Role of the reverse transcriptase tryptophan repeat motif in HIV-1 replication

Johanna A. Wapling

BSc. (Hons)

A thesis submitted for consideration towards the degree of

Doctor of Philosophy

December 2011

Department of Microbiology

Monash University

and

Centre for Virology

Burnet Institute

Copyright Notices

Notice 1

Notice 2

Table of contents

Summary

The HIV-1 enzyme, reverse transcriptase (RT), is a successful target for antiretroviral agents used for the treatment of HIV/AIDS. Ongoing research indicates that RT may yet reveal further targets for the development of novel chemotherapeutic agents that act to inhibit HIV-1 replication. RT is an asymmetric heterodimer composed of the p66 (66 kDa) and p51 (51 kDa) subunits. Since characterisation of RT as an obligate dimer, subunit dimerisation has been suggested as a novel drug target. Further, the ability of RT to dimerise is suggested to play a regulatory role in Gag-Pol processing and proteolytic generation of the mature RT heterodimer. Thus targeting RT dimerisation could potentially disturb both the early and late phases of HIV-1 replication, achieving dual modes of inhibition with a single compound. The present study validates this concept, and provides insight into the role of the RT domain in the late phase of HIV-1 replication. These observations were made upon examining the effect of mutating residues belonging to or associated with the highly conserved RT tryptophan repeat motif (TRM).

The TRM is comprised of a cluster of six tryptophan residues at RT codons 398, 401, 402, 406 and 410, and includes a tyrosine at codon 405. The motif is located in the connection subdomain, falling within secondary structural elements αL, β20 and the intervening loop linking these structures. The p66 αL-β20 loop protrudes into the p51 subunit, contributing to a major point of interaction at the RT heterodimer interface. Non-conservative mutation of the TRM residue W401 to alanine or leucine significantly diminishes RT subunit interaction, and accordingly RT activity. The dimerisation defect conferred by these mutations is predominantly mediated through the p66 subunit. In the p66 subunit W401 does not directly contribute to the heterodimer interface. Rather, W401 is located at the C-terminal of αL where it is proposed to have an essential role in maintaining the position of the p66 αL-β20 loop, and hence the interactions contributed by αL-β20 loop residues to the heterodimer interface. In contrast, the conservative substitution, W401F, does not affect the ability of the RT subunits to dimerise, indicating the importance of an aromatic residue at this location.

The role of the p66 αL-β20 loop in RT subunit interaction is supported by mutagenic analysis of other residues in this region. Non-conservative mutation of the TRM residue W414, which anchors the C-terminal of the loop in β20, and of K331, which interacts with the p66 αL-β20 loop in the p51 subunit, also perturb RT subunit dimerisation. A second-site compensatory mutation, T409I, which partially suppresses the dimerisation defected conferred by the W401A mutation, is located within the αL-β20 loop.

These data strongly support the proposal of an RT dimerisation defected mediated by the position of the αL-β20 loop at the heterodimer interface. It was proposed that mutation of these residues in HIV-1 would allow examination of the role of RT subunit interaction in HIV-1 replication in the absence of pleiotropic effects that have been described for other RT mutations.

Expression of TRM mutants that abrogate RT dimerisation (W401A/L) resulted in HIV-1 with significant decreases in levels of virion RT. Variation in the p51:p66 ratio in viral and producer cell lysates suggested that these mutations affected proteolytic generation of mature RT. These defects were RT specific with no accompanying decrease in virion Gag-Pol or IN. Virion particle production and Gag processing resembled that of wild-type HIV-1, indicating PR activation was not affected. A similar range of defects was apparent upon expression of the dimerisation defective K331A mutation in HIV-1.

In contrast expression of the W401F mutation, which does not adversely affect RT subunit dimerisation, conferred no significant defects when expressed in HIV-1. Furthermore, generation of a replication competent virus by passage of the W401A HIV-1 mutant identified three second-site mutations, C162Y, K366R and A534T. These mutations also restored RT dimerisation to the W401A mutant in a recombinant protein binding assay. These observations strongly suggested that the defects observed upon expression of dimerisation defective mutations were representative of the role of RT dimerisation in HIV-1 replication.

While the effect of the W401 mutations in HIV-1 replication corresponded well with their role in RT heterodimerisation, examination of other TRM residues indicated an independent role in HIV-1 replication. Expression of TRM mutants W398A and W414A in HIV-1 resulted in reduced levels of virion Gag-Pol, RT and IN. These mutations were also found to change the Gag-Pol processing profile in a recombinant Gag-Pol expression system. The W401A second-site compensatory mutation identified in recombinant protein studies, T409I, also resulted in a similar profile when expressed in HIV-1 and recombinant Gag-Pol. Accordingly, this mutation did not act to suppress the defects conferred by W401A in HIV-1 replication. Interestingly, neither T409I nor W398A inhibit RT subunit dimerisation or RT activity in recombinant RT. The contrasting effect of these mutations in recombinant RT compared to HIV-1 demonstrates the dynamic nature of the RT domain during maturation. This may be representative of a role for the TRM in regulation of Gag-Pol cleavage events performed by the embedded PR either directly, or by interaction with regulatory host cell factors.

These findings confirm that dimerisation of the HIV-1 RT domain has an important role in both the early and late phases of HIV-1 replication. Late phase defects were restricted to the proteolytic generation of mature RT, and no adverse effect on PR activation was observed. However this study identified the TRM as a key region in two independent stages of the late phase of HIV-1 replication, that being a defect in generation of a mature RT heterodimer upon disturbing RT dimerisation, and a dimerisation independent Gag-Pol processing defect. However, mutational analysis of W414, and the combined defect of the W401A and T409I mutations indicate that these defects can occur simultaneously. These data confirm the role of the TRM as a key region for RT interactions necessary for RT maturation and activity.

General Declaration

In accordance with Monash University Doctorate Regulations for Doctor of Philosophy, the following declarations are made:

This thesis contains no material which has been accepted for the award of any other degree or diploma in any university or other institution and affirms that to the best of my knowledge the thesis contains no material previously published or written by another person, except where due reference is made in the text of the thesis.

Signed

Date

25 April 2012

Acknowledgments

The primary objectives of the nascent Macfarlane Burnet Centre for Medical Research Centre, now the Burnet Institute, included; the development of new measures of infection control for hospitals and the community, to provide opportunities for graduates seeking careers in medical research, and to provide a focal point for the study of infection in the western Pacific region (Anderson, 2002). I hope these aspirations continue to guide the institute, so that it may continue to inspire and provide opportunities to young researchers such as myself.

Many aspects of the Burnet Institute have made it a special place for me. The diversity of research, from public health programs to cutting-edge basic science, creates a unique environment that I have enjoyed immensely. The calibre of the senior researchers, whose generosity with their time, advice, reagents and encouragement, is a great boon for the institute. And significantly, the staff and students whose intelligence and camaraderie I admired and deeply appreciated. To these wonderful friends and colleagues at or associated with the Burnet, I am amazed by you all, and am excited that you are taking to take your amazingness to the far corners of the world!

A particular note of thanks goes to the past and present members of the Tachedjian, Mak and Greenway laboratories, for their support and friendship. I would like to acknowledge Katie Moore, research assistant extraordinaire, for her assistance and advice over the years.

I would like to thank Dr Michael Kuiper for his enthusiasm in interpreting the effect of mutations from the point of the molecule itself, and for providing the beautiful images as acknowledged in each chapter.

Thanks to A/Prof Nicolas Sluis-Cremer and Jessica Radzio for their advice and review of the circular dichroism analysis performed in Chapter 4. Also to Prof Mibel Aguilar and her staff for the use of equipment and assistance in performing the circular dichroism spectroscopy.

Dr Steve Pettit generously provided advice on the recombinant Gag-Pol processing assay presented in Chapters 4 and 6. Dr Ron Swanstrom kindly supplied the original plasmids generated by Dr Pettit for use in this system, and thanks to his staff for their time spent locating these plasmids.

Dr Con Sonza provided reagents and equipment used in the detection of reverse transcription intermediates presented in Chapter 1, and the recombinant Gag-Pol processing assays presented in Chapters 4 and 6. Con's assistance and advice throughout this study, as well as his appreciation of coffee, were greatly valued.

Thanks to A/Prof Johnson Mak for providing the plasmids as acknowledged in Chapter 2, and to Penny Buxton and Dr Miranda Shehu-Xhilaga for their advice on these constructs. Also to Dr Mel Hill and Dr Andy Poumbourios for plasmids and reagents as acknowledged in Chapter 2. Tim Spelman provided much valued assistance in statistical analysis of data presented in this thesis.

This opportunity would have not have been possible without the financial support of an Australian Postgraduate Award administered though the Department of Microbiology at Monash University. And nor would it have been possible without the following people who enabled this fantastic opportunity.

To my primary supervisor A/Prof Gilda Tachedjian, thank you for accepting this little undergrad into your laboratory, and thank you for your continued support throughout this endeavour. I can still clearly remember the moment, peering down the microscope at some happily fluorescing, transiently transfected cells when you spoke those words; 'So, you wana do a PhD?'!

To my co-supervisor A/Prof Peter Wright, thank you for your support and advice, and especially for your stories. I am a little disappointed that your retirement means that future students will not experience your vast knowledge and wonderful tales of the early days of molecular biology.

Thank you to my friends, many of who do not share in my (over)excitement about all things science, but nevertheless offer their encouragement every step of the way. Finally, to my family. Thank you for putting up with me on the good days and the bad. Thank you for your continuing love and support, regardless of the endeavour I embark upon.

This work is humbly dedicated to Dianne Louise Wapling
1971-1996

List of Figures

List of Tables

Abbreviations

aa	amino acid/s
AIDS	acquired immune deficiency syndrome
ART	antiretroviral therapy
ARV	antiretroviral
AZT	zidovudine
CA	HIV capsid protein (p24)
cART	combination antiretroviral therapy
CPE	cytopathic effect
ECL	enhanced chemiluminescence
EFV	efavirenz
eGFP	enhanced green fluorescent protein
dsDNA	double stranded DNA
dNTP	deoxyribonucleotide triphosphate
kDa	kilodalton
h	hour/s
HIV	human immunodeficiency virus
HRP	horseradish peroxidase
HX	HIV-1 molecular clone HXB2
IN	integrase
K_d	dissociation constant
K_M	Michaelis constant
mAb	monoclonal antibody
M	molar
MA	matrix
min	minute/s
NNBP	NNRTI binding pocket
NC	nucleocapsid
NL	HIV-1 molecular clone NL4.3
NLS	nuclear localisation sequence
NNRTI	non-nucleoside reverse transcriptase inhibitor
NRTI	nucleoside reverse transcriptase inhibitor
NVP	nevirapine
p	plasmid
p24	HIV CA protein
PAGE	polyacrylamide gel electrophoresis
PBS	primer binding site
PBS(-)	phosphate-buffered saline, magnesium and calcium free
PI	protease inhibitor
PIC	pre-integration complex
Pol	HIV precursor protein including PR, RT and IN
PPT	polypurine tract
PR	HIV protease

RDDP	RNA-dependent DNA polymerase
RE	restriction endonuclease
RNase H	ribonuclease H
RT	HIV reverse transcriptase
RTC	reverse transcription complex
SDS-PAGE	SDS-polyacrylamide gel electrophoresis
SEC	size exclusion chromatography
T/P	template/primer
TRM	tryptophan repeat motif
TSAO-T	tert-butyldimethylsilyl-spiroaminooxathioledioxide-thymine
$TCID_{50}$	50% tissue culture infectious dose
Y2H	yeast two-hybrid
VLP	virus like particles

Chapter 1

Introduction

1.1. General and historical introduction

The human immunodeficiency virus (HIV) is the aetiological agent of acquired immunodeficiency syndrome (AIDS). HIV specifically infects cells of the human immune system, predominantly CD4+ T lymphocytes and macrophages. HIV replication results in the progressive depletion of CD4+ T lymphocytes, disabling the immune system. The resulting immunosuppression allows for opportunistic infections, and left untreated these infections incapacitate, and ultimately result in death.

Although there is evidence that HIV had been present in the human population since the 1920s (Worobey *et al.*, 2008), the herald of the current pandemic was a report published in 1981 (Gottlieb *et al.*, 1981). It describes five cases of a rare infection usually limited to severely immunosuppressed patients occurring without apparent cause in previously healthy young homosexual men from Los Angeles, USA. The accompanying editor's comment suggested *'the possibility of a cellular-immune dysfunction related to a common exposure that predisposes individuals to opportunistic infections'.* Reports of similar cases of immunosuppression followed from locations across the USA (Centers for Disease Control, 1981; Hymes *et al.*, 1981; Hungnes *et al.*, 1992). In September of 1982 the fatal affliction was given the name AIDS. By 1985 over 15,000 cases had been reported worldwide, the majority occurring in the USA (Centers for Disease Control, 1985). In North America and Europe the epidemic was most prominent in populations of men who have sex with men and intravenous drug users (Centers for Disease Control, 2001; UNAIDS, 2002). In contrast, the emerging African epidemic was characterised by heterosexual transmission (Piot *et al.*, 1984; Van de Perre *et al.*, 1984; Serwadda *et al.*, 1985).

In Australia the AIDS epidemic effectively began 18 months after it was first reported in the USA (Penny *et al.*, 1983). Australia's approach to AIDS prevention in the early 1980s is recognised as one of the most innovative and successful in the world (Sendziuk, 2003; Pitt *et al.*, 2007). A progressive national minister of health, world-class infectious diseases experts and proactive members of the at-risk communities all contributed to this outcome.

Upon briefing of the emerging AIDS epidemic in 1983 the newly appointed minister of health, Neal Blewett, established a task force to coordinate a national response. In the ethos of harm reduction, this included a safe sex media campaign, needle exchange programme and peer mediated sex-worker education programme (Sendziuk, 2003; Pitt *et al.*, 2007). These initiatives were in stark contrast to the actions of contemporary conservative governments. In the USA, President Ronald

Regan did not publicly address the topic of AIDS during his first term of office from 1981 to 1985, the period spanning the emergence and rapid expansion of the epidemic within the USA (Sendziuk, 2003).

At this time within the scientific field, the novel human retrovirus eventually to become known as HIV type-1 (HIV-1) was isolated by Luc Montagnier's research team at the Pasteur Institute in France (Barre-Sinoussi *et al.*, 1983), and subsequently by researchers in the USA (Gallo *et al.*, 1984; Levy *et al.*, 1984). These three independently isolated viruses referred to as lymphadenopathy associated virus, human T cell leukaemia virus type III and AIDS associated retrovirus, respectively, were confirmed to be variants of the same virus (Ratner *et al.*, 1985). However, a protracted controversy eventuated between the French and American research groups led by Montagnier at the Pasteur Institute and Gallo at the National Cancer Institute. Gallo claimed the discovery of HIV-1 and received the patent for commercial tests developed to detect the presence of HIV-1 antibodies. In 1987 an agreement between the then US president Ronald Reagan and French Prime Minister Jacques Chirac recognised both Montagnier and Gallo equally for the discovery, and arranged to share the royalties generated by the patent. With the name of the virus, HIV, decreed by an international commission on virological nomenclature in 1986 (Brown, 1986; Coffin *et al.*, 1986) the public feud abated. Any remaining ambiguity was firmly put to rest in 2008 with the awarding of the Nobel Prize in Medicine to the French scientists, Barre-Sinuossi and Montagnier.

During the early years of the AIDS epidemic, Australia emerged as a world leader in HIV research. In December of 1984 the virology laboratory associated with the Fairfield Hospital in Melbourne was one of three World Health Organisation collaborating centres for AIDS research. By 1985 it was one of five laboratories evaluating candidate HIV antibody detection kits. This facilitated implementation of a fundamental AIDS prevention measure in Australia - HIV antibody screening in all blood banks (Resnik, 1999). In 1986 the virology laboratory was formally transformed into the Macfarlane Burnet Centre for Medical Research, now the Burnet Institute, named after the Australian virologist and Nobel laureate Sir Frank Macfarlane Burnet. Professor Ian Gust was the founding scientific director of the institute (Anderson, 2002). Earlier in 1983, Gust had attended a meeting on the emerging threat of AIDS, where he first met the young French scientist, Luc Montagnier.

Amidst the rapid expansion of the epidemic (Centers for Disease Control, 1985), and failure in early attempts in vaccine development (Francis *et al.*, 1985), the first antiretroviral (ARV) drug was approved for use in the treatment of AIDS in 1987. The nucleoside analogue, zidovudine (AZT), was shown to block HIV-1 replication by preventing reverse transcription (Mitsuya *et al.*, 1985). AZT therapy decreased mortality and the frequency of opportunistic infections in AIDS patients in

short-term trials (Yarchoan *et al.*, 1986; Fischl *et al.*, 1987), and the drug received fast-track approval for release. However, AZT was set to retail at approximately $7000-$10,000 USD per annum, a prohibitive cost for most AIDS patients. Pressure from advocacy groups and the USA Congress resulted in a 20% reduction in price in December of 1987, followed by a further reduction in September of 1989 (Delaney, 2005). From this first instance, access to ARV therapy remains an ongoing issue, and the role of advocacy groups in campaigning for universal access has not abated.

Following a contentious medium-term double-blind study, AZT monotherapy was confirmed neither to retard the progression to AIDS nor improve survival (Concorde Coordinating Committee, 1994). The mechanisms resulting in the rapid generation and selection of drug resistance mutations, characteristic of HIV-1, were not understood until several years following the release of AZT (Larder *et al.*, 1989). HIV-1 infection is characterized by continuous viral replication and rapid turnover of infected CD4+ lymphocytes (Ho *et al.*, 1995). Combined with the low fidelity of the HIV-1 RT (Bebenek *et al.*, 1989), and recombination of the viral genome during replication (Hu *et al.*, 1990), HIV-1 can rapidly generate highly heterogeneous populations within a single host (Perelson *et al.*, 1996). Such diversity provides a broad base of variants that can escape from both the host immune response and antiretroviral therapy (ART) (reviewed by Freed *et al.*, 2001 and Menendez-Arias *et al.*, 2002).

The breakthrough in chemotherapeutic control of HIV-1 infection came in 1996 with the development of highly active antiretroviral therapy (HAART), now referred to as combination antiretroviral therapy (cART). The availability of two new classes of ARV drugs, protease inhibitors (PIs) in 1995, and non-nucleoside reverse transcriptase inhibitors (NNRTIs) in 1996, allowed dosing with at least two independent classes of ARV. This dramatically increased the genetic barrier against generation of resistant HIV-1 (Perelson *et al.*, 1996).

ART remains the sole method to control HIV-1 infection, as an efficacious vaccine remains elusive after some 30 years of research. ART also forms the basis of prophylactic measures such as prevention of mother to child transmission (PMTCT) and more recently, as microbicides (Karim *et al.*, 2010). The ARV repertoire has expanded for treatment-experienced patients to include the fusion inhibitor T20/enfuvirtide (James, 1997) in 2003, the CCR5 co-receptor antagonist maraviroc (Wood *et al.*, 2005) and the IN inhibitor raltegravir (Markowitz *et al.*, 2006; Grinsztejn *et al.*, 2007) in 2007. Structural data has facilitated the development of new NNRTIs, with the latest generation, rilpivirine (Janssen *et al.*, 2005), released in 2011. Continued development of ART is a necessity as the efficacy of current cART regimens is limited by cross-resistance to inhibitors of the same class, the accumulation of drug resistance mutations and transmission of multi-drug resistant HIV-1 (reviewed by Clavel *et al.*, 2004; Shafer *et al.*, 2008). Increased cost effectiveness, decreased toxicity, convenient dosing and supply chain requirements are also demanded of novel therapies.

Since 1981, more than 25 million people have died from AIDS related illnesses. This is but a preliminary manifestation of the human cost, as current estimates place the number of people living with HIV at 33 million (UNAIDS, 2010). While at a local level individual HIV epidemics can be found to be expanding, stabilising or contracting, the global HIV prevalence has stabilised since 2000 as prevention and treatment protocols begin to yield results. The decline in AIDS related deaths observed for the 2005 - 2007 period is partially attributed to increased access to cART (UNAIDS, 2008).

For those in high-income countries with access to quality healthcare, cART has transformed HIV infection from a debilitating disease culminating in premature death, to a chronic condition with life expectancies approaching that of the general population (Antiretroviral Therapy Cohort Collaboration, 2008). Yet in low and middle-income countries, where the overwhelming burden of HIV infection is borne, only 30% of HIV-1 positive people have access to cART (UNAIDS, 2010), and the 2010 target date for universal access to HIV treatment and care has passed unfulfilled. Moreover, universal access is only part of the solution. During 2009, 1.2 million HIV positive people gained access to cART, while 2.6 million were newly infected (UNAIDS, 2010). UNAIDS has recognised community involvement as a critical element in the success of HIV prevention programs (UNAIDS, 2010). Combating the pandemic requires not only improved antiretroviral drugs and up scaling of comprehensive treatment and care programs, but increased investment in multidisciplinary, comprehensive prevention programs.

1.2 HIV taxonomy and phylogeny

HIV-1 is a primate lentivirus of the Retrovirus family. The *Retroviridae* are enveloped RNA viruses whose replicative strategy involves reverse transcription of the RNA genome into a DNA intermediate. This once counterintuitive process was ushered from theory to fact by Temin and Baltimore with the discovery of RNA dependent DNA polymerase activity in Rous sarcoma virus particles in 1970 (Baltimore, 1970; Temin *et al.*, 1970). The reversal of the 'central dogma of biology', the unidirectional flow of information from DNA to RNA, earned the terminology *retro* from the Latin for 'backward'.

The genus name *lentivirus* is derived from the Latin for 'slow', referring to the characteristic delay in the onset of symptoms after infection by a lentivirus. Five serotypes are defined on the basis of the hosts they infect, primates, sheep and goats, horses, cats and cattle (Los Alamos National Laboratory, 2008a). The primate serotype includes HIV-1, HIV type 2 (HIV-2) and simian immunodeficiency virus (SIV). The two HIV types are distinguished on the basis of their genome organisation and phylogeny. Significant sequence divergence exists between the two types (Los Alamos National Laboratory, 2008a) and HIV-2 is reportedly less pathogenic than HIV-1 (Popper

et al., 1999). HIV-2 was isolated in 1986 from AIDS patients from west Africa (Clavel *et al.*, 1986), where it remains endemic.

HIV-1 clusters into three distinct phylogenetic groups, group M (main), group O (outlier) group N (non-M/non-O), and group P (reviewed in Sharp *et al.*, 2011). Group M viruses, which are the cause of the current pandemic, are further divided into subtypes that vary in prevalence around the world. Of increasing relevance to the pandemic are inter-subtype recombinants known as circulating recombinant forms (Los Alamos National Laboratory, 2008b).

1.3 The zoonotic origin and spread of HIV

Despite the genetic and structural similarities between HIV and SIV, the simian immunodeficiency viruses have not been observed to cause disease in their natural hosts (Hahn *et al.*, 2000). Each simian species carries its own subtype of SIV (Los Alamos National Laboratory, 2008a). The observation that infection of a primate with an SIV derived from a different species results in an AIDS-like disease (Daniel *et al.*, 1985; Letvin *et al.*, 1985) gave rise to the theory of AIDS as a zoonosis. HIV-2 was the first of the human lentiviruses to be recognised as cross species transmission of SIV from sooty mangabeys to humans (Hahn *et al.*, 2000). Phylogenetic studies demonstrating that HIV-1 is most closely related to chimpanzee SIV (SIVcpz) (Peeters *et al.*, 1989; Huet *et al.*, 1990) were confirmed in molecular epidemiological field studies that traced the origins of group M and group N HIV-1 to two distinct and geographically isolated chimpanzee communities in Cameroon (Keele *et al.*, 2006; Van Heuverswyn *et al.*, 2007). The origin of HIV-1 group O remains unknown but is also suspected to be an independent zoonotic event.

Analysis of historical biological samples retrospectively found to be HIV-1 positive has facilitated estimation of when such a zoonotic event may have occurred. The two oldest known HIV-1 positive samples were collected in 1959 (Zhu *et al.*, 1998) and 1960 (Worobey *et al.*, 2008) in Leopoldville, now Kinshasa in the Democratic Republic of Congo. These samples belong to two distinct subtypes, demonstrating that HIV-1 diversity at this point in history was greater than previously thought (Worobey *et al.*, 2008). Worobey and colleagues (2008) estimate the most recent common ancestor of the group M viruses to have been present in the human population between 1902 and 1921. At this time Leopoldville was one of the largest cities of Central Africa, located on the major trade route of the Sangha River. These factors probably facilitated arrival and dispersal of HIV-1 from Leopoldville. However, it is thought the particular social, economic, and behavioural changes that occurred in the mid 20th century, including the formation of large cities and international travel, enabled the rapid expansion of HIV-1, resulting in the pandemic experienced today (Yusim *et al.*, 2001; Worobey *et al.*, 2008).

1.4 Genetic organisation and structure of HIV-1

The HIV-1 genome (Fig. 1.1) is a single stranded RNA, approximately 9000 nucleotides in length. HIV-1 utilises overlapping reading frames and multiple mRNA splicing events to make efficient use of this relatively compact genome. Common to all replication-competent retroviruses HIV-1 has three major open-reading frames: *gag*, *pol*, and *env*. Reverse transcription of the RNA genome into a double-stranded DNA copy duplicates the terminal 'unique' and 'repeat' regions to form the long terminal repeat elements (LTR) at each end of the double-stranded DNA copy. LTRs contain the regulatory elements essential for transcription of the HIV-1 genome once integrated into the host.

The *gag* reading frame encodes the viral structural proteins, matrix (MA), capsid (CA/p24), and nucleocapsid (NC); *pol* encodes the viral enzymes protease (PR), reverse transcriptase (RT) and integrase (IN); and *env* encodes the surface and transmembrane envelope glycoproteins gp120 and gp41. HIV-1 is classified as a complex retrovirus due to the presence of regulatory proteins Tat and Rev, and accessory proteins Vif, Nef, Vpr and Vpu, which are encoded in independent reading frames.

HIV-1 virions are pleomorphic but generally spherical and approximately 80-100 nm in diameter (Fig. 1.2). Viral particles are enveloped by a host cell derived lipid bilayer, which is studded with the envelope complex. The envelope complex is formed by a trimer of gp120:gp41 heterodimers, in which gp120 is anchored to the membrane via non-covalent interactions with transmembrane glycoprotein gp41. A MA lattice lines the lipid bilayer, within which CA multimers form the electron dense cone-shaped core characteristic of HIV-1 particles. The core contains two copies of the positive-sense RNA genome, which is dimeric in structure and complexed with the viral nucleoprotein, NC. The HIV-1 enzymes PR, RT and IN are found in the core along with viral accessory and regulatory proteins and host cell factors (Vogt, 1997).

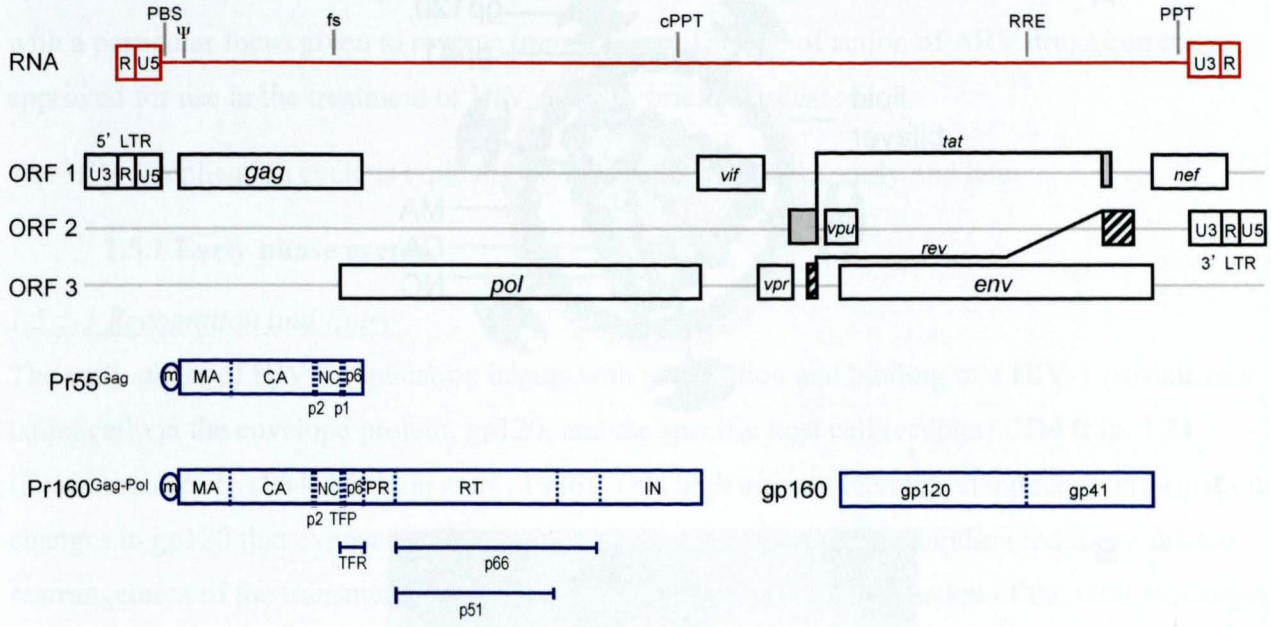

Figure 1.1. Organisation of the HIV-1 genome.

The positive sense RNA genome (red) of approximately 9000 nucleotides is bordered by identical repeat sequences (R) and a unique region at the 5' (U5) and 3' (U3) end of the genome. RNA elements important for replication are indicated at their approximate position, including the primer binding site (PBS), RNA encapsidation sequence (Ψ), frameshift site (fs), central and terminal polypurine tracts (cPPT and PPT respectively), and the RRE (Rev responsive RNA element). Reverse transcription of the genomic RNA duplicates the terminal repeat and unique regions to form long terminal repeat (LTR) elements at each end of the reverse transcribed DNA (black). The LTRs contain transcriptional elements essential for mRNA production. Common to all replication-competent retroviruses are the *gag*, *pol*, and *env* coding regions, which are expressed as polyprotein precursors named for their molecular weight; $Pr55^{Gag}$, $Pr160^{Gag\text{-}Pol}$ and $gp160^{Env}$ respectively (blue). The *gag* reading frame encodes the structural proteins matrix (MA or p17), capsid (CA or p24), nucleocapsid (NC or p7), $p6^{Gag}$ and two spacer peptides, p2 and p1. The *pol* reading frame encodes the retroviral enzymes, protease (PR), reverse transcriptase (RT), and integrase (IN). Expression of *pol* is dependent on a ribosomal slippage event during *gag* translation into the overlapping *pol* reading frame, generating the Gag-Pol fusion protein $Pr160^{Gag\text{-}Pol}$. This results in replacement of the Gag proteins p1 and p6 with the transframe octapeptide (TFP) and $p6^{pol}$ ($p6^{*}$) collectively referred to as the transframe region (TFR). Both $Pr55^{Gag}$ and $Pr160^{Gag\text{-}Pol}$ are post-translationally myristoylated (m). The *env* reading frame encodes the surface glycoprotein gp120, and transmembrane glycoprotein gp41. HIV-1 also encodes regulatory proteins, Tat and Rev, and accessory proteins Vif, Nef, Vpr and Vpu. Diagram adapted from the Los Alamos HIV Sequence Database (2008), and Petropoulos (1997).

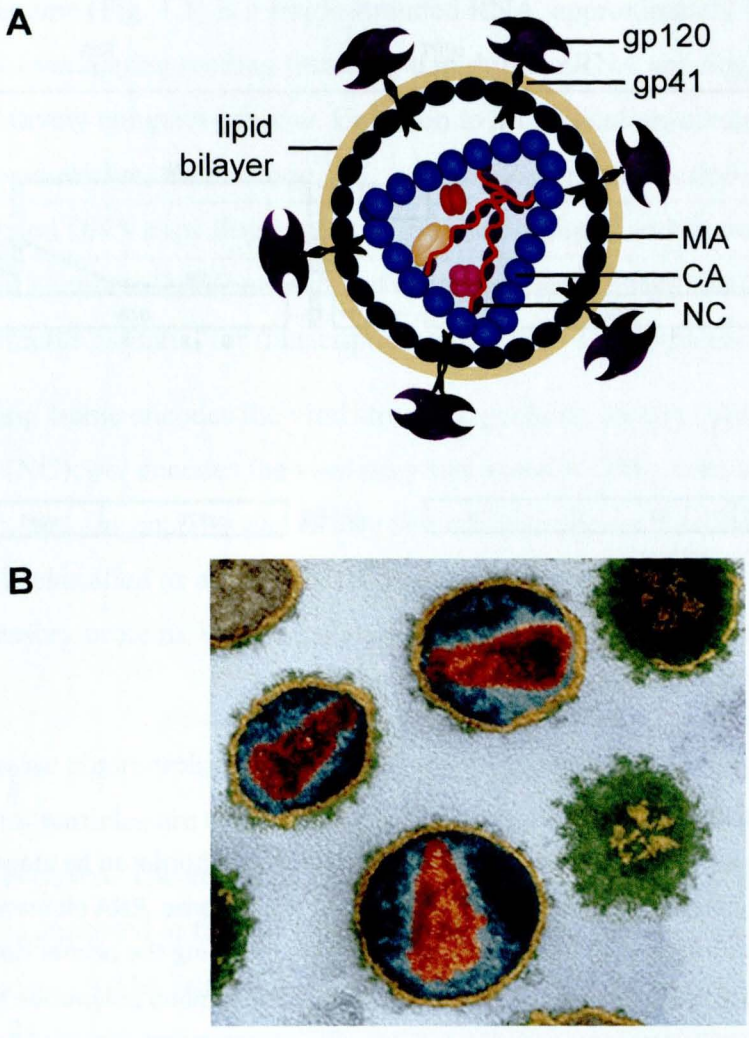

Figure 1.2. Structure of a mature HIV-1 particle.

Diagram of a mature HIV-1 viral particle (**A**) and colour-enhanced electron microscopy image of HIV-1 particles (**B**), obtained from Wellcome Images (Wellcome Photo Library, 2008). HIV-1 particles are spherical to pleiomorphic, approximately 100 nm in diameter and icosahedral in structure. The viral particle is enveloped by a host derived lipid bilayer that is studded by the HIV-1 envelope complex, occasionally observable as surface projections in electron micrographs. The surface protein gp120 is anchored by non-covalent interactions with the gp41 transmembrane protein, which associate into a trimer of heterodimers. A network of MA molecules line the envelope, occasionally observable in electron micrographs as a thin layer of submembrane protein. The characteristic cone-shaped electron dense core of HIV-1 is formed by CA multimers. The core encapsidates two copies of the HIV-1 RNA genome, which associates as a dimeric complex stabilised by NC. The HIV-1 enzymes RT, PR and IN, together with p6, Vpr and Vif, are found in the HIV core.

1.5 HIV-1 replication

An overview of the HIV-1 replication cycle is provided in Fig. 1.3, and briefly described below, with a particular focus given to reverse transcription. The site of action of ARV drugs currently approved for use in the treatment of HIV/AIDS is briefly discussed.

The HIV-1 replication cycle is typically divided into two phases, early and late.

1.5.1 Early phase events

1.5.1-1 Recognition and Entry

The early phase of HIV-1 replication begins with recognition and binding of a HIV-1 particle to a target cell via the envelope protein, gp120, and the specific host cell receptor, CD4 (Fig. 1.3) (Klatzmann *et al.*, 1984; Maddon *et al.*, 1986). This high affinity interaction induces conformational changes in gp120 that expose the co-receptor binding site. Co-receptor binding induces a drastic rearrangement of the transmembrane domain of gp41 which results in fusion of the viral and target cell membrane (Melikyan *et al.*, 2000, and reviewed by Sterjovski *et al.*, 2006). While HIV-1 can utilise a number of molecules as co-receptors, the chemokine receptors CXCR4 (R4) and CCR5 (R5) are the predominant cellular co-receptors for HIV-1 attachment and entry. Co-receptor usage has been associated with cell tropism, with X4 viruses exhibiting T-lymphocyte tropism and R5 viruses exhibiting macrophage tropism. However co-receptor usage is not an absolute predictor of tropism (reviewed by Gorry *et al.*, 2004).

Following membrane fusion and release of the HIV-1 core into the host cell cytoplasm, the CA lattice that forms the core disassembles in a process referred to as uncoating. Uncoating is important for viral infectivity, however the mechanism remains unclear. CA mutations that either increase or decrease core stability reduce HIV-1 infectivity (Forshey *et al.*, 2002). This suggests that the timing or extent of core disassembly is important for successful replication, presumably by directly influencing the efficiency of reverse transcription (reviewed by Ganser-Pornillos *et al.*, 2008).

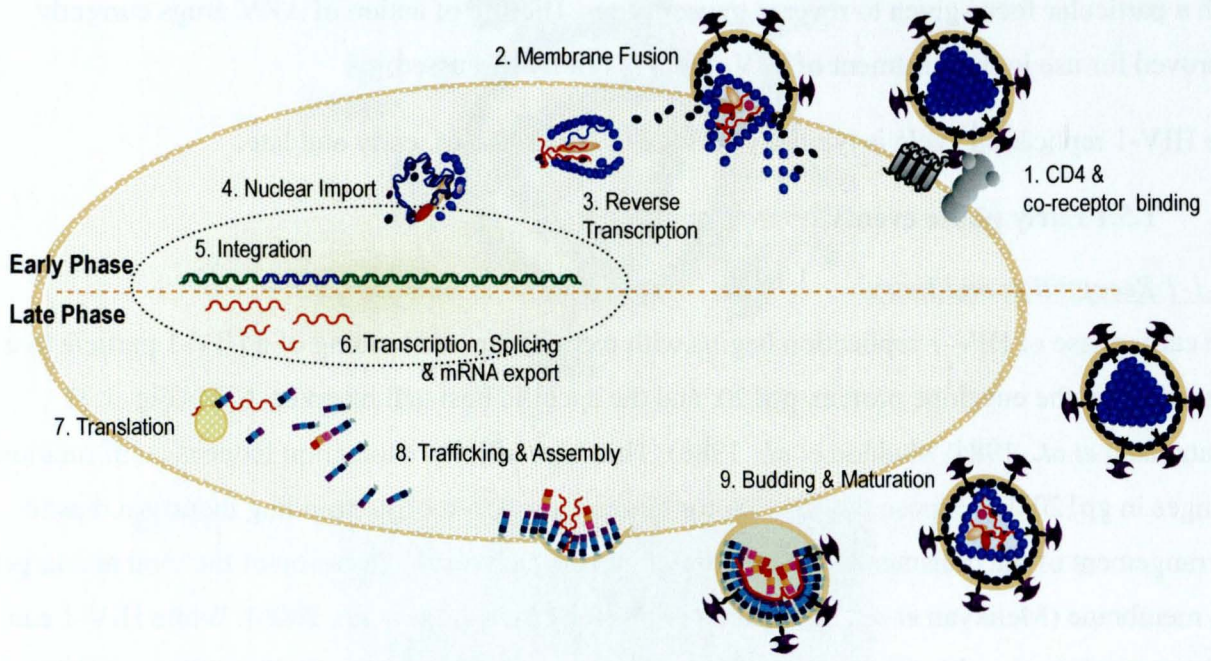

Figure 1.3. The HIV-1 replication cycle.

The early phase begins with binding of HIV-1 envelope protein, gp120, to the host cell receptor CD4 and either the CCR5 or CXCR4 chemokine co-receptor (1). Fusion of the viral and cell membranes releases the viral core into the host cell cytoplasm (2). Uncoating allows restructuring of the core and incorporation of host cell factors to form the reverse transcription complex, where the RT catalyses the conversion of the single-stranded viral RNA genome into a double-stranded DNA copy (3). The reverse transcription complex matures into the preintegration complex which is trafficked across the nuclear membrane (4) and the HIV-1 cDNA is integrated into the host chromosomal DNA (5). Transcription of the integrated provirus begins the late phase of HIV-1 replication (6). Unspliced, singly and multiply spliced mRNA transcripts are exported and translated utilising the host cell machinery (6, 7). Viral polyprotein precursors, proteins and RNA are trafficked to microdomains in the plasma membrane where viral particle formation occurs (8). As progeny virions bud from the cell surface the HIV-1 protease is activated and cleaves the polyprotein precursors. The formation of the mature structural proteins and enzymes generates a morphologically mature and infectious virion in a process known as maturation (9). Antiretroviral therapies currently target entry (i.e. the CCR5 agonist maraviroc), fusion (i.e. T20), reverse transcription (i.e. NRTIs and NNRTIs), integration (i.e. raltegravir) and maturation (i.e. PIs).

1.5.1-2 Reverse transcription

Reverse transcription of the single-stranded viral RNA genome into a double-stranded DNA copy is essential for establishment of a productive HIV-1 infection. To a limited degree, reverse transcription can occur within the HIV-1 core (Lori *et al.*, 1992; Trono, 1992; Arts *et al.*, 1994; Oude Essink *et al.*, 1996; Huang *et al.*, 1997; Warrilow *et al.*, 2007). A combination of the low dNTP concentration, lack of interacting host cell factors and secondary structures in the HIV-1 RNA template in the HIV-1 core are proposed to physically limit intra-particle reverse transcription (reviewed by Abbink *et al.*, 2008). In the target cell, reverse transcription occurs within the reverse transcription complex (RTC).

The RTC is formed from core contents and host cell factors following uncoating. Due to the dynamic nature and technical difficulty in isolating intact RTCs, the components have not been consistently defined. Presence in the RTC or a role in reverse transcription is described for viral proteins NC (Amacker *et al.*, 1997; Lener *et al.*, 1998; Anthony *et al.*, 2007), MA (Kiernan *et al.*, 1998) and IN (Wu *et al.*, 1999). Regulatory protein Tat (Ulich *et al.*, 1999; Kameoka *et al.*, 2001), and multifunctional accessory proteins Vif (Dettenhofer *et al.*, 2000) and Nef (Aiken *et al.*, 1995; Schwartz *et al.*, 1995; Fournier, 2002) have also been implicated. Host cell factors that contribute to reverse transcription or the RTC are continually being identified (Lemay *et al.*, 2008a; Lemay *et al.*, 2008b; Warrilow *et al.*, 2008), although the role of some of these factors is controversial and remains to be confirmed (Ahn *et al.*, 2010).

Although HIV-1 proteins and host cell factors have been shown to participate in reverse transcription, the enzymatic activities supplied by the HIV-1 RT are both necessary and sufficient for reverse transcription. The RT enzyme contains two active sites that coordinate three catalytic functions, RNA and DNA dependent DNA polymerase activity (RDDP and DDDP respectively) and ribonuclease H activity (RNase H), which specifically degrades RNA in RNA:DNA duplexes. Reverse transcription is a complex and quite remarkable process that coordinates DNA synthesis, RNA degradation, multiple strand transfer events, primer generation and removal (Fig. 1.4). The process of reverse transcription is also responsible for generating the genetic diversity characteristic of HIV-1. Reverse transcriptase does not possess exonucleolytic proofreading activity, and exhibits lower fidelity *in vitro* than proofreading-defective DNA polymerases (Bebenek *et al.*, 1989). Theoretically, this corresponds to a single amino acid substitution for each genome transcribed (Telesnitsky *et al.*, 1997). Recombination or template switching between the two packaged RNA genomes during reverse transcription also facilitates generation of genetic diversity in progeny virions (Hu *et al.*, 1990).

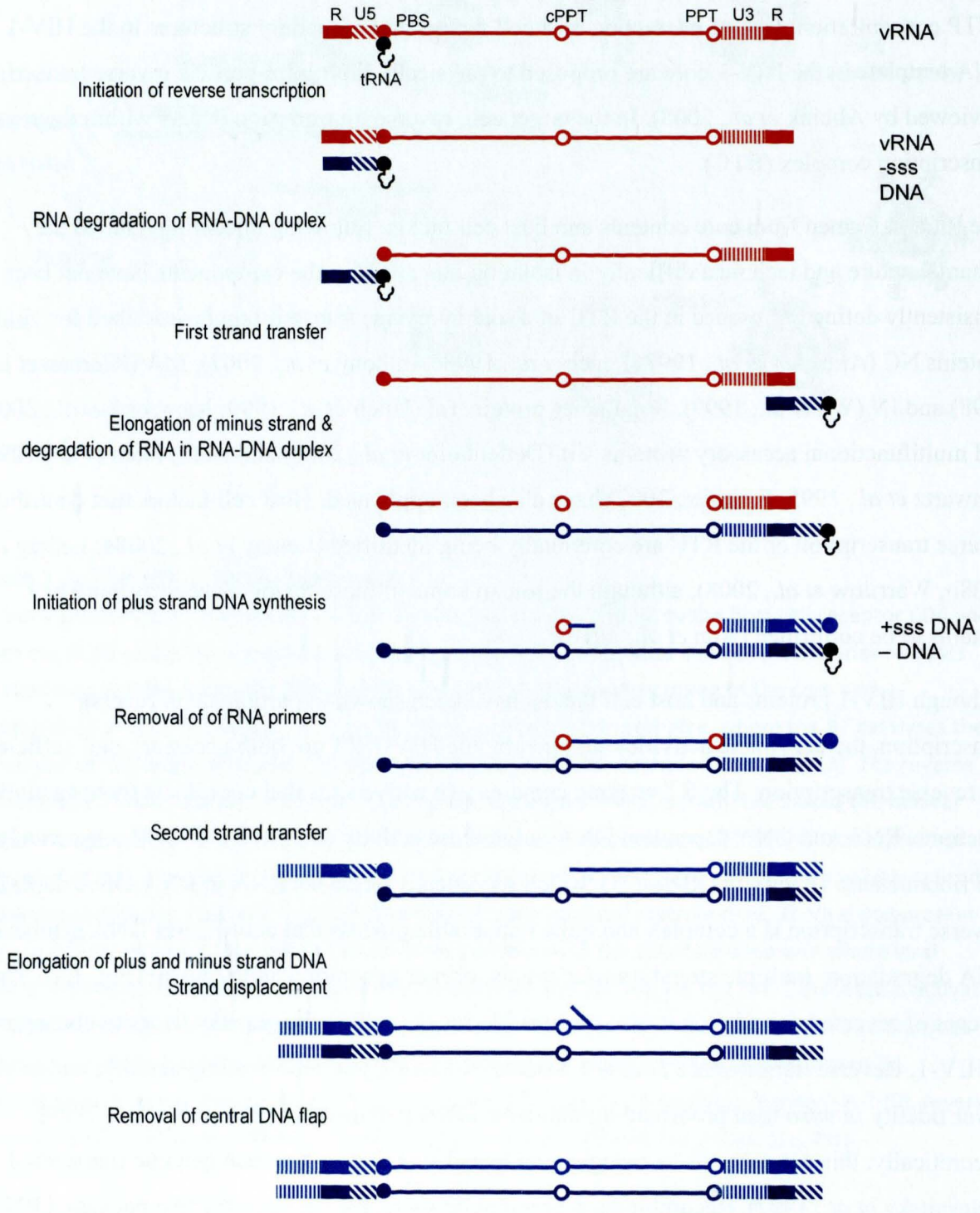
R U5
PBS
cPPT
PPT U3 R
vRNA
tRNA
Initiation of reverse transcription
vRNA
-sss
DNA
RNA degradation of RNA-DNA duplex
First strand transfer
Elongation of minus strand &
degradation of RNA in RNA-DNA duplex
Initiation of plus strand DNA synthesis
+sss DNA
– DNA
Removal of of RNA primers
Second strand transfer
Elongation of plus and minus strand DNA
Strand displacement
Removal of central DNA flap

Figure 1.4. Reverse transcription of the HIV-1 genome.

The positive sense RNA genome is primed with a host derived $tRNA^{lys3}$. RT facilitates annealing of the 3' end of the tRNA to the complementary primer-binding site (PBS) within the 5' untranslated region (U5) of the HIV-1 RNA genome (Goff, 1990; Mak *et al.*, 1994). RDDP activity extends the primer to the 5' end of the genome, generating a DNA intermediate known as minus strand strong stop (-sss) DNA. RNase H degradation of the RNA template facilitates the first strand transfer event in which the –sssDNA is transferred to the 3' end of the HIV-1 RNA genome via interaction with the complementary repeat (R) sequence. The –sssDNA now serves as a primer for extension of the minus strand. Minus strand elongation is accompanied by RNase H degradation of the RNA template. Two regions resist cleavage; the 3' polypurine tract (PPT) and the central polypurine tract (c-PPT) (Sarafianos *et al.*, 2001). These RNA fragments serve as primers for plus-strand synthesis with the nascent negative strand acting as the template. Elongation continues until the first modified base of the incorporated tRNA is encountered (Artzi *et al.*, 1996). Removal of the tRNA by RNase H allows the second strand transfer event, where the positive strand fragment is transferred to the complementary minus strand PBS. Elongation of the minus and plus strands completes the formation of the 5' and 3' LTRs. Elongation of the plus strand displaces the strand initiated from the cPPT via a mechanism called strand displacement, creating the central DNA flap. Elongation is terminated at the central termination sequence approximately 80–100 nucleotides downstream of the cPPT. Reverse transcription has produced a linear double stranded DNA with a discontinuous positive strand and central DNA flap. A role for the flap has been proposed in nuclear import (Charneau *et al.*, 1992) after which the flap is ligated by a cellular enzymes (Rumbaugh *et al.*, 1998). However the importance of the flap for HIV-1 infectivity remains somewhat contentious (Marsden *et al.*, 2007 and reviewed by Abbink *et al.*, 2008). The resulting double stranded DNA is flanked by two LTRs, duplicating 3' and 5' ends of the RNA genome at each end of the DNA copy, allowing the viral DNA to serve as the template from which RNA can be transcribed (reviewed by Sarafianos *et al.*, 2009). Diagram adapted from Abbink *et al.*, (2008).

Reverse transcription of the HIV-1 RNA genome is generally complete within 8-12 hours following entry of a HIV-1 particle (Telesnitsky *et al.*, 1997). However, reverse transcription products have been detected in the nucleus within four hours following entry (Fassati *et al.*, 2001). Only a small proportion of RTCs produced in each cell successfully integrate to give rise to progeny virions (Iordanskiy *et al.*, 2006).

1.5.1-3 Nuclear import and integration

Upon completion, or progressively during reverse transcription, the RTC undergoes qualitative and quantitative changes in protein content to form a pre-integration complex (PIC) (Iordanskiy *et al.*, 2006). The PIC is shuttled to the nuclear membrane via the microtubule network (McDonald *et al.*, 2002), and is actively transported into the nucleus. This critical stage of replication is a unique feature of lentiviruses such as HIV - the ability to infect non-dividing cells.

It is still unclear how many molecules of IN comprise the functional complex, however IN is known to function as a multimer and is likely a tetramer (reviewed by Chiu *et al.*, 2004b). Integrase preferentially inserts the reverse transcribed HIV-1 genome at transcriptionally active sites in the host chromosome (Schroder *et al.*, 2002). Integrase catalyses the cleavage and subsequent ligation of the 3' ends of the double-stranded HIV-1 DNA and the 5' end of host chromosomal DNA. The resulting unligated 3' ends or 'nicks' in the DNA are subsequently extended and ligated by DNA repair enzymes, completing the process of integration (Brown, 1997).

1.5.2 Late phase events

1.5.2-1 Transcription, translation and trafficking

The integrated provirus behaves essentially as a cellular gene. Transcription is initiated from the promoter in the U3 region of the LTR. Basal transcriptional activity is low and is greatly increased upon production of the Tat protein, which recruits cellular transcription factors to the LTR (Dayton *et al.*, 1986; Fisher *et al.*, 1986; Wei *et al.*, 1998). Unspliced RNA transcripts act as both mRNA for the Gag and Gag-Pol polyproteins, and as the viral genomic RNA that is packaged into the virion. Single and multiple splicing events generate specific mRNAs coding for other viral proteins (see Fig. 1.1) (Purcell *et al.*, 1993). Splicing and export of mRNA species is regulated by the interaction of the HIV-1 Rev protein (regulator of expression of viral proteins) with the *cis* acting Rev responsive element (RRE) found in unspliced and singly spliced RNAs.

The host cell machinery is appropriated for expression of HIV-1 proteins following mRNA export. The coding regions *gag* and *env* are translated as polyprotein precursors ($Pr55^{Gag}$ and $gp160^{Env}$ respectively). As the *pol* coding region lacks a start codon, transcription is dependent on ribosomal slippage during *gag* translation into the overlapping *pol* reading frame, producing the Gag-Pol fusion protein ($Pr160^{Gag\text{-}Pol}$) (Jacks *et al.*, 1988b). Interaction of multiple RNA elements facilitate

ribosomal frameshifting, the key regions being a heptanucleotide AU-rich 'slippery' sequence and a downstream RNA stem loop structure located at the 3' end of the NC coding region (Jacks *et al.*, 1988b; Kollmus *et al.*, 1994 and reviewed by Hill *et al.*, 2005; Brierley *et al.*, 2006). In the resulting Gag-Pol fusion protein the terminal Gag proteins p1 and p6 are replaced by the transframe region (TFR), which links the Gag and Pol proteins. The TFR is comprised of an octapeptide transframe protein (TFP) followed by a 48–60 amino acid variable region known as $p6^{Pol}$, separated by a HIV-1 PR cleavage site (Fig. 1.1) (Candotti *et al.*, 1994; Louis *et al.*, 1998). Ribosomal frameshifting is an infrequent event occurring approximately once for every 20 Gag transcripts, resulting in a 1:20 Gag:Gag-Pol ratio. Maintenance of this ratio is important for HIV-1 particle formation (Park *et al.*, 1991) and maturation (Shehu-Xhilaga *et al.*, 2001). Similar frameshifting mechanisms are used by other retroviruses to regulate *pol* expression (Jacks *et al.*, 1985; Jacks *et al.*, 1987; Jacks *et al.*, 1988a). The known exception is human foamy virus, in which the Pol protein is expressed from a separately spliced mRNA and naturally incorporated into virus particles (Yu *et al.*, 1996).

Both Gag and Gag-Pol are co-translationally myristoylated at the amino terminus, which facilitates oligomerisation and trafficking to the plasma membrane (Gottlinger *et al.*, 1989; Bryant *et al.*, 1990; Pal *et al.*, 1990; Halwani *et al.*, 2003). Both the myristoylation signal and a conserved basic amino acid region within the MA domain of Gag and Gag-Pol facilitate interaction with the plasma membrane (Ono *et al.*, 1999; Ono *et al.*, 2000). In contrast, Env is trafficked through the host cell secretory pathway where it is cleaved to its mature components by host cell endoproteases.

Accessory proteins Nef, Vif and Vpr are actively packaged into the budding viral particle, whereas Rev Tat and Vpu are not (Turner *et al.*, 1999). Host cell proteins are also passively or actively packaged into the virion. For some of these proteins the mechanisms of packaging and role in HIV-1 replication is well defined, such as that for $tRNA^{Lys3}$. Novel roles for other host cell factors are currently being characterised, such as clathrin (Popov *et al.*, 2011; Zhang *et al.*, 2011) and for many others remains to be verified (Brass *et al.*, 2008).

1.5.2-2 Assembly and budding

Viral particle assembly at lipid microdomains or 'rafts' in the plasma membrane of T lymphocytes is well characterised (Lindwasser *et al.*, 2001; Ding *et al.*, 2003; Holm *et al.*, 2003). The location of viral assembly in macrophages has been under some debate since the description of HIV-1 particles budding into intracellular compartments in infected macrophages (Pelchen-Matthews *et al.*, 2003). This occurrence is also observed as a phenotype of HIV-1 trafficking mutants in T lymphocytes (Joshi *et al.*, 2009). However recent studies provide a new interpretation of the data that once again places assembly at the plasma membrane (Jouvenet *et al.*, 2006; Welsch *et al.*, 2007; Marsh *et al.*, 2009).

Multiple Gag/Gag, Gag/Gag-Pol and Gag/RNA interactions work in concert to facilitate particle assembly, which is assisted by host cell factors including trafficking factors and assembly chaperones (reviewed by Freed, 1998; Ganser-Pornillos *et al.*, 2008). However it is Gag multimerisation that drives particle assembly, and Gag alone can self assemble into virus like particles (VLPs) in the absence of other viral proteins (Gheysen *et al.*, 1989). Both unmyristoylated Gag and Gag-Pol can be incorporated into assembly complexes via Gag/Gag interactions with myristoylated Gag (Park *et al.*, 1992; Morikawa *et al.*, 1996). The envelope complex is incorporated by interaction between the gp41 cytoplasmic tail and MA domain of Gag (Freed, 1998). Hence mutations that prevent Gag myristoylation and misdirect Gag trafficking inhibit viral particle production (Gottlinger *et al.*, 1989; Bryant *et al.*, 1990; Facke *et al.*, 1993; Morikawa *et al.*, 1996).

Additional to Gag/Gag interactions, interactions between Gag and the RT domain have been implicated in recruiting Pol proteins to the assembly complex (Chiu *et al.*, 2002; Cen *et al.*, 2004b). More recently it as been demonstrated that the host cell factor, clathrin, may also facilitate the incorporation of Pol products into the budding virion (Popov *et al.*, 2011; Zhang *et al.*, 2011). It is suggested that multiple mechanism of Pol incorporation reflect its essential role in HIV-1 replication, including the those of the HIV-1 enzymes within the Pol precursor protein, as well as the role of specific regions within Pol in incorporation and annealing of the host derived tRNA for initiation of reverse transcription (Mak *et al.*, 1994; Mak *et al.*, 1997; Cen *et al.*, 2004a).

A range of enveloped viruses, including HIV, have been found to encode specific sequences that promote particle release, collectively referred to as 'late' (L) domains. These domains are recognised by host cell factors that are recruited to facilitate the late stages of viral budding. The HIV-1 late domain is located within Gag p6 (Gottlinger *et al.*, 1991; Huang *et al.*, 1995) and can interact with host cell factors TSG101 and ALIX (Garrus *et al.*, 2001; Martin-Serrano *et al.*, 2001; VerPlank *et al.*, 2001; Strack *et al.*, 2003). These proteins recruit host cell factors belonging to the endosomal sorting complex required for transport (ESCRT) pathway to facilitate viral budding (reviewed by Weiss *et al.*, 2011). More recently it has been proposed that the recruitment of ESCRT complexes may be essential for particle release in a temporal sense (Carlson *et al.*, 2008). Approximately 2000 Gag molecules form a virion (Turner *et al.*, 1999). Spatial calculations demonstrate that this forms an incomplete sphere in the context of the viral particle. Thus it is hypothesised that budding is completed in an ESCRT-dependent manner, rather than upon formation of a sphere induced by Gag multimerisation at the site of assembly (Briggs *et al.*, 2009).

1.5.2-3 HIV-1 particle maturation

The sequential and ordered processing of Gag (Pettit *et al.*, 1998; Cote *et al.*, 2001) and Gag-Pol (Lindhofer *et al.*, 1995; Pettit *et al.*, 2003) by the HIV-1 PR is critical for generation of an infectious viral particle (Kohl *et al.*, 1988). Maturation sets in motion a series of structural

rearrangements in which a non-infectious HIV-1 particle is transformed into infectious particles with the electron dense cone shaped core typical of HIV-1. Regulation of PR function is critical for production of mature viral particles (Section 1.9). Inhibition of PR activity, or premature PR activation results in non-infectious viral particles (Kaplan *et al.*, 1991; Krausslich, 1991; Louis *et al.*, 1999a).

The HIV-1 PR is formed by the symmetrical association of two subunits. As PR is expressed as part of the Gag-Pol precursor, PR activation within the precursor is dependent on Gag-Pol multimerisation. The spatial and steric constraints of dimerisation of the PR domain within Gag-Pol are thought to regulate PR activation (Navia *et al.*, 1990). The exact mechanisms remain undefined, however PR appears to be activated shortly before or during viral budding and PR mediated processing is complete in HIV-1 particles examined 10 seconds post release (Kaplan *et al.*, 1994). Recent research indicates that host cell factors may also have an essential role to play in regulating virion morphogenesis (Section 1.8) (Popov *et al.*, 2011; Zhang *et al.*, 2011).

1.5.3 Targets of antiretrovirals in HIV-1 replication

Six classes of ARV are now available that target five stages of viral replication, namely, co-receptor binding, entry, reverse transcription, integration and maturation.

1.5.3-1 Co-receptor binding

Interaction between the HIV-1 envelope protein and cellular co-receptors is essential for viral particle entry (Liu *et al.*, 1996; Samson *et al.*, 1996). Co-receptor antagonists block interaction of the HIV-1 envelope protein gp120 with the target cell co-receptor. Currently only the CCR5 antagonist, maraviroc, is approved for use in the treatment of HIV-1 infected individuals. As HIV-1 commonly uses either the CXCR4 or CCR5 molecules as co-receptors, use of maraviroc is limited to individuals harbouring R5 viruses, and further only to those who have access to co-receptor tropism testing. A second CCR5 antagonist, vicriviroc, is being evaluated, while CXCR4 agonists are in development (reviewed in Moore *et al.*, 2009).

1.5.3-2 HIV-1 entry

During viral particle entry the envelope glycoprotein gp41 undergoes conformational changes that facilitate fusion of the viral and target cell membranes. Two conserved heptad repeat units within gp41 form a six-helix bundle, which is an essential structural intermediate in the process of fusion (Weng *et al.*, 1998). The entry inhibitor T20 (enfurvitide) is a synthetic 36 amino acid peptide corresponding to the C-terminal heptad repeat unit. T20 acts by competitively binding and preventing formation of the six-helix bundle (Eggink *et al.*, 2010). T20 is the only peptidic inhibitor currently in use, and its delivery is limited to subcutaneous injection.

1.5.3-3 Reverse transcription

Of the six classes of ARV currently available, two classes target RT by independent mechanisms; the nucleoside/nucleotide reverse transcriptase inhibitors (NRTIs) and non-nucleoside reverse transcriptase inhibitors (NNRTIs). Together, RT inhibitors constitute greater than half of the ARV drugs available for treatment of HIV/AIDS (U.S. Department of Health and Human Services, 2009). NRTIs are nucleoside or nucleotide analogues that lack a 3'-hydroxyl group on the ribose. Incorporation into the nascent DNA chain during reverse transcription results in premature termination of the transcript (Goody *et al.*, 1991). However, NRTIs require intracellular conversion to their corresponding triphosphate forms by host-cell enzymes before being able to compete against the natural dNTP substrate. NRTIs can result in undesirable levels of toxicity due to their incorporation by cellular polymerases.

In contrast, NNRTIs are non-competitive, allosteric inhibitors of the HIV-1 RT. The first NNRTIs were identified by screening of compound libraries for antiviral activity, whereas second generation NNRTIs have been developed with the aid of structural data and molecular modelling (reviewed in Campiani *et al.*, 2002). NNRTIs bind to an induced fit pocket in the p66 polymerase domain referred to as the NNRTI binding pocket (NNBP). NNRTI binding induces local and global distortions in RT structure that prevents RT polymerase activity (reviewed by Balzarini, 2004). Interestingly, inhibitory effects on HIV-1 maturation have been described for some NNRTIs, however it is unknown whether this affect contributes to the inhibition of HIV-1 replication *in vivo* (Figueiredo *et al.*, 2006) (Section 1.8). NNRTIs are highly specific for HIV-1 RT, do not require intracellular metabolism and generally confer less cytotoxicity than NRTIs, however also more readily result in the selection of drug resistant HIV-1 (Davey *et al.*, 1993; Saag *et al.*, 1993; Richman *et al.*, 1994).

1.5.3-4 Integration

The IN inhibitor raltegravir prevents integration of the reverse transcribed viral DNA into the host cell chromosome, an event that is essential for the establishment of a productive HIV-1 infection. Raltegravir binds to the IN active site to inhibit strand transfer of the proviral DNA precursor to the host DNA (Espeseth *et al.*, 2000; Hazuda *et al.*, 2000).

1.5.3-5 Maturation

The development of PIs was the first success for structure informed design of HIV-1 ARV drugs. Protease inhibitors specifically target the PR active site, and bind with high specificity and affinity (Wlodawer *et al.*, 1998). Protease inhibitors act during the late phase of viral replication, preventing PR mediated virion maturation and the production of infectious virions by infected cells.

1.6 Reverse transcriptase structure and function

1.6.1 Composition of lentiviral RTs

Retroviral RTs vary in composition, however subunit dimerisation appears to be a common prerequisite for activity. For example, avian sarcoma leucosis virus contains three enzymatically active RT isoforms that are monomeric, homodimeric and heterodimeric (reviewed by Hizi *et al.*, 2008). In contrast moloney murine leukaemia virus (MMLV) RT is monomeric in solution (Roth *et al.*, 1985) but dimerises in the presence of template/primer (T/P) (Telesnitsky *et al.*, 1993). The generation of a heterodimeric RT via an internal cleavage appears to be peculiar to lentiviruses, and is observed for the primate lentiviruses and the non-primate lentiviruses feline immunodeficiency virus (FIV), equine infectious anaemia virus (EIAV), and bovine immunodeficiency virus (BIV) (reviewed by Hizi *et al.*, 2008).

The HIV-1 RT heterodimer consists of a p66 and a p51 subunit, named for their molecular weight of 66 and 51 kDa, respectively. The p66 subunit is the full-length product of the RT coding region; a 560 amino acid protein with an N terminal polymerase (aa 1-440) and C terminal RNase H domain (aa 441-560) (Telesnitsky *et al.*, 1997). The p51 subunit consists of the polymerase domain only (Fig. 1.5A), and is generated by HIV-1 PR mediated cleavage between the polymerase and RNase H domains (F440/Y441) (Mizrahi *et al.*, 1989). While both p66 and p51 can form homodimers, the heterodimer is the most stable configuration (Venezia *et al.*, 2006) and is the dominant species in virions (di Marzo Veronese *et al.*, 1986) and infected cells (Lightfoote *et al.*, 1986). RT heterodimer formation can occur upon expression of recombinant p66 in *E.coli* following cleavage by cellular proteases (Hizi *et al.*, 1988; Lowe *et al.*, 1988), or by co-expressed HIV-1 PR (Mizrahi *et al.*, 1989; Tachedjian *et al.*, 2000), or upon co-expression of both the p66 and p51 subunits (Muller *et al.*, 1989). However, neither the immediate precursor of the mature RT heterodimer, nor the Gag-Pol processing events that lead to the generation of the RT heterodimer have been comprehensively described.

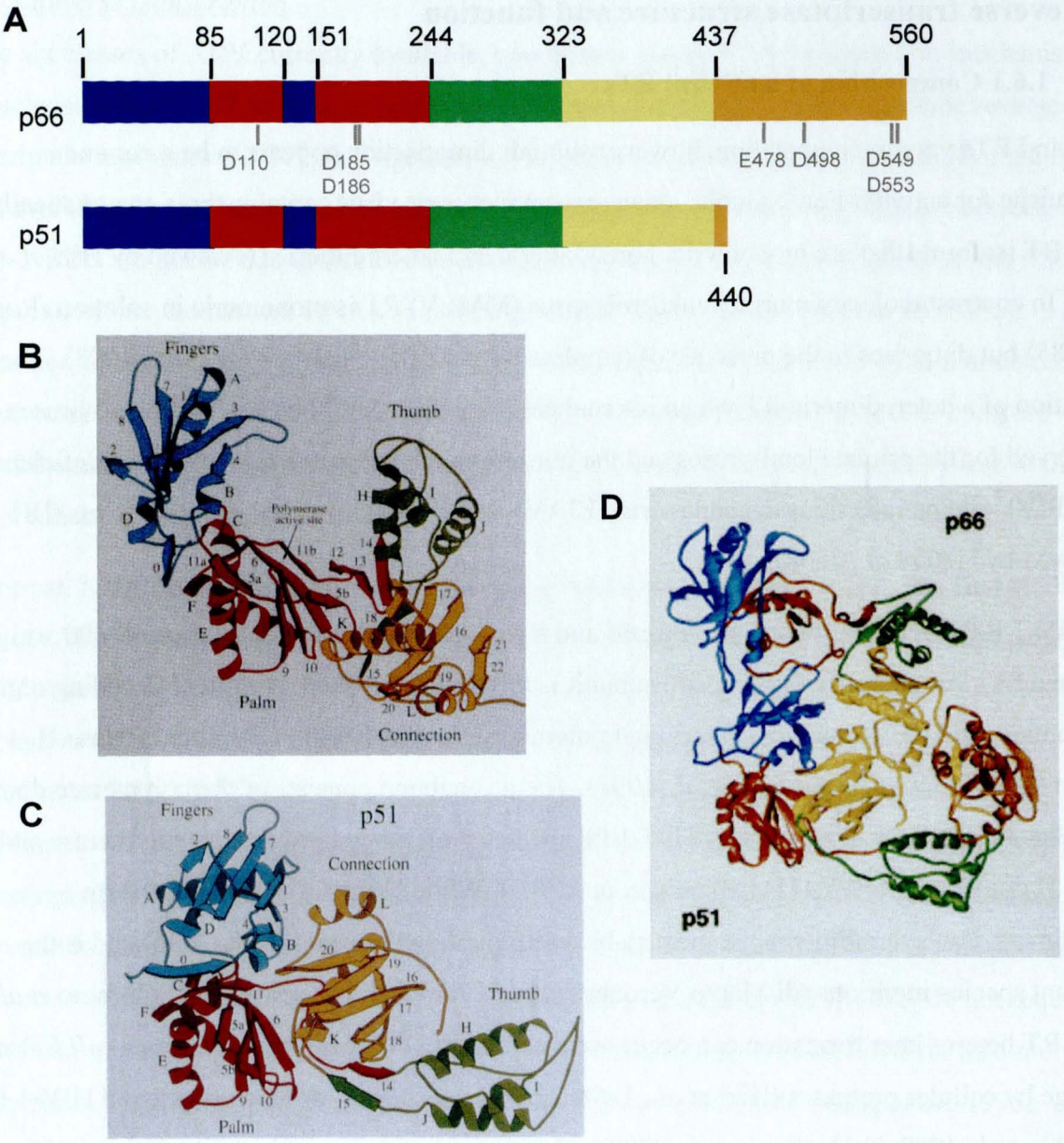

Figure 1.5. Structure of the RT heterodimer.

The p66 and p51 subunits share identical polymerase domains that fold into spatially distinct subdomains. The boundaries of the RT polymerase subdomains and RNase H domain in (A) are taken from the unliganded RT structure described by Rodgers and colleagues (1995) with the fingers subdomain coloured blue (residues 1–84, 120–150), palm subdomain coloured red (86–119, 151–243), thumb subdomain coloured green (244–322), connection subdomain coloured yellow (323–437), and the RNase H domain coloured orange (438–560). The polymerase and RNase H active site residues are indicated. Despite similar organisation of the secondary structural elements in the polymerase subdomains, the contrasting organisation of the subdomains between the p66 (B) and p51 (C) subunits result in the asymmetry of the heterodimer (D). This is predominantly facilitated by the connection subdomain, which in the p66 subunit is located between the polymerase and RNase H domains, whereas in the p51 subunit it is sandwiched between the fingers, palm and thumb subdomains, burying the polymerase active site. Images B, C and D were reproduced from Jacobo-Molina *et al.*, (1993).

1.6.2 HIV-1 RT structure

The RT crystal structure has been determined in a number of configurations, including the unliganded enzyme (Rodgers *et al.*, 1995; Hsiou *et al.*, 1996), inhibitor bound (Kohlstaedt *et al.*, 1992), complexed with DNA:DNA or RNA:DNA T/P (Jacobo-Molina *et al.*, 1993; Ding *et al.*, 1998; Sarafianos *et al.*, 2001), and as a stalled catalytic complex with bound T/P and dNTP (Huang *et al.*, 1998). Structural studies have revealed the asymmetric nature of the heterodimer, location of the NNRTI binding site, and provided insight into the dynamic nature of the enzyme. Structural studies continue to be important tools for elucidation of mechanisms of drug resistance and rational drug design (Ren *et al.*, 2001; Hopkins *et al.*, 2004; Bauman *et al.*, 2008).

The first high resolution crystal structure described was of the HIV-1 RT complexed with the NNRTI nevirapine (Kohlstaedt *et al.*, 1992). The authors observed the similarity between the tertiary structure of the p66 polymerase domain and that of the *E.coli* Klenow fragment, whose structure had been anthropomorphically likened to that of a right hand (Ollis *et al.*, 1985). Thus the nomenclature was extended to the HIV-1 RT with polymerase subdomains designated as fingers, palm, and thumb, with the connection subdomain linking the polymerase and RNase H domains (Fig. 1.5). Kohlstaedt and colleagues (1992) assigned the nomenclature for the secondary structure elements, identifying each α-helix alphabetically and β-strand numerically. Jacobo-Molina and colleagues (1993) further defined the location of these structural elements in the primary sequence. This nomenclature is conserved in subsequently published structures, however the boundaries of secondary structure elements vary depending on the structure analysed (Jacobo-Molina *et al.*, 1993; Ren *et al.*, 1995; Rodgers *et al.*, 1995).

One of the most intriguing revelations upon resolution of the RT structure was the asymmetric nature of the heterodimer. While the p66 and p51 polymerase domains are identical in amino acid composition and share highly similar folding of the secondary structure elements into subdomains, the spatial arrangement of the subdomains is radically different between the subunits (Fig. 1.5 B and C). The p66 subunit assumes an 'open' catalytically competent conformation. The fingers and thumb subdomains form a nucleic acid binding cleft with the polymerase active site located at the base of the cleft in the palm subdomain.

In contrast the p51 subunit assumes a 'closed' catalytically inactive conformation in which the connection subdomain is folded on top of the palm between the fingers and thumb, burying the polymerase active site within the subunit. Subunit-selective mutagenesis of the polymerase active site residues in the p66 subunit confirmed that the p51 subunit is catalytically inactive (Le Grice *et al.*, 1991; Hostomsky *et al.*, 1992). Consequently in the RT heterodimer all enzymatic activity is conferred by the p66 subunit.

However, subunit interaction is essential for efficient reverse transcription, and ongoing investigations continue to reveal more on the interactions that facilitate the dynamic activities of the heterodimer (Abbondanzieri *et al.*, 2008; Venezia *et al.*, 2009; Zheng *et al.*, 2010).

As the RT heterodimer is intrinsically asymmetric, so is the dimer interface (Wang *et al.*, 1994) (Fig. 1.6). Residues that contribute to the heterodimer interface in the p66 subunit are distinct from residues that contribute to the interface in the p51 subunit, with the exception of a unique region in the connection subdomain (Section 1.6.2-3). The residues buried at the heterodimer interface upon dimerisation are predominantly hydrophobic and generally well conserved across the available crystals structures. Three major points of interaction occur between the p66 palm (D86-L92) and the p51 fingers (P52-P55 and I135-P140), the RNase H domain (P537–E546) and the p51 thumb (C280–E291) and the connection subdomains from both p66 (W401-W410) and p51 (P392-W401) (Srivastava *et al.*, 2006).

1.6.2-1 The p66 subunit

The p66 subunit is comprised of the N terminal polymerase domain (residues 1-440) and C-terminal RNase H domain (residues 441-560). The open, catalytically competent conformation of the p66 polymerase domain corresponds with its substantial flexibility. The two most mobile elements of p66 are the thumb and fingers subdomains. Molecular dynamics studies indicate that the motion of these subdomains is coupled, moving from the same hinge region (Bahar *et al.*, 1999). In unliganded RT, the p66 thumb lies across the palm, partially occluding the nucleic acid binding cleft (Rodgers *et al.*, 1995; Hsiou *et al.*, 1996). In the presence of nucleic acid, the p66 thumb rotates out and away from the nucleic acid binding cleft, while the fingers and palm of both p66 and p51 move to accommodate the T/P (Rodgers *et al.*, 1995; Hsiou *et al.*, 1996) (Fig. 1.5B).

The nucleic acid binding cleft is configured so that bound nucleic acid is positioned at both the polymerase and the RNase H active sites. Approximately 60 Å separates the polymerase and RNase H active sites, which accommodates approximately 17 bp of a bound a DNA/DNA substrate and 18 bp for an RNA/DNA hybrid (Jacobo-Molina *et al.*, 1993; Ding *et al.*, 1998; Sarafianos *et al.*, 2001). The T/P adopts a bend of approximately 40° (Jacobo-Molina *et al.*, 1993; Ding *et al.*, 1998) which facilitates an A-DNA helical structure at the region of the polymerase active site and B-DNA helical structure at the RNase H active site (Huang *et al.*, 1998). Such distortion is typical of nucleic acids bound to a polymerase and is important for polymerase activity (reviewed by Turner *et al.*, 1999). The nucleic-acid binding cleft is primarily composed of residues from the p66 fingers, palm and thumb. Residues from RNase H, the connection subdomain of both subunits, and the p51 thumb subdomain also contribute (Arnold *et al.*, 1992; Kohlstaedt *et al.*, 1992; Jacobo-Molina *et al.*, 1993; Ding *et al.*, 1998).

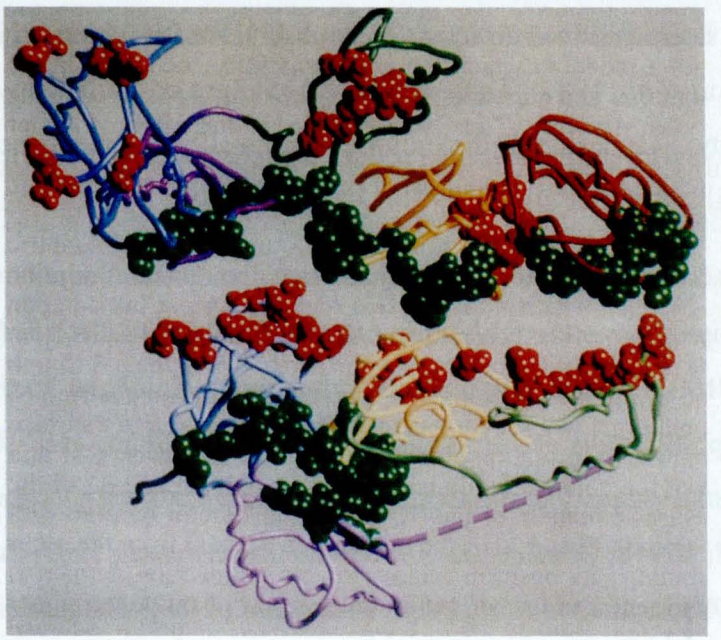

Figure 1.6. Asymmetric nature of the RT heterodimer interface.
Representation of the RT heterodimer with the polymerase subdomains, -fingers, thumb, palm and connection, coloured blue, green, purple and yellow respectively. The RNase H domain is coloured orange. Residues that form the heterodimer interface are indicated in space-fill representation in each subunit. Residues that form the p66 interface are coloured green, and the p51 interface coloured red. This highlights the asymmetry of residues in the heterodimer. Image reproduced from Wang *et al.*, (1994).

Residues from the αI and αH helices of the p66 thumb interact with both template and primer strands to position the T/P at the polymerase active site (Arts *et al.*, 1998; Huang *et al.*, 1998), which is located within the heart of the p66 palm. The polymerase catalytic triad is formed by amino acids D110, D185 and D186, which are contributed by the β6-β10-β9 β-sheet (Larder *et al.*, 1987). The D185 and D186 residues form part of the YXDD motif which is highly conserved across retroviral RTs (Johnson *et al.*, 1986). These active site residues co-ordinate two divalent cations that are required for activity. Magnesium is the preferred cation although manganese and other divalent cations can also be utilised (Filler *et al.*, 1997).

Adjacent to the polymerase active site is a structural motif known as the polymerase primer grip. The primer grip is a highly conserved β-hairpin motif (β12-β13, aa 227-235) (Xiong *et al.*, 1990; Jacobo-Molina *et al.*, 1993) which plays a crucial role in maintaining the 3' end of the primer strand in position for nucleophilic attack at the polymerase active site (Huang *et al.*, 1998). Because of its role in positioning the T/P, mutation of the primer grip can affect both polymerase and RNase H activity (Jacques *et al.*, 1994b; Ghosh *et al.*, 1996; Palaniappan *et al.*, 1997; Powell *et al.*, 1997; Wisniewski *et al.*, 1999; Sarafianos *et al.*, 2001; Julias *et al.*, 2002).The nucleic-acid binding cleft is primarily composed of residues from the p66 fingers, palm and thumb. Residues from RNase H, the connection subdomain of both subunits, and the p51 thumb subdomain also contribute (Arnold *et al.*, 1992; Kohlstaedt *et al.*, 1992; Jacobo-Molina *et al.*, 1993; Ding *et al.*, 1998).

The RNase H domain of the p66 subunit is spatially distinct from the polymerase domain. The domain is comprised of a five stranded mixed β-sheet surrounded by four α-helices (Davies *et al.*, 1991). The HIV-1 RNase H shares structural similarities with ribonucleases isolated from other organisms including MLV RT, *E.coli* and humans, despite low amino acid similarity (reviewed by Schultz *et al.*, 2008). The RNase H active site comprises four acidic amino acid residues D443, E478, D498, D549 (Davies *et al.*, 1991) which coordinate two divalent cations essential for catalytic activity (De Vivo *et al.*, 2008). The crystal structure of RNase H has been determined as part of the RT heterodimer (Kohlstaedt *et al.*, 1992) and as the free RNase H (Davies *et al.*, 1991). The structure is highly similar in both contexts (reviewed by Klumpp *et al.*, 2006). Correspondingly, intrinsic activity of recombinant RNase H has been described and is not dependent on expression as part of RT (Hang *et al.*, 2004). However RNase H activity of the HIV-1 RT is limited by the low affinity of the RNase H domain for nucleic acid substrates, as the majority of nucleic acid interactions are located in the polymerase domain (Smith *et al.*, 1993, and reviewed by Klumpp *et al.*, 2006).

The RNase H primer grip is a region adjacent to the RNase H active site that interacts with nucleotides in the primer strand of the bound T/P, upstream of the RNase H active site (Sarafianos

et al., 2001). Unlike the polymerase primer grip, the RNase H primer grip is not a distinct structural motif but consists of multiple residues from the RNase H domain and connection subdomain of both RT subunits (Sarafianos *et al.*, 2001). Mutation of the RNase H primer grip can influence both RNase H and polymerase activity, although not to the degree of mutations in the polymerase primer grip (Arion *et al.*, 2002; Julias *et al.*, 2002; Rausch *et al.*, 2002; McWilliams *et al.*, 2006).

1.6.2-2 The p51 subunit

In contrast to the p66 subunit, the p51 subunit assumes a closed, catalytically inactive conformation (Kohlstaedt *et al.*, 1992) that is essentially rigid (Bahar *et al.*, 1999). Compared to p66, the fingers are closer to the palm, and the thumb has moved away from the palm (Fig. 1.5). The connection subdomain is sandwiched between the fingers, palm and thumb, obscuring the equivalent nucleic acid binding cleft and burying the polymerase active site compared to p66 (Kohlstaedt *et al.*, 1992; Jacobo-Molina *et al.*, 1993; Ding *et al.*, 1998; Huang *et al.*, 1998). Within the subdomains, the organisation of the secondary structure elements into subdomains is highly similar between the subunits, excluding secondary structures αL-β20-β21. This is proposed to facilitate the contrasting position of the connection subdomain between the subunits (Wang *et al.*, 1994).

Although the p51 subunit does not directly contribute to RT enzymatic activity, the essential role of p51 is well documented. Multiple studies demonstrate that RT activity is confined to dimeric species and monomers are devoid of polymerase activity (Restle *et al.*, 1990; Goel *et al.*, 1993; Jacques *et al.*, 1994a; Wohrl *et al.*, 1997; Sluis-Cremer *et al.*, 2000; Tachedjian *et al.*, 2000; Pandey *et al.*, 2001; Tachedjian *et al.*, 2005b). The p51 subunit is suggested to perform a structural role in the heterodimer, maintaining the catalytic competent conformation of the p66 subunit. However analysis of chimeric RT heterodimers revealed that certain aspects of the heterodimer are conferred by p51 rather than the p66 subunit, such as heterodimer stability, NNRTI susceptibility and aspects of enzyme activity (Amacker *et al.*, 1998; Menendez-Arias *et al.*, 2001). Other studies also indicate that the p51 subunit is essential for interaction with the T/P (Divita *et al.*, 1993; Harris *et al.*, 1998; Pandey *et al.*, 2001), the host derived $tRNA^{Lys}$ primer (Jacques *et al.*, 1994a) and initiation of reverse transcription (Arts *et al.*, 1996).

1.6.2-3 The RT tryptophan repeat motif

An integral region to this study is the RT tryptophan repeat motif (TRM). The motif was first described by Baillon and colleagues (1991) and consists of a cluster of six tryptophans located at RT codons 398, 401, 402, 406, 410 and 414, and a tyrosine at codon 405 (Baillon *et al.*, 1991). The motif is highly conserved across primate lentiviral RTs, but not in non-primate lentiviral RTs (Figure. 1.7A). The TRM residues are housed within α-helix L (αL), β-strand 20 (β20) and the loop linking these secondary structures (Fig. 1.7 B and C) in the connection subdomain.

A

	395	396	397	398	399	400	401	402	403	404	405	406	407	408	409	410	411	412			413	414	415	416	Acc. No.
HIV-1 consensus M-group	K	E	T	W	E	T	W	W	T	E	Y	W	Q	A	T	W	I	P	-	-	E	W	E	F	
HIV-1 N YBF106	K	E	V	W	E	T	W	W	T	E	H	W	Q	A	T	W	I	P	-	-	E	W	E	F	Q9IDV9
HIV-1 N YBF30	K	E	V	W	E	A	W	W	T	D	H	W	Q	A	T	W	I	P	-	-	E	W	E	F	O91080
HIV-1 O ANT	R	E	T	W	E	T	W	W	A	D	Y	W	Q	A	T	W	I	P	-	-	E	W	E	F	Q77373
HIV-1 O MVP5180	R	E	T	W	E	T	W	W	A	E	Y	W	Q	A	T	W	I	P	-	-	E	W	E	F	Q79666
HIV-2 BEN	R	E	T	W	E	Q	W	W	D	N	Y	W	Q	V	T	W	I	P	-	-	E	W	D	F	P18096
HIV-2 ROD	R	E	I	W	E	Q	W	W	D	N	Y	W	Q	V	T	W	I	P	-	-	D	W	D	F	P04584
HIV-2 EHO	R	E	T	W	D	Q	W	W	T	D	Y	W	Q	V	T	W	I	P	-	-	E	W	D	F	Q89928
HIV-2 UC1	R	E	T	W	D	Q	W	W	T	D	Y	W	Q	V	T	W	I	P	-	-	E	W	D	F	Q76634
SIVagm155	R	D	T	W	E	Q	W	W	A	D	Y	W	Q	V	S	W	I	P	-	-	E	W	D	F	P27973
SIVagm3	R	E	V	W	E	Q	W	W	A	D	Y	W	Q	V	S	W	I	P	-	-	D	W	E	F	P27980
SIVagm TYO1	R	E	V	W	E	Q	W	W	A	D	Y	W	Q	V	S	W	I	P	-	-	E	W	D	F	P05895
SIVcpz EK505	K	E	V	W	E	T	W	W	T	E	Y	E	Q	A	T	W	I	P	-	-	D	W	E	F	Q1A249
SIVcpz MB66	K	E	T	W	E	A	W	W	T	D	Y	W	Q	A	T	W	I	P	-	-	E	W	E	Y	Q1A267
SIVcpz TAN1	K	E	T	W	S	Q	W	W	T	D	Y	W	Q	V	T	W	V	P	-	-	E	W	E	F	Q8AII1
SIVmac 17E-Cl	K	D	V	W	E	Q	W	W	T	D	Y	W	Q	V	T	W	I	P	-	-	E	W	D	F	AAK64203
SIVmac 17E-Fr	K	D	V	W	E	Q	W	W	T	D	Y	W	Q	V	T	W	I	P	-	-	E	W	D	F	AAK64194
SIVmac K6W	R	D	V	W	E	Q	W	W	T	D	Y	W	Q	V	T	W	I	P	-	-	-	W	D	F	P05897
SIVmac Mm142-83	K	D	V	W	E	Q	W	W	T	D	Y	W	Q	V	T	W	I	P	-	-	E	W	D	F	P05896
SIVmnd GB1	R	E	I	W	E	D	W	W	H	E	Y	W	Q	C	T	W	I	P	-	-	E	V	E	F	P22382
SIVmnd-2	R	E	V	W	D	Q	W	W	P	E	Y	W	Q	A	T	W	I	P	-	-	E	W	E	F	NP_758887
SIVmon	K	E	Q	W	D	T	W	W	A	D	N	W	Q	V	T	W	I	P	-	-	E	I	E	P	CAD70671
SIVolc	R	K	D	W	E	A	W	A	F	D	D	W	Q	V	H	W	I	P	-	-	D	I	E	F	CAQ60125
SIVsm F236/smH4	R	E	I	W	E	Q	W	W	T	D	Y	W	Q	V	T	W	I	P	-	-	D	W	D	F	P12502
SIVsm PBj14/BCL-3	R	E	I	W	E	Q	W	W	T	D	Y	W	Q	V	T	W	I	P	-	-	E	W	D	F	P19505
SIVwrc	K	D	I	W	D	M	W	W	S	E	Y	W	Q	A	T	W	I	P	-	-	E	V	E	H	CAP72504
SIVqu	Q	E	Q	W	N	T	W	W	A	E	H	W	Q	A	N	W	I	P	-	-	E	V	K	A	CAD83157
BIV	S	E	D	W	E	A	A	L	Q	K	E	E	S	L	T	Q	I	F	P	-	-	-	-	-	AAA91271
CAEV	E	E	D	W	R	L	E	L	Q	L	G	N	-	I	T	W	M	P	-	-	K	F	W	S	AAA91826
FIV	R	E	A	W	E	S	N	L	I	N	S	P	-	Y	L	K	A	P	P	P	E	V	E	Y	AAB59937
EAIV	K	E	R	V	K	W	E	M	E	K	G	W	Y	Y	S	W	L	P	-	-	E	I	V	Y	AAB59862

B

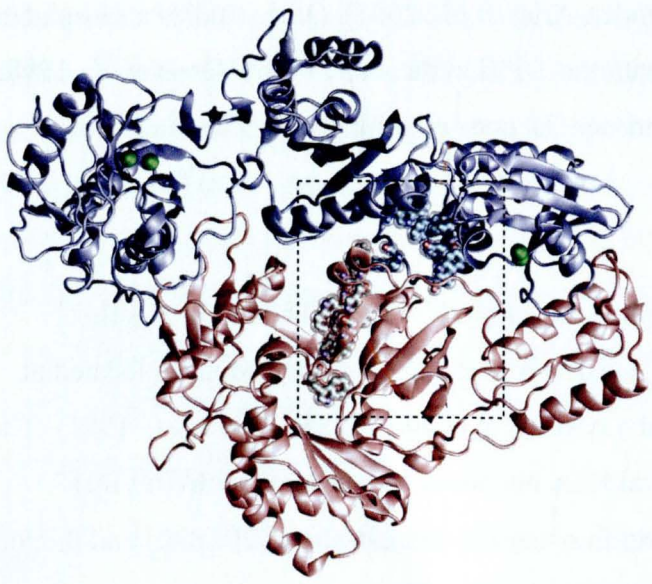

C

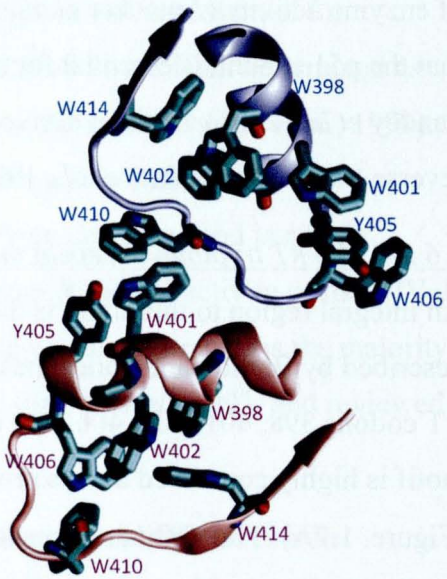

Figure 1.7 Conservation and location of the RT tryptophan repeat motif.
(A) RT or Pol sequences from representative strains of lentiviruses were aligned using the ClustalW2 multiple sequence alignment program (Chenna *et al.*, 2003). The alignment displays RT residues 395-416 in reference to the HIV-1 M group consensus sequence from the Los Alamos HIV sequence database (2008b). (B) Ribbon diagram of the RT heterodimer with the p66 subunit coloured blue, and p51 subunit in pink, and polymerase and RNase H active site cations in green. The region of the heterodimer harbouring the TRM is boxed and the side-chains of TRM amino acids are displayed in a ball and stick model. A detail of this region is shown in (C). Figures (B) and (C) are based on the stalled catalytic complex RT crystal structure (PDB ID 1RTD, Huang *et al.*, 1998). (B) and (C) were created by M. Kuiper at the Victorian Partnership for Advance Computing using the Visual Molecular Dynamics (VMD) program and rendered using POV-Ray (http://www.povray.org).

Interestingly this is a region where the organisation of the secondary structures within the connection subdomain differs between the two subunits. This is proposed to allow the radically different position of the connection subdomain assumed in the two subunits (Wang *et al.*, 1994). However this also facilitates another unique feature of the TRM in the asymmetric heterodimer; TRM residues from both subunits contribute to the RT heterodimer interface (Wang *et al.*, 1994; Tachedjian *et al.*, 2003; Mulky *et al.*, 2005b). The TRM was identified as an important region for RT subunit heterodimerisation and stability in early studies (Becerra *et al.*, 1991; Divita *et al.*, 1995a), which was later confirmed by mutagenic analysis (Tachedjian, 2003; Mulky *et al.*, 2005b).

1.6.3 Molecular mechanisms of RT activity

1.6.3-1 Polymerisation

The mechanism of DNA polymerisation is reasonably well understood due to extensive biochemical and crystallographic data, as well as homology with other polymerases (Das *et al.*, 2004; Gotte, 2006; Cote *et al.*, 2008; Sarafianos *et al.*, 2009). In most contexts, RT preferentially binds the T/P so that the 3' end of the primer strand is located at the priming site (P site), adjacent to the polymerase active site. An incoming dNTP is bound at the nucleotide-binding site (N site) to form the ternary catalytic complex (Huang *et al.*, 1998). The rate-limiting step in the polymerisation reaction is the conformational change in the p66 fingers subdomain in which the fingers close down upon the incoming dNTP. The β3–β4 loop of the 'fingertips' align the 3' hydroxyl group of the primer, the α-phosphate of the dNTP, and the polymerase active site (Huang *et al.*, 1998). Hence the integrity of the β3–β4 loop influences many aspects of polymerase activity including fidelity, processivity and strand displacement synthesis (Garforth *et al.*, 2007).

The two divalent cations of the polymerase active site coordinate phosphodiester bond formation between the primer strand and nucleotide. The active site cations are also suspected to have a role in release of the concomitantly generated pyrophosphate from the active site as the fingers return to their original position. The extended T/P is then translocated in order to vacate the N site allowing another nucleotide to bind and repeat the cycle. Recent crystal structures of RT in pre- and post-translocation states have added to our understanding of this process (Sarafianos *et al.*, 2002 and reviewed by Gotte, 2006).

1.6.3-2 RNase H activity

RNase H is a non-specific nuclease that hydrolyses the phosphodiester bonds of RNA in an RNA:DNA duplex (Schatz *et al.*, 1990). RNase H differs from that of conventional ribonucleases in that cleavage produces a 3'-hydroxyl and 5'-phosphate terminated product. This property of the enzyme is central to its role in reverse transcription, as the 3'-hydroxyl of oligoribonucleotides formed by RNase H cleavage subsequently act to prime polymerisation (Telesnitsky *et al.*, 1997).

RNase H is known to employ a two-ion mechanism of RNA cleavage, however the details are yet to the elucidated. This is an area of active research employing high-resolution structural studies and molecular dynamics (Klumpp *et al.*, 2003; De Vivo *et al.*, 2008).

RNase H activity can be polymerase dependent or independent (reviewed by Klumpp *et al.*, 2006; Schultz *et al.*, 2008). In polymerisation-dependent RNase H activity the 3' terminus of the nascent DNA strand at the polymerase active site positions the RNA template strand 17–19 nucleotides downstream at the RNase H active site (Furfine *et al.*, 1991; Gopalakrishnan *et al.*, 1992). Polymerisation-dependent RNase H activity initiates the degradation of the RNA genome. As RNA hydrolysis occurs at a slower rate relative to polymerisation, RNA fragments remain bound to the newly synthesised DNA (DeStefano *et al.*, 1991; Kati *et al.*, 1992). These fragments are subsequently cleaved into smaller fragments by polymerisation-independent RNase H activity (Wisniewski *et al.*, 2000b; Wisniewski *et al.*, 2000a). It is polymerisation-independent RNase H cleavage events that generate the RNA PPT primer for plus strand synthesis, and removes the tRNA primer from the nascent DNA to define the end of the proviral DNA that is the substrate for integration (Gopalakrishnan *et al.*, 1992; Peliska *et al.*, 1992; Telesnitsky *et al.*, 1997).

The RNase H active site does not recognise specific RNA sequences, rather cleavage is regulated by positioning of the substrate at the active site by the RNase H primer grip, and the width of the minor groove of the substrate (reviewed by Sarafianos *et al.*, 2009). The PPT RNA resists RNase H degradation due to the composition of the RNA resulting in an atypical narrow minor groove structure compared to typical RNA-DNA substrates. This places the RNA strand outside of the RNase H active site (Sarafianos *et al.*, 2001).

1.6.3-3 Coordination of enzymatic activities

Using fluorescence resonance energy transfer (FRET) to observe the interaction of a single RT molecule with a labelled T/P, Abbondanzieri and colleagues (2008) defined factors which influence whether RT interacts with the T/P in either of two orientations; placing the 3' end of the primer strand at the polymerase active site for primer extension, or at the RNase H active site, preventing polymerisation. The primary determinant is the composition of the sugar backbone of the T/P at the polymerase and RNase H primer grip regions. Typically, RT binds to DNA primed with a DNA oligonucleotide in the polymerisation mode, while DNA primed with RNA oligonucleotide binds so that primer extension is not possible. Remarkably, on duplexes containing the unique PPT RNA primer, RT is observed to rapidly switch or 'flip' between orientations. The rate of flipping is influenced by the local concentration of dNTPs, and the presence of NNRTIs (Abbondanzieri *et al.*, 2008). NNRTIs and dNTPs have opposite effects on the structural dynamics of the p66 fingers and thumb subdomains in the heterodimer (Huang *et al.*, 1998). Whereas dNTPs bring the fingers and thumb regions closer together to form a clamp on the T/P, NNRTIs induce separation of the

subdomains. Thus Abbondanzieri and colleagues (2008) propose that the ability of RT to switch orientation on the substrate is the result of the relaxation of the fingers and thumb, allowing reorganization of the RT-T/P complex without dissociation.

1.6.4 NNRTI binding and its effects on RT structure and activity

The NNBP does not exist in the free RT structure. Rather, the repositioning of amino acid side-chains upon NNRTI interaction forms the NNBP. The pocket is located between β-sheets that contribute to the polymerase active site (β6-β10-β9) and the polymerase primer grip (β12-β13-β14), approximately 10 Å from the polymerase active (Kohlstaedt *et al.*, 1992) (Fig. 1.8A). Residues from the p66 palm and thumb subdomains form the pocket, while residues from the p51 fingers subdomain also contribute. The side-chains that line the pocket are predominately aromatic or hydrophobic, with some charged residues (Smerdon *et al.*, 1994; Ding *et al.*, 1995; Das *et al.*, 2008) (Fig. 1.8B). A solvent accessible entrance to the pocket is located at the heterodimer interface (Rodgers *et al.*, 1995; Hsiou *et al.*, 1996).

NNRTI binding induces both local and global distortions that inhibit polymerase activity (reviewed by Balzarini, 2004; Sluis-Cremer *et al.*, 2004b; Sluis-Cremer *et al.*, 2008). The most significant structural change upon NNRTI binding is rotation of the p66 thumb away from the fingers, resulting in a hyper-extended conformation (Fig. 1.8C) (Kohlstaedt *et al.*, 1992; Ding *et al.*, 1995; Ren *et al.*, 1995; Rodgers *et al.*, 1995). Molecular modelling suggests this distortion is due to interference with the hinge region that controls the cooperative motions of the fingers and thumb domains (Temiz *et al.*, 2002). NNRTI binding also induces rotation of the β12-β13-β14 sheet, distorting the position of the primer grip (Rodgers *et al.*, 1995; Hsiou *et al.*, 1996), and the relative position of the β9-β10 loop that contains the YXDD motif of the polymerase active site. This is suggested to affect the geometry of the active site and adversely affect translocation of the T/P during polymerisation (Esnouf *et al.*, 1995; Das *et al.*, 2007). Minor conformational changes are also observed to occur in the p66 connection subdomain and RNase H domain, as well the p51 subunit (reviewed by Sluis-Cremer *et al.*, 2004b).

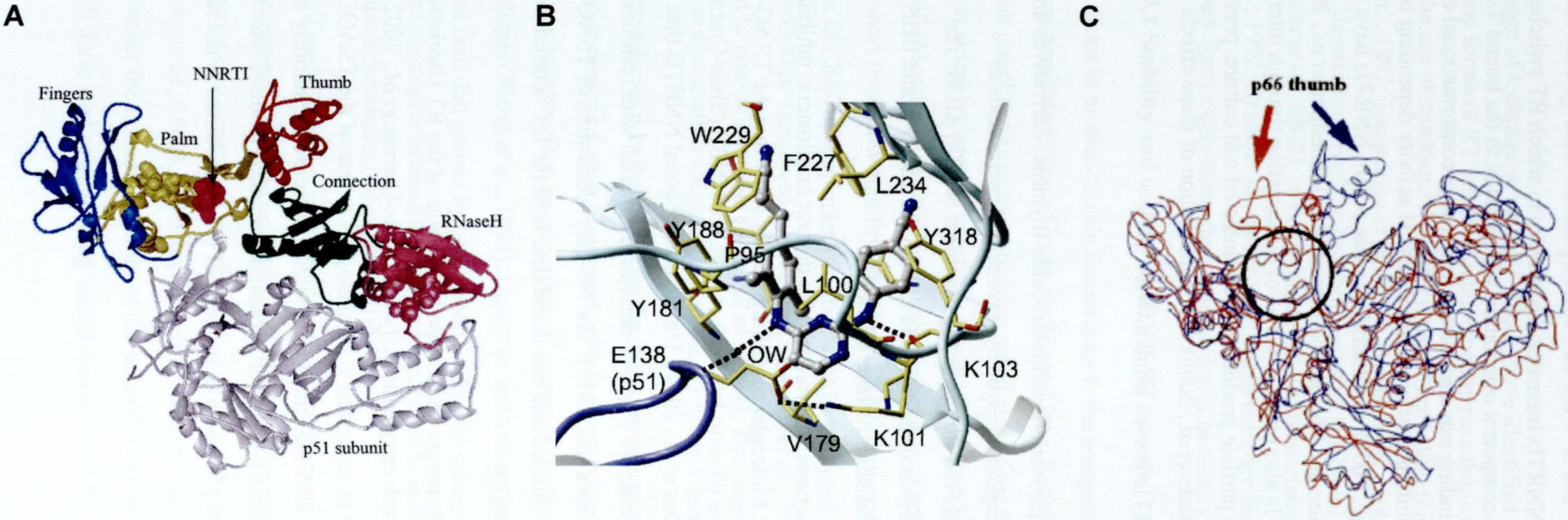

Figure 1.8. Location of the NNBP and conformational changes to the RT heterodimer upon NNRTI binding.

(A) Ribbon diagram of the RT heterodimer with the p66 fingers, palm, thumb, connection subdomains coloured blue, yellow, red and green with the RNase H domain coloured magenta and the p51 subunit in grey. The polymerase and RNase H active sites are shown in space-fill representation. The NNRTI nevirapine is shown in pink space-fill at the NNBP. Residues from the p66 palm, thumb and p51 fingers contribute to the NNBP. (B) The NNBP is formed by repositioning the side-chains (yellow), shown here interacting with the NNRTI TMC278. NNRTI binding induces long and short-range conformational changes in RT structure. (C) The unliganded (red) and NNRTI bound RT (blue) structures are superimposed, displaying the hyper-extended conformation of the p66 thumb. The position of the β6-β10-β9 and β12-β13-β14 sheets (circled), which harbour the polymerase active site and primer grip, is also affected by NNRTI binding. (A) Image reproduced from Sluis-Cremer *et al.*, 2004b, (B) from Das *et al.*, 2008, and (C) from Hsiou *et al.*, 1996.

Additional to the inhibitory effects on polymerisation, NNRTIs have been found to affect other aspect of RT activity. The presence of NNRTIs increases the kinetics in which RT switches from a polymerase-competent to the RNase H-competent orientation with regards to the bound T/P (Abbondanzieri *et al.*, 2008). NNRTI binding can also induce long-range conformational changes that affect RNase H activity, either inhibiting or stimulating RNase H activity depending on the composition of the substrate (Hang *et al.*, 2007). Additionally, some potent NNRTIs have been found to enhance RT subunit dimerisation and p66 homodimerisation (Tachedjian *et al.*, 2001; Tachedjian *et al.*, 2005a). These NNRTIs also enhance Gag-Pol dimerisation through interaction with the RT domain, and decrease viral particle production from infected cell culture, presumably due to premature PR activation (Figueiredo *et al.*, 2006). The contribution of these effects to inhibition of HIV-1 replication by NNRTIs *in vivo* is unknown.

1.6.4-1 Unconventional NNRTIs

The TSAO-T (tert-butyldimethylsilyl-spiroaminooxathioledioxide-thymine) derivatives and BBNH (N-[4-tert-butylbenzoyl]-2-hydroxy-1-naphthaldehyde hydrazone) are two classes of unconventional NNRTI that are not approved for use in the treatment of HIV/AIDS. The mechanism of action is distinct from conventional NNRTIs as both the TSAO-T and BBNH derivatives inhibit RT activity by destabilising the heterodimer.

The TSAO-T derivatives are highly functionalised nucleosides that act as allosteric inhibitors of RT, of which TSAO-T is the prototype. Molecular modelling studies show that the TSAO-T molecules bind to the RT dimer interface close to but distinct from the NNBP (Sluis-Cremer *et al.*, 2000; Rodriguez-Barrios *et al.*, 2001; Das *et al.*, 2011). Unlike conventional NNRTIs that primarily interact with residues from the p66 subunit, the TSAO-T derivatives interact with residues from both subunits (Jonckheere *et al.*, 1994 Das *et al.*, 2011). The N3-ethyl derivative of TSAO-T, (TSAO-e3T) has been most extensively studied and can destabilise both the RT heterodimer and p66 homodimers (Sluis-Cremer *et al.*, 2000).

BBNH interacts with both the DNA polymerase and RNase H domains of the RT (Borkow *et al.*, 1997; Arion *et al.*, 2002), and inhibits both enzymatic activities (Sluis-Cremer *et al.*, 2002). BBNH interaction with the polymerase domain is suggested to be analogous to that of the TSAO-T derivatives (Sluis-Cremer *et al.*, 2002). Although these compounds decrease the stability of the heterodimeric enzyme, they are not sufficient to induce subunit dissociation (Sluis-Cremer *et al.*, 2000). Thus complete dissociation of the p66 and p51 subunits of RT heterodimer is not necessary in order to inhibit enzymatic function.

1.7 The necessity and consequences of HIV-1 RT subunit heterodimerisation

Using a range of techniques, multiple studies have identified that polymerase activity is associated with dimeric forms of RT rather than the monomeric subunits. Methodologies employed have included the use of mutations that inhibit dimer formation (Goel *et al.*, 1993; Jacques *et al.*, 1994a; Wohrl *et al.*, 1997; Tachedjian *et al.*, 2000; Pandey *et al.*, 2001; Pandey *et al.*, 2002; Tachedjian *et al.*, 2003), destabilisation of the heterodimer using small molecules (Sluis-Cremer *et al.*, 2000; Sluis-Cremer *et al.*, 2002), or denaturant mediated dissociation of the subunits (Restle *et al.*, 1990; Basu *et al.*, 1992; Restle *et al.*, 1992a). Although there are limitations to each of these studies, taken together they form a consensus that dimerisation is necessary for optimal RT activity.

1.7.1 Stability and activity of HIV-1 RT species

A driving factor in protein-protein interactions is the energetic benefit in reducing solvent exposed surface area, particularly that of hydrophobic residues (Keskin *et al.*, 2005). RT subunit dimerisation greatly reduces the solvent exposed area of the individual subunits and in turn generates an extensive protein interface. A standard protein interface encompasses between 1200 and 2000 $Å^2$ (Moreira *et al.*, 2007b). Smaller interfaces of approximately 1200 $Å^2$ normally constitute short lived, low stability complexes, while large interfaces range from 2000 to 4660 $Å^2$ (Moreira *et al.*, 2007b). Depending on the structure analysed, the RT heterodimer interface ranges from 4300-5300 $Å^2$ (reviewed by Rodriguez-Barrios *et al.*, 2001) of which 2800-3300 $Å^2$ correspond to non-polar atoms (Wang *et al.*, 1994). This extensive heterodimer interface correlates with the low dissociation constant (K_d) of the RT heterodimer.

The RT heterodimer is calculated to be the most energetically favourable configuration of monomeric or dimeric forms. Monomeric p66 is proposed to assume a p51-like structure, reducing the solvent exposed surface area by 1600 $Å^2$ compared to the open conformation assumed by p66 in the heterodimer (Wang *et al.*, 1994). However heterodimerisation buries significantly greater surface area than that gained by conversion of the p66 subunit to a p51-like conformation. The free energy generated upon heterodimerisation is proposed to stabilise the open conformation assumed by p66 in the heterodimer (Wang *et al.*, 1994).

A number of methodologies have been employed to measure the free energy of RT heterodimerisation, including analytical gel filtration (Becerra *et al.*, 1991), analytical gel filtration in the presence of a denaturant (Restle *et al.*, 1990; Divita *et al.*, 1995b; Sluis-Cremer *et al.*, 2000; Sluis-Cremer *et al.*, 2002), and analytical ultracentrifugation (Becerra *et al.*, 1991; Lebowitz *et al.*, 1994). However the inherent stability of the heterodimer has hampered accurate determination of the K_d, with these studies generating values ranging from 0.4 nM to 2 μM.

Experimental parameters such as differences in RT expression constructs, pH, and mathematical models used to analyse data contribute to this imprecision. Venezia and colleagues (2006) critiqued these studies and offered arguably the most accurate estimation of heterodimer stability using a 'thermodynamically rigorous' method of analytical ultracentrifugation, providing a K_d of 310 ± 60 nM (Venezia *et al.*, 2006).

Both p66 and p51 homodimers can be generated in recombinant systems, and the reported K_d for each also varies between studies (Becerra *et al.*, 1991; Basu *et al.*, 1992; Cabodevilla *et al.*, 2001; Zheng *et al.*, 2010). However, both p66 and p51 homodimers are consistently characterised as less stable compared to the heterodimer. From the aforementioned Venezia study, the K_d of the p66 homodimer is reported at 4.2 ± 0.8 μM and the p51 homodimer 230 ± 30 μM (Venezia *et al.*, 2006).

While a crystal structure of either p66 or p51 homodimer has not been determined, theoretical models have been proposed (Wang *et al.*, 1994) and supported by experimental data (Zheng *et al.*, 2010). Homodimers are proposed to mimic the asymmetric nature of the heterodimer as formation of symmetrical homodimers is prevented by steric hindrance between the polymerase domains (Wang *et al.*, 1994). Such was later reported using NMR and small angle X-ray scattering to observe the conformation of p51 homodimers (Zheng *et al.*, 2010).

It is proposed that the decreased stability of homodimers compared to the heterodimer is in part due to the RNase H domain. In the case of the p51 homodimer, this is due to the absence of stabilising interactions contributed by the RNase H domain, and in p66 homodimers, due to the steric clash of two RNase H domains (Wang *et al.*, 1994). Correspondingly, the RNase H domain is observed in unique positions with respect to the polymerase domain in the heterodimer, p66 homodimer and p66 monomer (Restle *et al.*, 1992b).

Homodimers demonstrate varying degrees of polymerase activity when assayed on homopolymeric templates (Muller *et al.*, 1989; Restle *et al.*, 1990; Anderson *et al.*, 1992; Basu *et al.*, 1992; Bavand *et al.*, 1993), and RNase H activity in the case of the p66 homodimer (Restle *et al.*, 1992a). These studies conclude that polymerase activity of homodimers is mechanistically similar to that of the heterodimer, giving weight to the suggestion that homodimers assume an asymmetric heterodimer-like structure with one competent polymerase active site. However, these studies are divided on whether p66 homodimers exhibit comparable polymerase activity to the heterodimer, or whether the heterodimer has a distinct catalytic advantage. Reports describing the latter also do not concur, with the advantage of the heterodimer being attributed to increased processivity, catalytic constant (K_{cat}) or Michaelis constant (K_M) (Anderson *et al.*, 1992; Bavand *et al.*, 1993; Beard *et al.*, 1993). As the biochemical and biological preference for heterodimer formation is well documented, these studies

provide insights to the role of dimerisation in RT function, rather than imply a direct role for homodimers in HIV-1 replication.

1.7.2 Consequences of heterodimerisation for RT structure and activity

The necessity of heterodimerisation for RT activity is predominantly attributed to conformational changes conferred upon dimerisation. Bahar and colleagues (1999) examined changes to subunit conformation and flexibility using Gaussian Network modelling - a crude form of molecular dynamics that allows modelling of large molecules. As did Wang and colleagues (1994) for their analysis, Bahar and colleagues (1999) utilised structural data from the heterodimeric structure to analyse the p66 and p51 subunits separately.

The fingers and thumb subdomains of p51, and the fingers, thumb and RNase H domain of p66 demonstrate intrinsic flexibility when monomeric. Upon heterodimerisation, the mobility of the entire p51 subunit is subdued, the p66 fingers remain mobile, and the flexibility of the p66 thumb is enhanced. A decrease in flexibility is observed for the RNase H domain, which correlates with stabilising interactions formed between the RNase H domain and p51 thumb. The residues most severely constrained upon dimerisation are located at the dimer interface, which generally correspond with residues calculated to make the largest contribution to the heterodimer interface (Table 1.1 and Table 1.2) (Bahar *et al.*, 1999; Menendez-Arias *et al.*, 2001; Rodriguez-Barrios *et al.*, 2001; Srivastava *et al.*, 2006).

Significant changes in secondary structure are observed by circular dichroism (CD) analysis upon heterodimerisation of independently produced recombinant RT subunits, or proteolysis of a recombinant p66 precursor (Anderson *et al.*, 1992). Mature RT heterodimers appear to be resistant to further proteolysis. This is attributed to the changes in conformation upon heterodimerisation (Lowe *et al.*, 1988; Anderson *et al.*, 1992; Chattopadhyay *et al.*, 1992; Abram *et al.*, 2005). However recent attempts to produce the mature heterodimer by incubation of recombinant p66 homodimers with recombinant HIV-1 PR have been unsuccessful, leading to the suggestion that the conformation of purified recombinant p66 may be different to the intermediate formed during RT maturation in the virion (Abram *et al.*, 2005).

In addition to these large-scale changes, there is evidence that dimerisation influences the structure of the polymerase active site. The RT TRM contributes to the heterodimer interface, and is spatially isolated from both polymerase and RNase H active sites. A conservative TRM mutation, W401F, does not affect RT secondary structure or subunit heterodimerisation in recombinant protein dimerisation assays (Tachedjian *et al.*, 2005b), but changes the cation preference and optima of the polymerase active site (Tachedjian *et al.*, 2005b).

Furthermore, the RT dimerisation defect conferred by the W401A and W401L mutations can be suppressed by a single second-site mutation, the polymerase active site residue, D110G (Tachedjian *et al.*, 2003). These data suggest a relationship between the construction of the RT heterodimer interface and the polymerase active site.

Compared to polymerase activity, data linking RNase H activity with the dimeric nature of the enzyme is not definitive. An early study describes RNase H activity only in dimeric species (Restle *et al.*, 1992a). However, it is not known whether the use of a denaturant (i.e. 15% acetonitrile) resulted only in subunit dissociation and not protein unfolding, as such has been described for incubation of RT in urea, another commonly used denaturant (Menendez-Arias *et al.*, 2001; Sluis-Cremer *et al.*, 2002).

RT mutations have been described which prevent subunit dimerisation, and also result in RT with defective polymerase and RNase H activities (Ghosh *et al.*, 1996; Wohrl *et al.*, 1997). However the pleiotropic nature of these mutations confound whether the lack of enzymatic activity is due to the inability to dimerise or conformational changes induced by the mutation. Non-conservative mutation of the TRM residue W401 results in a dimerisation defect due to localised disturbance at the heterodimer interface (Tachedjian *et al.*, 2003; Tachedjian *et al.*, 2005b). While polymerase activity is abolished for these mutants, polymerase-dependent (DNA 3'-end directed) and polymerase-independent (RNA 5'-end directed) RNase H activity is observed albeit at a decreased catalytic rate (Tachedjian *et al.*, 2005b).

The ability of W401 dimerisation defective mutants to form transient or unstable heterodimers was not excluded by Tachedjian and colleagues (2003). Therefore it is not clear whether RNase H activity was facilitated by the formation of transient heterodimers, or whether monomeric p66 subunits are capable of RNase H activity. The inability of W401 mutants to efficiently utilise manganese as an RNase H active site cation may be indicative of a relationship between the RT heterodimer interface and RNase H active site, as is implied for the polymerase active site (Tachedjian *et al.*, 2005b).

Ultimately the association of RNase H activity with dimeric RT species remains unresolved. It is however, without question that dimerisation is necessary for proper RT function, and that conformational changes are conferred by RT heterodimerisation. Chimeric RT with subunits derived from HIV and FIV RT demonstrates that these changes also directly inform RT activity. Aspects of DNA synthesis, RNase H activity and susceptibility to RT inhibitors is associated with the origin of the p51 subunit, rather than the p66 subunit (Amacker *et al.*, 1998). Interestingly, FIV RT lacks the TRM, and the secondary structure of the β7-β8 loop differs significantly, both motifs important for RT heterodimerisation (Pandey *et al.*, 2001; Tachedjian *et al.*, 2003).

This may be suggestive of a role for these motifs in the structure the heterodimer interface, and correspondingly, RT activity. These studies imply more is yet to be discovered on the relationship between RT heterodimerisation and RT activity.

1.7.3 RT heterodimer formation *in vitro*

In order to observe the process of RT subunit heterodimerisation, early studies used the organic solvent acetonitrile to dissociate RT heterodimers into monomeric subunits, and assayed RT heterodimer formation by intrinsic tryptophan fluorescence and polymerase activity upon dilution of the solvent (Restle *et al.*, 1990; Divita *et al.*, 1993; Divita *et al.*, 1995a; Divita *et al.*, 1995b). These studies describe subunit association as biphasic. An initial, rapid, concentration dependent association of the subunits forms a heterodimeric intermediate devoid of polymerase activity, however which can bind T/P with high affinity (Divita *et al.*, 1995a). This is followed by a slow isomerisation, potentially involving conformational changes at the polymerase active site and the p51 thumb, resulting in an active heterodimer (Divita *et al.*, 1993; Divita *et al.*, 1995a). Following a dearth of publications on the topic, two recent publications challenge the hypothesis of a biphasic association.

The most accurate assessment of dissociation constants for the RT heterodimers and homodimers (Venezia *et al.*, 2006) facilitated astute experimental design using appropriate protein concentrations to monitor RT heterodimer association in the absence of denaturants (Venezia *et al.*, 2009). This study found no evidence of biphasic heterodimer formation, rather a second-order reaction that is dependent on monomer concentration, with a relatively slow association constant (approximately 1.7 M-1 s-1) (Venezia *et al.*, 2009). While the authors caution the need for confirmatory studies, they suggest the slow association of the subunits is best suited to a conformational selection model, where only two monomers in the correct conformation associate.

This model is favoured by a study of p51 homodimer formation. Zheng and colleagues (2010) observed the conformation of p51 in solution by NMR and small angle X-ray scattering (SAXS). While the majority of p51 subunits are monomeric and assume a closed conformation, p51 homodimers occur in which one subunit assumes a p66 like conformation. The authors suggest this can be explained by a conformational selection model where the predominant monomeric species is able to select the low concentration of p51 monomer in the p66 like open conformation. Expression of the RT L289K mutation, which prevents RT heterodimerisation through the p66 subunit, results in p51 subunits with a greater preference for the closed conformation compared to the wild-type p51. In the conformational selection model, this reduces homodimer formation due to the decrease in subunits in the open conformation.

The authors caution that these experimental data do not necessarily rule out alternative models (Zheng *et al.*, 2010), and further studies are required to confirm the validity of the conformational selection model.

1.8 The role of the reverse transcriptase domain in the late stages of HIV-1 replication

In the late phase of viral replication, the HIV-1 enzymes, PR, RT and IN, are expressed as part of the Gag-Pol precursor protein and trafficked to the site of virion assembly. The process of maturation is initiated upon interaction of Gag-Pol molecules facilitating dimerisation of the PR domain and PR activation. The sequential cleavage of the Gag and Gag-Pol precursor proteins liberates the mature viral proteins and results in morphological restructuring of the viral particle generating an infectious virus particle.

Multiple roles are indicated for RT in the late phase of replication, including regulation of PR activation, maturation of the RT heterodimer, and incorporation into the virion independently of Gag-Pol. These processes are at present poorly described, predominantly due to the inability to accurately detect and monitor late-phase events. What is known of the late-phase events that affect RT maturation, or involve the RT domain, are briefly described here.

1.8.1 Regulation of PR activation

The sequential and ordered processing of the polyproteins Gag (Pettit *et al.*, 1998; Cote *et al.*, 2001) and Gag-Pol (Lindhofer *et al.*, 1995; Pettit *et al.*, 2003) by the HIV-1 PR is critical for generation of an infectious viral particle (Kohl *et al.*, 1988). Activation of the HIV-1 PR must be tightly regulated as premature activation or partial inhibition results in defects in virion particle production, maturation or infectivity (reviewed by Hill *et al.*, 2005). At a fundamental level, PR activity is proposed to be regulated by its expression as part of Gag-Pol (Navia *et al.*, 1990).

In contrast to cellular aspartyl proteases that are comprised of a single polypeptide, the HIV-1 PR is a homodimeric aspartyl protease formed by the symmetrical association of two 99 amino acid subunits. Homodimerisation generates both the substrate-binding pocket and the active site (Cheng *et al.*, 1990). As the HIV-1 PR is expressed as part of the Gag-Pol polyprotein, multimerisation of Gag-Pol is required to facilitate dimerisation of the PR domains, forming an active Gag-Pol embedded PR. It is this embedded PR that mediates the initial Gag-Pol cleavages (Pettit *et al.*, 2004).

Experimental data supports the hypothesis that PR activation and activity is in part regulated by the inherent spatial and temporal restrictions of expression within Gag-Pol and the architecture of the budding virion (Navia *et al.*, 1990).

For example, maintenance of the 1:20 Gag:Gag-Pol ratio (Shehu-Xhilaga *et al.*, 2001), association of the viral polyproteins with the host cell membrane (Kaplan *et al.*, 1994), and the integrity of the Gag-Pol molecule (Bukovsky *et al.*, 1996; Quillent *et al.*, 1996; Wang *et al.*, 2000) all affect virion production or infectivity by means of HIV-1 PR activity. The role of the RT domain in PR activation is most clearly demonstrated in the use of potent NNRTIs including efavirenz (EFV), TMC120, and TMC125, which are known to enhance both RT heterodimerisation and p66 homodimerisation (Tachedjian, 2003; Figueiredo *et al.*, 2006). HIV-1 generated in the presence of these compounds demonstrates enhanced intracellular processing of the HIV-1 polyproteins and decrease in viral particle production, defects characteristic of premature PR activation (Figueiredo *et al.*, 2006). Thus the ability of the RT domain to dimerise in Gag-Pol or Gag-Pol processing intermediates appears to be a positive factor in PR activation.

A role for other factors in regulating PR activation, such as host cell factors, pH, and calcium flux (Swanstrom *et al.*, 1997), are yet to reveal the extent of their influence. One currently unfolding story is that of the host cell factor clathrin (Popov *et al.*, 2011; Zhang *et al.*, 2011). Clathrin is specifically incorporated into the virion via interaction with multiple, but as yet uncharacterised, domains within Pol. Reduced levels of clathrin in the virion does not affect viral particle production, but decrease HIV-1 infectivity. Clathrin is suggested to act by regulating PR activation, or stabilising Gag-Pol and Pol processing intermediates in the presence of active PR (Zhang *et al.*, 2011), however the precise mechanism is not as yet defined.

1.8.2 Gag-Pol maturation

The process of PR mediated Gag maturation has been well characterised in recombinant protein studies (Krausslich *et al.*, 1989; Pettit *et al.*, 1994; Pettit *et al.*, 1998; Wiegers *et al.*, 1998; Pettit *et al.*, 2002) and in HIV-1 infected cell-culture (Pettit *et al.*, 1994; Almog *et al.*, 1996; Pettit *et al.*, 2002, reviewed by Ganser-Pornillos *et al.*, 2008). In contrast, the process of Gag-Pol maturation is not as well described. This is due to a combination of factors including the inherent difficulties in expression of recombinant Gag-Pol, and detection of short-lived processing intermediates in virions and HIV-1 infected or transfected cells.

Expression of full-length Gag-Pol in bacteria has not been described. Shorter 'model' fragments have been used to characterise PR autocatalysis and to a lesser degree, RT maturation (Sluis-Cremer *et al.*, 2004a). Using an *in vitro* transcription/translation strategy in which full-length Gag-Pol is transcribed from a DNA construct and translated incorporating radiolabeled amino acids, Kaplan and Pettit describe the processing of the Gag-Pol precursor by both the Gag-Pol embedded PR (Pettit *et al.*, 2003) and mature PR (Pettit *et al.*, 2005b).

The observation of processing intermediates by Pettit and colleagues correlate with observations in HIV-1 infected cells (Lindhofer *et al.*, 1995) and viral lysates (unpublished data, A. Figueiredo, Burnet Institute, Melbourne, Australia). The data generated in Pettit and Kaplan's studies provide the most comprehensive, albeit incomplete understanding of Gag-Pol maturation.

The HIV-1 PR does not recognise a specific cleavage site, rather cleavage is dependent on amino acid composition (Pearl *et al.*, 1987; Partin *et al.*, 1990; Pettit *et al.*, 1991; Tozser *et al.*, 1997) and accessibility of the site (Prabu-Jeyabalan *et al.*, 2002). As a result, PR cleavages sites are processed with differing efficiency. The resulting sequential processing of Gag-Pol is hypothesised to be important for proper condensation of the structural proteins and incorporation of the Pol proteins in the viral particle (Pettit *et al.*, 1998; Pettit *et al.*, 2002; Pettit *et al.*, 2005a). Figure 1.9 summarises the data generated by Pettit and colleagues (2005a, 2005b) using the *in vitro* transcription/translation system to express full-length recombinant Gag-Pol, processed by the Gag-Pol embedded PR (Fig. 1.9A) and mature PR (Fig. 1.9B). In both conditions the initial Gag-Pol cleavage occurs at the p2/NC junction. This cleavage event liberates the active PR complex from the membrane-tethered Gag fragment. Using the Gag-Pol associated PR, only one more cleavage event is observed in this system, between the TFP and $p6^{Pol}$ (Pettit *et al.*, 2003). Both of these cleavages are performed in an intramolecular manner. The lack of virion assembly acting to spatially organise Gag-Pol is thought to restrict the cleavage events detected in this system. However, additional cleavage events can be observed by introducing mutations in the embedded PR, which are hypothesised to increase the flexibility of the precursor associated PR (Fig. 1.9) (Pettit *et al.*, 2003).

In contrast, the addition of mature PR can completely process recombinant Gag-Pol to liberate the mature proteins (Pettit *et al.*, 2005b). Following the initial cleavage at p2/NC, the secondary cleavage occurs at the RT/IN site. This is followed by partial processing at the p51/RNase H site within RT. Thereafter a series of 'paired intermediates' are observed - with or without the RNase H domain. This implies that following IN liberation, RT containing processing intermediates are dimeric, which regulates the cleavage of p51/RNase H site generating the heterodimeric species (Pettit *et al.*, 2005b) The final cleavage observed in this system between PR/RT releases the mature PR (Pettit *et al.*, 2005b). In the virion, Gag-Pol processing is likely to be a combination of *trans* and *cis* PR events, mediated by the relative amounts of substrate, mature and precursor associated PR.

1.8.2-1 Characteristics of the immature versus the mature PR

The Gag-Pol embedded PR and mature PR demonstrate significantly different characteristics in terms of sensitivity to PIs and affinity for certain cleavage sites. The Gag-Pol embedded PR is up to 10,000-fold less sensitive to particular PIs compared to the mature enzyme, and successive Gag-Pol cleavage events increase the susceptibility of the precursor associated PR (Pettit *et al.*, 2004). This

is also observed in HIV-1 infected cells where early cleavage events (p2/NC and TFP/p6^{Pol}) can occur in the presence of high concentrations of PI, while subsequent cleavage events are inhibited (Lindhofer *et al.*, 1995). Interestingly, PR mutations proposed to enhance the flexibility of the embedded PR result in enhanced processing of distal sites, and increased susceptibility to PIs (Pettit *et al.*, 2003; Pettit *et al.*, 2005a) (Fig. 1.9).

The two cleavage events required to liberate the mature PR are p6^{Pol}/PR and PR/RT. Cleavage of the p6^{Pol}/PR site in model systems is accompanied by a large increase in wild-type like PR activity (Louis *et al.*, 1991a; Partin *et al.*, 1991; Louis *et al.*, 1994; Zybarth *et al.*, 1995; Wondrak *et al.*, 1996). Several model systems have been used to examine PR autocatalysis, including Gag-PR fusion proteins (Zybarth *et al.*, 1994), mini precursors consisting of PR flanked by short native sequences (Co *et al.*, 1994; Wondrak *et al.*, 1996; Louis *et al.*, 1999a), and truncated model Gag-Pol proteins (Louis *et al.*, 1994; Sluis-Cremer *et al.*, 2004a). In these model systems, cleavage at the PR N-terminus occurs prior to the C-terminal cleavage. In studies where the precursor includes the TFR/p6^{Pol} cleavage site, cleavage of this site occurs prior to p6^{Pol}/PR (Louis *et al.*, 1999a; Louis *et al.*, 1999b). The presence of p6^{Pol} reduces the efficiency and stability of the PR-fusion protein compared to the mature PR (Louis *et al.*, 1991a; Louis *et al.*, 1991b; Zybarth *et al.*, 1994; Zybarth *et al.*, 1995; Almog *et al.*, 1996; Louis *et al.*, 1999b; Paulus *et al.*, 1999; Sluis-Cremer *et al.*, 2004a; Chatterjee *et al.*, 2005), and confers defects in Gag maturation and infectivity when expressed in HIV-1 (Tessmer *et al.*, 1998; Ludwig *et al.*, 2008). The p6^{Pol}/PR cleavage has been characterised as an intramolecular event (Louis *et al.*, 1994; Wondrak *et al.*, 1996; Louis *et al.*, 1999b) or a mixed intra/intermolecular event Co *et al.*, 1994, which may be indicative of the changing characteristics of the PR upon liberation of p6^{Pol}. The final PR/RT cleavage event is intermolecular (Louis *et al.*, 1994; Wondrak *et al.*, 1996).

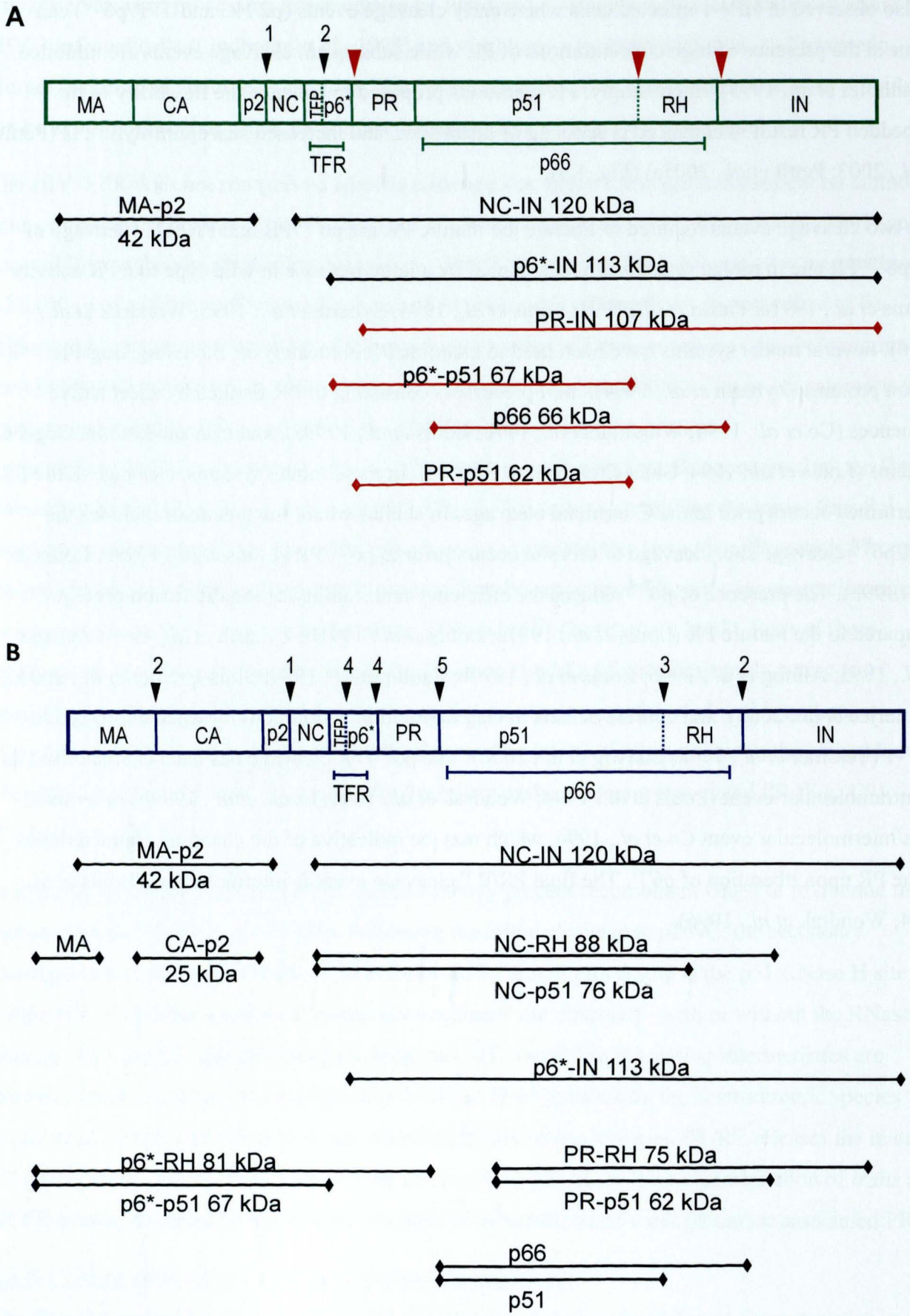
A
1
2
MA
CA
p2
NC
TFR
p6*
PR
p51
RH
IN
TFR
p66
MA-p2
42 kDa
NC-IN 120 kDa
p6*-IN 113 kDa
PR-IN 107 kDa
p6*-p51 67 kDa
p66 66 kDa
PR-p51 62 kDa
B
2
1
4
4
5
3
2
MA
CA
p2
NC
TFR
p6*
PR
p51
RH
IN
TFR
p66
MA-p2
42 kDa
NC-IN 120 kDa
MA
CA-p2
25 kDa
NC-RH 88 kDa
NC-p51 76 kDa
p6*-IN 113 kDa
p6*-RH 81 kDa
p6*-p51 67 kDa
PR-RH 75 kDa
PR-p51 62 kDa
p66
p51

Figure 1.9. Protease mediated processing of recombinant Gag-Pol.

Schematic of cleavage of recombinant Gag-Pol mediated by the embedded PR (A) or mature PR (B) as described by Pettit and colleagues (2004, 2005b). Each cleavage event is marked with a black arrowhead and is numbered to indicate its occurrence. The cleavage products are designated by the N- and C-terminal domains, and size in kDa. When employing the Gag-Pol embedded PR (A), cleavage is initiated at the p2/NC site, followed by cleavage between TFP and $p6^{Pol}$, resulting in 120-kDa NC-IN and 113-kDa $p6^{Pol}$-IN processing intermediates (Pettit *et al.*, 2003). Mutation of the terminal residues of PR, such as the PR P1A mutation, relax the constraints of the embedded PR and allows cleavage of the $p6^{Pol}$/PR, p66/IN and p51/RNase H sites, indicated by a red arrowhead. Recombinant Gag-Pol can be completely processed by addition of mature PR (B) (Pettit *et al.*, 2005b). The initial cleavage occurs at the same point as for that performed by the Gag-Pol embedded PR, at the p2/NC junction. Secondary cleavages at p66/IN and MA/CA occur at a similar rate. Cleavage at the p51/RNase H site can proceed once IN has been released, which results in paired processing intermediates with or without the RNase H domain. These paired intermediates are subsequently processed at the N-terminal cleavage sites.

1.8.2-2 Models for maturation of the reverse transcriptase heterodimer

Three cleavage events are required to generate the mature RT heterodimer, at PR/RT, RH/IN, and at the internal p51/RNase H site to form the p51 subunit. Two models of RT maturation have been proposed and discussed in the literature to a limited extent; the sequential and the concerted model (Divita *et al.*, 1995a; Sluis-Cremer *et al.*, 2004a). The concerted model proposes that each RT subunit is independently cleaved to maturity, after which the subunits associate to form the heterodimer. In the sequential model the immediate precursor to the heterodimer is a p66 homodimer, the structural constraints of which regulate generation of the RT heterodimer.

The HIV-1 PR mediated cleavage of p51/RNase H occurs between amino acids 440 and 441 (Graves *et al.*, 1990; Tomasselli *et al.*, 1993). In the crystal structure of both the RT heterodimer and free RNase H, this site is buried within the protein and is presumably inaccessible to the PR (Davies *et al.*, 1991; Hostomska *et al.*, 1991; Kohlstaedt *et al.*, 1992; Jacobo-Molina *et al.*, 1993; Wang *et al.*, 1994). The sequential model proposes that due the steric interference between connection subdomains and RNase H domains of a p66 homodimer, it must assume an asymmetric conformation, exposing the p51/RNase H cleavage site in one of the subunits (Hostomska *et al.*, 1991; Wang *et al.*, 1994).

This model concurs with other observations from studies in recombinant protein and HIV-1 (Sluis-Cremer *et al.*, 2004a; Pettit *et al.*, 2005b). In virions produced in the presence of PIs, formation of p51 is abolished while the p66 subunit is present (Sluis-Cremer *et al.*, 2004a). This implies that p51 formation is subsequent to that of the p66 subunit. Pettit and colleagues (2004a) also observed the generation of the RT heterodimer in a bacterially expressed 90 kDa model Pol protein, encompassing four C-terminal amino acid of NC through to the first 46 amino acid of IN. In this system the p51 subunit is generated only after accumulation of the p66 subunit (Sluis-Cremer *et al.*, 2004a). Further, expression of the RT L234A mutation, which prevents RT subunit dimerisation (Ghosh *et al.*, 1996; Tachedjian *et al.*, 2000), prevents generation of the p51 subunit, but not p66 (Sluis-Cremer *et al.*, 2004a).

While these data support the role of p66 homodimerisation in the generation of the heterodimer, recombinant Gag-Pol studies indicate that processing of the p51/RNase H site is not restricted to p66, but is observed in a range of RT containing intermediates (Pettit *et al.*, 2005b). Liberation of IN from recombinant Gag-Pol by the mature PR is an early event, occurring after the initial cleavage event at p2/NC. Following liberation of IN, a series of 'paired intermediates' are observed, which correspond to partial cleavage at the p51/RNase site (Fig. 1.9). Pettit and colleagues (2005) suggest that release of IN allows dimerisation of the processing intermediate, which facilitates the regulated cleavage at the p51/RNase H site as proposed in the sequential model of RT maturation.

Subsequent cleavages of the N-terminal of the heterodimeric processing intermediates liberate the mature heterodimer (Pettit *et al.*, 2005b). These data imply a variation to the sequential model in which dimerisation, but not necessarily p66 homodimerisation, is necessary. As yet, no data exits which clearly supports the role any of these models *in situ*.

1.8.2-3 Cleavage events required to liberate a reverse transcriptase heterodimer

As previously stated, three cleavage events are required to generate the mature RT heterodimer, at PR/RT, RH/IN, and at the internal p51/RNase H site to form the p51 subunit. However in the bacterially expressed model Pol protein described by Sluis-Cremer and colleagues (2004a), cleavage at the PR/RT site is not necessary for cleavage at p51/RH. Introduction of PR/RT cleavage site mutations result in PR-RT fusion proteins which form a heterodimer comprised of PR-p66 and PR-p51 (Sluis-Cremer *et al.*, 2004a). Expression of PR/RT cleavage site mutations in HIV-1 also results in these PR-extended species (Cherry *et al.*, 1998a; Cherry *et al.*, 1998b). These virions are up to 20 times less infectious than wild-type HIV-1. Since these mutations do not appear to affect virion maturation in any other aspect, the defect is likely due to a direct effect on RT activity (Cherry *et al.*, 1998a; Cherry *et al.*, 1998b).

Blocking the RT/IN site is also tolerated in the bacterial model Pol system, and generates a p66-IN fusion protein and mature p51 (Sluis-Cremer *et al.*, 2004a). The kinetics of formation is analogous to that of the RT heterodimer in this recombinant system. However it should be noted that only the first 46 amino acid of IN are expressed in this model protein. In contrast liberation of IN from full-length Gag-Pol is required prior to cleavage at the p51/RNase H site (Pettit *et al.*, 2005b). The effect of blocking cleavage of the RT/IN site in HIV-1 is unknown.

Interestingly, mutation of the p51/RNase H cleavage site in p66 bacterial expression vectors results in a number of phenotypes depending on the mutation, ranging from prevention of p51 generation, enhanced cleavage, or altered cleavage resulting in aberrantly-sized products and protein degradation (Hostomska *et al.*, 1991; Jupp *et al.*, 1991). In the context of HIV-1, p51/RNase H cleavage site mutations result in virions with reduced RT content. Interestingly, the RT in these virion is primarily composed of the p51 rather than the p66 subunit, regardless of the nature of the cleavage site mutation (Abram *et al.*, 2005). Preventing formation of the mature heterodimer by inhibiting generation of p51 results aberrant proteolysis. As had been observed in recombinant protein studies, formation of a mature heterodimer results in changes to secondary structure which confer resistance to further proteolysis (Lowe *et al.*, 1988; Anderson *et al.*, 1992; Chattopadhyay *et al.*, 1992; Abram *et al.*, 2005). This also appears to be true of RT in the context of HIV-1 (Abram *et al.*, 2005).

1.8.3 Virion incorporation of RT

At the most fundamental level, the HIV-1 enzymes are incorporated into the virion due to their expression as part of the Gag-Pol precursor protein. However, it has been displayed in both engineered (Wu *et al.*, 1997) and natural systems (Cen *et al.*, 2004b; Liao *et al.*, 2007) that Pol products can be incorporated into the virion independently of Gag-Pol.

Wu and colleagues (1997) utilised a *trans*-complementation system in which incorporation of RT and IN into the budding virion is dependent on expression as Vpr-RT-IN, or both Vpr-RT and Vpr-IN fusion proteins. Mulky and colleagues (2004) adapted the system to use a Vpr-p51 fusion protein that co-packages p66 only upon interaction with Vpr-p51. While demonstrating that an intact Gag-Pol molecule is not absolutely necessary for viral particle formation, *trans*-complementation is inefficient, with RT activity and virus infectivity approximately 20% of wild-type levels (Wu *et al.*, 1997; Mulky *et al.*, 2004).

Regions of Pol have been identified that directly interact with Gag and mediate incorporation of Pol into Gag VLPs (Chiu *et al.*, 2002; Cen *et al.*, 2004b; Chiu *et al.*, 2004a; Liao *et al.*, 2007). A consensus on the role of the RT and IN domains involved in virion incorporation of Pol remains unclear. Both Cen and colleagues (2004b) and Liao and colleagues (2007) reported that Pol fragments encompassing RT are incorporated into Gag VLPs. While PR is dispensable for this interaction, Cen and colleagues (2004b) found that IN was not required for incorporation, and Liao and colleagues (2007) found IN to directly inhibit incorporation. Attempts by Liao and colleagues (2007) to identify regions of RT responsible for mediating Pol incorporation by deletion mutagenesis are confounded by poor expression levels and stability of these Pol fragments. However, it does appear that the RNase H domain and the C-terminal region of the RT connection subdomain (from 305 onwards) are dispensable for virion incorporation.

Within Gag, the MA (Liao *et al.*, 2007) and p6 (Cen *et al.*, 2004b; Liao *et al.*, 2007) domains are required for incorporation of Pol. The ability of p6 to interact with Pol proteins during viral assembly and maturation has previously been reported (Yu *et al.*, 1998b; Dettenhofer *et al.*, 1999). These earlier reports support that these interactions are biologically relevant and not artefacts of the over expression of viral proteins characteristic of cell transfection systems employed by Cen (2004b) and Liao (2007). While a direct interaction between the Pol fragments and Gag has been suggested (Cen *et al.*, 2004b; Liao *et al.*, 2007), host cell factors may also have a role in facilitating this interaction (Popov *et al.*, 2011; Zhang *et al.*, 2011).

The incorporation of Pol into the virion independently of expression as Gag-Pol is not without precedent. Human foamy virus does not produce a Gag-Pol fusion protein, instead Pol is translated from a separately spliced mRNA and this protein is actively packaged into virions (Lochelt *et al.*, 1996; Yu *et al.*, 1996). Murine leukaemia virus (MLV) Pol is also incorporated into VLPs independently of Gag-Pol (Buchschacher *et al.*, 1999). For HIV-1, incorporation of Pol or RT independently of Gag-Pol is generally suggested to prevent loss of Pol from the budding virion upon PR activation (Navia *et al.*, 1990).

1.9 Protein:protein interactions as a novel means of inhibition of HIV enzymes

For each of the three HIV enzymes, subunit multimerisation is necessary for activity. Thus preventing or modulating subunit multimerisation by targeting specific protein:protein interactions has been proposed as a novel means to inhibit HIV-1 replication (reviewed by Wapling *et al.*, 2007). This has been explored to varying degrees for each the HIV-1 enzymes, usually utilising peptides derived from a protein interface, and to a lesser degree identification of compounds that destabilise the protein interface. Currently there are no molecules with sufficient potency to warrant further development (reviewed by Loregian *et al.*, 2002; Camarasa *et al.*, 2006; Wapling *et al.*, 2007). Increasing knowledge of basic protein interactions and structure-function relationships will hopefully aid in future identification and development of novel inhibitory compounds.

Historically it had been assumed that protein–protein interactions were the result of numerous low energy interactions across the interface. However, studies characterising various protein complexes reveal that the free energy of binding is not evenly distributed across the protein interface. Rather small subsets of residues at the protein interface contribute 'hot spots' of binding energy (Bogan *et al.*, 1998). A hot spot is defined as a residue whose substitution by alanine leads to a decrease in the free energy of protein binding of at least 2 kcal/mol (Bogan *et al.*, 1998).

Systematic analysis of hot spots reveals a preferential amino acid composition, predominantly tryptophan (21%), arginine (13.3%) and tyrosine (12.3%), and to a lesser extent proline, leucine, aspartic acid and lysine (Keskin *et al.*, 2005; Moreira *et al.*, 2007a). Tryptophan appears to play a unique function in protein-protein interactions owing to its size and chemical properties. Tryptophan has a large hydrophobic surface, which generates a gain in free energy upon movement from a solvent exposed environment (Clore *et al.*, 1995). Its hydrophobic nature also protects nearby hydrogen bonds from water (Ma *et al.*, 2007). Due to its aromatic nature, tryptophan can participate in π-stacking interactions, and can also act as a hydrogen-bonding donor (Ma *et al.*, 2007).

Hot spots are typically densely packed, forming clusters that have been referred to as 'hot regions' (Halperin *et al.*, 2004; Keskin *et al.*, 2005). Hot spots within a hot region contribute to binding energy in a cooperative manner, whereas individual hot regions are additive (Keskin *et al.*, 2005). Hot regions tend to couple across the protein interface, showing complementarity in shape so that the hot region of one protein interface packs against the hot region of the opposing protein interface (Halperin *et al.*, 2004). This is observed in the RT heterodimer, where clusters of residues from the p66 palm interact with the p51 fingers, residues in the RNase H domain interact with the p51 thumb, and the residues from the connection subdomains from both p66 and p51 interact (Section 1.9.1).

Due to the typically dense packing of hot spots into hot regions, substitution of a hot spot residue often results in steric clashes or destabilisation. Correspondingly, hot spots correlate with structurally conserved residues (Keskin *et al.*, 2005). Algorithms have been developed to identify theoretical hotspots within proteins utilising the protein sequence and structural data (Kitchen *et al.*, 2004; Ofran *et al.*, 2007). Identification of critical binding residues at the protein interface allows a targeted approach for inhibitor design. Such a peptide mimetic or drug-like compound is anticipated to have high affinity and specificity.

In terms of the development of novel therapies for the treatment of HIV-1, this approach has been realised to some extent in the peptide fusion inhibitor, T20. Knowledge of the sequence, conformation and role of the heptad repeat region in the HIV-1 transmembrane protein, gp41, allowed design of the synthetic peptide, T20. T20 specifically binds to the heptad repeat regions to prevent conformational changes necessary to induce fusion between the host cell and HIV-1 membranes (Wild *et al.*, 1994).

RT dimerisation as a novel antiretroviral drug target is attractive for a number of reasons. RT activity is associated with dimeric species and the monomers are devoid of polymerase activity (Restle *et al.*, 1990; Goel *et al.*, 1993; Jacques *et al.*, 1994a; Wohrl *et al.*, 1997; Sluis-Cremer *et al.*, 2000; Tachedjian *et al.*, 2000; Pandey *et al.*, 2001). Studies also indicate an essential role of the RT domain within Gag-Pol in Gag-Pol oligomerisation and PR activation (Figueiredo *et al.*, 2006). Further, expression of RT dimerisation defective mutations in HIV-1 confer defects in reverse transcription and putatively, RT maturation (Wapling *et al.*, 2005). Thus a RT dimerisation inhibitor could potentially have a dual mechanism of action, affecting both early and late phases of HIV-1 replication. Furthermore, inhibition of reverse transcription retards the generation of HIV-1 diversity, potentially delaying the development of drug-resistant HIV-1. RT dimerisation was first reported as a novel means of enzyme inhibition in 1990 (Restle *et al.*, 1990). Although dimer interface peptides have been described (Divita *et al.*, 1994; Debyser *et al.*, 1996; Morris *et al.*, 1999a; Morris *et al.*, 1999b; Depollier *et al.*, 2005) the lack of RT dimerisation inhibitors approved

for HIV therapy during the past 20 years is indicative of the challenges faced in designing protein interface inhibitors.

1.9.1 The RT heterodimer interface and theoretical hotspots

A number of studies have used different approaches to identify interface residues that contribute significantly to the heterodimer interface and thus form potential hot spots. These approaches include loss of solvent accessibility upon RT dimerisation (Menendez-Arias *et al.*, 2001; Rodriguez-Barrios *et al.*, 2001), constriction of movement upon RT dimerisation (Bahar *et al.*, 1999) or calculated buried surface area at the heterodimer interface (Srivastava *et al.*, 2006). Tables 1.1 and 1.2 summarise these data for the p66 and p51 subunit, respectively. These studies generally correlate, and identify residues within the three main regions of interaction at the RT heterodimer interface described by Wang and colleagues (1994); those being the p66 palm and the p51 fingers, the RNase H domain of p66 and the p51 thumb, and the connection subdomain of both subunits.

While these studies indicate the location of potential hot spots, as stated by Keskin and colleagues (2008), the '*computational predictions are mere candidates for the experiment to tes*t'. Although a number of RT heterodimer interface residues have been subject to mutational analysis, rarely has validation as a hot spot, i.e. alanine mutagenesis resulting in a decrease of subunit binding energy by at least 2 kcal/mol, been an objective of the analysis. Regardless, these mutational studies provide insight into the relationship between the heterodimer interface, heterodimer stability, and RT activity. Studies of interest or relevance to this work are briefly discussed in Section 1.10.

1.9.2 Inhibition of HIV-1 replication using peptides directed at the RT heterodimer interface

While this study contributes to the proof of concept for of dimerisation as a potential drug target, the theory is by no means new. Two strategies have been utilised to generate peptides designed to target the RT dimer interface in order to block HIV-1 RT function, including peptides corresponding to regions that are known to have an important role in RT dimerisation (Divita *et al.*, 1994; Debyser *et al.*, 1996; Morris *et al.*, 1999a; Morris *et al.*, 1999b; Depollier *et al.*, 2005), and rationally designed peptides (Campbell *et al.*, 2002).

Table 1.1. Identification of p66 residues that contribute to the HIV-1 RT heterodimer interface.

Sub-domain	Structure/Feature	Residue	Reference*			
			RB	MA	Ba	Sr
palm		D86		★		★
palm		F87			★	★
palm		W88	★	★	★	★
palm		E89				★
palm		V90				★
palm		Q91				★
palm		L92		★		★
palm		P95		★		
palm		Y181		★		
connection		Q373	★	★		★
connection		T376				★
connection		T377				★
connection		I380	★	★		★
connection		V381		★		★
connection		I382				★
connection		W383				★
connection		G384	★	★		★
connection	αL, TRM	W402	★	★		★
connection	αL/αL-β20 loop	T403		★	★	
connection	αL/αL-β20 loop	E404			★	
connection	αL/αL-β20 loop, TRM	Y405			★	
connection	αL-β20 loop, TRM	W406	★	★	★	★
connection	αL-β20 loop	Q407		★	★	★
connection	αL-β20 loop	A408	★	★	★	★
connection	αL-β20 loop	T409			★	★
connection	αL-β20 loop, TRM	W410	★	★	★	★
connection		P433		★		
RNase H		Y441	★	★		
RNase H		N460		★		
RNase H		N507	★			
RNase H		W535		★		
RNase H		P537		★		★
RNase H		K540		★	★	★
RNase H		G541			★	★
RNase H		I542			★	★
RNase H		G543		★	★	★
RNase H		G544				★
RNase H		E546				★

* RB, amino acid residues that bury greater than 60 Å^2 upon heterodimerisation (Rodriguez-Barrios *et al.*, 2001); MA, amino acids with accessibility score of greater than 10, (Menendez-Arias *et al.*, 2001); Ba, amino acids most severely constrained upon dimerisation (Bahar *et al.*, 1999); Sr, amino acids that significantly contribute to the total buried surface area of the subunit (Srivastava *et al.*, 2006).

Table 1.2. Identification of p51 residues that contribute to the HIV-1 RT heterodimer interface.

Sub-domain	Structure/Feature	Residue	Reference*			
			RB	MA	Ba	Sr
fingers		P25		★		★
fingers		L26			★	
fingers		T27		★	★	
fingers		E28			★	
fingers		P52	★	★	★	★
fingers		E53	★	★	★	★
fingers		N54			★	★
fingers		P55		★	★	★
fingers	β7-β8 loop	S134			★	
fingers	β7-β8 loop	I135		★	★	★
fingers	β7-β8 loop	N136	★	★	★	★
fingers	β7-β8 loop	N137	★	★	★	★
fingers	β7-β8 loop, NNBP	E138	★	★	★	★
fingers	β7-β8 loop	T139			★	★
fingers	β7-β8 loop	P140	★	★	★	★
fingers	β7-β8 loop	G141			★	
thumb		N255		★		
thumb		Q258	★	★		
thumb		N265		★		
thumb		C280			★	★
thumb		K281			★	
thumb	Leucine repeat motif	L282			★	
thumb		L283			★	★
thumb		R284			★	★
thumb		G285			★	★
thumb		T286	★	★	★	★
thumb		K287			★	★
thumb		A288		★	★	★
thumb	Leucine repeat motif	L289	★	★	★	★
thumb		T290	★	★	★	★
thumb		N291			★	
connection		K331	★	★		★
connection		N363		★		
connection		D364	★	★		
connection		P392				★
connection		Q394	★	★		★
connection	αL	E396		★		★
connection	αL	T397		★		★
connection	αL	T400		★		★
connection	αL, TRM	W401	★	★		★
connection		P421	★	★		
connection		L422		★		

* RB, amino acid residues that bury greater than 60 $Å^2$ upon heterodimerisation (Rodriguez-Barrios *et al.*, 2001); MA, amino acids with accessibility score of greater than 10, (Menendez-Arias *et al.*, 2001); Ba, amino acids most severely constrained upon dimerisation (Bahar *et al.*, 1999); Sr, amino acids that significantly contribute to the total buried surface area of the subunit (Srivastava *et al.*, 2006).

An early study identified a 19 amino-acid synthetic peptide derived from the TRM (RT residues 389–407, Divita *et al.*, 1994). While the peptide could not induce dissociation of the heterodimer, re-association of RT subunits dissociated by acetonitrile could be prevented in a concentration dependent manner (Divita *et al.*, 1994). This peptide was shortened (residues 395–404) and optimised for stability and cellular uptake, and shown to suppress viral replication in HIV-1 infected cells (Morris *et al.*, 1999b). This peptide preferentially interacts with the p51 subunit and acts to destabilise the heterodimer (Depollier *et al.*, 2005). Residues W24 and F61 in the fingers subdomain of p51 are essential for biding, and are in close proximity to p66 TRM residues. However, as the concentration of peptide required to inhibit HIV-1 replication is significantly less than the peptide concentration required to inhibit RT dimerization *in vitro*, the mechanism of action of this peptide is unconfirmed (Morris *et al.*, 1999b).

Interestingly this corresponds with the region identified to interact with two naturally occurring metalloporphyrins, haeme and zinc protoporphyrin (Argyris et al., 1999; Argyris et al., 2001). These compounds have been found to inhibit RT activity, putatively via interaction with a region spanning the TRM in the p66 subunit, from W398 to Q407 (Argyris *et al.*, 1999; Argyris *et al.*, 2001). Unfortunately at this point of time, neither of these lines of investigation has yielded further data nor lead compounds.

Screening for small molecule inhibitors that target this region has yielded a hit, MAS0, which inhibits both polymerase and RNase H activity. However, inhibition is only observed upon pre-incubation of recombinant RT with MAS0 in the presence of acetonitrile (Grohmann *et al.*, 2008).

More recently, rational design strategies have been employed using the available RT structures to direct the design of peptide mimetics targeting subunit interaction (Campbell *et al.*, 2002; Hosokawa *et al.*, 2004). These studies have led to the synthesis of a peptide, TLMA2993, which is designed to target the RT connection subdomain (383-413). TLMA2993 inhibits RT activity at micromolar concentrations (Campbell *et al.*, 2002) and when stably expressed can protect cells against HIV-1 infection by inhibition of reverse transcription (Hosokawa *et al.*, 2004).

Although these studies are promising, they also demonstrate the difficulties in designing peptide inhibitors, including stability and delivery. Ideally, such inhibitors could be evolved to peptidomimetic or small molecule inhibitors.

1.10 RT mutations and their effects on HIV-1 replication

Reverse transcriptase has multiple roles in HIV-1 replication in addition to its essential role in reverse transcription of the HIV-1 RNA genome. A role for the RT domain within Gag-Pol or in RT containing processing intermediates has been indicated in regulation of PR activation, RT maturation, RT incorporation into the virion (Section 1.8), and incorporation and annealing of the tRNA primer (Section 1.5). Thus manipulation of the RT domain can affect multiple aspects of HIV-1 replication. Mutagenic studies that describe such effects are briefly discussed here. RT mutations have been described to have a global affect on Gag-Pol stability and processing, or a precise localised effect on RT maturation. With regards to RT heterodimerisation, these studies indicate that formation of a stable RT heterodimer, whether mediated by the p66 or the p51 subunit, is necessary for HIV-1 infectivity.

1.10.1 The ß7–ß8 loop

The ß7–ß8 loop is located in the fingers subdomain and is defined by two prolines at codons P133 and P140 that bracket the amino acids SINNET, which form the loop between β7 and β8. The interaction between the p51 β7-β8 loop and the p66 subunit forms a significant interaction at the RT heterodimer interface (Table 1.2). The loop protrudes into the p66 subunit to interact with residues 381-382 in the connection subdomain, and palm residues 83 - 106 located at the base of the nucleic acid binding cleft (Kohlstaedt *et al.*, 1992). The β7-β8 loop residues and interacting partners in the p66 subunit are highly conserved across primate lentiviral RTs (Menendez-Arias *et al.*, 2001; Mulky *et al.*, 2007).

Correct configuration of the p51 β7-β8 loop is required for formation of a stable RT heterodimer. Deletion, mutation or duplication of the p51 β7-β8 loop results in reduced dimer stability and enzymatic activity (Pandey *et al.*, 2001; Pandey *et al.*, 2002). The role of this structure in subunit interaction is also implied by the observation that the loop residue E138 is critical for binding of the non-conventional NNRTI, TSAO-T, which inhibits RT activity by destabilising, but not dissociating the RT heterodimer (Sluis-Cremer *et al.*, 2000).

Structural analysis of this region has identified specific interactions between the p51 β7-β8 loop residue N136 with p66 residues P95, H96, V381, and I382 (Auwerx *et al.*, 2005; Balzarini *et al.*, 2005; Mulky *et al.*, 2007), and N137 with p66 residues L92, G93, I94 (Pandey *et al.*, 2001; Auwerx *et al.*, 2005) (Fig. 1.10). In recombinant RT, mutation of $p51^{N136}$ or $p51^{N137}$ destabilises the heterodimer but does not result in subunit dissociation (Auwerx *et al.*, 2005; Balzarini *et al.*, 2005). The decrease in RT dimer stability correlates with a significant decrease in RDDP activity (Auwerx *et al.*, 2005; Balzarini *et al.*, 2005).

Mutation of β7-β8 residue, $p51^{P140A}$, or interacting partner $p66^{P95A}$ also causes a significant decrease in RDDP activity, however the effect of these mutations on subunit interaction is uncharacterised (Auwerx *et al.*, 2005). While it is possible that these mutations affect RT subunit interaction, the proximity of $p66^{P95}$ to the polymerase primer grip may also provide an alternative mechanism of action for inhibition of RT activity by altering the positioning of this motif (Auwerx *et al.*, 2005).

Mulky and colleagues (2007) also performed mutational analysis of the β7-β8 loop where RT subunit interaction was assayed in the context of the virus particle. Based on the Vpr *trans*-complementation system developed by Wu and colleagues (1997), packaging of the p66 subunit into the virion is dependent on interaction with the Vpr-p51 fusion protein (Mulky *et al.*, 2004). This system circumvents the possibility of pleiotropic effects of the RT mutation on Gag-Pol, enabling specific evaluation of mutations on RT subunit interaction and activity. The effect of the mutations on RT subunit interaction is measured as a function of *trans*-complemented viral particle infectivity and RT activity, and p66 incorporation can be directly detected by Western blot analysis (Mulky *et al.*, 2004).

In this context Mulky and colleagues (2007) found that $p51^{N136}$ decreases incorporation of p66 compared to wild-type, with corresponding decreases in viral infectivity and virion-associated RT activity. When expressed in HIV-1, N136A results in a decrease in virion RT levels that is in part due to proteolysis by the viral protease (Mulky *et al.*, 2007). Virion Gag maturation and virion-associated IN are indistinguishable from wild-type suggesting that N136A does not adversely affect Gag-Pol incorporation or generation of mature IN.

Thus this dimerisation defective mutation appears to affect RT heterodimer stability and RT activity in HIV-1, independently of the maturation of other Pol proteins. Interestingly, while Auwerx and colleagues (2005) report that $p51^{N137A}$ or $p51^{P140A}$ significantly decreases RDDP activity, Mulky and colleagues (2007) observed no significant effect on mutating these residues on RT expression or viral infectivity when expressed either in the p51 subunit in the Vpr *trans*-complementation system, or in HIV-1.

1.10.2 The polymerase primer grip

The polymerase primer grip is a highly conserved structural motif, which in the p66 subunit has a crucial role in positioning the primer strand for polymerisation (Xiong *et al.*, 1990). The primer grip is a β-hairpin motif formed by β12 and β13 (aa 227-235) (Jacobo-Molina *et al.*, 1993). Primer grip residues L234, F227 and W229 also form part of the NNBP (Smerdon *et al.*, 1994). Mutagenic analysis of primer grip residues in recombinant RT (Jacques *et al.*, 1994b; Ghosh *et al.*, 1996; Palaniappan *et al.*, 1997; Powell *et al.*, 1997; Wohrl *et al.*, 1997; Wisniewski *et al.*, 1999) and in

HIV-1 (Yu *et al.*, 1998a) has contributed to our understanding of the role of the motif in RT function and HIV-1 replication. The primer grip is adjacent to the RT heterodimer interface, however in neither subunit do primer grip residues contribute to the heterodimer interface. Nonetheless mutagenic analysis of the motif reveals a role in RT subunit dimerisation.

Of the primer grip residues studied by mutagenic analysis, W229 (Jacques *et al.*, 1994b; Wohrl *et al.*, 1997), G231 (Wohrl *et al.*, 1997) and L234 (Ghosh *et al.*, 1996; Wohrl *et al.*, 1997; Tachedjian *et al.*, 2000) affect RT subunit dimerisation. Subunit specific mutation of $p66^{W229}$ or $p66^{G231}$ to alanine retards interaction with $p51^{WT}$ (Wohrl *et al.*, 1997). As neither W229 nor G231 are located at the dimer interface, they are hypothesised to affect dimerisation indirectly, by inducing conformational changes to the subunit. For the W229A mutant, it is proposed that replacement of the tryptophan with the smaller alanine side-chain causes the adjacent residues to collapse. Consequently the interactions between the p51 β7-β8 loop and the p66 subunit are disturbed (Rodgers *et al.*, 1995; Wohrl *et al.*, 1997; Pandey *et al.*, 2001). In contrast, replacement of $p66^{G231}$ with a the larger alanine residue is suggested to change the architecture of the primer grip in turn affecting a conformational change in the surrounding residues which affects dimer stability (Wohrl *et al.*, 1997).

Mutation of $p66^{L234}$ to alanine abolishes interaction with $p51^{WT}$ in recombinant protein studies (Ghosh *et al.*, 1996; Tachedjian *et al.*, 2000). Subunit specific analysis in the yeast two-hybrid (Y2H) system adapted by Tachedjian and colleagues (2000) to quantitatively assay RT subunit interaction confirms that the L234A mutation mediates its effect predominantly through the p66 subunit. Expression in the p66 subunit reduces subunit interaction by 32-fold compared to wild-type levels, compared to a 2-fold decrease when expressed in the p51 subunit only (Tachedjian *et al.*, 2000). The effect of the L234A is cumulative when expressed in both subunits (Tachedjian *et al.*, 2000).

The proximity of L234 to P95 in the p66 subunit led to the proposal that mutation of L234 causes heterodimer instability by a similar mechanism as proposed for mutation of $p66^{W229}$; by conformational changes that disturb proper interaction with the p51 β7-β8 loop (Wohrl *et al.*, 1997). To gain insight into the mechanism of inhibition of RT dimerisation by L234A, Tachedjian and colleagues (2000) identified second-site mutations in the p66 subunit that restore interaction with p51 as detected in the Y2H system. Four compensatory mutations were identified in p66, two located at the polymerase active site, D110G and D186V, and two within the TRM, W402R, and W406R. The ability of polymerase active site mutations to suppress the dimerisation defective phenotype conferred by L234A mutation suggests interplay between dimerisation and the structure of the polymerase active site.

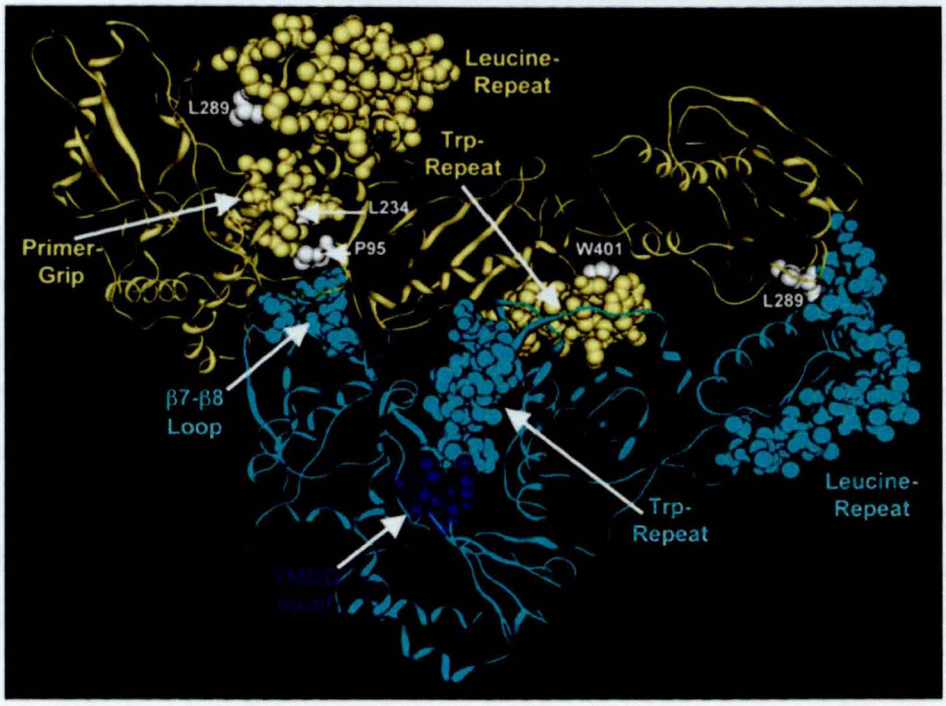

Figure 1.10. Motifs and residues that contribute to the RT heterodimer interface.

The HIV-1 structure (PDB ID: 1DLO, Hsiou *et al.*, 1996) is displayed in ribbon rendering with the p66 subunit in yellow and p51 subunit in cyan. Important motifs in RT heterodimer interaction or stability are indicated in space-fill, with specific residues highlighed in white space-fill. The asymmetry of the RT heterodimer interface is apparent as these motifs and residues are indicated in both subunits. Image reproduced from Srivastava *et al.*, (2006).

Interestingly, co-expression of L234A with either of the second side compensatory mutations, W402R and W406R, increases RT subunit interaction and RDDP activity above that observed for the wild-type recombinant protein. W402 and W406 comprise part of the highly conserved TRM, which is surrounded by highly conserved charged residues. Replacement of these tryptophan residues with basic residues may maintain electrostatic interactions at the interface while allowing flexibility required to accommodate conformational changes conferred by L234A. These analyses of L234 highlight a role for multiple regions at the RT heterodimer interface, including the β7-β8 loop and the TRM. These data suggest that additional to formation of a stable complex, the RT heterodimer interface has an important role in regulation of DNA polymerase activity.

In HIV-1 replication, polymerase primer grip mutations that abrogate RT subunit dimerisation also result in defects in the context of Gag-Pol. Introduction of L234D or W239A (Yu *et al.*, 1998a) into HIV-1 results in non-infectious virions which display immature or aberrant particle morphology, incomplete Gag processing and reduced levels of virion RT and IN.

Expression of the L234A mutation in HIV-1 does not appear to adversely affect Gag processing, but also results in decreased levels of virion RT and IN (Buxton *et al.*, 2005). In recombinant RT the L234A mutation prevents p66 homodimerisation and heterodimerisation (Tachedjian *et al.*, 2000; Tachedjian *et al.*, 2005a), and prevents generation of the p51 subunit from a bacterially expressed model Pol fragment, presumably by preventing formation of the required p66 homodimer for processing to the heterodimer (Sluis-Cremer *et al.*, 2004a). The lack of effect of L234A RT mutation on viral particle production (Zhang *et al.*, 2011) and Gag processing (Buxton *et al.*, 2005) indicates that Gag-Pol expressing the L234A mutation is incorporated at wild-type levels. The effect on maturation of Pol products is suggested to be due both to effects on the dimeric stability of Pol expressing RT processing products (Sluis-Cremer *et al.*, 2004a) and loss of interaction with clathrin, a Pol stabilising host cell factor (Popov *et al.*, 2011; Zhang *et al.*, 2011).

However, the L234D and W239A mutations display evidence of cell-associated HIV-1 PR-mediated processing of Gag-Pol, and these mutations are proposed to affect conformational changes in Gag-Pol that result premature PR activation, and decreased incorporation of Gag-Pol into the budding virion (Yu *et al.*, 1998a).

1.10.3 The F130W mutation

F130 is located within the core of the fingers subdomain, which in the p51 subunit is buried within the RT heterodimer (Olivares et al, 2004). Despite the conservative nature of the mutation, F130W is proposed to destabilise the p51 subunit, inturn affecting both heterodimer stability and PR activation (Olivares *et al.*, 2004; Olivares *et al.*, 2007).

Expression of F130W HIV-1 results in incomplete Gag processing, aberrant Gag-Pol processing and delayed replication kinetics (Olivares *et al.*, 2004; Olivares *et al.*, 2007). Only in the absence of an active HIV-1 PR is Vpr-p51^{F130W} detected in viral lysates using the Vpr-p51 *trans*-complementation system (Olivares *et al.*, 2007). In contrast to dimerisation defective RT mutants previously examined in this system such as N136A (Mulky *et al.*, 2007), expression of p51^{F130W} does not prevent co-packaging of the p66 subunit. However the presence of p66 breakdown products indicates that this p51 mutation results in heterodimer instability (Olivares *et al.*, 2007).

A second-site suppressor mutation was generated upon serial passage of the F130W mutant HIV-1, which restores infectivity, virion-associated RT activity and Gag maturation. This mutation, T85S, appears to directly interact with F130W to stabilise the p51 subunit (Olivares *et al.*, 2004; Olivares *et al.*, 2007). Of note, Olivares and colleagues (2007) identified transitory PR mutations located in the C-terminal β-sheet that contributes to the PR dimer interface, which act to reduce PR stability. These PR mutations were only observed in intermediate passages of F130W HIV-1, and resolved upon selection of the T85S RT mutation. The authors hypothesise that these transitory PR mutations serve to prevent PR mediated degradation of unstable RT, allowing generation and selection of an RT compensatory mutation (Olivares *et al.*, 2007).

1.10.4 p51/RNase H cleavage site mutations

The generation of a heterodimeric RT by internal cleavage of the RT subunit is unique to primate lentiviral RTs (reviewed by Hizi *et al.*, 2008). However, as p66 homodimers also demonstrate polymerase and RNase H activity (Restle *et al.*, 1990; Restle *et al.*, 1992a), what is the necessity for generation of the p51 subunit? Abram and colleagues (2005) addressed this question by mutating the PR cleavage site between the polymerase and RNase H domains. In contrast to recombinant protein studies in which cleavage site mutations can decrease, increase or have no effect on PR mediated cleavage (Hostomska *et al.*, 1991; Jupp *et al.*, 1991; Mizrahi *et al.*, 1994; Tozser *et al.*, 1997) in HIV-1, mutation of this cleavage site results in aberrant RT processing, regardless of the predicted severity of the mutation (Abram *et al.*, 2005). Conservative and non-conservative cleavage site mutations demonstrate extreme or complete loss of immunoreactive RT protein. However in all mutants with detectable levels of virion RT, the p51:p66 ratio is increased compared to wild-type. Thus blocking the natural cleavage sites does not prevent generation of p51 to result in a concomitant increase in virion p66, rather forces proteolysis of mutant p66 subunits at alternative sites (Abram *et al.*, 2005). Virions produced in the presence PIs indicated that the aberrant proteolysis is due to the HIV-1 PR, and that p66 species rather than higher-mass intermediates were most susceptible to degradation.

Wild-type Gag processing profiles for all p51/RNase H cleavage site mutants suggest that the reduction in virion RT arose from proteolytic instability rather than decreased incorporation of Gag-Pol. However, some cleavage site mutants display decreases in virion Gag-Pol and IN, which is attributed to Gag-Pol stability and PR-mediated processing (Abram *et al.*, 2005).

Generation and selection of the second-site compensatory mutation, T477A, restores wild-type processing and viral infectivity to a subset of the cleavage site mutants (Abram *et al.*, 2010). T447A purportedly acts to allow access to a secondary, as yet undefined cleavage site to allow generation of functional RT (Abram *et al.*, 2010). These data suggest that formation of the RT heterodimer is essential to generate a stabilised complex that is resistant to aberrant proteolysis, as has been described in recombinant protein studies (Section 1.7).

1.10.5 Mutations within the RT thumb subdomain

The thumb subdomain of p51 forms multiple contacts with the RNase H domain of the p66 subunit, whereas the p66 thumb does not contribute to the dimer interface but has an integral role in manipulation of the T/P during polymerisation (Section 1.6.3). It is the elucidation of this latter role for which mutagenic studies of thumb residues have been performed. Of interest to this study are two recent publications characterising mutations of the thumb residues that result in RT-specific defects (Dunn *et al.*, 2009; Zhang *et al.*, 2009). Zhang and colleagues focused on the role of residues contributing to the conserved loop between helices αH and αI (residues 271-277), which form the 'helix clamp' motif (Wang *et al.*, 2008; Zhang *et al.*, 2009). Expression of the Y271A and I274A mutations decrease viral replication when expressed in HIV-1, which does not correlate with the role of these mutations in RT activity (Wang *et al.*, 2008). In HIV-1 these mutations result in undetectable virion RT, while demonstrating wild-type levels of virion IN and PR. Together with a wild-type like distribution of Gag-Pol within the producer cell, it is unlikely that these mutations effect Gag-Pol stability or virion incorporation. Further, there is also no evidence of premature PR activation as observed by decreased particle production or enhanced processing of viral proteins in producer cell lysates (Zhang *et al.*, 2009). Zhang and colleagues (2009) conclude that this profile is representative of an RT specific defect. Production of mutant HIV-1 in the presence of the PI indinavir (IDV) indicates that the HIV-1 PR is in part responsible for the decrease in virion RT.

Interestingly, expression of these mutations in recombinant p66 results in the formation of higher order oligomers as well as dimers, the latter being the predominant form observed for wild-type recombinant p66. The authors suggest this is indicative of conformational changes affected by the mutations, which affect protein stability and hence formation of an active and stable RT heterodimer.

Dunn and colleagues (2009) performed a comprehensive analysis of 20 non-conservative mutations within the RT thumb subdomain to find greater than 80% of mutations result in an RT specific defect in viral lysates. A range RT phenotypes in HIV-1 viral lysates was observed, from substantial amounts of the mature RT subunits to complete absence of the RT subunits with only small molecular weight RT reactive fragments observed by Western blot. The size profile of RT breakdown products in the virion are relatively consistent across the various mutations, which they suggest is due to these mutations increasing exposure of pre-existing PR cleavage sites rather than the mutation generating a new PR cleavage site. These mutants showed delayed reverse transcription kinetics as judged by real time PCR of early and late reverse transcription intermediates. Interestingly, this was also true for mutations with undetectable RT by Western blot analysis.

This effect is reminiscent of the defects in virion RT observed by Abram and colleagues (2005) and Zhang and colleagues (2009), that being an RT specific defect, with some mutants demonstrating wild-type levels of virion PR and IN. Similar to these studies, Dunn and colleagues (2009) also observe that generation of mutant virus in the presence of the PI ritonavir results in an increase in RT subunits in the virion, indicating the role of the HIV-1 PR in actively degrading unstable or malformed RT heterodimers.

The mutations in the RT thumb domain characterised by Dunn and colleagues (2009) are not located at the dimer interface, and their effect on RT heterodimerisation was not examined in these studies. The majority of the mutations that result in a severe defect are located within the hydrophobic core of the thumb domain, and involve a hydrophobic to hydrophilic substitution. It is proposed that these mutations destabilise the subunits, or may cause partial unfolding and allow aberrant proteolysis. Dunn and colleagues (2009) suggest these effects are indicative that the design of novel RT inhibitors that force the HIV-1 to generate resistance mutations at a significant cost to viral fitness may be a viable possibility.

1.10.6 The tryptophan repeat motif

The TRM is a highly conserved cluster of aromatic amino acids consisting of six tryptophans located at RT codons 398, 401, 402, 406, 410 and 414, and a tyrosine at codon 405 (Baillon *et al.*, 1991). These residues span αL, β20, and the loop linking these secondary structures, which are located in the connection subdomain. Uniquely in the context of the asymmetric heterodimer, the TRM from each subunit interact at the heterodimer interface (Kohlstaedt *et al.*, 1992; Jacobo-Molina *et al.*, 1993; Wang *et al.*, 1994) (Fig. 1.10). This is facilitated by the contrasting conformation of the connection subdomain in the p66 and p51 subunits respectively, which in turn

is facilitated by the differing arrangement of secondary structures αL, β20 and β21 in the subunits (Wang *et al.*, 1994) (Section 1.6.2-3).

The p66 αL-β20 loop is buried upon subunit dimerisation, and both TRM and intervening residues from W402 through to W410 are calculated to make significant contributions to the heterodimer interface (Table 1.1). In the context of p51, the majority of αL, β20 and the linking loop region are internalised within the subunit. Only T400 and W401 calculated to make a significant contribution to the p51 heterodimer interface (Table 1.2), with Y405 identified to contribute to interface interactions (Mulky *et al.*, 2005b; Srivastava *et al.*, 2006).

The intervening residues that fall within the TRM (RT codons E399, T403, E404, Q407, A408, T409, I411, P412 and E413) are conserved across HIV-1 and HIV-2 comparably to the TRM, however are generally more varied across primate lentiviral RTs (Fig. 1.7). The role of the intervening residues in RT function and HIV-1 replication has not been investigated previously. What is known of the role of the TRM and associated residues is briefly described here.

Both Tachedjian and colleagues (2003) and Mulky and colleagues (2005b) have analysed the RT crystal structure and utilised subunit specific mutagenesis to characterise the role of specific residues in this highly conserved motif. Both studies identify a potential interaction between the side-chains of $p51^{W401}$ and $p66^{W410}$, while Mulky and colleagues (2005b) also identify interactions between the side-chain of $p66^{W410}$ with $p51^{N363}$ and $p51^{Y405}$. Tachedjian and colleagues (2003) propose that the backbone carbonyl residues of the p66 αL-β20 loop also contribute interactions with the p51 subunit.

Non-conservative mutation of W401 (W401A/L) (Tachedjian *et al.*, 2003; Mulky *et al.*, 2005b; Tachedjian *et al.*, 2005b) or W414 (W414A) (Tachedjian *et al.*, 2003) results in an RT dimerisation defect, predominantly mediated through the p66 subunit. The extent of the defect varies depending on the system in which these mutations are examined, ranging from very low levels of interaction in biological systems including yeast two-hybrid (Tachedjian *et al.*, 2003) and HIV-1 *trans*-complemented virions (Mulky *et al.*, 2005b), to the absence of interaction in recombinant protein binding assays (Tachedjian *et al.*, 2003; Tachedjian *et al.*, 2005b).

TRM residues W401 and W414 residues do not directly contribute to the heterodimer interface (Table 1.1). Tachedjian and colleagues (2003) propose that $p66^{W401}$ and $p66^{W414}$, located in the terminal ends of αL and β20 respectively, are essential in positioning the p66 αL-β20 loop, and therefore affect multiple interactions contributed by loop residues to the heterodimer interface (Table 1.1). The presence of a bulky aromatic at W401 appears to be essential for this role in positioning the p66 αL-β20 loop, as the conservative mutation W401F does not affect RT subunit

interaction or activity (Tachedjian *et al.*, 2003). Non-conservative mutation of W401 in the p51 subunit results in minor decreases in interaction with the p66 subunit, which is likely due to the loss of the direct interactions between the side-chains of $p51^{W401}$ with $p66^{W410}$ (Tachedjian *et al.*, 2003; Mulky *et al.*, 2005b). Expression of these mutations in both RT subunits appears to act cumulatively (Tachedjian *et al.*, 2003; Mulky *et al.*, 2005b).

The W401A, W401L and W401F mutations do not result in detectable changes to RT spectra observed by CD analysis, implying that these mutations do not induce changes in the composition α-helices, β-strands and random coils in the RT, and that any structural effect of these mutations is confined to the αL-β20 loop (Tachedjian *et al.*, 2005b). Several lines of evidence support the proposed role for the p66 αL-β20 loop in RT heterodimerisation (Tachedjian *et al.*, 2003). T409 is located within the TRM, in the middle of the p66 αL-β20 loop. Expression of T409I restores subunit interaction to W401A mutant RT in recombinant protein binding assays (Tachedjian *et al.*, 2003). The replacement of threonine with the bulkier side-chain of isoleucine at 409 is proposed to restore the position of the αL-β20 loop (Tachedjian *et al.*, 2003). However, the W401A/T409I double mutant exhibits only partial restoration of RT activity.

Further, $p51^{K331}$, located in β16 of the connection subdomain of the p51 subunit, contributes to the p51 heterodimer interface (Table 1.2). The $p51^{K331}$ side-chain is predicted to form multiple hydrogen bonds with the backbone carbonyls of p66 αL and αL-β20 loop residues W402, Y405 and Q407 (Tachedjian *et al.*, 2003). Mutation of K331 to alanine in both subunits (Tachedjian *et al.*, 2003), or specifically in the p51 subunit (Grohmann *et al.*, 2008) also inhibits RT subunit interaction in recombinant RT binding studies. The location of K331 on the solvent exposed face of the p66 subunit supports the presumption that the mutation acts via the p51 subunit. However the role of K331A specifically in the p66 subunit has not been defined.

Interestingly, expression of the W398L, W402L, Y405L, W406L or W410L mutations in both subunits does not prevent RT subunit interaction (Tachedjian *et al.*, 2003). Nor does simultaneous mutation of the evenly spaced TRM residues in the p66 subunit, (W398L, W402L, W406L, W410L and W414L), significantly reduce interaction with wild-type p51 in the Y2H system (Tachedjian *et al.*, 2003). Thus apparently the loss of interactions contributed by these side-chains is not sufficient to destabilise the heterodimer directly, or affect positioning of the αL-β20 loop. Tachedjian and colleagues (2003) propose that this implies the importance of the interaction between the backbone carbonyl resides of the p66 αL-β20 loop with the p51 subunit.

In contrast to recombinant RT binding assays and the Y2H system employed by Tachedjian and colleagues (2003), Mulky and colleagues (2005b) utilised the Vpr-p51 virion *trans*-complementation system (Mulky *et al.*, 2004) to examine the role of TRM residues in RT subunit interaction. Mulky and colleagues (2005b) propose side-chain interactions between $p66^{W410}$ with $p51^{W401}$, $p51^{Y405}$ and $p51^{N363}$, and an internal interaction between $p51^{N363}$ and $p51^{Y405}$ are key interactions for heterodimer stability. Subunit specific mutation of these residues in Vpr-p51 *trans*-complemented virions, where incorporation of p66 is dependent on interaction with Vpr-p51, results in reduced infectivity (Mulky *et al.*, 2005b). Simultaneous mutagenesis of proposed interacting residues results in a greater decrease in infectivity than that observed for either mutation alone, implying the loss of these interactions is additive. Thus the decrease in infectivity likely directly corresponds to the loss of interactions at the heterodimer interface. As the *trans*-complemented virion RT profile was not examined, whether these mutations affect a decrease in infectivity due to a reduction in p66 incorporation is unknown.

Mulky and colleagues (2005b) examined the effect of mutating TRM residues W398, W402, Y405, W406 or W414 specifically in p51 subunit, an analysis that was not conducted by Tachedjian and colleagues (2003) due to defects in protein expression. Mutation of these residues to alanine decreases infectivity of *trans*-complemented virions by 30-75% compared to wild-type. The p66 subunit appears to be co-packaged in equivalent amounts compared to the p51 subunit, however proteolysis of co-packaged p66 subunit is observed. This effect was also observed for the p51 F130W mutation in this system (Olivares *et al.*, 2004). Thus this may be indicative of subunit instability induced by incorrect interaction with the p51 subunit. Mulky and colleagues (2005b) suggest that p51 mutations mediate their effect through proximity to p51 residues Y405, W401, and N363.

The RT mutations W401A, W401L, K331A and W414A prevent RT heterodimerisation and demonstrate significantly reduced DNA polymerase activity (Tachedjian *et al.*, 2003; Tachedjian *et al.*, 2005b). While the essential role of RT subunit dimerisation in RT activity is well characterised (Section 1.7), mutational analysis also indicates a relationship between the TRM, RT heterodimer interface and the construction of the RT active sites. As mentioned in Section 1.10.2, the $p66^{W402R}$, $p66^{W406R}$, and $p66^{D110G}$ mutations can suppress the RT dimerisation defect conferred by the L234A mutation (Tachedjian *et al.*, 2000). Furthermore, while expression of the W401F mutation does not adversely affect RT subunit interaction (Tachedjian *et al.*, 2003; Tachedjian *et al.*, 2005b), expression of this mutation in recombinant RT changes the cation optima and ability to utilise manganese for DNA polymerisation (Tachedjian *et al.*, 2005b). Tachedjian and colleagues (2005b) propose this is indicative of the role the heterodimer interface mediating formation of a competent polymerase active site. Interestingly, the W401A/L dimerisation defective RT mutants display both

3' and 5' directed RNase H activity, however they also affect a change in cation optima and inability to utilise manganese, also indicating a relationship with the RNase H active site (Tachedjian *et al.*, 2005b).

Expression of the dimerisation defective mutants W401A, W414A and K331A in HIV-1 demonstrate defects in the early and late phases of HIV-1 replication specific to RT (Mulky *et al.*, 2005b; Wapling *et al.*, 2005, Chapter 3, Chapter 6). The expression of TRM mutations that prevent RT subunit dimerisation in HIV-1 significantly reduces infectivity and virion-associated RT activity. This is in part due to reduced levels of virion RT, which in turn is due to aberrant proteolysis mediated by the HIV-1 PR. These mutations do not affect levels of virion IN, viral particle production or Gag processing, implying that these mutations do not affect Gag-Pol stability or incorporation as has been described for other RT mutations. This is also observed for the W401A and N136A dimerisation defective mutants examined in HIV-1 by Mulky and colleagues (2005b, 2007)

Mutation of TRM residues can also result in defects in HIV-1 replication characteristic of Gag-Pol mediated defects (Chiang *et al.*, 2009; Chiang *et al.*, 2010, Chapter 4, Chapter 6). Non-conservative mutation of TRM residue W402 to alanine or leucine in VSV-G pseudotyped HIV-1 severely reduces viral particle production from transfected cells as determined by Western blot analysis profile (Chiang *et al.*, 2010). Interestingly in the context of recombinant RT, mutation of this residue does not appear to affect RT subunit interaction (Tachedjian *et al.*, 2003; Mulky *et al.*, 2005b). Due to the similar profile observed upon production of VSV-G pseudotyped HIV-1 in the presence of EFV (Chiang *et al.*, 2009), Chiang and colleagues (2010) suggest that these mutations enhance Gag-Pol multimerisation, resulting in premature PR activation. Interestingly, both the effect of EFV and mutation of W402 on viral particle production can be partially mediated by the W401A mutation. Expression of the conservative W402F mutation demonstrates a wild-type like profile with respect to viral particle production (Chiang *et al.*, 2010). Chiang and colleagues (2010) propose that an aromatic side-chain at this location may play a stabilizing role in Gag-Pol conformation. Following the description of a role for the host cell factor clathrin in regulating PR activation, stabilising Gag-Pol processing intermediates, and mediating Pol dependent incorporation into the virion (Popov *et al.*, 2011; Zhang *et al.*, 2011), it would be of interest to define any potential role of TRM residues in clathrin recruitment as a part of future studies.

1.11 Study rationale

It has been suggested that perturbing RT dimerisation would adversely affect both early and late phases of HIV-1 replication. In its most basic aim, this project was designed to test these hypothesises utilising the TRM mutations characterised by Tachedjian and colleagues (2003). Non-conservative mutation of W401 in the RT TRM to either alanine or leucine prevents RT subunit heterodimerisation in recombinant protein binding studies (Tachedjian *et al.*, 2003; Tachedjian *et al.*, 2005b). These mutations mediate their effect predominately through the p66 subunit and are proposed to disturb the position of the p66 αL-β20 loop, resulting in loss of multiple interactions that it contributes the p66 heterodimer interface. In contrast, the W401F mutation has no effect on RT dimerisation. The ability to dimerise correlates with polymerase activity for all W401 mutants. Furthermore, no change in CD spectra of recombinant RT subunits is observed upon mutation of W401 (Tachedjian *et al.*, 2005b), implying that mutation of W401 does not affect long-range conformational changes, or changes to regular secondary structure elements.

The initial hypothesis was that expression of these mutations in HIV-1 would allow examination of the role of RT dimerisation independent of Gag-Pol pleiotropic effects. The W401A and W401L mutations, which result in subunit dimerisation defects when expressed in recombinant RT, will significantly reduce virion-associated RT activity and thus HIV-1 infectivity. The generation of mature RT in the late phase of HIV-1 replication will also be affected by these mutations. As the RT domain of Gag-Pol is hypothesised to have a positive regulatory role in PR activation, these mutations may delay PR activation. As dimerisation of the RT domain is proposed to have an essential role in generation of the mature RT heterodimer, these mutations may delay RT maturation. Examination of these mutations will discern whether the p66 homodimer is an essential processing intermediate in the generation of the mature RT heterodimer, as W401A/L mutations prevent homodimerisation of recombinant p66 (unpublished data, G. Tachedjian, Burnet Institute). Defects in HIV-1 replication upon mutation of W401 will be associated with the W401A or W401L mutations that abrogate RT dimerisation, and will not be observed for W401F, as this mutation has no effect on subunit dimerisation in recombinant RT.

This hypothesis is tested in Chapter 3, and forms the core of this study. The remaining Chapters are informed by these results. Chapter 4 examines the role of the W401A compensatory mutation T409I, identified by Tachedjian and colleagues (2003) in their recombinant protein study of TRM mutations. The T409I mutation is located within the αL-β20 loop and is hypothesised to suppress the effect of W401A on RT dimerisation by restoring the position of the loop.

Given the association between defects conferred by dimerisation defective mutations in recombinant RT and HIV-1, presented in Chapter 3, it was hypothesised that T409I would also act to suppress the defects conferred by W401A in HIV-1. However, this hypothesis was disproven due to pleiotropic effects of the T409I mutation on Gag-Pol. Chapter 5 discusses the generation of W401A compensatory mutations by serial passage of HIV-1 expressing the W401A mutation. Given the proposed local mechanism of action of W401A on the p66 αL-β20 loop, it was hypothesised that compensatory mutations would occur at the dimer interface. Indeed, replication competent W401A mutant HIV-1 was selected with three naturally occurring polymorphisms, which in the p66 subunit were located at the heterodimer interface and adjacent to the TRM.

Chapter 6 examines the role of residues in HIV-1 replication that form part of, fall within or interact with the TRM. This includes the RT mutations W414A and K331A, reported by Tachedjian and colleagues (2003) to abrogate RT dimerisation, and the highly conserved RT residues W398 and Q407.

Since the inception of this study there have been publications illuminating the role of the RT domain of Gag-Pol in PR activation. Most significantly, the description of EFV mediated enhancement of Gag-Pol dimerisation and PR activation (Figueiredo *et al.*, 2006). There have also been publications describing the effect of mutating TRM residues, in particular W401, in HIV-1 replication (Mulky *et al.*, 2005b; Chiang *et al.*, 2009; Chiang *et al.*, 2010). These studies complement the data generated in this thesis to enhance understanding of the roles of the highly conserved TRM in HIV-1 replication.

Chapter 2

Materials and methods

2.1 Plasmids and plasmid propagation

2.1.1 GFP expression vector

A GFP expression vector was used as a positive control to detect successful transfection of mammalian cell lines. The plasmid pEGFP-N1 (Clontech) was provided by Dr M. Hill (Burnet Institute, Melbourne, Australia). pEGFP-N1 encodes a red shifted variant of the wild-type green fluorescent protein, which has been optimised for fluorescence in mammalian cells and is expressed from a CMV promoter. The plasmid contains a bacterial origin of replication, kanamycin resistance gene for expansion and selection in *E.coli*.

2.1.2 HIV-1 molecular clones

A summary of all HIV-1 constructs used in this study is provided in Table 2.1.

2.1.2-1 HXB2 molecular clones

The plasmid pSVC21 was a gift from H. Gottlinger (Virology and Immunology program, University of Massachusetts Medical School, Boston, MA, USA). It contains HIV-1 HXB2 infectious molecular clone, a clade B laboratory strain (Ratner *et al.*, 1987). This clone does not encode the HIV-1 accessory proteins Vpr, Nef or Vpu. The plasmid contains a bacterial origin of replication and an ampicillin resistance gene for expansion and selection in *E.coli*. The RT mutations W401A, W401L and W401F were introduced into pSVC21 by G. Tachedjian (Burnet Institute) and are designated pSVC21-W401A, pSVC21-W401L and pSVC21-W401F (Table 2.1).

2.1.2-2 NL4.3 molecular clones

The HIV-1 isolate NL4.3 is a clade B laboratory strain that expresses all HIV-1 accessory proteins (Adachi *et al.*, 1986), encoded by the plasmid pNL4.3. The plasmid pNL4.3 was provided by J. Mak (Burnet Institute) and is described in Buxton *et al.*, 2005). This construct contains an introduced *Not*I site at nucleotides 6088-6096, which falls in the RNase H coding region and does not alter the amino acid sequence. The plasmid contains a bacterial origin of replication and ampicillin resistance gene for expansion and selection in *E.coli*.

The pNL4.3 plasmid encoding the RT mutations L234A and W401A were also provided by J. Mak (Burnet Institute) are designated pNL4.3-L234A and pNL4.3-W401A, also described in (Buxton *et al.*, 2005).

The RT mutations W398A, T409I and W414A were introduced into the RT coding region of pNL4.3 by site-directed mutagenesis as follows. The *Apa*I-*Not*I fragment of pNL4.3 was inserted into the multi-cloning site of pBluescript SK+ (Stratagene, La Jolla, CA, USA) creating the plasmid pBpolAN. Mutations were introduced using the 'Gene Editor in vitro Site Directed Mutagenesis system' (Promega, Madison, WI, USA) according to the manufacturer's instructions, using the mutagenic primers detailed in Table 2.2. The presence of the desired mutation in pBpolAN was confirmed by DNA sequence analysis using oligonucleotide primers detailed in Table 2.8. The mutated *Apa*I-*Sal*I fragment was inserted into the *Apa*I-*Not*I sites of wild-type pNL4.3.

The RT mutation A534T was introduced into the RT coding region by site-directed mutagenesis using the 'QuikChange Site-directed mutagenesis kit' (Stratagene). The *Not*I-*Sal*I fragment of pNL4.3 was cloned into the multi-cloning site of pBluescript SK+ (Stratagene) creating pBpolNS, and the mutation introduced using the relevant mutagenic primers (Table 2.2) according to the manufacturer's instructions. The presence of the desired mutation in pBpolNS was confirmed by DNA sequence analysis, and the mutated *Not*I-*Sal*I fragment inserted into the *Not*I-*Sal*I sites of pNL4.3-W401A and pNL4.3-AYR (described below), generating pNL4.3-AT and pNL4.3-AYRT, respectively.

The RT mutations C162Y and K336R were cloned into pNL4.3 from the relevant pB-PRRT plasmid described in Section 2.4.3. The RT mutation C162Y was excised from pB-PRRT and inserted into pNL4.3-W401A using the *Age*I-*Sbf*I sties, generating pNL4.3-AY. The K366R mutation and double mutation C162Y/K366R were excised from pB-PRRT and inserted into pNL4.3-W401A using the *Age*I-*Not*I sites. These fragments were inserted into pNL4.3-W401A, generating pNL4.3-AR and pNL4.3-AYR respectively.

All HX and NL constructs were confirmed by restriction endonuclease (RE) digest analysis and DNA sequence analysis, and are listed in Table 2.1. Oligonucleotide primers used for DNA sequence analysis are listed in Table 2.8.

Table 2.1 HIV- 1 molecular clones

HIV-1 molecular clone	Plasmid	Backbone[a]	RT mutation
HX	pSVC21	HXB2	Wild-type
HX-W401A	pSVC21-W401A	HXB2	W401A
HX-W401L	pSVC21-W401L	HXB2	W401L
HX-W401F	pSVC21-W401F	HXB2	W401F
NL	pNL4.3	NL4.3	Wild-type
NL-K331A	pNL4.3-K331A	NL4.3	K331A
NL-W398A	pNL4.3-W398A	NL4.3	W398A
NL-W401A	pNL4.3-W401A	NL4.3	W401A
NL-T409I	pNL4.3-T409I	NL4.3	T409I
NL-W414A	pNL4.3-W414A	NL4.3	W414A
NL-W401A/T409I	pNL4.3-AI	NL4.3	W401A, T409I
+C162Y	pNL4.3-AY	NL4.3	W401A, C162Y
+K366R	NL4.3-AR	NL4.3	W401A, K366R
+A534T	NL4.3-AT	NL4.3	W401A, A534T
+2x[b]	NL4.3-AYR	NL4.3	W401A, C162Y, K366R
+3x	NL4.3-AYRT	NL4.3	W401A, C162Y, K366R, A534T

[a] The molecular clone HXB2 does not encode accessory proteins Nef, Vpr or Vpu.

[b] Not used in this study other than for cloning purposes.

Table 2.2 Oligonucleotides used for site-directed mutagenesis

RT mutation	Oligonucleotide name	Sequence (5'-3')[a]	Location[b]
K331A	K331A	CTTAATAGCAGAAATACAGGCGCAGGGGCAAGGCC	5679-5713
W398A	W398A	CCATACAAAAGGAAACAGCTGAAGCATGGTGGAC	5882-5915
T409I	T409I	GACAGAGTATTGGCAAGCCATATGGATTCCTGAGTGGG	5913-5950
W414A	W414A	GCCACCTGGATTCCTGAGGCGGAGTTTGTCAATACCCC	5929-5967
A534T	5'Nln-A534T	GGAAAAAGTCTACCTGACATGGGTACCAGC	6291-6320
	3'Nln-A534T	GCTGGTACCCATGTCAGGTAGACTTTTTC	6291-6320

[a] Underlined nucleotides indicate mutated codons

[b] Coordinates correspond to the pNL4.3N sequence described in Buxton *et al.* 2005

2.1.3 Recombinant RT expression vector - pNLRT6H/PR

The bacterial expression vector pNLRT6H/PR is a modified version of the plasmid pRT6H/NB-PROT, was a gift from V. Prasad (Albert Einstein College of Medicine, New York City, NY, USA). pRT6H/NB-PROT contains a dual cassette for expression of HIV-1 p66 and HIV-1 PR from independent promoters. Recombinant p66 subunit is expressed with additional N terminal amino acids MRGSAAA, and additional C-terminal amino acids RS followed by a hexahistidine tag (Kew *et al.*, 1998). The vector contains a bacterial origin of replication, kanamycin resistance gene for expansion and selection in *E.coli*. For this study the p66-coding region of pRT6H/NB-PROT was replaced with the corresponding coding region from pNL4.3, resulting in the construct pNLRT6H/PR. The p66 coding region was PCR-amplified with primers 5'RT*Not*I-NL43 and 3'RT*Bgl*II-NL43 (Table 2.4), which contain engineered *Not*I and *Bgl*II sites respectively. The PCR amplicon was gel purified using the Compass DNA Purification Kit (American Bioanalytical, Natick, MA, USA) according to the manufacturer's recommendations and cloned into the *Not*I–*Bgl*II sites of pRT6H/NB-PROT. Due to the presence of the *Not*I site in the RNase H domain of pNL4.3 (Section 2.1.1-2), this was completed by partial digestion of the amplicon and isolation of the correctly sized product by agarose gel electrophoresis.

RT mutations were inserted into pNLRT6H/PR by the same methodology, utilising the relevant mutant pNL4.3 construct containing the desired RT mutation. The resulting plasmids are listed in Table 2.4. All constructs were confirmed by RE digest analysis and the presence of the desired RT mutation by DNA sequence analysis. Oligonucleotide primers used for sequencing analysis are detailed in Table 2.8.

2.1.4 Gag-Pol expression vector for use in the Promega TNT T7 Quick Coupled Transcription/Translation System - pGPtfs

The vector pGPtfs was designed to express Gag-Pol derived from the NL4.3 HIV-1 molecular clone in the TNT T7 Quick Coupled Transcription/Translation System (Promega). For this purpose pGPtfs contains the Gag-Pol coding region with a constitutive Gag-Pol frameshift, a polyA tail and a T7 terminator signal under the control of a T7 promoter. pGPtfs also contains a bacterial origin of replication and ampicillin resistance gene for expansion and selection in *E.coli*.

The vector pGPtfs was constructed as follows. The Gag-Pol coding region was derived from the plasmid pNL4.3-GPPR+, a gift from J. Mak (Burnet Institute). This plasmid contains HIV-1 molecular clone NL4.3 DNA with an optimised frameshift mutation in the overlapping *gag* and *pol* reading frames, facilitating constitutive expression of Gag-Pol (Shehu-Xhilaga *et al.*, 2001).

RE digestion of pNL4.3-GPPR+ with *Hha*I and *Sal*I allowed isolation of a 5075 bp fragment encompassing 75 nucleotides upstream of the Gag initiation site, to 697 nucleotides downstream of the Pol termination site. This fragment was cloned into the *Kpn*I and *Sal*I sites of pGem3Z+ vector (Promega) using linker oligonucleotides for ligation of the mismatched *Hha*I and *Kpn*I sites. These oligonucleotides conserved the *Kpn*I site and destroyed the *Hha*I site. The linker oligonucleotide sequences are presented in Table 2.5.

This placed the Gag-Pol coding region under the control of the pGem3Z+ T7 promoter. A 134 bp *Sal*I-*Pvu*I fragment from the pTNT vector (Promega) containing the polyA tail and T7 terminator signal was inserted into the *Sal*I site by ligating the complementary *Sal*I sticky ends, polishing the non-complementary ends with Klenow fragment (Promega) and blunt-end ligation. This resulted in the vector pGPtfs.

RT mutations were introduced into pGPtfs from the relevant pNL4.3 construct, and referred to as pGPtfs followed by the RT mutation i.e. pGPtfs-W401A (Table 2.6). These plasmids were generated by cloning the *Apa*I-*Not*I fragment from the relevant pNL4.3 encoding the W401A, T409I, W401A/T409I, W398A and W414A RT mutations (Section 2.1.2-1) into the *Apa*I-*Not*I sites in pGPtfs. All constructs were confirmed by RE digest analysis and DNA sequence analysis. Oligonucleotide primers used for sequence analysis of constructs are detailed in Table 2.8.

2.1.5 Plasmid propagation

Plasmids were transformed into *E.coli* strain Top10 (Invitrogen, Carlsbad, CA, USA) by heat-shock as previously described (Sambrook, 1989). All colonies and cultures were incubated at 30°C to minimise recombination (Joshi *et al.*, 1993). A single transformed colony was inoculated into Luria-Bertani medium (LB) containing 100 μg/ml ampicillin and/or 50 μg/mL kanamycin as required, and incubated at 30°C with shaking. Broths were inoculated and grown as recommended for DNA isolation using the QIAGEN mini, midi or maxi prep kits (QIAGEN, Hilden, Germany). Purified plasmid DNA was quantified by linearising the plasmid and DNA electrophoresis with a DNA of known concentration including the λ DNA-*Bst*EII (New England Biolabs, Beverly, MA, USA) and GeneRuler™ 1 kb Ladder (Fermentas Molecular Biology Tools, Thermo Fisher Scientific, Waltham, MA, USA). DNA was quantified using the Bio-Rad Molecular Imager Gel Doc XR System (Bio-Rad, Hercules, CA, USA). Plasmid DNA concentration and purity was confirmed by absorbance at 280 nm and 260 nm using the NanoDrop™ spectrophotometer (Thermo Fisher Scientific, Waltham, MA, USA).

Table 2.3. Bacterial expression vector pNLRT6H/PR constructs

Plasmid	RT mutation present
pNLRT6H/PR	Wild-type
pNLRT6H/PR-W401A	W401A
pNLRT6H/PR-T409I	T409I
pNLRT6H/PR-AI	W401A, T409I
pNLRT6H/PR-AY	C162Y, W401A
pNLRT6H/PR-AR	K366R, W401A
pNLRT6H/PR-AT	W401A, A534T
pNLRT6H/PR-AYRT	C162Y, K366R W401A, A534T

Table 2.4 Oligonucleotide primers for PCR amplification of the RT coding region and cloning into pNLRT6H/PR

Oligonucleotide	Oligonucleotide sequence (5'-3')	Location[a]
5'RTNotI-NL43[b]	GGCTGCACTGCGGCCGCTCCCATTAGTCC	4680-4723
3'RTBglII-NL43[c]	CCATCAGATCTTAGTACTTTCCTGATTCC	6370-6398

[a] Coordinates correspond to the pNL4.3N sequence described in (Buxton *et al.*, 2005)

[b] Underlined bases indicate the introduced *Not*I RE site

[c] Underlined bases indicate the introduced *Bgl*II RE site

Table 2.5. Linker oligonucleotides used to ligate the NL4.3 *Apa*I-*Sal*I fragment into the *Kpn*I and *Sal*I sites of pGem3Z+

Oligonucleotide	Oligonucleotide sequence (5'-3')[a]
upsGag_KpnHha+	CCACCATTATCACAGGCG
upsGag_KpnHha+	GGACACTTATTACCACCATG

[a] Underlined bases indicate nucleotides contributing to *Kpn*I site

Table 2.6. pGPtfs constructs for expression of Gag-Pol in the Promega TNT T7 Quick Coupled Transcription/Translation System

Plasmid[a]	RT mutation present
pGPtfs	Wild-type
pGPtfs-W401A	W401A
pGPtfs-T409I	T409I
pGPtfs-W401A /T409I	W401A, T409I
pGPtfs-W398A	W398A
pGPtfs-W414A	W414A

[a] Expresses full length Gag-Pol derived from NL4.3

Table 2.7 Oligonucleotides used to amplify the PR-RT and RT-IN coding regions for cloning into the vector pBluescript

Oligonucleotide	Oligonucleotide sequence (5'-3')[a]	RE site	NL4.3 Coordinates[b]
5'usPR	GCTGTTGGAAATGTCGACAGGAAGGACACC	SalI	4181-4211
3'dsRT401	CACTCAGGGATCCAGGTGGCTTGC	BamHI	5923-5950
5'usRT366	GGAGATTCTAAAGGATCCGGTACATGG	BamHI	5627-5654
3'dsIN	CCTAGTGGGATGTCGACTTCTGAAC	SalI	7352-7378

[a] Location of the RE site is underlined

[b] As referred to in Buxton *et al.* 2005

Table 2.8. Oligonucleotides primers for DNA sequence analysis

Oligonucleotide	Oligonucleotide Sequence (5'-3')	HXB2 Coordinates[a]	NL4.3N Coordinates[b]
SpCA	GGATGACAGAAACCTTGTTG	1282-1301	3894-3913
RspPR	GCTTTAATTTTACGTGTACAG	2115-2135	4727-4747
Sp1aV2	CTGAAAATCCATACAATACTC	2250-2270	4862-4882
Sp2a	TAGATATCAGTACAATGTG	2521-2539	5133-5151
Rsp2a	CACATCCAGTACTGTTAC	2411-2428	5023-5040
Sp3a	GATTTGTATGTAGGATCTG	2651-2669	5263-5281
Sp4a	GGACTGTCAATGACATACAG	2850-2869	5462-5481
Sp5a	CCATACAAAAAGAAACATG	3194-3211	5882-5900
Sp9a	GCAGGAAGATGGCCAG	4088-4103	6700-6715
Rsp9a	CTGGCCATCTCCCTGC	4088-4103	6700-6715
Sp10	CCTAGGTGTGAATATCAAGC	4977-4996	7589-7608

[a] As for HXB2 reference sequence NC_001802

[b] As referred to in Buxton *et al.* 2005

2.2 Cell Culture

2.2.1 Description and maintenance of cell lines

2.2.1-1 Media

DMEM-10 and RF-10 media was used for culturing of cell lines employed in this study. DMEM-10 is Dulbecco's Modified Eagle's Medium (DMEM, Invitrogen) supplemented with 10% heat inactivated Cosmic Calf Serum (Progen, Darra, Australia), 1% L-glutamine (Invitrogen), 100 U/mL of penicillin (Invitrogen), and 100 μg/ml of streptomycin (Invitrogen).

RF-10 is RPMI 1640 (Invitrogen) supplemented with 10% heat inactivated Cosmic Calf Serum (Progen, Qld, Australia), 1% L-glutamine (Invitrogen), 100 U/mL of penicillin (Invitrogen), and 100 μg/ml of streptomycin (Invitrogen).

2.2.1-2 HEK293T cells

The HEK293T cell line is an adherent cell line derived from human embryonic kidney cells that are readily transfectable, and express high levels of transfected material. These cells were obtained from R. Axel (Columbia University, New York City, NY, USA) and had been selected for increased adherence. Cells were maintained in DMEM-10 (Section 2.2.1-1) at 37°C with 5% CO_2 in a humidified incubator, and passaged approximately every four days by a 1/10-1/20 dilution.

2.2.1-3 MT-2 cells

MT-2 cells are a non-adherent HTLV-1 transformed lymphocyte line (Harada *et al.*, 1985). MT-2 cells were maintained in RF-10 (Section 2.2.1-4) and incubated at 37°C with 5% CO_2 in a humidified incubator. MT-2 cells were passaged every four days by a 1/4-1/10 dilution in RF-10 (Section 2.2.1-1).

2.2.1-4 TZM-bl cells

The TZM-bl indicator cell line was obtained through the NIH AIDS Research and Reference Reagent Program, contributed by Dr John C. Kappes, Dr Xiao Yun Wu and Transomed Inc. (Platt *et al.*, 1998; Derdeyn *et al.*, 2000; Wei *et al.*, 2002). Previously designated JC53-bl (clone 13), the TZM-bl cell line is a HeLa derivative that expresses high levels of CD4 and CCR5 along with endogenously expressed CXCR4, and is highly sensitive to infection with diverse isolates of HIV-1. TZM-bl cells contain β-galactosidase (β-gal) and luciferase reporter cassettes, expressed from a HIV LTR-driven promoter activated by HIV Tat expression. TZM-bl cells were maintained in DMEM-10 (Section 2.2.1-4) at 37°C with 5% CO_2 in a humidified incubator. Cells were passaged approximately every seven days by a 1/10 dilution in DMEM-10 (Section 2.2.1-1).

2.3 Production of HIV-1 by transfection and preparation of viral and cell lysates.

2.3.1 Transfection

Wild-type and mutant HIV-1 was generated by transient transfection of HEK293T cells with plasmids containing the NL or HX molecular clones by calcium phosphate co-precipitation (Pear *et al.*, 1993). Briefly, 24 h prior to transfection, 2x 10^6 HEK293T cells were seeded into 10 cm diameter tissue culture plates. The cell layer was approximately 70% confluent at the time of transfection. Ten micrograms of the plasmid encoding the relevant HIV-1 molecular clone (Sections 2.1.2-1 and 2.1.2-2), or pUC19 (New England Biolabs, Beverly, MA, USA) for mock controls, together with 2μg of an eGFP reporter plasmid (Section 2.1.1) was added to 50 μl 2.5 M $CaCl_2$ and sterile ddH_2O to a total volume of 500 μl. This mixture was added drop wise to 500 μl 2x HBS (Appendix I) and mixed by pipetting. When the formation of the $Ca_3(PO_4)_2$-DNA complex formed a visible precipitate, the mixture was added drop wise to the plated HEK293T cell culture, gently but thoroughly rocked then incubated at 37°C with 5% CO_2. Approximately 10 h post transfection, cells were washed with warm PBS(-) (Invitrogen) and replaced with fresh DMEM-10 (Section 2.2.1-1).

2.3.2 Preparation of virus stocks and viral lysates

Approximately 36 h post transfection the culture supernatant was collected and clarified by centrifugation at 1500 rpm (400 g) for 10 min (Beckman Tabletop Centrifuge GS-6R, Beckman Coulter, Pasadena, CA, USA) and filtered through a sterile 45-micron syringe filter. The clarified supernatant was split into two aliquots and stored at -80°C for infectivity (Section 2.6) or RDDP assays (Section 2.7). The remainder subjected to concentration by ultracentrifugation.

For ultracentrifugation the supernatant was overlayed on 2 mL of 25% w/v sucrose in TEN (Appendix I) and centrifuged for 1 h at 4°C at 26,500 rpm (87,000 g) in SW 28 rotor (Optima™ L-90 K Ultracentrifuge, Beckman Coulter). The supernatant was decanted and the virus pellet resuspended in 150 μL of 2x SDS sample buffer (Appendix I), which was immediately denatured by incubation at 95°C for 3 min, and stored at –20°C prior to Western blot analysis (Section 2.5).

2.3.3 Preparation of transfected cell lysates

Following harvesting of the supernatant (Section 2.3.2), transfected HEK293T cell cultures were washed with 10 mL of warm PBS(-), collected in 5 mL of PBS(-) and pelleted by centrifugation at 400 g (1500 rpm) for 10 min (Beckman Tabletop Centrifuge GS-6R, Beckman Coulter). The cell pellet was resuspended in 250μl of TEN (Appendix I) and lysed by the addition of 250μl of 2x TNEN lysis buffer (Appendix I). Cell lysates were clarified by centrifugation at 14,000 rpm (18,500 g) for 30 min at 4°C (5417R Refrigerated Microcentrifuge, Eppendorf, Hamburg, Germany).

An aliquot was taken for immediate eGFP quantification (Section 2.3.5). The remaining sample was added to an equal amount of 2×SDS sample buffer (Appendix I), denatured by incubation at 95°C for 3 min, and stored at –20°C prior to Western blot analysis.

2.3.4. Production of HIV-1 by transfection in the presence of indinavir

Indinavir (IDV) as the sulphated form was obtained through the NIH AIDS Research and Reference Reagent Program, and prepared as a 10 μM stock in dimethyl sulfoxide (DMSO, Sigma Aldrich, St. Louis, MO, USA). For the production of HIV-1 in the presence of IDV, the following adaptations were made to the transfection protocol described in Sections 2.3.1-2.3.3. IDV was added to seeded HEK293T cells 1 h prior to transfection, at a final concentration of 0, 0.1, 1.0 or 10 μM. The same concentration of IDV was added to PBS(-) and DMEM-10 used for subsequent washes and media changes. Upon harvesting of supernatant and cell cultures, a 2-fold excess of IDV was added to PBS(-) used for washes and collection.

2.3.5 Determination of transfection efficiency

A series of 2-fold dilutions of clarified cell lysate in TEN buffer (Section 2.3.3) was prepared in a black-walled 96 well flat bottom plate (BD Biosciences, Franklin Lakes, NJ, USA). The transfection efficiency was directly related to the amount of fluorescence generated by the co-transfected eGFP in cell lysates. Fluorescence was detected using the Fujifilm FLA-3000 Fluorescence and Storage Phosphor Imager (FujiFilm Life Science, Tokyo, Japan) and quantified using the Image Gauge software, version 3.3 (FujiFilm Life Science). Low transfection efficiencies were defined as fluorescence less than 90% of the pUC 19 control transfected cell lysates. These viral and cell lysates were not used in subsequent experiments.

2.4 Serial passage and cloning of HIV-1 from culture.

2.4.1 Serial passage of replication defective W401A HIV-1

NL-W401A was produced from transfection of HEK293T cells with pNL4.3-W401A as described in Section 2.3. Approximately 30 mL of clarified culture supernatant from HEK293T cells transfected with pNL4.3-W401A was concentrated by ultracentrifugation as described in Section 2.3.2 and resuspended in 1 mL of RF-10 (Section 2.2.1-1). The concentrated NL-W401A stock was used to infect 4×10^5 MT-2 cells in a total of 4 mL of RF-10, which was incubated for 2 h in a humidified incubator at 37°C with 5% CO_2, after which RF-10 was added to a total volume of 10 mL. An infection was performed in parallel using 1 mL of clarified supernatant from HEK293T cells transfected with pNL4.3 wild-type as described in Section 2.3.

Infected MT-2 cultures were passaged approximately every four days by a 1:4 dilution in RF-10. HIV-1 induced cytopathic effect (CPE) was monitored by light microscopy. For wild-type infected cultures, where CPE was frequently observed at greater than 80% at the time of passage, 500 µL of culture supernatant was added to 4×10^5 uninfected MT-2 cells in a total of 10 mL RF-10. Evidence of increasing CPE in NL-W401A infected cultures was monitored, and aliquots harvested at passage 14 and passage 25.

2.4.2 Biological cloning of serial passaged virus by terminal dilution

In order to isolate a single clone of HIV-1 from infected MT-2 cultures, the infected culture was biologically cloned by three sets of terminal dilutions in MT-2 cells. 1.8×10^4 MT-2 cells were seeded in a 96 well plate and inoculated with serial 10-fold dilutions of culture supernatant from MT-2 cells infected with NL-WT or NL-W401A undergoing serial passage (Section 2.4.1). Six days post-infection supernatant from MT-2 cells displaying CPE at the highest dilution was collected and the procedure repeated.

After the third terminal dilution, virus present in supernatant from infected cells from a single well at the most dilute inoculum was used to infect 4×10^5 MT-2 cells in a total of 10 mL or RF-10. Infected cells were incubated at 37°C with 5% CO_2 in a humidified incubator until CPE reached 80%. Culture supernatant was collected and clarified by centrifugation at 1500 rpm (400 g) for 10 min (Beckman Tabletop Centrifuge GS-6R, Beckman Coulter) and filtered through a sterile 45 micron syringe filter. The clarified supernatants were stored in aliquots at -80°C.

2.4.3 Molecular cloning of the *pol* regions from serial passaged HIV-1.

An aliquot of serially passaged biologically cloned HIV-1 (Section 2.4.2) was used to infect 4×10^5 MT-2 cells. The culture was incubated in a humidified incubator at 37°C with 5% CO_2 and inspected daily until HIV-1 induced CPE was observed in approximately 75% of the culture. Infected cells were collected by low speed centrifugation at 1500 rpm (400 g) for 10 min (Beckman Tabletop Centrifuge GS-6R, Beckman Coulter). The cell pellet was washed by suspension in warm PBS(-) and pelleted again by low speed centrifugation. The cell pellet was resuspended in 200 µL PBS(-), and the genomic DNA isolated using the QIAamp Blood Kit (QIAGEN) as per the manufacturer's instructions.

The Pol coding region was amplified from the isolated genomic DNA in two overlapping fragments. The PR-RT coding region was amplified with primer pair 5'usPR and 3'dsRT401, and the RT-IN coding region amplified with primer pair 5'usRT366 and 3'dsIN. Each primer was designed with a *Bam*HI or *Sal*I site for cloning. The primer sequences are detailed in Table 2.7.

The resulting PCR amplicons were digested with the relevant RE and cloned into the MCS of pBluescript SK(+) (Stratagene). The resulting plasmids were screened following propagation and purification as described in Section 2.1.5. Clones containing the desired insert were identified by RE digest analysis, and subjected to DNA sequence analysis using the primers listed in Table 2.8.

2.5 Western blot analysis

At the commencement of this study a quantitative Western blotting system was not available, and for all data presented in Chapter 3, the western blots were performed as described in Section 2.5.2. Densitometry analysis performed on the blots provided semi-quantitative analysis. For all other chapters, Western blot imaging and quantitation was performed using the Odyssey Infrared Imaging System (Section 2.5.3).

Transfection efficiency (2.3.5) was used to normalise both viral and cell lysates for Western blot analysis using antibodies directed against p24 (CA) (Section 2.5.5-1) to determine viral particle production (Section 2.5.4-1). Viral and transfected cell lysates were then normalised to equivalent amounts of p24 and subject to Western blot analysis using antibodies against HIV-1 proteins RT, IN, and polyclonal antibodies (Section 2.5.5).

2.5.1 SDS polyacrylamide gel electrophoresis

Viral and cell lysates were prepared for Western blot analysis as described in Section 2.3. Samples in SDS-sample buffer were heated to 95°C for 3 min directly before loading onto a 7.5-10% SDS-polyacrylamide gel. Samples were electrophoresed at 200 V in a Bio-Rad Mini Protean 3 cell (Bio-Rad) for 45-55 min.

2.5.2 Western blot detection using enhanced chemiluminescence

The SDS-PAGE gel was subjected to wet transfer for electroblotting of proteins onto a PVDF membrane (Immobilon-P Transfer membrane, Millipore, Billerica, MA, USA) using a Bio-Rad Mini Protean 3 cell (Bio-Rad) for 1.5 h at 300 mA.

The membrane was blocked for 30 min in TBST-(0.5%) (Appendix I) containing 5% skim milk at room temperature with rocking. The membrane was rinsed in TBST-(0.5%) then incubated with primary antibody diluted in TBST-(0.5%) at room temperature with rocking for 1 h. The membrane was washed three times for 5 min in TBST-(0.5%), then incubated with the appropriate secondary horseradish peroxidase conjugated antibody diluted in TBST-(0.5%) with 5% skim milk for 45 min. The membrane was again washed three times for 5 min in TBST-(0.5%). The membrane was visualised using enhanced chemiluminescence (Amersham ECL Plus™, GE Healthcare, Little Chalfont, UK). The membrane was incubated with ECL Plus according to the manufacturers instructions, exposed to film (Amersham Hyperfilm, GE Healthcare), manually developed and

fixed. Films were scanned and quantified by densitometry using Image Gauge software, version 3.3 (FujiFilm Life Science) as previously described (Klein *et al.*, 2001).

2.5.3 Western blot detection using the Odyssey Infrared Imaging System

For Western blot analysis using the Odyssey Infrared Imaging System (LI-COR Biosciences, Lincol, NE, USA) the SDS-PAGE gel (Section 2.5.1) was subjected to wet transfer and proteins electroblotted onto a supported mixed ester nitrocellulose membrane (Amersham Hybond™-C Extra, GE Healthcare) using a Bio-Rad Mini Protean 3 cell (Bio-Rad) for 1.5 h at 300 mA. The membrane was blocked for 30 min in TBS (Appendix I) containing 2% skim milk at room temperature with rocking. The membrane was rinsed in TBS, and then incubated with primary antibody diluted in TBST-(0.2%) at room temperature with rocking for 1 hr. The membrane was washed four times for 3 min in TBST-(0.2%), then incubated with the appropriate secondary antibody in TBST-(0.2%) supplemented with 0.01% SDS and 2% skim milk at room temperature with rocking for 45 min. The membrane was washed four times for 3 min in TBST (0.2%) and rinsed in TBS. Blots were imaged on the Odyssey Imager. Scan resolution of the instrument was set at 169 μm. Quantification was performed using Odyssey software version 2.0.

2.5.4 Protein quantification and calculation of viral particle production

2.5.4-1 HIV-1 protein quantification

The quotient of the protein of interest and p24 was determined in each experiment and expressed as the percentage of the wild-type quotient. Data from at least three independent assays were subjected to statistical analysis (Section 2.11).

2.5.4-1 Calculation of HIV-1 particle production

Viral particle production of wild-type and mutant HIV-1 from transfected cells was calculated following Western blot analysis of viral and transfected cell lysates. Viral particle production was determined as the total p24 and $Pr55^{Gag}$ in viral lysates divided by the total p24 and $Pr55^{Gag}$ in viral and transfected cell lysates Shehu-Xhilaga *et al.*, 2004. Data from independent assays were subjected to statistical analysis (Section 2.11).

2.5.5 Antibodies used in Western blot analysis

2.5.5-1 Monoclonal antibodies

Monoclonal antibody preparations and hybridomas producing RT monoclonal antibodies (5B2, 7E5, 11G10) (Szilvay *et al.*, 1992) and monoclonal anti-IN antibody (8E5) (Nilsen *et al.*, 1996) were kindly provided by D. Helland (University of Berger, Berger, Norway). These monoclonal antibodies were used at a 1:100 dilution. Monoclonal RT antibodies included 11G10, which recognises an epitope 1 (aa 193-284), RT antibody 5B2 recognises epitope 2 (aa 294-319), and RT

antibody 7E5 recognises an epitope in the RNase H domain and is hence p66 specific. The IN monoclonal antibody 8E5 recognises an epitope in the C-terminal of IN (aa 262-271).

Monoclonal antibody and hybridomas producing monoclonal antibody 183-H12-5C were provided by A. Poumbourios (Burnet Institute), which was contributed by Bruce Chesebro to the NIH AIDS Research and Reference Reagent Program, Division of AIDS, NIH (Chesebro *et al.*, 1992). This antibody recognises mature p24, p24 within Gag, and p24 containing Gag processing intermediates. 183-H12-5C was used at 1:1000 dilution.

The secondary antibody Amersham ECL™-HRP linked sheep anti-mouse IgG antibody (GE Healthcare, Little Chalfont, UK) was used for visualisation of viral proteins by ECL with all monoclonal primary antibodies. For visualisation using the Odyssey Imager, secondary antibody Alexa Fluor 680 goat anti-mouse IgG (Molecular Probes, Invitrogen) was used with all monoclonal primary antibodies.

2.5.5-2 Polyclonal antibodies

Pooled HIV-1 positive patient serum and secondary anti-human HRP linked antibody (Dako) was kindly provided by J. Mak (Burnet Institute) Hill *et al.*, 2002. Rabbit polyclonal RT antibodies were generated by IMVS custom antibody service (IMVS, Adelaide, Australia) using recombinant HIS-tagged p66 as the immunogen. Recombinant p66-HIS for rabbit immunisation was prepared by K. Moore (Tachedjian laboratory) using the methodology described in Section 2.8. Sera was used at a 1:7,500 dilution. For visualisation using ECL, the secondary antibody used was Amersham ECL™-HRP linked donkey anti-rabbit IgG whole antibody (GE Healthcare, Little Chalfont, UK). For use with Odyssey Imager the secondary antibody used was IR Dye 800 goat anti-rabbit IgG (LI-COR Biosciences) used at a 1:5000 dilution.

2.6 Viral Infectivity Assays

2.6.1 Normalisation of HIV-1

HIV-1 produced by transfection of HEK293T cells was normalised to equivalent amounts of virion p24 as determined by Western blot analysis. For virus obtained from infected MT-2 cell cultures, HIV-1 was normalised to equivalent amounts of virion p24 as determined by p24 ELISA, using the Vironostika HIV-1 Antigen MicroElisa system (bioMerieux Marcy l'Etoile, France) according to the manufacturer's instructions

2.6.2 Determination of the HIV-1 $TCID_{50}$ in MT-2 cell culture

MT-2 cells (1.8×10^4) were seeded into a flat-bottomed 96-well tissue culture plate (BD Biosciences, Franklin Lakes, NJ, USA) and inoculated with 10-fold serial dilutions of virus in quintuplicate. Cultures were observed daily for HIV-1 induced syncytium formation by light microscopy. Six

days post infection, the presence of virus induced CPE was scored in each well as either positive or negative, and the median tissue culture infective dose ($TCID_{50}$/mL) of each virus was calculated using the Karber formula (Hawkes, 1979). Independent experiments were subjected to statistical analysis (Section 2.11).

2.6.3 Determination of the HIV-1 titre in the TZM-bl cell line

TZM-bl cells (2×10^4) were seeded in a flat-bottomed 96-well tissue culture plate 24 h prior to infection. The following day media was removed and replaced with serial dilutions of virus stock in quadruplicate in DMEM-10 with a 40 μg/mL final concentration of DEAE-dextran (GE Healthcare, Little Chalfont, UK) in a final volume of 50 μl. Each dilution was assayed in quadruplicate. Mock-infections were performed using DMEM-10 containing 40 μg/mL DEAE-dextran. Cultures were incubated for 1 h at 37° C after which 150 μl of DMEM-10 was added to each well and incubated for a further 48 h at 37° C in 5% CO_2. Culture supernatant was aspirated and cells fixed (Fixing solution, Appendix I) for 5 min at room temperature, washed in warm PBS(-) then stained for 1 h at 37°C for β-galactosidase activity (Staining Solution, Appendix I). Following two washes with PBS(-), blue foci were counted by microscopy as previously described (Derdeyn *et al.*, 2000). Mock-infected cells typically showed no blue stained cells. The number of infectious units was calculated for the dilution factor where between 25-250 blue foci were counted. The count was multiplied by the dilution factor, replicates averaged and expressed as infectious units (IU) per mL of culture supernatant. The percentage of the wild-type titre was determined, and independent experiments were subjected to statistical analysis (Section 2.11).

2.7 Reverse Transcription assays

2.7.1 RDDP activity assay

The RDDP assay was used to detect RDDP activity of virion-associated RT produced from transfection of HEK293T cells with HIV molecular clones (Section 2.3) or recombinant RT (Section 2.8). For the former, clarified supernatants from virus cultures stored at -20°C were rapidly thawed at 37° C, lysed with an equal volume of 0.3% IGEPAL CA-630 (Sigma Aldrich, St. Louis, MO, USA) and maintained on ice until use. Equivalent amounts of lysate as determined by p24 Western blot analysis and quantification (Section 2.5.3) were subjected to the RDDP assay. Supernatant from mock transfected cells were used as a negative control.

Following purification, bacterially expressed recombinant RT (Section 2.8) was diluted 1:5 (v/v) in dilution buffer and normalised equivalent amounts of p66 as determined by Western blot analysis and quantification using the Odyssey Imaging system (Section 2.5.3). Dilution buffer was used as a negative control.

Each sample was tested in triplicate. A 20 µL sample was added to 40 µL of RT buffer (Appendix I) containing Poly(rA)/oligo(dT) template/primer and ^{33}P dTTP, gently mixed, and incubated at 37° C for 1 h. A 5 µL aliquot of the reaction was spotted onto Whatman DE81 anion exchange paper (Sigma Aldrich, St. Louis, MO, USA) and left for 5 min to air dry. The membrane was washed with gentle rocking in 2× SSC (Appendix I) at room temperature for 5 min, followed by two 15 min washes in 2× SSC. A final rinse was performed in 95% ethanol. The membrane was dried thoroughly by incubation in a 65°C oven for 30-60 min depending on the size of the membrane. The membrane was exposed to a FujiFilm imaging plate for 24 h. Incorporated radiolabel was detected as photo-stimulated luminescence (PSL) using the Fujifilm FLA-3000 Phosphor Imager (FujiFilm Life Science) and quantified using Image Gauge software, version 3.3 (FujiFilm Life Science). The background signal generated by the mock reaction was subtracted and the mean of triplicates was determined. The PSL for each mutant was expressed as the percentage of wild-type, and independent experiments were subjected to statistical analysis (Section 2.11).

2.7.2 Detection of intracellular reverse transcription products

Specific stages of reverse transcription can be detected using primer combinations to target reverse transcriptase intermediates. The primers M667 (5' GGCTAACTAGGGAACCCACTG 3'), AA55 (5' CTGCTAGAGATTTTCCACACTGAC 3'), and M667 (5'CTGCTAGAGATTTTCCACACTGAC 3') were employed to detect late and early transcripts as described by Zack and colleagues (1990). Primer pair M667/AA55 was used to amplify the R/U5 junction and can be used to detect early HIV-1 transcripts. The primer pair M667/M661 was used to amplify the [LTR]/gag region and hence can be used to detect late transcripts as described in (Zack *et al.*, 1990). Semi-quantitative PCR was used to detect early and late viral DNA synthesis in infected MT-2 cell lysates. To degrade any residual plasmid DNA introduced by transfection, clarified HIV-1 stocks produced by transfection (Section 2.3.1-2.3.2) were treated with RNase-free DNase I (Roche, Basil, Switzerland) at a concentration of 10 U/mL of supernatant in the presence of 10 mM $MgCl_2$ at 37°C for 30 min. The supernatant was subjected to PCR using the M667/AA55 primer pair. Each reaction contained 5 µL of supernatant, 2.5 mM $MgCl_2$, 400 nM of each primer, 200 µM each dNTP, and 2.5 U HotStarTaq (QIAGEN). The thermocycler program contained an initial activation step of 95°C for 15 min, followed by 30 cycles of 94°C for 30 sec, 60°C for 30 sec, 72°C for 1 min, followed by a final extension step of 72°C for 15 min. A 10 µL aliquot of the PCR reaction was analysed by gel electrophoresis on a 2% agarose gel. The absence of an amplicon of 140 bp indicated that the treated supernatant was negative for residual plasmid DNA, and was used to infect MT-2 cells.

Approximately 4×10^5 MT-2 cells were infected with the equivalent of 500 ng p24 in a total of 2 mL. Infection proceeded for 1 h in a humidified incubator at 37°C with 5% CO_2, after which the culture was made up to 10 mL with RF-10. At 6 h post infection cells were pelleted by low speed centrifugation (1500 rpm/400 g for 10 mins, Beckman Tabletop Centrifuge GS-6R, Beckman Coulter), washed with warm PBS(-) pelleted again and the supernatant removed. The cell pellet was lysed with 100 µL of PCR lysis buffer (Appendix I) followed by the addition of 20 mg of Proteinase K (Roche, Basil, Switzerland) incubation at 60°C for 1 h. Proteinase K was then heat inactivated by incubation at 95°C for 15 min. Treated cell lysates were standardised to equivalent amounts of cellular DNA as determined by PCR for the cellular locus HLA-DQα using the primer pair GH26/GH27 (Lee *et al.*, 1991). A 10 µL aliquot of the PCR reaction was subjected to electrophoresis on a 2% agarose gel to resolve the 242 bp product, visualised using the Fuji Film LAS-1000plus (FujiFilm Life Science) and quantified using Image Gauge software, version 3.3 (FujiFilm Life Science). Undiluted, 1:3, 1:10, and 1:30 dilutions of normalised cell lysates were subject to the PCR described above with the exception that the number of cycles was reduced from 30 to 25, and both the M667/AA55 and M667/M661 primer pairs were used in separate reactions to detect early and late HIV-1 transcripts, respectively. A serial dilution of ACH-2 cell lysates was also subjected to these PCR reactions to provide both standards and a positive control as previously described Sonza *et al.*, 1996. ACH-2 cells are a chronically infected T lymphocyte cell line that contain a single copy of the integrated HIV provirus per cell Folks *et al.*, 1989. A 10 µL aliquot of the PCR reaction was subjected to electrophoresis on a 2% agarose gel to resolve the 140 bp product.

2.8 Expression and purification of recombinant RT.

Recombinant RT was generated using the bacterial expression vector pNLRT6H/PR (Section 2.1.3) as previously described for pRT6H/NB-PROT (Tachedjian *et al.*, 2003). Briefly, pNLRT6H/PR expressing wild-type or mutant RT (Table 2.3) were propagated in *E.coli* strain M15, induced with isopropyl-β-D-thiogalactopyranoside (IPTG), and incubated with shaking at 37°C for 3 h. Bacterial cultures were harvested by centrifugation at 2500 g for 10 min (Beckman J2-21M/E centrifuge, Beckman Coulter). The bacterial pellets were washed in 50 mM phosphate buffer pH 7.8 (Appendix I) and resuspended in A/78 buffer (Appendix I). Pellets were lysed by the addition of lysozyme at a final concentration of 1 mg/mL and incubated on ice with occasional mixing for 30 min. Benzonase nuclease (Merck, Whitehouse Station, NJ, USA) was added to lysates at a final concentration of 5 U/mL and incubated on ice for a further 30 min. NaCl was added to a final concentration of 500 mM prior to centrifugation at 100,000 g 1 h at 4°C (SW 41 rotor, Optima™ L-90 K Ultracentrifuge, Beckman Coulter).

The soluble fraction was harvested and imidazole was added at a final concentration of 10 mM. Heterodimer formation was determined by subjecting lysates to metal chelate chromatography. Lysates were adjusted to 10 mM imidazole. A 50% slurry of Ni-NTA agarose equilibrated in buffer A/78+ containing 20 mM imidazole was prepared, and added to the lysates and incubated for 1 h at 4°C with rocking. This was applied to Poly-Prep Column (Bio-Rad) and washed twice with 10 volumes of A/78+ containing 20 mM imidazole at 4°C.

HIS tagged p66 and co-associating p51 bound to the Ni-NTA agarose was eluted with A/78+ buffer containing 200 mM imidazole. The eluate was dialyzed overnight in dialysis buffer (Appendix I). Dialysed RT was diluted 1:5 (v/v) in dilution buffer and subject to Western blot analysis (Section 2.5.2) using RT monoclonal antibody 11G10 (Section 2.5.4-1). Equivalent amounts of purified recombinant RT based on the p66 subunit were assayed for RDDP activity as described in Section 2.7.1.

2.9 Far UV Circular dichroism analysis of recombinant RT

CD spectra were collected for recombinant RT, expressed and purified as described in Section 2.8. Prior to CD analysis recombinant RT was dialyzed overnight at 4°C in 50 mM sodium phosphate buffer, pH 7.4 (Appendix I). The protein concentration was adjusted to 300μg/mL as determined using a NanoDrop™ 1000 photospectrometer (Thermo Fisher Scientific, Waltham, MA, USA). The CD spectra were collected at ambient room temperature over the 190-250 nm range using an Aviv Instruments Circular Dichroism Spectrometer Model 202 (Aviv Biomedical, Lakewood, NJ, USA).

2.10 In vitro transcription/translation of $Pr160^{Gag\text{-}Pol}$

The T7 TNT® Quick Coupled Transcription/Translation System (Promega) was used to assay the initial Gag-Pol cleavage events mediated by the embedded PR as previously described (Pettit *et al.*, 2003). The reticulocyte lysate system with methionine/cysteine ^{35}S translabel was used. The pGPtfs plasmids were designed for use in this system (Section 2.1.4) and encode a full-length, frameshifted $Pr160^{Gag\text{-}Pol}$ derived from the NL4.3 HIV-1 molecular clone, with wild-type or mutant RT as detailed in Table 2.6. According to the manufacturer's instructions, 1 μg of circular plasmid was incubated with 40μL TNT Quick Master Mix and 2 μL of Promega enhancer mix at 30°C. Aliquots of 10 μL were taken at 30 min, 1,2,4 and 6 h, and added to 50 μL ddH_2O and 60μl 2x SDS sample buffer (Appendix I). The samples were heated to 65°C for 20 min prior to SDS-PAGE electrophoresis on a 9% acrylamide gel using the Gibco-BRL V16-2 (Biometra) apparatus, at 35 mA per gel for 550 min at 4°C. Dried gels were exposed to a FujiFilm imaging plate for 24 h and imaged on the Fujifilm FLA-3000 Phosphor Imager (FujiFilm Life Science).

2.11 Statistical analysis

Statistical analysis was performed by program GraphPad Prism (GraphPad Software, San Diego, CA, USA), which determined the mean, standard error of the mean, and p value for data sets. All data was assumed to have a non-Gaussian distribution and as such were analysed using nonparametric tests. Data sets consisting of two groups were compared using the Wilcoxon matched-pairs signed rank test. Data sets consisting of three or more groups were compared using the Kruskal-Wallis test to determine whether the means varied significantly, and the Dunn's post-test was employed to determine significant differences between two nominated groups.

Chapter 3

The role of tryptophan repeat motif residue W401 in HIV-1 replication: implications for the role of RT dimerisation

3.1 Introduction

The tryptophan repeat motif (TRM) is an important region for RT subunit interaction (Divita *et al.*, 1993; Tachedjian *et al.*, 2003; Mulky *et al.*, 2005b; Tachedjian *et al.*, 2005b). The TRM is a series of highly conserved hydrophobic residues consisting of six tryptophans and a single tyrosine located at RT codons W398, W401, W402, Y405, W406, W410, and W414. These amino acids are located in secondary structure elements αL, β20, and the loop that spans these two elements (Jacobo-Molina *et al.*, 1993). Within the asymmetric heterodimer, the TRM is unique as it is the only instance where a residues belonging to a motif in both the p66 and p51 motif interact at the heterodimer interface.

The p66 αL-β20 loop is buried upon heterodimerisation and forms multiple interactions at the heterodimer interface (Menendez-Arias *et al.*, 2001; Rodriguez-Barrios *et al.*, 2001; Srivastava *et al.*, 2006). Interestingly, mutational analyses suggest that it is the p66 αL-β20 peptide main chain, as well as side-chains that form interactions with residues in the p51 subunit (Tachedjian *et al.*, 2003; Mulky *et al.*, 2005b). In p51 subunit the majority of the αL-β20 secondary structures are internalised and only TRM residues W401 and Y405 contribute to the p51 heterodimer interface (Menendez-Arias *et al.*, 2001; Rodriguez-Barrios *et al.*, 2001; Srivastava *et al.*, 2006).

Non-conservative mutation of W401 to alanine or leucine prevents RT subunit dimerisation (Tachedjian *et al.*, 2003; Mulky *et al.*, 2005b). Subunit specific analysis reveals that the dimerisation defect is mediated primarily through the p66 subunit. However, as $p66^{W401}$ does not directly contribute to the p66 dimer interface, this effect cannot be directly attributed to the loss of inter-subunit interactions contributed by W401. Tachedjian and colleagues (2003) hypothesise that the presence of an aromatic side-chain at this position is essential for maintaining the position of the p66 αL-β20 loop, and consequently the multiple interface interactions formed between the loop and the p51 subunit (Tachedjian *et al.*, 2003). Correspondingly, mutation of W401 to phenylalanine maintains wild-type levels of subunit interaction (Tachedjian *et al.*, 2003; Tachedjian *et al.*, 2005b).

Mutation of $p51^{W401}$ alone is not sufficient to prevent RT subunit dimerisation, but does reduce subunit interaction consistent with the loss of a single interface interaction (Tachedjian *et al.*, 2003; Mulky *et al.*, 2005b). Non-conservative mutation of W401 in both subunits has a cumulative effect on RT subunit interaction (Tachedjian *et al.*, 2003; Mulky *et al.*, 2005b).

Pleiotropic effects on Gag-Pol stability and/or virion incorporation have been described for previously characterised RT mutations in HIV-1 (Section 1.10), notably the dimerisation defective L234D/A mutation (Yu *et al.*, 1998a; Buxton *et al.*, 2005). It is hypothesised that these mutations confer long-range conformational changes that affect both conformation of RT and Gag-Pol.

In contrast, introduction of a non-conservative mutation at W401 is hypothesised to mediate an RT dimerisation defect by changes localised to the p66 αL-β20 loop (Tachedjian *et al.*, 2003). Loops are characterised by the absence of regular secondary structure, and can typically exist in a range of conformations (Leszczynski *et al.*, 1986). Loop regions are not well-defined chiroptically (Woody, 1996). Correspondingly, the W401 mutations result in no detectable change to RT secondary structure as observed by CD analysis (Tachedjian *et al.*, 2003).

Hence the RT W401 mutations characterised by Tachedjian and colleagues (2003) provide a unique tool with which to investigate the effect of perturbing RT dimerisation on HIV-1 replication. It was hypothesised that as mutation of W401 does not result in changes to regular secondary structure elements in RT as observed by CD analysis, mutation of this residue would not adversely affect Gag-Pol structure. Thus expression of mutations that confer a dimerisation defect, W401A and W401L, would allow the role of RT dimerisation in HIV-1 replication to be discerned, independent of pleotropic effects on Gag-Pol conformation, stability, or virion incorporation. Further, the role of RT subunit dimerisation would be confirmed by the absence of such defects upon examination of the RT dimerisation competent W401F mutation in HIV-1.

Corresponding with this hypothesis, mutation of W401 in HIV-1 did not adversely affect viral particle production, the virion Gag processing profile, or levels of virion Gag-Pol and IN, indicative that these mutations did not affect virion incorporation of Gag-Pol or stability. However, specific decreases in the levels of mature RT were observed in W401A/L mutant HIV-1. These mutant viruses also demonstrated significant reductions in RT activity and HIV-1 infectivity. While a role for the RT domain in PR activation has been described (Figueiredo et al., 2006), no evidence of delayed PR activation was observed in W401A/L mutant HIV-1. Lastly, these defects were not observed upon expression of the W401F mutation, confirming that these defects were specific to mutations that confer a RT dimerisation defect.

3.2 Results

3.2.1 Mutation of RT residue W401 does not affect HIV-1 viral particle production or maturation.

Mutations within the RT domain can adversely affect the production of mature virus particles (Quillent *et al.*, 1996; Yu *et al.*, 1998a; Olivares *et al.*, 2004; Chiang *et al.*, 2010). Hence HIV-1 expressing mutations at W401 were examined for decreases in viral particle production from HIV-1 transfected cell culture (Section 2.3). The RT mutations W401F, W401A and W401L were examined in the HIV-1 molecular clone, HX, which does not express the viral accessory proteins Vif, Nef and Vpu. These proteins are dispensable for the generation of infectious HIV-1 in cell culture although they are important in promoting viral replication and infectivity *in vivo*. To confirm the role of RT dimerisation in HIV-1 replication W401A was also examined in the HIV-1 molecular clone NL, which expresses the full complement of accessory proteins.

The presence of the RT mutations at W401 in either HX or NL did not affect viral particle production from transfected HEK293T cell cultures (Fig. 3.1). The effect of the W401 mutations on viral particle maturation was assessed qualitatively by Western blot analysis of the virion Gag processing profile as observed by detection of mature and precursor associated p24 in both viral lysates (Fig. 3.2A) and transfected cell lysates (Fig. 3.2B). All W401 mutants demonstrated a similar profile to their respective wild-type with respect to immature Gag, mature p24, and Gag processing intermediates which likely correspond to previously characterised Gag processing intermediates pi49 and p39 (Pettit *et al.*, 1994; Pettit *et al.*, 2002) (Fig. 3.2). These data demonstrate that the W401 RT mutants do not effect the production of viral particles or PR mediated Gag maturation in viral particles.

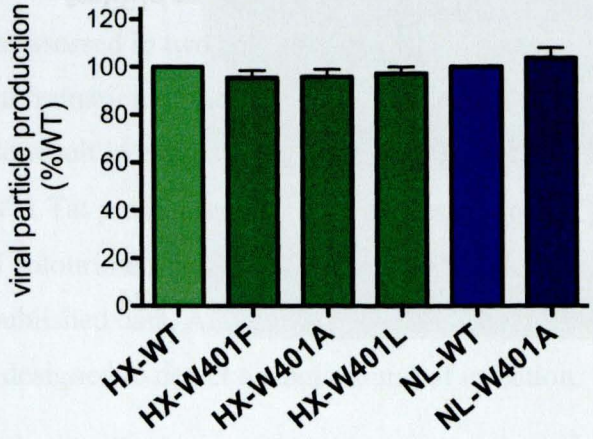

Figure 3.1. HIV-1 particle production of wild-type and W401 mutant HIV-1.

The HIV-1 molecular clones HXB2 (HX) or NL4-3 (NL) encoding wild-type (WT) or W401 RT mutations were used to transfect HEK293T cells. Transfection efficiency was monitored by co-transfection with an eGFP producing plasmid. Equivalent amounts of viral and transfected cell lysates, as determined by transfection efficiency, were subjected to Western blot analysis using p24 primary antibody 183-H12-5C and anti-mouse HRP conjugated secondary antibody. Blots were visualised by ECL, imaged on Hyperfilm and quantified by densitometry. Viral particle production was calculated as the ratio of virion-associated $Pr55^{Gag}$ and p24 to the total $Pr55^{Gag}$ and p24 in viral and transfected cell lysates as previously described by Shehu-Xhilaga *et al.*, 2004). Data are presented as the percentage of viral particle production of the respective wild-type. Bars represent the mean of four independent assays and error bars denote the standard error. No significant difference in viral particle production was observed upon expression of any W401 mutation in either HX ($p = 0.43$, Kruskal-Wallis and Dunn's post-test) or NL ($p = 0.63$, Wilcoxon matched-pairs signed rank test).

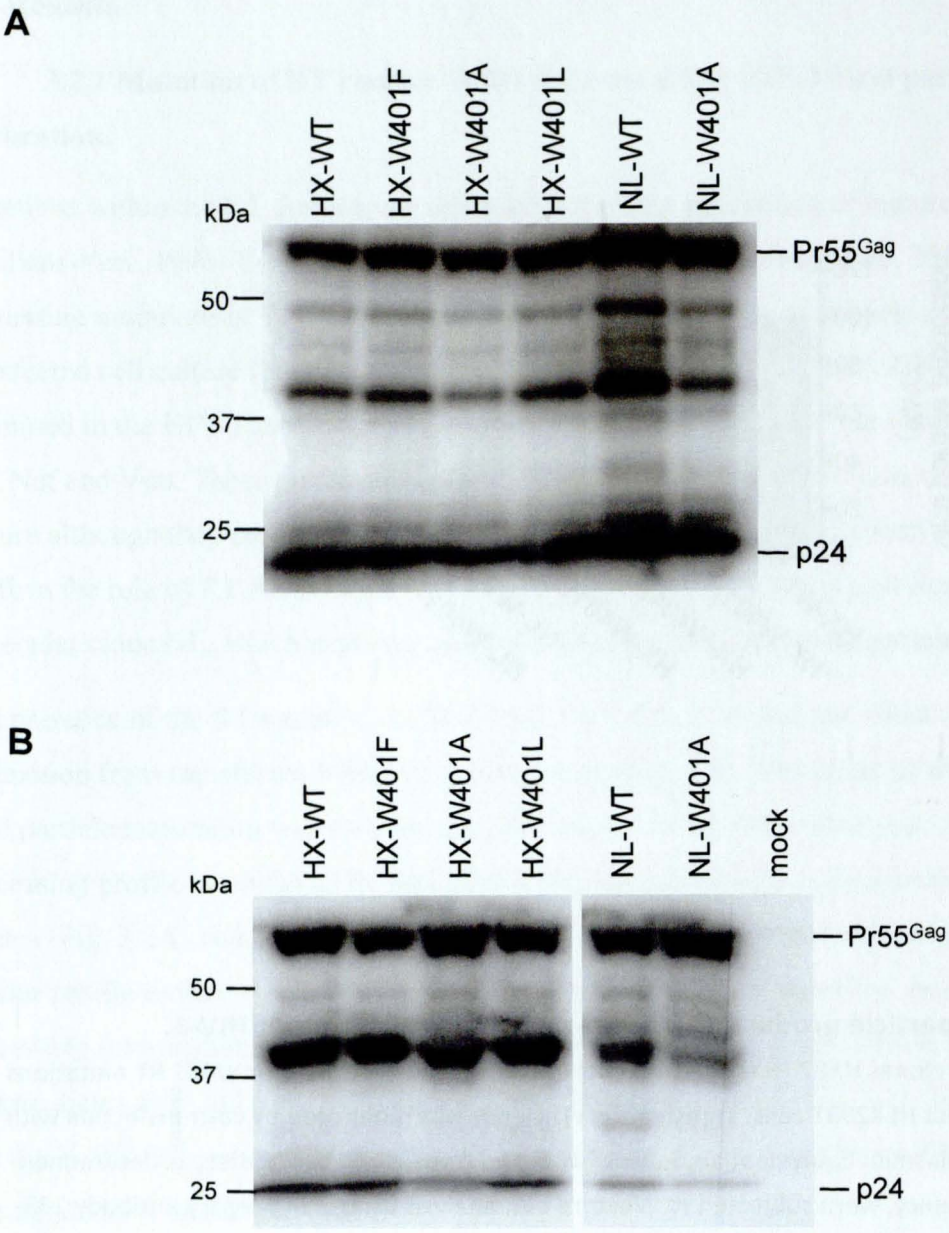

Figure 3.2. Gag processing profile W401 HIV-1 mutants in viral and transfected cell lysates.
The Gag processing profile was visualised by Western blot using p24 antibody 183-H12-5C and anti-mouse HRP conjugated secondary antibody. Clarified supernatants from HEK293T cells transfected with wild-type or mutant HIV-1 constructs were pelleted by ultracentrifugation. Virus pellets were lysed and subjected to Western blot (A), as were transfected HEK293T cell cultures (B). Blots were visualised by ECL and imaged on Hyperfilm.

3.2.2 Mutations at W401 that abrogate RT dimerisation confer reduced HIV-1 infectivity

Expression of W401A and W401L mutations in recombinant RT prevents subunit dimerisation and correspondingly these subunits are devoid of polymerase activity (Tachedjian *et al.*, 2005b). Due to the essential role of reverse transcription in HIV-1 replication, it was expected that HIV-1 expressing either W401A or W401L would demonstrate reduced HIV-1 infectivity. The affect on HIV-1 infectivity was assessed in two cell lines, the MT-2 T cell line and the TZM-bl indicator cell line (Section 2.6). Determination of the $TCID_{50}$ in MT-2 cells requires multiple rounds of productive infection to result in cytopathicity observed by light microscopy. In the TZM-bl cells, production of the HIV-1 Tat protein regulates the expression of the β-galactosidase reporter gene which can be assayed colourimetrically. As infected TZM-bl cells can produce low levels of viable HIV-1 particles (Unpublished data, A. Cornwall, Burnet Institute), the limited time frame used in this assay (48 h) was designed to detect a single round of infection.

Mutant HIV-1 expressing the W401A or W401L mutations demonstrated a significant reduction in infectivity, which was not observed for the W401F mutant (Fig. 3.3). Both HX-W401A and HX-W401L were incapable of inducing CPE in MT-2 cells under these assay conditions, and generated the minimal $TCID_{50}$ in this system of 16 $TCID_{50}$/mL, compared to 4.1×10^5 $TCID_{50}$/mL for HX-WT (Fig. 3.3A). The comparatively minor decrease in $TCID_{50}$ observed for HX-W401F (1.0×10^5 $TCID_{50}$/mL) was not statistically significant. In the NL isotype expression of the W401A mutation demonstrated CPE in infected cultures (30 $TCID_{50}$/mL), yet with a significant decrease of 10^3-fold ($p = 0.03$) compared to NL-WT (2.2×10^4 $TCID_{50}$/mL).

The effect of the W401 mutations in the TZM-bl cell line followed a similar trend to that observed in MT-2 cells (Fig. 3.3B). HX-W401A and HX-W401L demonstrated significant decreases in infectivity, reduced to 0.86% ($p < 0.05$) and 0.01% ($p < 0.01$) of wild-type, respectively. As observed for experiments performed in MT-2 cells, the effect of the W401A mutation in the NL isotype was not as dramatic as observed in HX (8.2% of wild-type, $p < 0.05$). In contrast, introduction of the W401F mutation in HX demonstrated infectivity of 44% of wild-type, which again was not a significant decrease. Thus expression of mutations at W401 that abrogate RT dimerisation displayed a strong association with significant reductions in HIV-1 infectivity that was apparent after a single round of replication. In contrast, expression of the W401F mutation, which does not affect recombinant RT subunit dimerisation, did not significantly reduce HIV-1 infectivity.

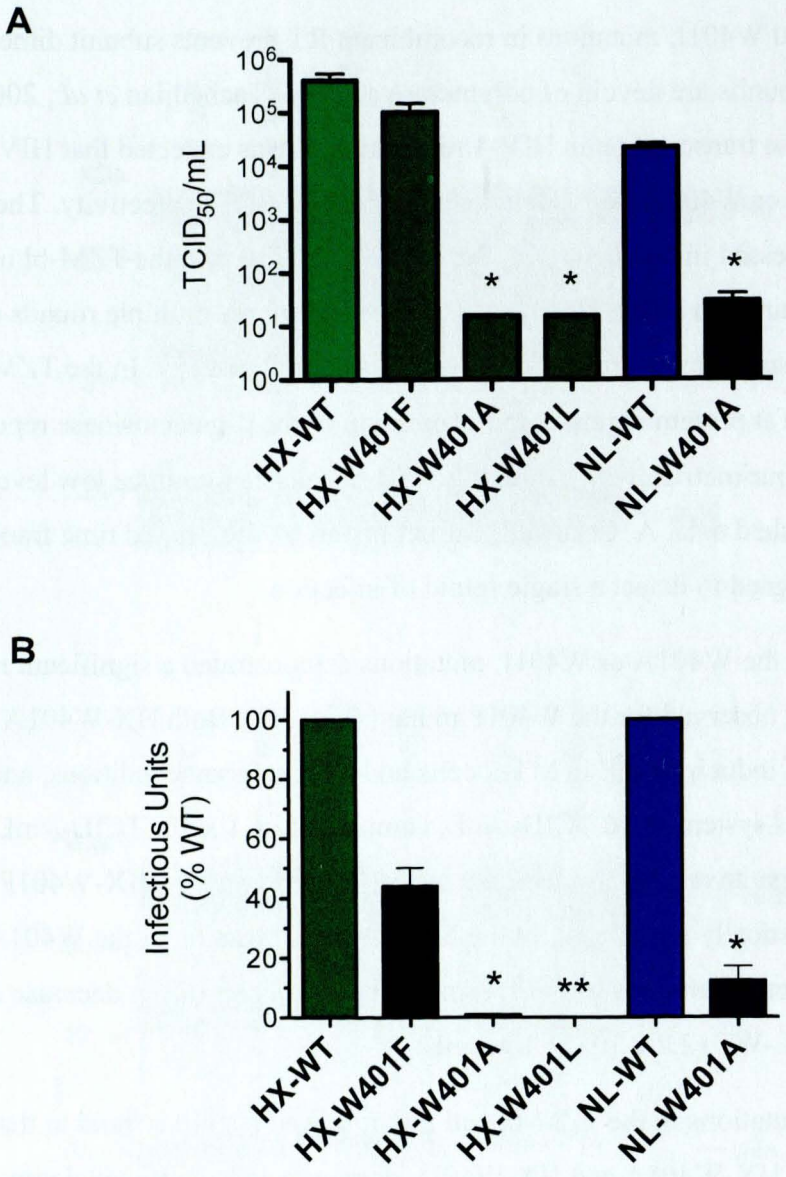

Figure 3.3. Effect of W401 mutations on HIV-1 infectivity

MT-2 cells (A) and the TZM-bl reporter cell line (B) were infected with clarified supernatants derived from HIV-1 transfected HEK293T cell cultures, normalised to equivalent amounts of p24 by Western blot analysis. Infected MT-2 cultures were scored for CPE six days post infection and the $TCID_{50}$/mL calculated using the Karber formula. Infected TZM-bl cultures were fixed 48 h post infection and stained to detect expression of the Tat activated reporter gene β-galactosidase. Infected blue-stained foci were counted by light microscopy to determine the infectious units, expressed as the percentage of the relevant wild-type infection. Each bar represents the mean of three independent assays and error bars denote the standard error. The Wilcoxon matched-pairs signed rank test was used to compare NL viruses, and the Kruskal-Wallis with Dunn's post test to compare HX viruses. Significant differences compared to wild-type are indicated by * ($p < 0.05$), and ** ($p < 0.01$).

3.2.3 Mutations at W401 that abrogate RT dimerisation confer reduced RT activity in HIV-1

The observed reductions in infectivity were predicted to correspond with reductions in RT activity. Accordingly, virion-associated RDDP activity of wild-type and mutant HIV-1 was determined. Wild-type and mutant HIV-1 produced by transfection were normalised to equivalent amounts of virion-associated p24 as determined by p24 Western blot analysis, and the virion-associated RDDP activity assayed on a homopolymeric T/P (Section 2.7.1). The HX-W401L mutant and W401A in both HX and NL demonstrated a significant decrease in RT activity of less than 5% and 1% of wild-type respectively. In contrast, virion-associated RDDP activity for HX-W401F was 80% of wild-type levels (Fig. 3.4).

The effect of W401A/L RT mutations was further investigated by PCR detection of intracellular reverse transcription intermediates in infected MT-2 cells (Section 2.7.2). The presence minus strand strong stop DNA, an early intermediate, was detected using primer pair *M667/AA55* to amplify the R/U5 junction. Amplification of the LTR/*gag* junction with primer pair *M667/M661*, indicative of extension of plus strand DNA was used as an indicator or late transcription events (Zack *et al.*, 1990). A serial dilution of ACH2 cell lysates, which contain a single proviral HIV-1 copy per cell, was used as a standard and demonstrated the dynamic range of detection to be from 3.7×10^3 to 45 proviral copies (Fig. 3.5A). MT-2 cells infected with NL-L234A served as a control for an RT mutation that results in non-infectious HIV-1 in T cell culture (Ghosh *et al.*, 1996). MT-2 cells were infected with equivalent amounts of virion-associated p24 as determined by p24 ELISA (Section 2.7.2).

Infection with HIV-1 expressing either the W401A or W401L mutation resulted in a decrease in reverse transcription intermediates, which was more pronounced in late transcripts compared to the respective wild-type virus (Fig. 3.5). Generally these data corresponded with the effect of the mutations on viral infectivity. HX-W401A affected a greater decrease in transcripts compared to expression in the NL background (Fig. 3.5B and D). The HX-W401L mutant demonstrated a greater reduction in both early and late transcripts compared to the HX-W401A mutant (Fig. 3.5C). Consistent with findings from a previous study (Yu *et al.*, 1998a), mutation of L234 resulted in reduced but detectable levels of early and late reverse transcripts compared to wild-type (Fig. 3.5E). These data indicate that the decrease in infectivity observed for W401A/L mutant HIV-1 is in part due to a reduction in reverse transcription.

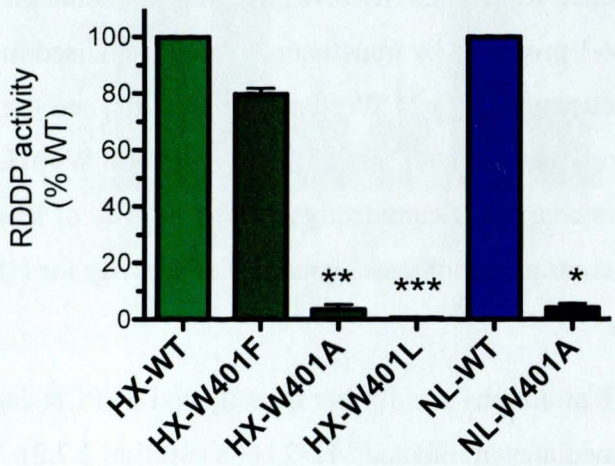

Figure 3.4. Virion-associated RDDP activity of wild-type and W401 mutant HIV-1.
Clarified supernatant derived from transfected HEK293T cell cultures were normalised to equivalent amounts of p24 as determined by Western blot analysis. The virion-associated RDDP activity was assayed on a homopolymeric poly(rA)/oligo(dT) T/P by incorporation of radiolabeled ^{33}P-dTTP. Incorporated radiolabel was detected and quantified using the Fujifilm FLA-3000 Phosphor Imager, and expressed as the percentage of wild-type activity. Each bar represents the mean of three independent assays and error bars denote the standard error. The Wilcoxon matched-pairs signed rank test was used to compare NL viruses, or the Kruskal-Wallis with Dunn's post test to compare HX viruses. Significant differences compared to wild-type are indicated by * where $p < 0.05$, ** where $p < 0.01$, and *** where $p < 0.001$.

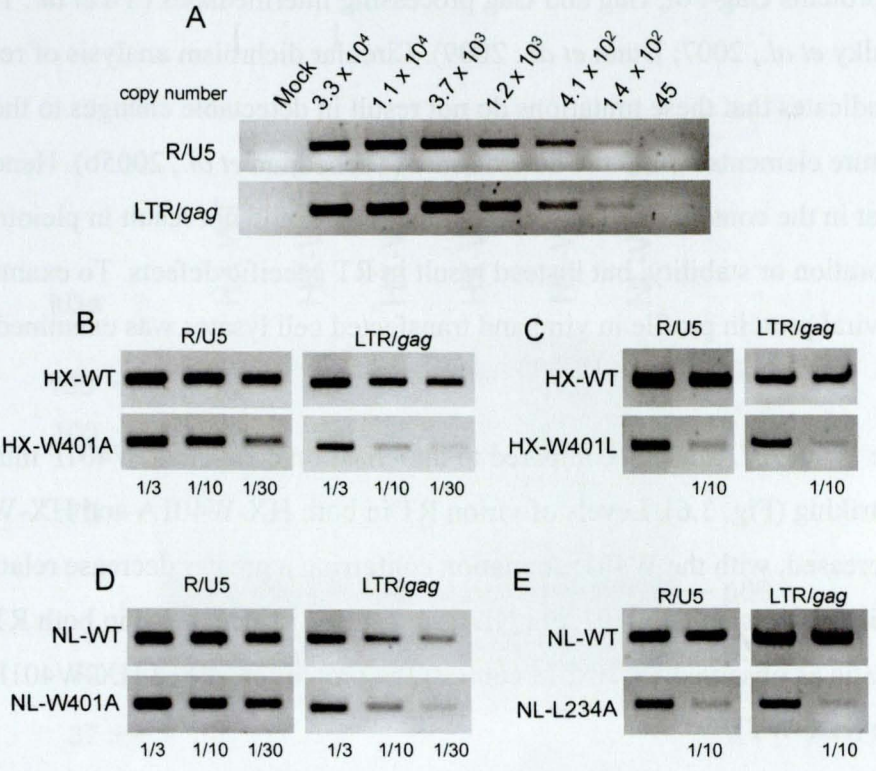

Figure 3.5. Detection of intracellular reverse transcription intermediates in HIV-1 infected MT-2 cells.

PCR was performed on serially diluted cell lysates of MT-2 infected with WT or mutant HIV-1. The primer pair AA55 and MM67 was used to detect early transcripts (R/U5). The MM61 and MM67 primer pairs were used to detect late transcripts (LTR/*gag*). PCR products were resolved in a 2% agarose gel and visualised by ethidium bromide staining. (A) Both PCRs were performed on a serial dilution of ACH2 cell lysates, which contain a single proviral HIV-1 copy per cell, to demonstrate the dynamic range of the assay from 3.7 x 10^3 to 45 proviral copies, indicating the range of the assay. (B-E) 4x10^5 MT-2 cells were infected with the equivalent of 500 ng of p24. Infected cultures were lysed six hours post infection and cell lysates normalised to equivalent amounts of the HLA-DQα reference gene prior to PCR analysis of viral transcripts. (B) HX-W401A, (C) HX-W401L, (D) NL-W401A, (E) NL-L234A were analysed compared to the respective WT virus.

3.2.4 W401A/L RT mutations result in a specific decrease HIV-1 RT

The expression of RT mutations in HIV-1 can result in defects that are not restricted to RT and affect the viral proteins Gag-Pol, Gag and Gag processing intermediates (Yu *et al.*, 1998a; Olivares *et al.*, 2004; Mulky *et al.*, 2007; Dunn *et al.*, 2009). Circular dichroism analysis of recombinant W401A/L RT indicates that these mutations do not result in detectable changes to the regular secondary structure elements within the heterodimer (Tachedjian *et al.*, 2005b). Hence it was hypothesised that in the context of HIV-1, these mutations would not result in pleiotropic effects on Gag-Pol incorporation or stability, but instead result in RT specific defects. To examine this hypothesis, the viral protein profile in viral and transfected cell lysates was examined by Western blot analysis.

The effect of the W401A/L mutants compared to dimerisation competent W401F mutation on virion RT was striking (Fig. 3.6). Levels of virion RT in both HX-W401A and HX-W401L were substantially decreased, with the W401L mutation conferring a greater decrease relative to W401A (Fig. 3.6A). While expression of W401A in NL also resulted in a decrease in both RT subunits, this was not as dramatic as observed for HX. In contrast the protein profile of HX-W401F was similar to that wild-type (HX-WT).

Examination of transfected cell lysates revealed a pronounced decrease in levels of p51 in the HX-W401A, HX-W401L and NL-W401A mutants. The same decrease was not observed for the p66 subunit (Fig. 3.7). Thus expression of these mutations resulted in a decreased p51:p66 ratio compared to wild-type. The RT protein profile of HX-W401F was again similar to wild-type. This profile was consistently observed using either of two antibodies, 11G10 and 5B2, which target two independent RT epitopes (Szilvay et al., 1993), and HIV positive pooled patient sera.

Wild-type levels of Gag-Pol (Fig. 3.6A), IN (Fig, 3.6B), and a wild-type Gag processing profile (Fig. 3.2A) for all W401 mutants indicated that these mutations did not affect Gag-Pol incorporation into the virion. This is further supported by the observation that there was no increase in levels of Gag-Pol in transfected cell lysates compared to wild-type (Fig. 3.7A). This suggests that the changes to the RT profile in viral and transfected cell lysates observed for mutations that confer a defect in RT dimerisation, those being HX-W401A, HX-W401L and NL-W401A, were not due to a loss of Gag-Pol. Further, the presence of wild-type levels of virion IN indicate that the defect was specific to the RT protein, and did not adversely affect other Pol proteins (Fig. 3.6B).

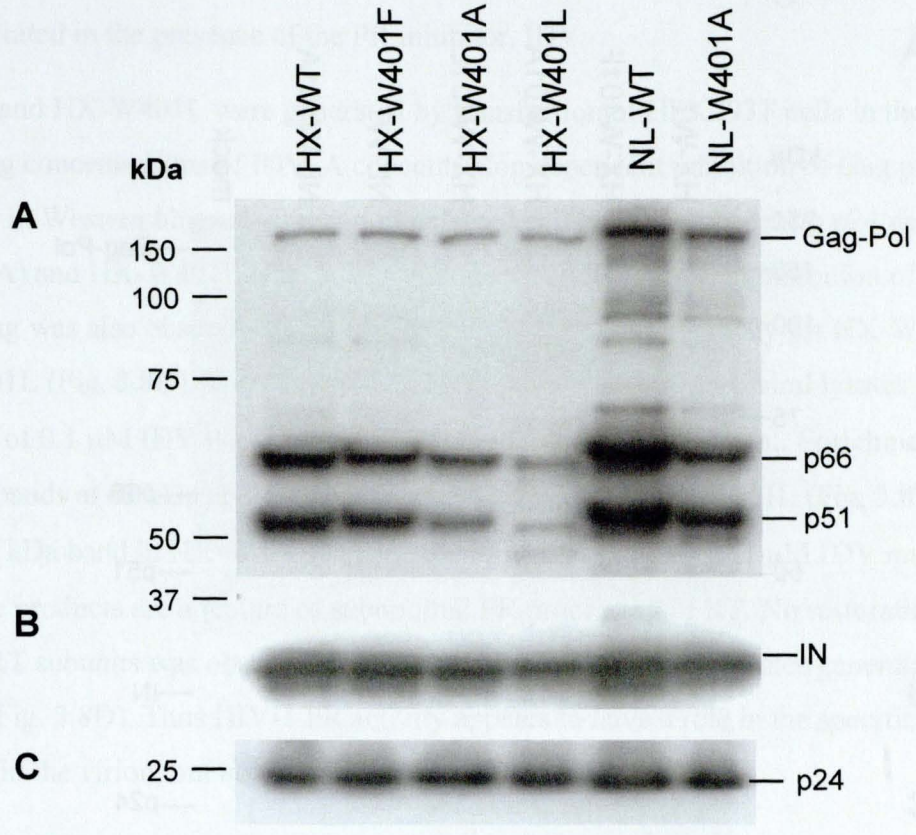

Figure 3.6. Western blot analysis of the HIV-1 protein profile of WT and W401 mutant viral lysates.

Clarified supernatants derived from HEK293T cells transfected with WT or W401 mutant HIV-1 constructs were concentrated by ultracentrifugation. Virus pellets were lysed, normalised to equivalent amounts of p24 and subjected to Western blot analysis. Western blot against using the primary RT antibody 11G10 (A), IN antibody 8E5 (B) or p24 antibody 183-H12-5C (C), with anti-mouse HRP conjugated secondary antibody. Proteins were visualised by ECL and imaged on Hyperfilm.

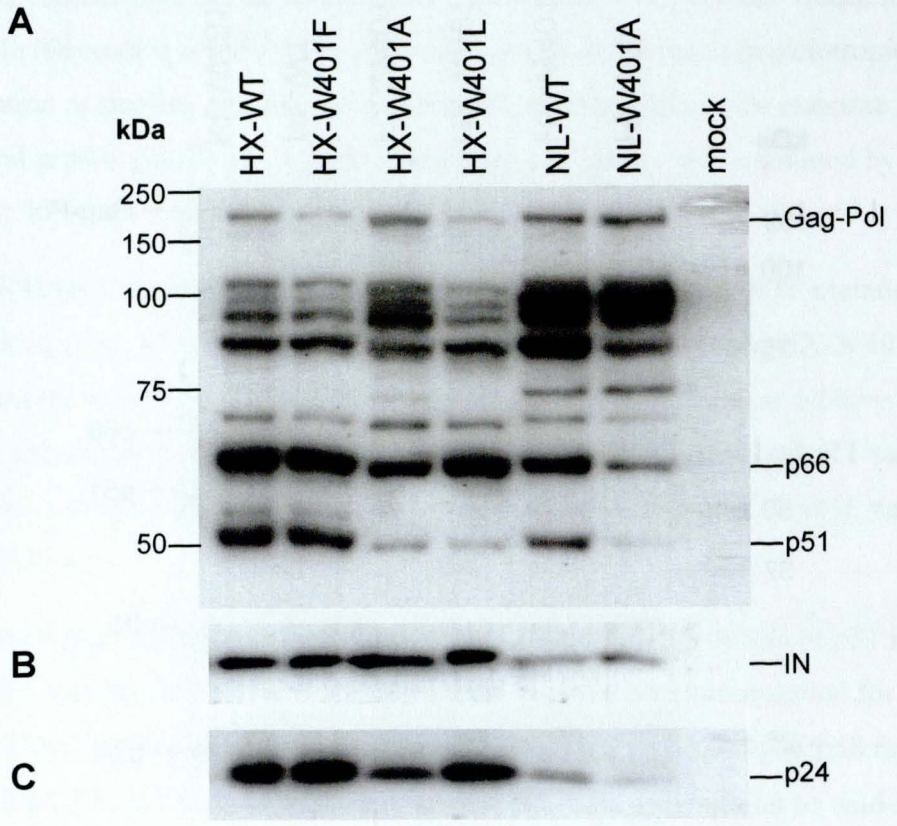

Figure 3.7. Western blot analysis of the HIV-1 protein profile of WT and W401 mutants in transfected cell lysates.

HEK293T cell cultures transfected with WT or W401 mutant constructs were normalised to equivalent amounts of p24 and subjected to Western blot analysis using the primary RT antibody 11G10 (A), IN antibody 8E5 (B), or anti-p24 antibody 183-H12-5C (C), and anti-mouse HRP conjugated secondary antibody. Proteins were visualised by ECL and imaged on Hyperfilm.

3.2.5 The HIV-1 PR mediates proteolysis of mutant RT in HIV-1

Previous studies demonstrate that expression of RT mutations can result in proteolysis of Pol proteins mediated by the HIV-1 PR (Yu *et al.*, 1998a; Mulky *et al.*, 2007; Olivares *et al.*, 2007; Dunn *et al.*, 2009). To determine whether the HIV-1 PR had a role in the decreased levels of virion RT upon expression of the W401A/L mutations, the most severely affected mutant, HX-W401L, was generated in the presence of the PR inhibitor, IDV.

HX-WT and HX-W401L were generated by transfection of HEK293T cells in the presence of increasing concentrations of IDV. A concentration dependent inhibition of Gag processing was observed in Western blots of viral and transfected cell lysates probed with p24 antibody for HX-WT (Fig. 3.8A) and HX-W401L (Fig. 3.8C). A concentration-dependent inhibition of Gag-Pol processing was also observed in viral lysates probed with RT antibody for HX-WT (Fig. 3.8B) and HX-W401L (Fig. 3.8D). The amount of RT subunits in HX-W401L viral lysates generated in the presence of 0.1 μM IDV was increased compared to no drug treatment. Enrichment of RT antibody reactive bands at 62 kDa and 45 kDa was also observed for HX-W401L (Fig. 3.8D). The presence of the 62 kDa band in HX-WT virus generated in the presence of 0.1 μM IDV may be indicative that these products are a feature of suboptimal PR processing of RT. No restoration of the amount ratio of RT subunits was observed in HX-W401L transfected cell lysates generated in the presence of IDV (Fig. 3.8D). Thus HIV-1 PR activity appears to have a role in the specific degradation of RT subunits in the virion, but not in transfected cell lysates.

3.2.6 The W401A dimerisation defective RT mutant does not affect the initial PR mediated cleavages of Gag-Pol

The virion protein profile of HIV-1 expressing W401A/L was indicative of RT specific, PR-mediated degradation of the RT subunits, with little effect on PR activation and Gag-Pol processing. The recombinant Gag-Pol processing assay developed by Pettit and Kaplan (Pettit *et al.*, 2003) was employed to observe the effect of W401 mutations that abrogate RT dimerisation on PR activation and early cleavage events in the context of Gag-Pol. In this assay, recombinant Gag-Pol is expressed and cleaved by the Gag-Pol embedded PR at the p2/NC site followed by the $p6^{Pol}$/TFP site (Fig. 1.9A). These are the only cleavage events observed when using wild-type constructs in this system (Pettit *et al.*, 2004).

The Gag-Pol processing assay uses the Promega Quick Coupled Transcription/Translation system (Section 2.10). A vector was created to express Gag-Pol derived from the NL HIV-1 molecular clone (Section 2.1.4). This vector demonstrated an identical cleavage profile to that of the previously published vector, pGPfs, which is derived from a HXB2 molecular clone (Pettit *et al.*, 2003).

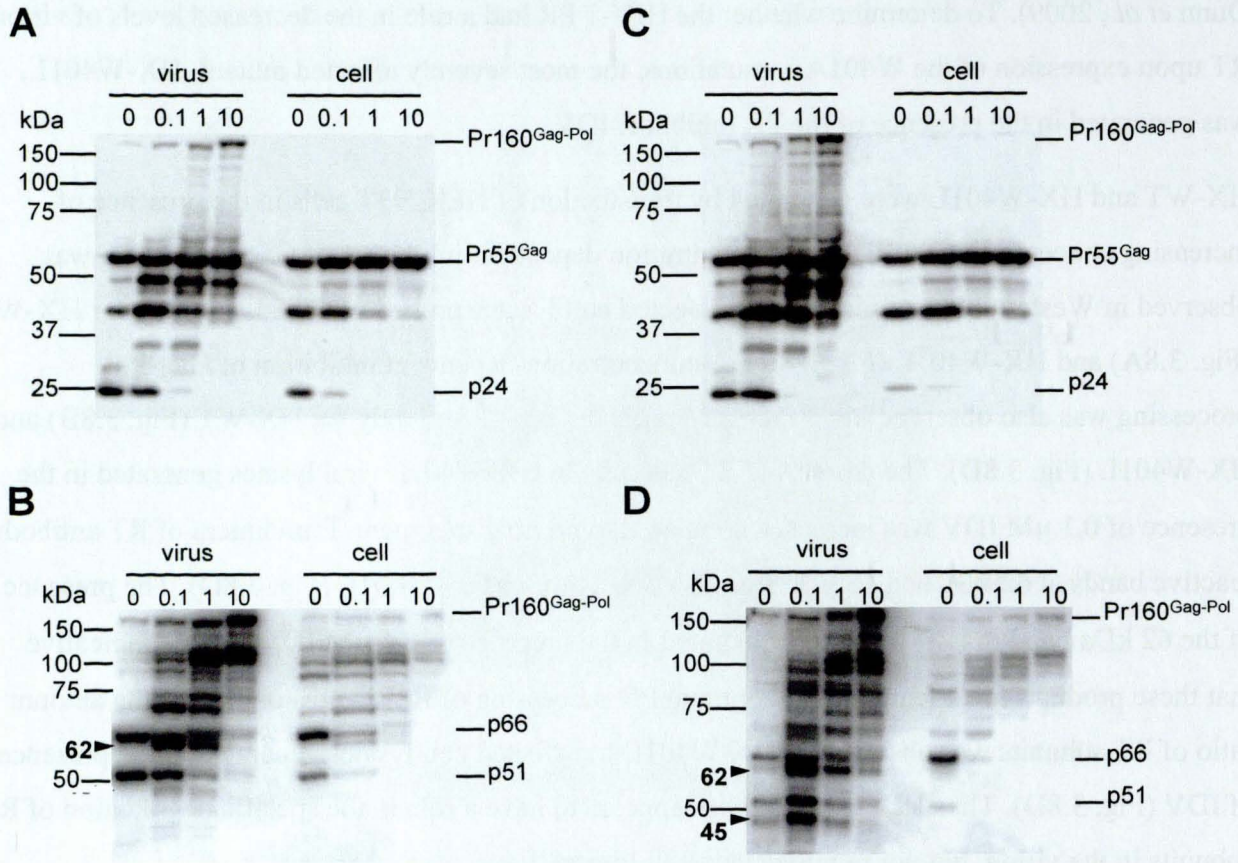

Figure 3.8. Western blot analysis of HX-WT and HX-W401L mutant HIV-1 generated in the presence of the HIV-1 protease inhibitor, indinavir.

HX-WT (A, B) or HX-W401L (C, D) HIV-1 were produced by HEK293T transfection in the presence of 0, 0.1, 1, or 10 μM indinavir. Transfection efficiency was monitored by co-transfection with an eGFP producing plasmid. Equivalent amounts of viral and transfected cell lysates, as determined by transfection efficiency, were subjected to Western blot analysis. Viral and cell lysates were probed using p24 antibody 183-H12-5C (A and C), and RT antibody 11G10 (B and D), with anti-mouse HRP conjugated secondary antibody. Proteins were visualised by ECL and imaged on Hyperfilm. Solid arrowheads denote RT antibody reactive bands migrating at approximately 62 and 45 kDa.

Upon expression of the W401A mutation in recombinant Gag-Pol this in vitro system, no variation in the cleavage profile was observed compared to wild-type Gag-Pol (Fig. 3.9). This further supports the inference that mutations at codon W401 that abrogate RT dimerisation do not affect PR activation or the initial PR-mediated cleavages of Gag-Pol. Instead, the defects are predominantly confined to the PR mediated events that liberate the mature RT heterodimer.

3.2.7 Location and potential mechanism of action of the W401A/L mutations

In the p66 subunit, W401 is proposed to be essential for correct positioning of the αL-β20 loop and subsequent interaction of this region with the p51 subunit. Correspondingly, non-conservative mutation of this RT residue results in a dimerisation defect mediated predominantly through the p66 subunit (Tachedjian *et al.*, 2003; Mulky *et al.*, 2005b). The structural consequences upon mutation of W401 appear to be confined to the loop, as W401 mutants do not affect RT standard secondary structure elements as determined by CD analysis (Tachedjian *et al.*, 2005b). The lack of detrimental effects on Gag-Pol stability, virion incorporation and PR activation demonstrated by this study suggest that mutation of W401 does not affect Gag-Pol structure. To further investigate the structural role of W401, the location of the p66 TRM was examined in several distinct crystal structures of the HIV-1 RT, including unliganded (1DLO [Hsiou *et al.*, 1996] and 1HMV [Rodgers *et al.*, 1995]), the trapped catalytic complex (1RTD [Huang *et al.*, 1998]), complexed with T/P (1HYS [Sarafianos *et al.*, 2001]), and inhibitor bound RT (1RTH [Jacobo-Molina *et al.*, 1993; Ren *et al.*, 1995]).

The position of the TRM residues within p66 αL-β20 was found to be relatively consistent amongst these structures, with $p66^{W401}$ and $p66^{W402}$ located at the carboxyl terminus of αL, $p66^{W414}$ at the N-terminus of β20, and the intermediary TRM residues spanning the αL-β20 loop (Fig. 3.10A). The side-chains of $p66^{W401}$, $p66^{Y405}$, and $p66^{W406}$ stack in a parallel manner, typical of the π interactions formed by planar aromatic side-chains (Fig. 3.10). This 'aromatic stack' potentially spans the dimer interface to involve the $p51^{P420}$ side-chain in this interaction. It is this π-stack beginning in αL with W401 and involving two αL-β20 loop residues, Y405 and W406, that is proposed to have an important role in positioning the p66 αL-β20 loop (personal communication, M. Kuiper, Victorian Partnership for Advanced Computing, Melbourne, Australia). The loss of this bulky aromatic by introducing a non-conservative mutation is hypothesised to collapse the stack and relax positioning of the αL-β20 loop (Fig 3.10 E-F). Incorrect positioning of the αL-β20 loop could disturb multiple interactions between the p66 loop and the p51 subunit.

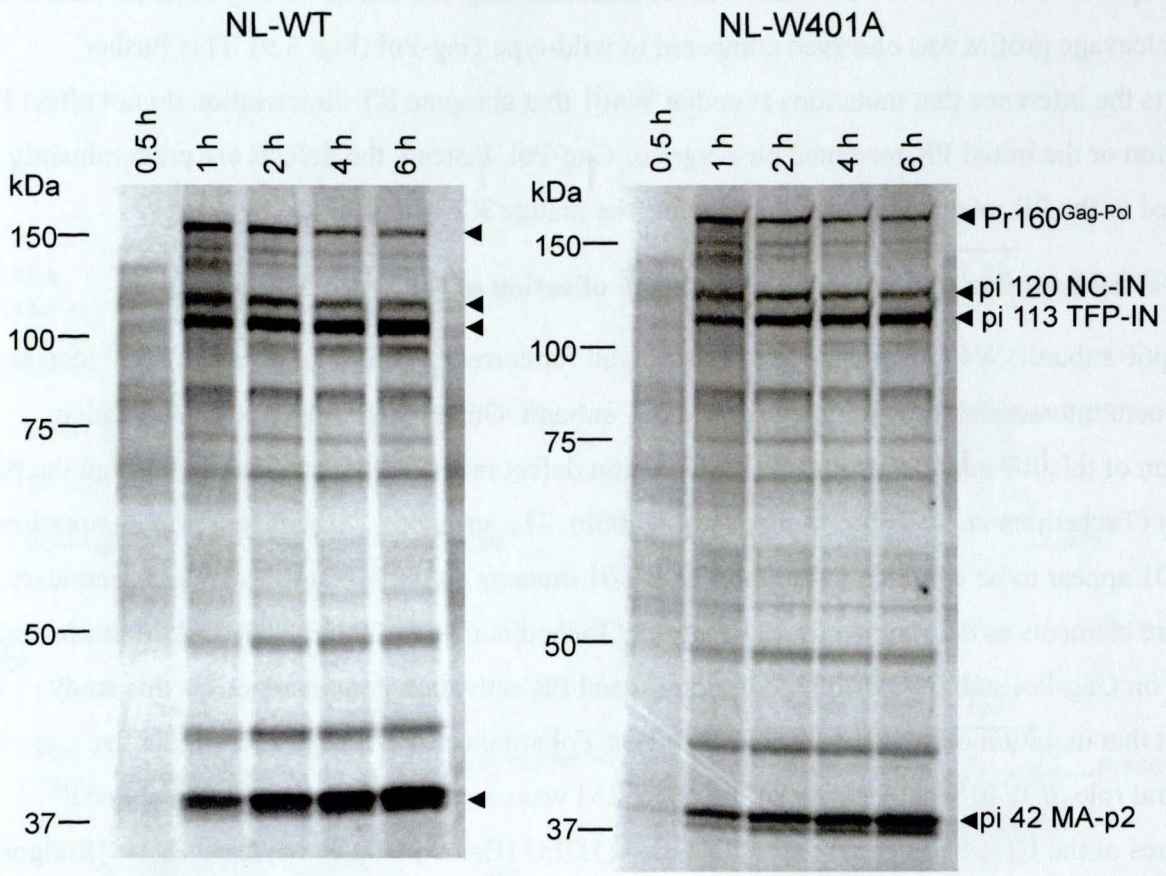

Figure 3.9. Effect of the RT mutation W401A on the initial Gag-Pol cleavage events mediated by the Gag-Pol embedded PR.

The full-length Gag-Pol coding region with frameshift mutation encoding wild-type or W401A mutant RT was expressed in the Promega Quick Coupled Transcription/Translation system. Aliquots were removed at the indicated time points, resolved by SDS-PAGE and imaged using the Fujifilm FLA-3000 Phosphor Imager. Molecular weight markers are indicated on the left, and the Gag-Pol processing intermediates (pi) by a solid triangle on the right of the blots. Gag-Pol processing intermediates were identified by their molecular weight and are notated as previously defined by Pettit and colleagues (2003).

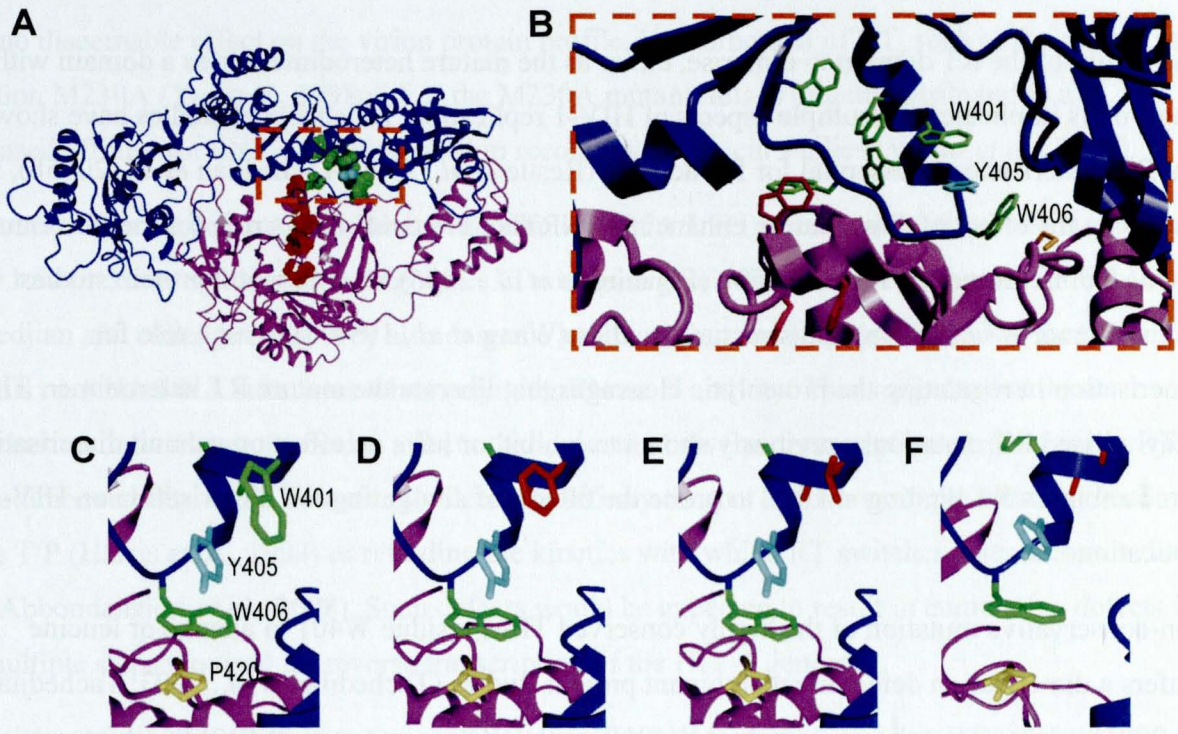

Figure 3.10. Representation of the W401 mutations in the p66 subunit of the RT heterodimer.

(A) Ribbon diagram of the RT heterodimer with the p66 subunit in blue and p51 subunit in pink. The tryptophan side-chains of the TRM in p66 are highlighted in green and Y405 in cyan, with the p51 TRM highlighted in red with Y405 coloured magenta. (B) Magnified representation of the boxed region in (A) displaying the TRM motif spanning αL-β20 in p66 and its proximity to the p51 subunit. (C) Side-chains of $p66^{W401}$ (green), $p66^{Y405}$ (cyan), $p66^{W406}$ (green) and $p51^{P420}$ (yellow) that potentially participate in a π stacking interaction that spans the dimer interface. W401 was mutated to phenylalanine (D), leucine (E) and alanine (F). The image was generated with YASARA (Krieger *et al.*, 2002) using coordinates for the RT crystal structure 1RTD (Huang *et al.*, 1998).

Hence non-conservative mutation of this single residue, W401, effectively disturbs multiple interactions between the subunits. This also provides an explanation as to why the conservative mutation, W401F, does not significantly affect subunit dimerisation, as the aromatic phenylalanine is expected to participate in the π interaction similarly to the tryptophan residue.

3.3 Discussion

The ability of the RT domain to dimerise, either as the mature heterodimer, or as a domain within Gag-Pol, is implicated in multiple aspects of HIV-1 replication. Biochemical studies have shown that RT dimerisation is essential for RT activity (Restle *et al.*, 1990; Tachedjian *et al.*, 2005b), and studies on the effect of dimerisation enhancing NNRTIs have confirmed a role for the RT domain of Gag-Pol in promoting PR activation (Figueiredo *et al.*, 2006). Recombinant protein studies (Sluis-Cremer *et al.*, 2004a) and structural studies (Wang *et al.*, 1994) suggest a role for dimerisation in regulating the proteolytic cleavages that liberate the mature RT heterodimer. This study utilised RT mutations previously shown to inhibit, or have no effect on subunit dimerisation in recombinant RT binding studies, to probe the effects of abrogating RT dimerisation on HIV-1 replication.

Non-conservative mutation of the highly conserved TRM residue W401 to alanine or leucine confers a dimerisation defect in recombinant protein studies (Tachedjian *et al.*, 2003; Tachedjian *et al.*, 2005b). In contrast the conservative W401F mutation does not prevent Rt subunit interaction (Tachedjian *et al.*, 2003; Tachedjian *et al.*, 2005b). Examination of the effect of these mutations in HIV-1 revealed a strong association between the dimerisation defective mutants and reductions in HIV-1 infectivity, RT activity and steady-state levels of RT. This was observed in the absence of defects in virion incorporation of Gag-Pol, characteristic of previously examined RT mutations (Yu *et al.*, 1998a; Chiang *et al.*, 2010). These data thus provide evidence of a RT dimerisation defect independent of pleiotropic effects Gag-Pol, and support the hypothesis that perturbing RT dimerisation can affect both early and late phases of HIV-1 replication.

Expression of W401A or W401L in HIV-1 resulted in decreases in RT activity demonstrated by a decrease in virion-associated RDDP activity, and intracellular reverse transcription intermediates. It is probable that both the decreased levels of virion RT and defects in RT function caused by these mutations contribute to this outcome. Previous studies describe RT mutants with no immunoreactive RT by Western blot analysis; however, demonstrate detectable virion-associated RT activity and HIV-1 infectivity (Abram *et al.*, 2005; Dunn *et al.*, 2009). This study shows that despite the presence of substantial immunoreactive RT in viral lysates, the W401A/L mutants demonstrated less than 5% virion-associated RDDP activity, and undetectable or low levels of HIV-

1 infectivity. Although the relative levels of virion RT and RT activity cannot be compared between these studies, it is in contrast to what was observed for W401A/L mutants examined here.

The decrease in late reverse transcription intermediates for the W401A/L mutants was greater than the decrease observed in early transcripts. Such has been observed for previously examined RT mutations that also result in reduced levels of virion RT (Yu *et al.*, 1998a; Dunn *et al.*, 2009), or have no discernable effect on the virion protein profile, including that of RT, such as the primer grip mutation M230A (Yu *et al.*, 1998a). For the M230A mutant, this is directly attributed to a decreased affinity for dNTPs characterised in recombinant protein studies (Wohrl *et al.*, 1997).

Previously reported polymerase activity of mutant W401A/L RT in recombinant protein studies is either low (< 5% of wild-type) or negligible (Tachedjian *et al.*, 2003; Tachedjian *et al.*, 2005b). Tachedjian and colleagues (2005b) also describe a reduced k_{cat} and increase in the K_M for these mutants on RNA:DNA substrates when engaging RNase H activity. This suggests that these dimerisation defective mutants also affect other aspects of reverse transcription. A decrease in RT heterodimer stability could conceivably decrease affinity for the T/P, for example either by loading of the T/P (Harris *et al.*, 1998) or retarding the kinetics with which RT switches orientation on the T/P (Abbondanzieri *et al.*, 2008). Such defects would be expected to result in cumulative defects in the multiple steps required for reverse transcription of the HIV-1 genome.

Expression of the W401A/L mutations in HIV-1 resulted in decreases in virion RT independent of a corresponding decrease in Gag-Pol. These mutants also displayed a decrease in the ratio of p51:p66 in transfected cell lysates. It is suggested that the concerted model of RT heterodimer formation via the putative p66 homodimer (Sluis-Cremer *et al.*, 2004a) could provide a mechanism to explain these data.

Formation of a p66 homodimer has been postulated to be an essential step in generation of the mature RT heterodimer, in which the conformational restrictions of the p66 homodimer regulate access to, and cleavage of the p51/RNase H site by the HIV-1 PR in one of the subunits which results in generation of the mature heterodimer (Wang *et al.*, 1994). This theory is supported by observation of PR mediated cleavage of a bacterially expressed model Pol protein, in which generation of p51 occurs subsequent to accumulation of the p66 subunit. Expression of the dimerisation defective L234A mutation in this system prevents generation of the p51 subunit (Sluis-Cremer *et al.*, 2004a). With regards to this study, the W401A/L mutations also prevent homodimerisation of recombinant p66 subunits (unpublished data, G. Tachedjian, Burnet Institute). Thus, the inability of W401A/L mutants to form a stable p66 homodimer in the virion may result in aberrant proteolysis of monomeric p66 or unstable p66 homodimers, resulting in a specific decrease in the RT subunits in the virion.

A similar effect has been described for RT mutants that are unable to form a stable heterodimer, whether due to p51/RH cleavage site mutations (Abram *et al.*, 2005), mutations that destabilise the subunit (Dunn *et al.*, 2009), or decrease RT subunit interaction (Mulky *et al.*, 2007). However, both the W401A and W401L mutants maintained an approximate 1:1 ratio of p51:p66 in viral lysates. It is proposed that this is indicative of inappropriate proteolysis occurred during proteolytic maturation of RT, rather than post-RT maturation, and that once formed, the W401A/L mutant RT heterodimer is somewhat protected from proteolysis.

While these mutations prevent association of the RT subunits in recombinant protein binding assays, in the context of the virion or transfected cell the dimeric status of the W401A/L mutant subunits was not directly examined. The presence of multiple interacting factors including T/P, viral proteins and host cell factors may act to stabilise the subunits and facilitate generation of the heterodimer. Indeed this could account for the difference in the extent of the defect observed in virion associated RDDP activity compared to that of intracellular reverse transcription and infectivity of the W401A/L mutants. For the latter, the presence of multiple factors in the host cell that have been characterised that act to stabilise the RTC and promote reverse transcription (reviewed by Warren *et al.*, 2009) may act to stabilise mutant RT subunits.

This study also examined the W401A/L virion protein profile in transfected cell lysates, where a distinctly different RT protein profile was observed compared to viral lysates. Steady-state levels of p66 were moderately reduced, however p51 was at the limit of detection. Due to the lower concentration of Pol products in transfected cell lysates compared to the confines of the virion, it is proposed that both p66 homodimerisation and proteolysis of mutant subunits was reduced, retarding RT maturation and decreasing the p51:p66 ratio compared to wild-type. This effect is reminiscent of inhibition of p51 formation upon expression of the dimerisation defective L234A mutation in the model Pol fragment described by Sluis-Cremer and colleagues (2004a). Thus these data can be interpreted to support the sequential model of RT heterodimer maturation (Sluis-Cremer *et al.*, 2004a).

Alternative explanations for the observed profile of cell lysates from cells transfected with W401A/L mutant virus include prevention of cleavage at the p51/RNase H site due to conformational changes caused by the mutations, or the selective degradation of p51 subunits. However, the observation of an approximately 1:1 ratio of p51:p66 demonstrated that these mutations do not prevent cleavage to the p51 subunit, nor is p51 selectively degraded. Ultimately while this study supports the sequential theory for RT heterodimerisation via a p66 homodimer intermediate, it is far from confirmatory data.

The possibility that RT heterodimer formation may occur in Pol processing intermediates present prior to generation of the p66 subunit is not addressed by these data. Cleavage of recombinant Gag-Pol demonstrates that following the release of IN, the p51/RNase H site can be cleaved from a number of dimeric processing intermediates (Pettit *et al.*, 2005b). Within the course of this study an assay was developed to observe the processing of radiolabeled Gag-Pol in HIV-1 transfected cells. However the methodology lacked the sensitivity to accurately observe the entire Gag-Pol processing cascade. Thus a role for larger RT containing dimeric processing intermediates on RT maturation, and the effect of mutations at W401 that abrogate RT dimerisation on this process was not investigated within this study.

HIV-1 PR mediated proteolysis of mutant RT subunits observed here does not appear to be unique to RT dimerisation mutants. RT specific PR mediated degradation has been reported on the expression of p51/RNase H cleavage site mutations (Abram *et al.*, 2005), and RT thumb subdomain mutations which reportedly destabilize the subunit (Dunn *et al.*, 2009; Zhang *et al.*, 2009). The loss of virion RT and an increase in small molecular weight (< 51 kDa) RT reactive species observed for particular mutations in these studies is reminiscent of the virion RT profile of the W401A/L mutants. The Western blot protocol employed by Dunn and colleagues (2009) included longer antibody incubation times than that used for this study, and reveals a relatively consistent population of small molecular weight RT antibody reactive species regardless of the RT mutation.

Also observed by Dunn and colleagues (2009), and in this study, is the aberrant processing of wild-type HIV-1 RT generated in the presence of a low concentration of HIV-1 PIs (≤ 1 μM). With reference to this study, the presence of RT antibody reactive species of approximately 47 kDa was observed in W401A/L mutants but also in wild-type virions generated in the presence of PI. While Dunn and colleagues (2009) employed the PI ritonavir, and this study utilised IDV for inhibition of the HIV-1 PR. The role of cellular proteases however in both studies is undefined. Dunn and colleagues (2009) suggest the presence of alternative pre-existing cleavage sites that are processed, and Abram and colleagues (2005) define the heterodimer as 'proteolytically stable'. Thus these alternative sites appear to be susceptible to proteolysis when formation of a stable RT heterodimer cannot occur or is delayed, whether due to partial PR inhibition, p51/RNase H cleavage site mutations (Abram *et al.*, 2005), mutations that induce subunit instability (Dunn *et al.*, 2009), inappropriate association of the subunits (Zhang *et al.*, 2009), or the presence of RT mutations that perturb dimerisation, as shown here and at another key point of RT subunit interaction, the β7-β8 loop (Mulky *et al.*, 2007).

The RT domain within Gag-Pol has a positive role in promoting Gag-Pol dimerisation and PR activation (Figueiredo *et al.*, 2006). Yet there was no indication that the W401A/L affected PR

activation in the context of Gag-Pol. Utilising the recombinant Gag-Pol processing assay developed by Pettit and Kaplan (Pettit *et al.*, 2003), no differences were observed for wild-type or W401A expressing Gag-Pol in PR activation or the initial cleavages mediated by the Gag-Pol embedded PR. Only the W401A mutant was examined in the course of this study, and it is postulated that a similar phenotype would be conferred by the W401L mutation.

Examination of the effect of the W401F in HIV-1, which does not affect subunit dimerisation in recombinant RT, was integral in assigning the defects observed upon mutation of W401A and W401L to their role in dimerisation, rather than mutation of this residue. The HX-W401F protein profile in virions and transfected cell lysates was indistinguishable from wild-type. HIV-1 expressing the W401F mutation did demonstrate a small decrease in infectivity compared to wild-type, which could be attributed to the subtle effects of this mutation on polymerase and RNase H activity as previously characterised in recombinant RT (Tachedjian *et al.*, 2005b). Tachedjian and colleagues (2000) propose that the construction of the heterodimer interface informs the optimal configuration of the polymerase active site (Section 1.10.6). Indeed it would appear that these interactions are also essential for optimal RT activity in the context of HIV-1, as in recombinant RT.

The differences in severity of the phenotype observed for the W401A mutant compared to W401L was unexpected. Previous characterisation of these mutations in recombinant RT does not provide a potential explanation (Tachedjian *et al.*, 2003; Mulky *et al.*, 2005b; Tachedjian *et al.*, 2005b). Structurally, a greater defect would be expected upon mutation of W401 to alanine, as this is associated with a greater loss in steric bulk compared to a mutation to leucine. HX-W401L consistently demonstrated a greater decrease in virion RT, which may be indicative of greater instability or susceptibility to PR.

Interestingly, the host cell factor clathrin is implicated in having a role in stabilisation of Pol processing intermediates, and sequestration of clathrin resulting in lower levels of mature IN (Zhang *et al.*, 2011). Clathrin incorporation depends on multiple, but as yet undefined regions in Pol, and is inhibited by the RT L234A mutation (Zhang *et al.*, 2011). As a significant decrease in virion IN was observed for the W401A and W401L mutants in these data, it suspected that clathrin does not play a major role in the defects conferred by these mutations. However, interaction of clathrin with either of these W401A or W401L mutants remains to be confirmed in future studies.

While the W401A mutation in both HX and NL isogenic strains demonstrated similar defects in HIV-1 replication, the magnitude of the defect conferred by the W401A mutation was more pronounced in the HXB2 background compared to NL4.3. This may indicate a role for the accessory proteins in which HXB2 is deficient namely Vif, Vpu and Nef. Both Vif (Dettenhofer *et*

al., 2000) and Nef (Aiken *et al.*, 1995; Schwartz *et al.*, 1995; Fournier, 2002) have been shown to enhance the efficiency of reverse transcription. The ability of these proteins to interact with RT may act to stabilise the mutant subunits, thereby decreasing aberrant processing in the NL4.3 background. Polymorphisms both in the RT coding region and other RT interacting proteins between the HIV-1 molecular clones may also have a role in this effect.

Recent studies have also examined the role of the W401A mutation in HIV-1 replication. The data presented here concurs with that of Mulky and colleagues (2005b), and partially with Chiang and colleagues (2010), who observed wild-type levels of particle production from transfected cells and virion Gag processing profile for the W401A mutant. Both studies observe a specific decrease in virion RT accompanied by the appearance of small molecular weight RT antibody reactive species. However, the RT profile in transfected cell lysates presented by Chiang and colleagues (2010) differs. Chiang and colleagues (2010) observe an increase in the p51:p66 RT ratio in transfected cell lysates for the W401A mutant, which is in direct contrast to the decrease in ratio observed here. As the characteristics of the W401A mutation generally concur well across these studies, this exception may be due to methodology. The Pol coding region used by Chiang and colleagues (2010) was derived from HXB2, and polymorphisms may have a role in this effect but are considered unlikely. Use of VSV-G pseudotyped HIV-1 is also unlikely to affect the stability of the RT subunits in transfected cells. There is however no indication of the use of cellular protease inhibitors when processing transfected cells lysates. Since cellular proteases can cleave the p66 subunit generating p51 (Lowe *et al.*, 1988) this could be responsible for the increase of p51 observed by Chiang (2010). Ultimately the reason for this discrepancy remains unknown.

The data presented in this study presents a comprehensive description of the effect of the W401 mutations characterised by Tachedjian and colleagues (2003) on HIV-1 replication. A strong association was observed between the RT dimerisation defective conferring mutations W401A/L and defects in HIV-1 replication, which where not observed upon expression of W401F. Furthermore, the defects described for W401A/L are consistent with recent studies of W401A (Mulky *et al.*, 2005b; Chiang *et al.*, 2010) and the RT dimerisation defective conferring mutation N136A (Mulky *et al.*, 2007). The W401A/L mutations resulted in HIV-1 with significantly reduced infectivity due to decreased reverse transcription and defects in RT maturation and stability. These data can be interpreted to support the sequential theory of RT maturation, although the evidence is circumstantial. There was no evidence that the effect of the W401A/L mutations on RT subunit interaction extended to Gag-Pol interaction or on PR activation. Therefore, the predominant effects of the W401A/L mutations in HIV-1 replication are to perturb RT subunit interaction leading to defects in RT activity and RT maturation.

Chapter 4

Analysis of the W401A compensatory mutation, T409I

4.1 Introduction

The highly conserved TRM is an important region for RT subunit interaction (Divita *et al.*, 1993; Tachedjian *et al.*, 2003; Mulky *et al.*, 2005b). The residues that comprise the TRM are located in secondary structures αL, β20 and the loop linking these structural elements. In the p66 subunit the αL-β20 loop contributes multiple residues to the heterodimer interface (Section 1.6.2-1). The presence of a bulky aromatic at W401 is proposed to have a fundamental role in maintaining the position of the p66 αL-β20 loop, and hence the interactions formed with the p51 subunit (Tachedjian *et al.*, 2003) (Chapter 3). Correspondingly, introduction of a non-conservative mutation at W401, such as W401A, prevents RT subunit dimerisation, a defect that is predominantly mediated by the p66 subunit (Tachedjian *et al.*, 2003). Second-site mutations that restore RT subunit interaction to the W401A mutant RT were identified upon random mutagenesis of $p66^{W401A}$ and screening for an increase in interaction with $p51^{W401A}$ in the Y2H system (Tachedjian *et al.*, 2003). Five different compensatory mutations were identified, of which T409I was both the most frequently occurring and the most potent (Tachedjian *et al.*, 2003).

T409 is located within the αL-β20 loop, and the larger branched side-chain of isoleucine compared to the native threonine at 409 is predicted to increase stearic hindrance, compensating for the collapse of the loop caused by the W401A mutation (Tachedjian *et al.*, 2003). Although T409I acts to restore subunit interaction, expression of T409I in the context of W401A only partially restores RDDP activity (Tachedjian *et al.*, 2003). Thus in this sense the T409I mutation is not restorative, but compensatory.

This Chapter extends the studies performed by Tachedjian and colleagues (2003) to determine the role of T409I in RT dimerisation and function, and on HIV-1 replication. Specifically, studies in recombinant RT were performed to confirm the role of T409I as a W401A compensatory mutation, and to determine the impact of T409I alone. Based upon the association of the effects of W401 mutations that confer a dimerisation defect and defects in HIV-1 replication, it was expected that the ability of T409I to suppress the defects conferred by W401A in recombinant RT would also extend to HIV-1 replication. However, these studies disproved this hypothesis. The T409I mutation caused aberrant Gag-Pol processing, which in the context HIV-1 compounded the defect conferred by W401A. These studies indicate a novel role for highly conserved residues within the TRM, and suggests that the roles of these residues in Gag-Pol and the mature RT heterodimer are functionally distinct.

4.2.1 Location and conservation of T409I

The RT TRM from both subunits clusters at the RT heterodimer interface (Fig. 4.1A). The RT residue T409I is located within the highly conserved TRM and the αL-β20 loop. In the p66 subunit T409 is located at the dimer interface, but buried within the subunit within p51 (Fig. 4.1B). In multiple structures that were analysed (i.e. 1DLO, 1HMV, 1RTD, 1HYS, 1RTH), the threonine side-chain appears to preferentially orientate towards the core of the p66 subunit, rather than directly interacting with the p51 subunit (Fig. 4.1B). Figure 4.1C displays an overlay of the W401A and T409I mutations in the context of the p66 αL-β20 loop. This demonstrates the loss of steric bulk upon mutation of W401 to alanine. The substitution of threonine with isoleucine at 409 introduces a bulkier hydrophobic residue where a small, polar side-chain naturally occurs. In the context of the W401A mutation, the increase in steric bulk due to T409I may act to reposition the αL-β20 loop to its original position (personal communication, M. Kuiper).

T409 is amongst the most highly conserved non-tryptophan residues located within the TRM. Expression of threonine at this location is conserved across HIV strains and nonhuman primate lentiviral RTs (Fig. 4.1D). The most common polymorphism at 409 is serine, which shares similar spatial and chemical properties to threonine. While this residue may not be essential for RT dimerisation and RDDP activity as demonstrated by Tachedjian and colleagues (2003), such high levels of amino acid conservation may be indicative of an important role in other aspects of HIV-1 replication.

4.2.2 Characterisation of the T409I mutation in recombinant RT

Previous studies demonstrate that co-expression of the W401A and T409I mutations result in a wild-type like profile with respect to RT subunit interaction and generation of the p51 subunit from a p66 precursor in recombinant protein studies (Tachedjian *et al.*, 2003). However, the presence of the T409I mutation only partially restores RDDP activity of the W401A mutant to 50% of wild-type levels (Tachedjian *et al.*, 2003). The effect of the T409I mutation alone on RT subunit interaction and RT activity has not been described. Hence the first aim of this study was to examine the effect of this mutation in recombinant RT, and to reproduce previously published data for the W401A/T409I double mutation (Tachedjian *et al.*, 2003).

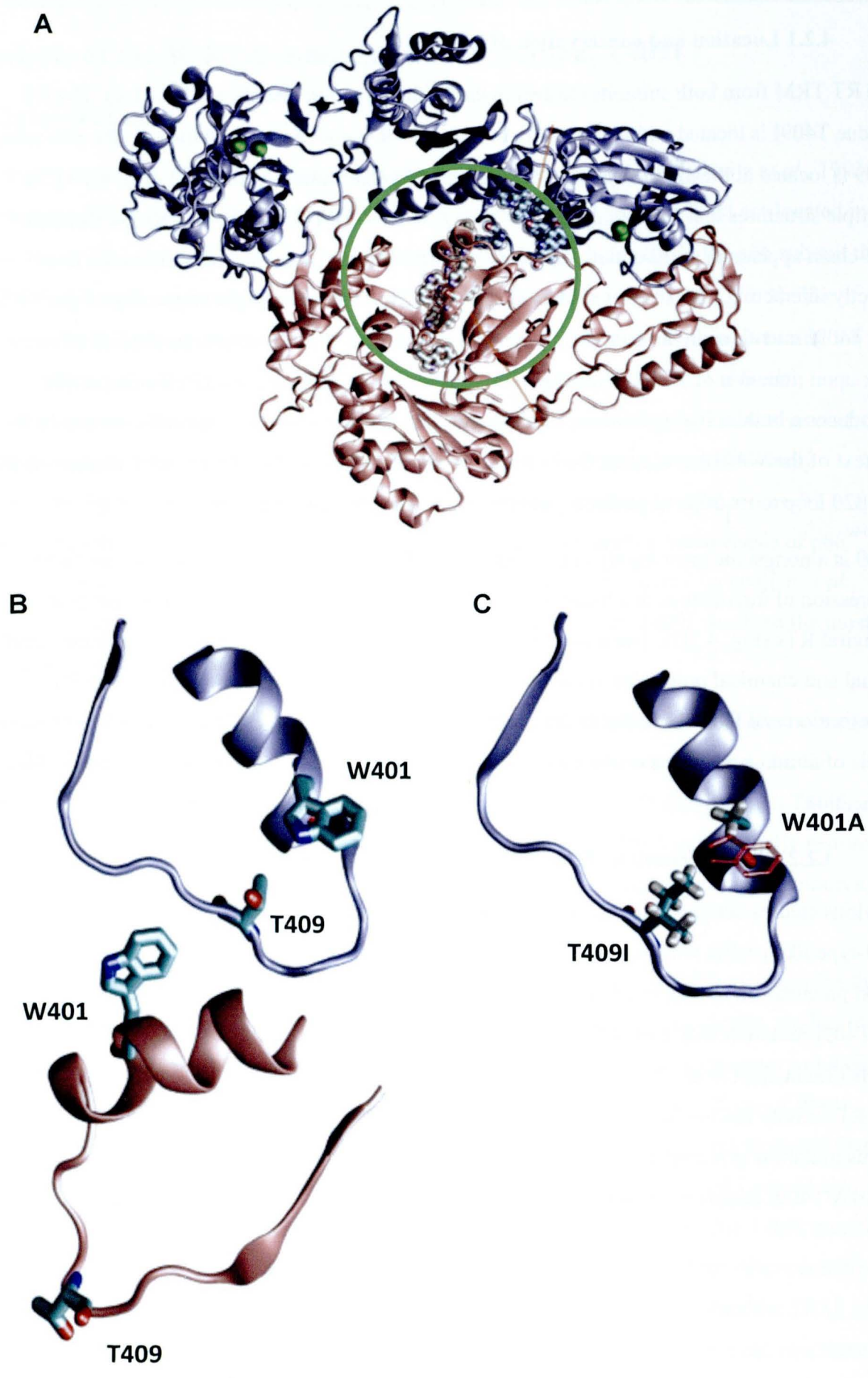
A
B
W401
T409
W401
T409
C
W401A
T409I

D

	398	399	400	401	402	403	404	405	406	407	408	409	410	411	412	413	414
HIV-1 M consensus	W	E	T	W	W	T	E	Y	W	Q	A	T	W	I	P	E	W
HIV-1 N YBF106	W	E	T	W	W	T	E	H	W	Q	A	T	W	I	P	E	W
HIV-1 N YBF30	W	E	A	W	W	T	D	H	W	Q	A	T	W	I	P	E	W
HIV-1 O ANT	W	E	T	W	W	A	D	Y	W	Q	A	T	W	I	P	E	W
HIV-1 O MVP5180	W	E	T	W	W	A	E	Y	W	Q	A	T	W	I	P	E	W
HIV-2 BEN	W	E	Q	W	W	D	N	Y	W	Q	V	T	W	I	P	E	W
HIV-2 ROD	W	E	Q	W	W	D	N	Y	W	Q	V	T	W	I	P	D	W
HIV-2 B_EHO	W	D	Q	W	W	T	D	Y	W	Q	V	T	W	I	P	E	W
HIV-2 B_UC1	W	D	Q	W	W	T	D	Y	W	Q	V	T	W	I	P	E	W
SIVagm 155	W	E	Q	W	W	A	D	Y	W	Q	V	S	W	I	P	E	W
SIVagm 3	W	E	Q	W	W	A	D	Y	W	Q	V	S	W	I	P	D	W
SIVagm TYO1	W	E	Q	W	W	A	D	Y	W	Q	V	S	W	I	P	E	W
SIVcpz EK505	W	E	T	W	W	T	E	Y	E	Q	A	T	W	I	P	D	W
SIVcpz MB66	W	E	A	W	W	T	D	Y	W	Q	A	T	W	I	P	E	W
SIVcpz TAN1	W	S	Q	W	W	T	D	Y	W	Q	V	T	W	V	P	E	W
SIVmac K6W	W	E	Q	W	W	T	D	Y	W	Q	V	T	W	I	P	W	D
SIVmac MM142-83	W	E	Q	W	W	T	D	Y	W	Q	V	T	W	I	P	E	W
SIVmac 17E-Cl	W	E	Q	W	W	T	D	Y	W	Q	V	T	W	I	P	E	W
SIVmac 17E-Fr	W	E	Q	W	W	T	D	Y	W	Q	V	T	W	I	P	E	W
SIVmnd GB1	W	E	D	W	W	H	E	Y	W	Q	C	T	W	I	P	E	V
SIVmnd-2	W	D	Q	W	W	P	E	Y	W	Q	A	T	W	I	P	E	W
SIVmon	W	D	T	W	W	A	D	N	W	Q	V	T	W	I	P	E	I
SIVolc	W	E	A	W	A	F	D	D	W	Q	V	H	W	I	P	D	I
SIVsm F236/SMH4	W	E	Q	W	W	T	D	Y	W	Q	V	T	W	I	P	D	W
SIVsm PBJ/BC13	W	E	Q	W	W	T	D	Y	W	Q	V	T	W	I	P	E	W
SIVwrc Pbt-05GM-X02	W	D	M	W	W	S	E	Y	W	Q	A	T	W	I	P	E	V
SIVqu	W	N	T	W	W	A	E	H	W	Q	A	N	W	I	P	E	V

Figure 4.1. Location and conservation of RT residues W401 and T409.

(A) Ribbon representation of the RT heterodimer with the p66 subunit in blue and p51 subunit in pink. The polymerase and RNase H active site divalent cations are green. The location of the TRM in the heterodimer is circled and the side-chains of each of the TRM residue highlighted in teal space fill modelling. A detail of the αL-β20 loop from each subunit (B) highlights the position of W401 and T409 with the side-chains shown in teal. (C) displays the p66 αL-β20 with the W401 and T409 wild-type residues overlayed by the W401A and T409I mutant side-chains in teal ball and stick model. These images were generated by M. Kuiper using coordinates for the RT structure 1RTD (Huang *et al.*, 1998). The image was creased using the Visual Molecular Dynamics (VMD) program and rendered using POV-Ray (http://www.povray.org). The conservation of T409 in the context of the TRM is shown in (D). The amino acid sequences from representative strains of lentiviral RTs were aligned using the ClustalW2 multiple sequence alignment program (Chenna *et al.*, 2003). The alignment is shown in reference to the HIV-1 M group consensus sequence generated by the Los Alamos HIV sequence database (Los Alamos National Laboratory, 2008a). All other sequences were obtained from the NCBI Entrez Protein Database and accession numbers are detailed in Figure 1.7.

RT heterodimer formation from a p66 precursor was examined using the bacterial expression vector pNLRT6H/PR (Section 2.1.3-1). This plasmid was derived from pRT6H/NB-PROT, which was previously used to examine the effect of the W401A/T409I double mutation on RT dimerisation (Tachedjian *et al.*, 2003). In this case the vector was modified to express the RT sequence from NL (Section 2.1.1). The pNLRT6H/PR vector expresses p66 with a C-terminal hexahistidine tag (p66-HIS) and the HIV-1 PR. Upon induction of expression in bacteria, p66-HIS is assumed to homodimerise, allowing HIV-1 PR mediated cleavage of one of the p66-HIS subunits to generate a p66-HIS/p51 heterodimer. Heterodimer formation was assessed by Western Blot analysis following affinity chromatography of p66-HIS and any interacting p51 (Section 2.8). Equivalent amounts of p66-HIS as determined by Western blot analysis were subject to an RDDP activity assay.

The profile of W401A, T409I or W401A/T409I RT was similar to wild-type RT as observed in the total and soluble fractions, indicating that all constructs were stably expressed and did not form inclusion bodies (Fig. 4.2A). As expected, a 1:1 ratio of p66-HIS to p51 was observed for wild-type RT. Expression of the T409I mutation did not affect either PR mediated processing of p66-HIS to the p51 subunit or RT subunit heterodimerisation (Fig. 4.2A). However, RDDP activity was approximately 55% of wild-type, indicating that despite normal heterodimer formation, the T409I affected RT function (Fig. 4.2B).

The W401A RT demonstrated significantly reduced heterodimer formation (6.7% of WT, $p < 0.05$, Fig. 4.2A and B). This was associated with significantly reduced RDDP activity (6.9% of WT, $p < 0.01$) (Fig. 4.2C). Co-expression of T409I partially restored heterodimer formation to approximately 40% of wild-type levels and was also associated with a corresponding increase in RDDP activity of 36% of wild-type. These data are generally consistent with a previous description of W401A and W401A/T409I RT mutants, with the exception that Tachedjian and colleagues (2003) described heterodimer formation of W401A/T409I RT as equivalent to wild-type. These data confirm that T409I acts as a suppressor mutation in recombinant RT by alleviating the dimerisation defect conferred by W401A and partially restoring associated RDDP activity.

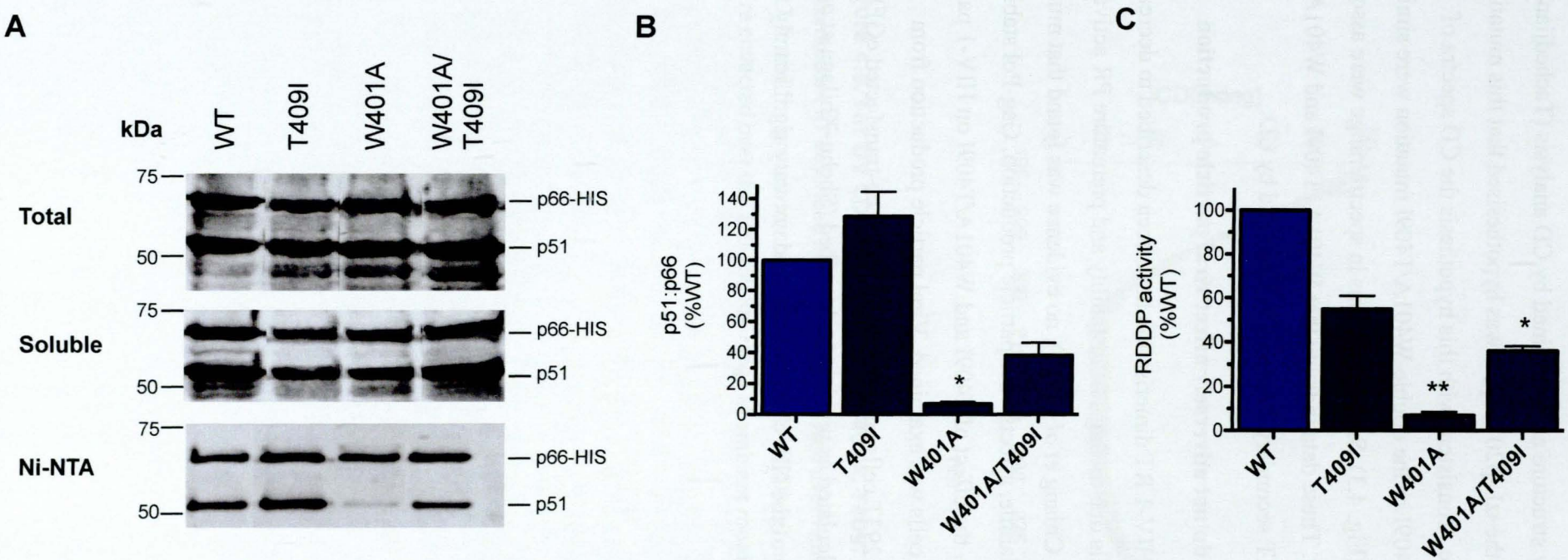

Figure 4.2. Heterodimer formation and RDDP activity of WT, W401A, T409I and W401A/T409I mutant HIV-1 RT.

RT heterodimer formation from a p66 precursor was assessed using the bacterial expression vector pNLRT6H/PR, encoding wild-type or mutant RT. (A) Transformed bacteria were induced, grown and then lysed (total). The soluble fraction (soluble) was affinity purified on Ni-NTA agarose and the eluate subjected to Western blot analysis using RT antibody 11G10 and Alexa Fluor 680 anti-mouse secondary antibody, which were visualised and quantitated using the Odyssey IR imaging system. The ratio of p51:p66-HIS was determined and expressed as the percentage of the wild-type ratio (B). Purified RT was normalised to equivalent amounts of p66 and assayed for RDDP activity on a poly(rA)/oligo(dT) T/P. Incorporation of ^{33}P dTTP was quantified using the Fujifilm FLA-3000 Phosphor Imager, and expressed as the percentage of wild-type activity (C). For (B) and (C) each bar represents the mean of five independent assays and error bars denote the standard error. Significant differences compared to wild-type were identified using the Kruskal-Wallis and Dunn's post test, and are indicated by * when $p < 0.05$, and ** when $p < 0.01$.

4.2.3 The T409I mutation does not affect RT secondary structure.

A previous study has shown that neither a conservative nor non-conservative mutation introduced at W401 confers changes to RT secondary structure as determined by CD analysis (Tachedjian *et al.*, 2005b). Given the location of T409I in the αL-β20 loop, it was hypothesised that this mutation would not affect RT secondary structure. Consistent with this hypothesis the CD spectra of recombinant RT expressing W401A, T409I or the double W401A/T409I mutation were similar to the spectra generated by wild-type RT (Fig. 4.3). Small variations in spectra range were associated with variations in protein concentration. These data indicate that W401A, T409I and W401A/T409I do not mediate significant changes to RT secondary structure as measured by CD.

4.2.4 T409I or W401A /T409I do not adversely affect viral particle production

While mutations that confer defects in HIV-1 RT dimerisation have been described to decrease viral particle production from transfected cells due to Gag-Pol instability and premature PR activation (Yu *et al.*, 1998a; Olivares *et al.*, 2004; Chiang *et al.*, 2010), no evidence was found that mutation of W401 to alanine, leucine or phenylalanine, affects viral particle production, Gag-Pol stability or PR activation (Chapter 3). Accordingly, the effect of T409I and W401A/T409I on HIV-1 particle production from transfected HEK293T cells was examined. Viral particle production from equivalent amounts of transfected HEK293T cells, as determined by the co-transfected eGFP reporter plasmid (Section 2.3.5) was calculated as previously described (Shehu-Xhilaga *et al.*, 2004). Viral particle production for any of the HIV-1 RT mutants did not vary significantly from wild-type (Fig. 4.4).

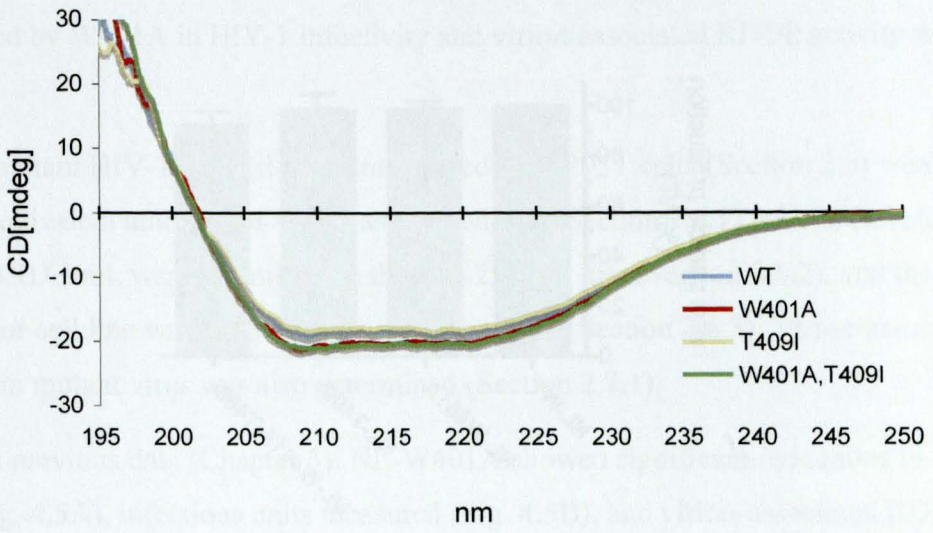

Figure 4.3. Far UV CD spectra of WT, W401A, T409I and W401A/T409I mutant RT.
Recombinant RT described in Fig. 4.2 was dialysed overnight at 4°C in 50 mM phosphate buffer, pH 7.4, and the protein concentration adjusted to 300μg/mL. The CD spectra of recombinant RT were collected over the 190-250 nm range at ambient room temperature.

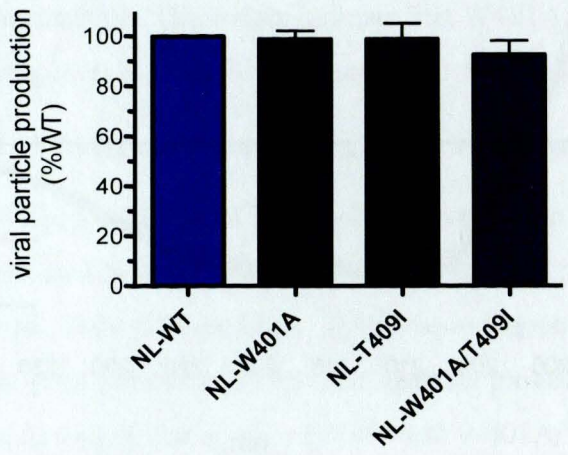

Figure 4.4. HIV-1 particle production of wild-type or RT mutants W401A, T409I and W401A/T409I.

HIV-1 particle production from transfected HEK293T cell cultures was determined by Western blot analysis. Transfection efficiency of wild-type and mutant RT HIV-1 constructs was monitored by co-transfection with an eGFP producing plasmid. Equivalent amounts of viral and transfected cell lysates, as determined by transfection efficiency, were subjected to Western blot analysis using p24 primary antibody 183-H12-5C and Alexa Fluor 680 anti-mouse secondary antibody. Western blots were visualised and quantified using the Odyssey IR imaging system. Viral particle production was calculated as the ratio of virion-associated $Pr55^{Gag}$ and p24 to the total $Pr55^{Gag}$ and p24 in viral and transfected cell lysates as previously described (Shehu-Xhilaga *et al.*, 2004), and expressed as the percentage of wild-type viral particle production. Bars represent mean of nine independent assays and error bars denote the standard error of the mean. No significant difference in viral particle production was observed for all mutants compared to wild-type using the Kruskal-Wallis test ($p = 0.47$).

4.2.5 T409I does not suppress defects conferred by W401A in HIV-1 infectivity or virion-associated RDDP activity

The W401A/L RT mutations prevent RT subunit dimerisation in recombinant RT binding studies, and expression in HIV-1 result in significant decreases in virion infectivity and RT activity. In the context of recombinant RT, T409I suppresses the defects in heterodimerisation and partially restored RDDP activity to the W401A mutant. Here the ability of the T409I mutation to suppress defects conferred by W401A in HIV-1 infectivity and virion-associated RDDP activity was examined.

Wild-type and mutant HIV-1 derived from transfected HEK293T cells (Section 2.3) were normalised to equivalent amounts of virion-associated p24 (Section 2.6.1) prior to infection of cell cultures. The $TCID_{50}$/mL was determined in the MT-2 T cell line (Section 2.6.2), and the titre in the TZM-bl indicator cell line was measured as infectious units (Section 2.6.3). Virion-associated RDDP activity in mutant virus was also determined (Section 2.7.1).

Consistent with previous data (Chapter 3), NL-W401A showed significant reductions in $TCID_{50}$/mL (Fig. 4.5A), infectious units measured (Fig. 4.5B), and virion-associated RDDP activity (Fig. 4.5C). Expression of the T409I mutant alone resulted in decreased levels of infectivity and RDDP activity, however these decreases were not as dramatic as those observed for NL-W401A, and were not found to be statistically significant. NL-T409I demonstrated a 24-fold decrease in $TCID_{50}$/mL and 50% decrease in infectious units compared to wild-type. Virion-associated RDDP activity was at 20% of wild-type.

Unexpectedly, the W401A/T409I mutant showed a greater decrease in infectivity and virion-associated RDDP activity compared to wild-type, and expression of either mutation alone. Evidence of cytopathicity in NL-W401A/T409I infected MT-2 cells was rare with a (26 ± 9 $TCID_{50}$/mL), approximately 10-fold lower than the W401A mutant (147 ± 37 $TCID_{50}$/mL). The infectious units in TZM-bl cells for NL-W401A/T409I was approximately 1% of wild-type levels compared to 9% for NL-W401A. The virion-associated RDDP activity of NL-W401A/T409I was less than 1% of wild-type. Compared to both NL-WT and NL-T409I, the infectivity of NL-W401A/T409I was significantly decreased.

Thus T409I did not act to suppress the defects conferred by the W401A mutation in the context of HIV-1, and appears to act in concert to produce a more defective virus compared to either mutant alone.

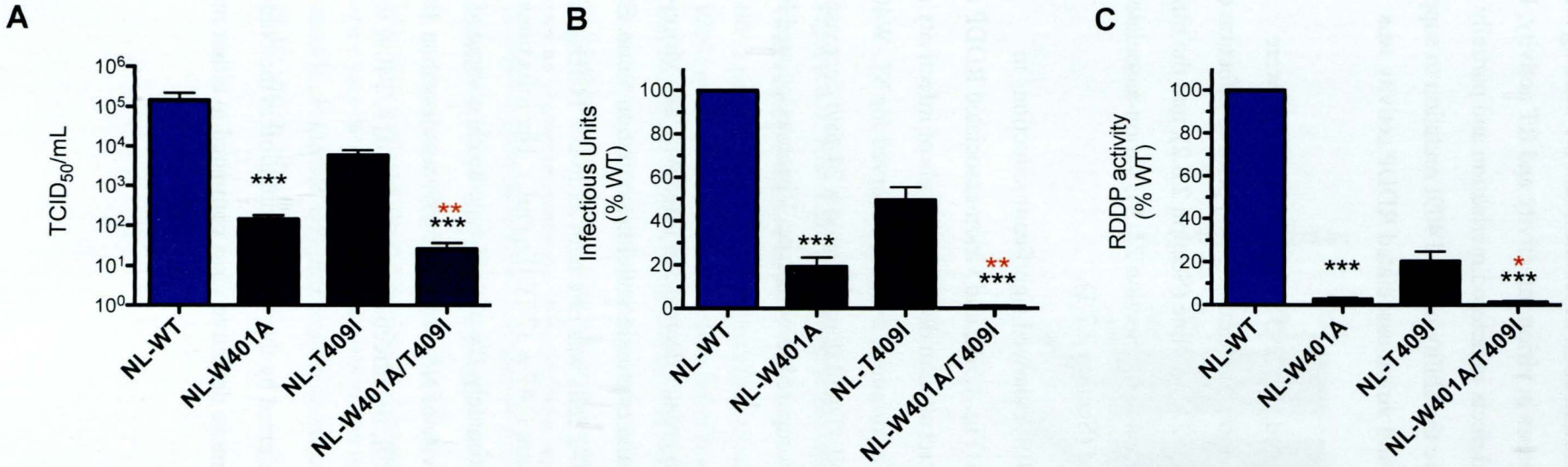

Figure 4.5. Infectivity and virion associated RDDP activity of HIV-1 expressing the RT mutations W401A and T409I.

MT-2 cells and the TZM-bl indicator cell line were infected with clarified supernatants from HIV-1 transfected HEK293T cells, normalised to equivalent amounts of p24 by Western blot analysis. Infected MT-2 cell cultures were scored for CPE six days post infection, and the $TCID_{50}$/mL calculated using the Karber formula (A). Infected TZM-bl cell cultures were fixed 48 h post infection and stained to detect expression of the Tat activated reporter, β-galactosidase. Infected blue-stained foci were counted by light microscopy to determine the infectious units (B). Clarified supernatants were also assessed for virion-associated RDDP activity on a homopolymeric poly(rA)/oligo(dT) T/P. Incorporated ^{33}P-dTTP radiolabel was detected and quantified using the Fujifilm FLA-3000 Phosphor Imager. Infectious units (B) and RDDP activity (C) was expressed as the percentage of wild-type for each individual experiment. Each bar represent the mean of nine independent experiments and error bars indicate standard error. Significant differences were identified using the Kruskal-Wallis with Dunn's post test. A significant difference compared to wild-type is indicated by * when $p < 0.05$, ** when $p < 0.01$ and *** when $p < 0.001$. Comparisons to NL-T409I are noted in red text (*).

4.2.6 T409I does not suppress defects in the viral protein profile of the W401A HIV-1 mutant

As described in Chapter 3, expression of the W401A/L mutations that abrogate RT dimerisation in HIV-1 result in reductions in virion RT, in part due to aberrant proteolysis by the HIV-1 PR. In transfected cell lysates these mutations result in a decrease in the p51:p66 ratio, which may be indicative of a role for p66 homodimer formation for RT maturation. The T409I mutation acts to restore recombinant RT heterodimer maturation from a p66 precursor expressing the W401A mutation. Accordingly, the ability of T409I to restore RT maturation in the context of the HIV-1 W401A mutant was determined by examining viral protein expression in both viral and cell lysates.

The protein profile of NL-W401A viral lysates was consistent with that of previous reports, resulting in a specific and significant decrease in RT subunits with no apparent defects in Gag-Pol virion incorporation or stability as indicated by wild-type levels of virion Gag-Pol (Fig. 4.6A and 4.6B, Table 4.1). No evidence of premature PR activation was observed as indicated by wild-type levels of virion IN, (Fig. 4.6C and Table 4.1), and wild-type Gag processing profiles in both viral (Fig. 4.6 D, Table 4.1) and transfected cell lysates (Fig. 4.7 C, Table 4.2).

Surprisingly, the presence of the T409I RT mutation resulted in significant decreases in virion RT and IN compared to wild-type (Table 4.1). Levels of virion Gag-Pol were significantly decreased when detected using RT (Fig. 4.6A) or p24 antibodies (Fig. 4.6D and Table 4.1). The decrease in Gag-Pol would largely account for the corresponding decrease in virion RT and IN. Low levels of Gag-Pol compared to wild-type were also observed in transfected cell lysates (Fig. 4.7A). An increase in the p24:Gag ratio compared to wild-type in viral lysates (143 ± 12 % of wild-type, $p < 0.05$) and in transfected cell lysates (181 ± 37 % of wild-type) is suggestive of enhanced PR-mediated processing of Gag-Pol rather than a decrease in Gag-Pol incorporation.

In light of these observations, it was perhaps not unexpected that T409I does not act to suppress the defects conferred by W401A in HIV-1. Of all the mutants, NL-W401A/T409I demonstrated the most extreme phenotype in terms of virion RT, with significantly reductions to approximately 10% of wild-type for both RT subunits (Fig. 4.6 and Table 4.1). In contrast to the T409I mutant, this decrease was not entirely attributable to a reduction in virion Gag-Pol. Detection of virion Gag-Pol in NL-W401A/T409I viral lysates using RT monoclonal antibody 11G10 showed no significant reduction compared to wild-type (Fig. 4.6A, Table 4.1). Similar results were observed using an RT monoclonal antibody 5B2, which targets an independent RT epitope to 11G10, where virion Gag-Pol was 83± 5% of wild-type, (n=2), an RNase H monoclonal antibody 18D7 where Gag-Pol was 102% ± 12% (n = 2) compared to wild-type, and a RT polyclonal antibody where Gag-Pol was 119% ± 5 (n=2) compared to wild-type (Fig. 4.6B).

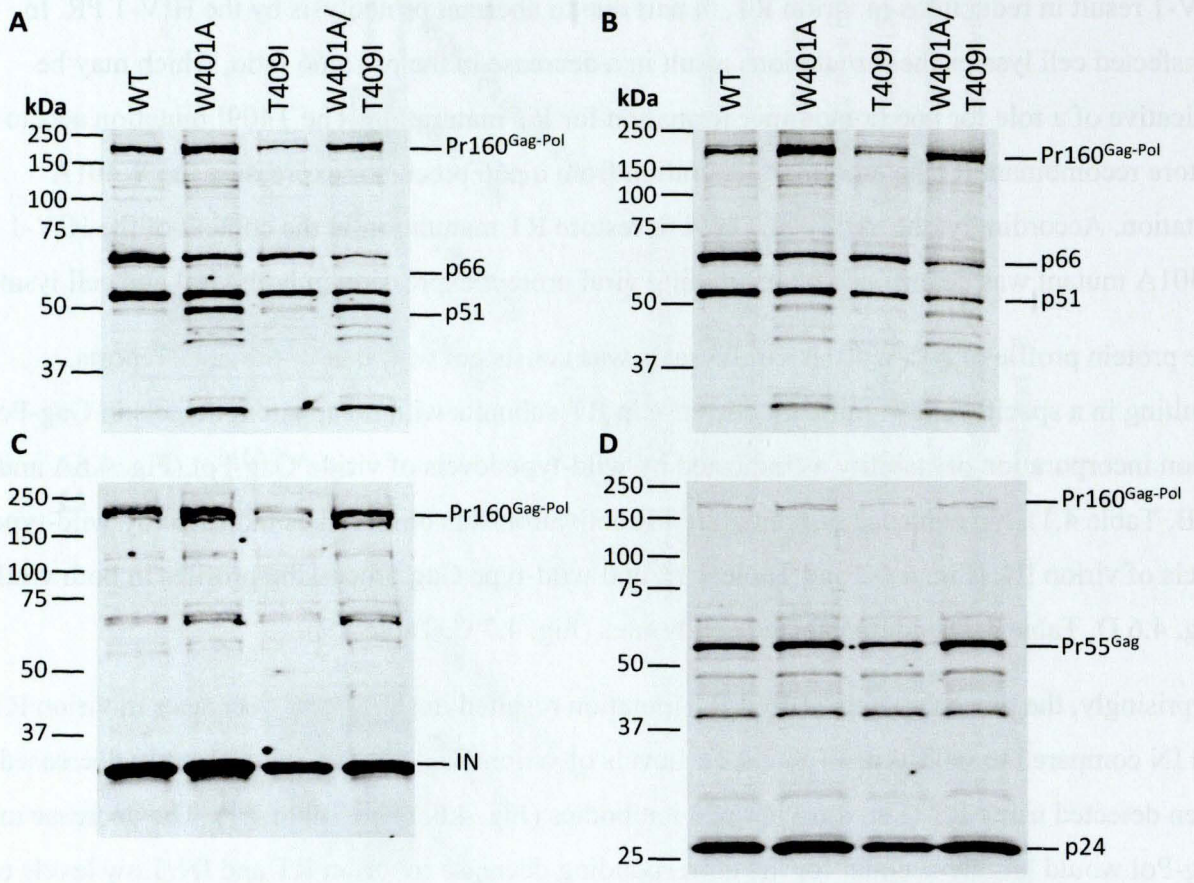

Figure 4.6. Protein profile of W401A, T409I and W401A/T409I mutant HIV-1 in viral lysates

Clarified supernatants from HEK293T cells transfected with wild-type or mutant HIV-1 constructs were pelleted by ultracentrifugation. Virus pellets were lysed normalised to equivalent amounts of p24 and subjected to Western blot analysis using RT antibody 11G10 (A), polyclonal RT antibody (B), IN antibody 8E5 (C) and p24 antibody 183-H12-5C (D). The secondary Alexa Fluor 680 anti-mouse antibody was used with the primary monoclonal antibodies and IR Dye 800 anti-rabbit IgG was used with the primary polyclonal antibody. Proteins were visualised and quantitated using the Odyssey IR imaging system. Blots are representative of seven independent experiments.

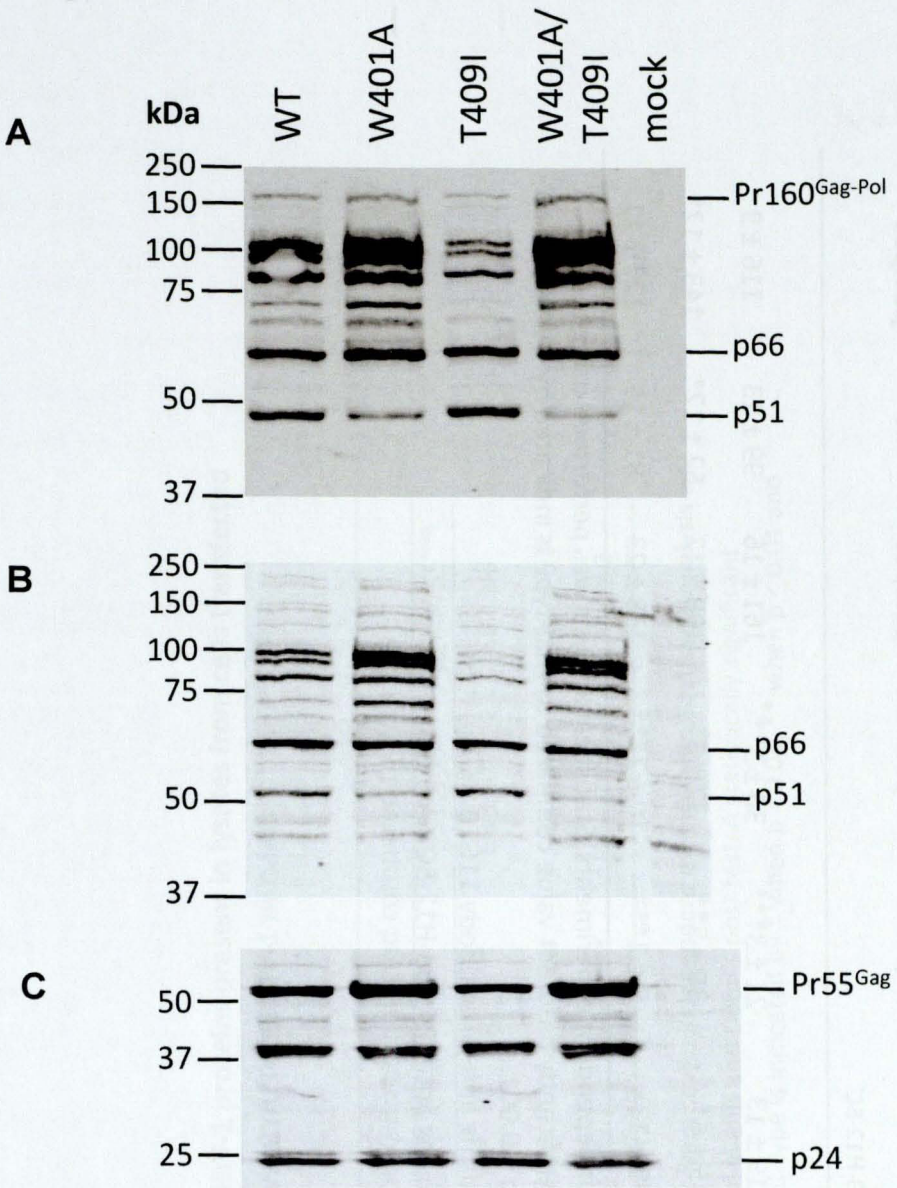

4.7. HIV-1 protein profile in lysates of cells transfected with the W401A, T409I or W401A/T409I HIV-1 mutants.

293T cells transfected with wild-type or mutant constructs were normalised to equivalent amounts of p24 and subjected to Western blot analysis using RT antibody 11G10 (A), RT polyclonal antibody (B) and p24 antibody 183-H12-5C (C). Alexa Fluor 680 anti-mouse secondary antibody was used with the primary monoclonal antibodies and IR Dye 800 anti-rabbit IgG with the primary polyclonal antibody. Proteins were visualised and quantitated using the Odyssey IR imaging system. Blots are representative of seven independent experiments.

Table 4.1. Quantification of viral proteins present in W401A, T409I and W401A/T409I HIV-1 viral lysates

Mutant	Protein or Ratio as indicated compared to WT (%)[a]						
	$Pr160^{Gag\text{-}Pol}$ 11G10[b]	$Pr160^{Gag\text{-}Pol}$ 183-H12-5C[c]	p66	p51	p51:p66	IN	$p24:p55^{Gag}$
NL-W401A	117 ± 21	119 ± 13	21 ± 3***	30 ± 5**	161 ± 16	99 ± 13	116 ± 9
NL-T409I	54 ± 5**	45 ± 6*	30 ± 5**	32 ± 6*	108 ± 12	52 ± 12*	143 ± 12*
NL-W40A/T409I	63 ± 11	98 ± 13	8 ± 2***	10 ± 2***	138 ± 23	81 ± 15	127 ± 11

[a] Mean ± the standard error from seven independent experiments. Statistical analysis was performed using the Kruskal-Wallis and Dunn's post test. A significantly different value compared to wild-type is indicated by * when $p < 0.05$, ** when $p < 0.01$ and *** when $p < 0.001$.

[b] Quantification of $Pr160^{Gag\text{-}Pol}$ detected using anti-RT antibody 11G10

[c] Quantification of $Pr160^{Gag\text{-}Pol}$ detected using anti-p24 183-H12-5C

Table 4.2. Quantification of HIV-1 proteins present in lysates from cells transfected with the W401A, T409I and W401A/T409I HIV-1 mutants

Mutant	Protein or Ratio as indicated compared to WT (%)[a]			
	p66	p51	p51:p66	p24:Pr55^{Gag}
NL-W401A	61 ± 12**	48 ± 5**	68 ± 9**	82 ± 8
NL-T409I	111 ± 2	102 ± 16	95 ± 9	181 ± 37
NL-W401A/T409I	64 ± 11*	40 ± 6***	52 ± 7***	77 ± 10

[a] Mean ± the standard error from seven independent experiments. Statistical analysis was performed using the Kruskal-Wallis and Dunn's post test. A statistically significant difference compared to wild-type is indicated by * when $p < 0.05$, ** when $p < 0.01$ and *** when $p < 0.001$.

In addition, no significant reduction in Gag-Pol levels was observed when viral lysates were probed with IN monoclonal 8E5 (107% ± 19, n = 4, Fig. 4.6C) or p24 antibody 183-H12-5C (98% ± 13) (Fig. 4.6D, Table 4.1). Levels of virion IN, and the p24:Gag ratio did not vary significantly from wild-type, 81 ± 15% and 125 ± 11% of wild-type respectively (Table 4.1).

The HIV-1 protein profile in transfected cell lysates for the W401A mutant was consistent with that described in Chapter 3, with a reduction in both RT subunits and a significant decrease in the p51:p66 ratio (Table 4.2). The NL-W401A/T409I mutant RT profile in transfected cell lysates was similar to the W401A mutant in this respect and a significant decrease in the p51:p66 ratio was observed. NL-T409I demonstrated wild-type levels of RT, however the p24:Gag ratio was increased compared to wild-type (182 ± 37 %, $p > 0.05$). This effect on the p24:Gag ratio was not apparent for NL-W401A/T409I.

Thus in the context of HIV-1, the T409I mutation conferred a defect in Gag-Pol stability or processing. This defect may be mediated by increased HIV-1 PR activity, as indicated by an increased p24:Gag ratio compared to wild-type. This enhanced or aberrant PR activity may be responsible for the decrease in virion Gag-Pol, and Pol products RT and IN. Presumably as a result of the effect of T409I on Gag-Pol, co-expression of T409I with W401A in HIV-1 did not act to suppress the defects conferred by W401A, in contrast to what was been demonstrated in recombinant RT. In contrast to NL-T409I, the profile of NL-W401A/T409I demonstrated a specific decrease in RT, which may be directly related to the effect of the W401A mutation in HIV-1, and exacerbated by the effect of T409I on Gag-Pol. Interestingly, it was apparent that the Gag-Pol defect observed for NL-T409I was not as severe in the double mutant.

4.2.7 Expression of T409I in recombinant Gag-Pol results in aberrant activity of the Gag-Pol embedded PR

The reduced levels of Gag-Pol and IN observed in viral lysates, together with increased Gag processing in viral and cell lysates observed for NL-T409I indicates that this mutation affects Gag-Pol processing or stability, possibly due to increased or aberrant HIV-1 PR activity. Accordingly, the role of T409I in PR-mediated cleavage of Gag-Pol was investigated using the recombinant Gag-Pol processing assay developed by Pettit and colleagues (2003) and described in Section 3.2.6.

Consistent with previous reports (Pettit *et al.*, 2003; Pettit *et al.*, 2004; Pettit *et al.*, 2005a) and the data presented in Chapter 3, expression of wild-type Gag-Pol resulted in cleavage by the Gag-Pol embedded PR at the p2/NC and TFP/$p6^{Pol}$ sites, generating the 120 kDa NC-IN and 113 kDa $p6^{Pol}$-IN processing intermediates, respectively at 1 h incubation (Fig. 4.8). As described in Chapter 3 (Fig. 3.9) the Gag-Pol processing profile of the W401A mutant was similar to wild-type. In contrast, expression of T409I in Gag-Pol resulted in the appearance of an additional 107 kDa processing intermediate corresponding to cleavage of the $p6^{Pol}$/PR site, generating PR-IN. The appearance of pi 107 PR-IN was accompanied by a concomitant decrease in full-length Gag-Pol compared to wild-type at 4 and 6 h post-induction and an increase in processing intermediates in the 60-70 kDa range (Fig. 4.9). Whereas identification of the 107 kDa processing intermediate by size migration analysis was accurate, identification of these smaller products was not (± 2-3 kDa). However the similarity of the profile to previous publications (Pettit *et al.*, 2005a) suggests these lower molecular weight products correspond to the p66 subunit and the processing intermediates $p6^{Pol}$-p51 and PR-p51 (67 and 62 kDa, respectively).

The Gag-Pol processing profile of the W401A/T409I mutant was similar to T409I where the appearance of the processing intermediate PR-IN was associated with an accelerated decrease in full length Gag-Pol compared to wild-type at 4 and 6 h post induction, and an increase in 60-70 kDa intermediates (Fig. 4.9). These data demonstrate that expression of T409I in the context of Gag-Pol alters the kinetics and cleavage of Gag-Pol mediated by the endogenous PR suggesting a mechanism for the increase in Gag and Gag-Pol processing observed upon expression of T409I.

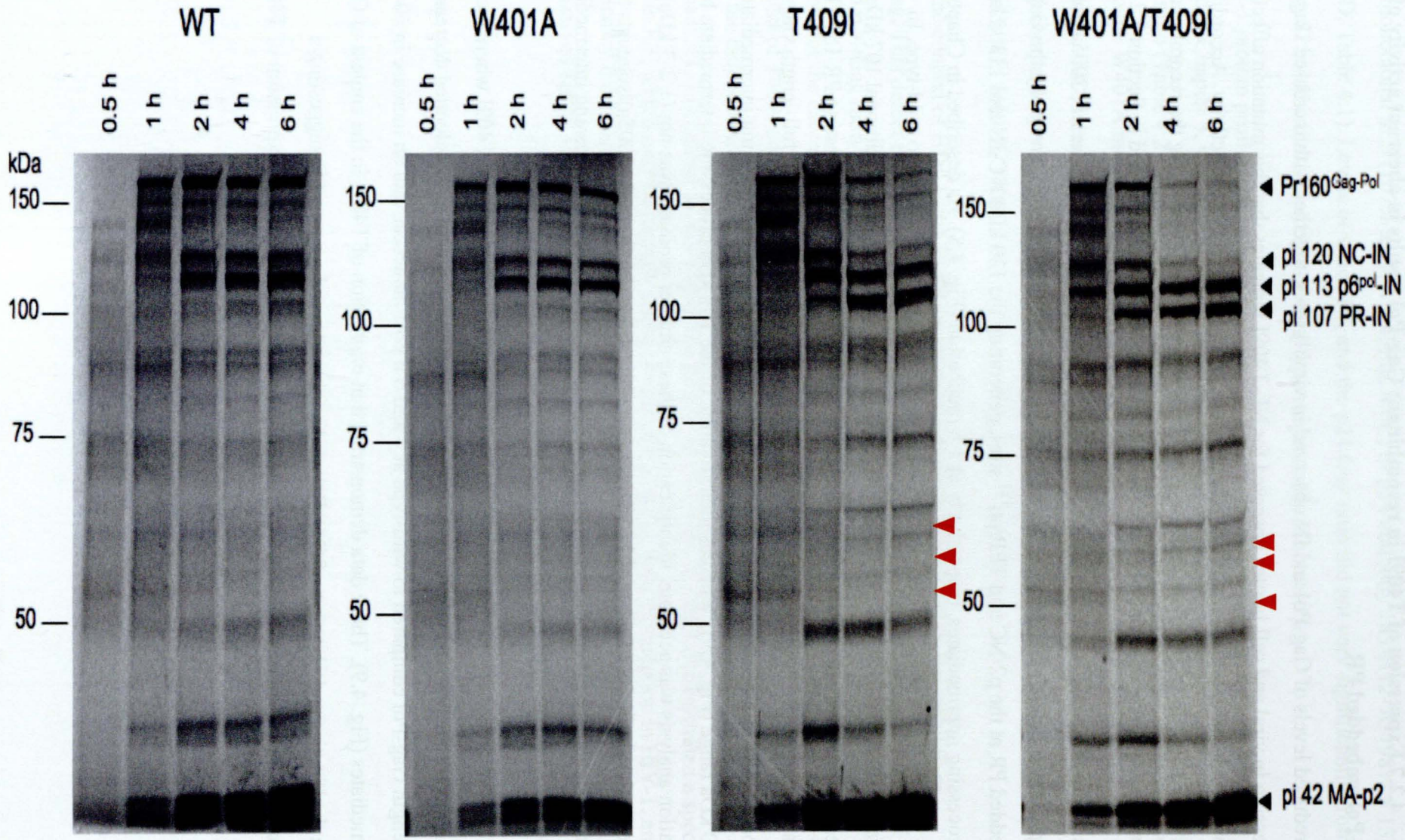
WT
W401A
T409I
W401A/T409I
0.5 h
1 h
2 h
4 h
6 h
kDa
150
100
75
50
Pr160Gag-Pol
pi 120 NC-IN
pi 113 p6pol-IN
pi 107 PR-IN
pi 42 MA-p2

Figure 4.8 Effect of the W401A, T409I and W401A/T409I mutations on the initial Gag-Pol cleavage events mediated by the Gag-Pol embedded PR.

The full-length Gag-Pol coding region derived from NL with a constitutive frameshift mutation, was expressed in the Promega RRL Transcription/Translation system. WT Gag-Pol (A) or Gag-Pol expressing RT mutations W401A (B), T409I (C), and W401A/T409I (D) and the processing intermediates were detected by incorporation of ^{35}S radiolabelled methionine and cysteine. Aliquots were removed at the indicated time points, added to an excess of 2 ×SDS sample buffer, resolved by SDS-PAGE and visualised using the Fujifilm FLA-3000 Phosphor Imager. Gag-Pol processing intermediates (pi) were identified by the calculated molecular mass and are denoted by solid arrowheads with the nomenclature previously defined by Pettit and colleagues (2003). Solid red arrows denote processing intermediates in the 60 to 70 kDa range that are predicted to correspond to $p6^{pol}$-p51, PR-RNase H and PR-p51. Molecular weight markers are indicated on the left of each blot. Blots are representative of five independent experiments.

4.3 Discussion

Tachedjian and colleagues describe the ability of the W401A mutation to prevent p66 homodimerisation, reduce RT heterodimer formation and correspondingly decrease the RDDP and DDDP activities of the mature HIV-1 RT heterodimer (Tachedjian *et al.*, 2003; Tachedjian *et al.*, 2005b). The W401A a second-site compensatory mutation, T409I, restores RT heterodimer formation, and partially restores RDDP activity (Tachedjian *et al.*, 2003). This study confirmed the role of T409I as a W401A compensatory mutation in recombinant RT. However, this role did not extend to suppressing defects conferred by W401A in the context of HIV-1. The T409I mutation conferred a Gag-Pol processing defect, which when combined with the W401A mutation in HIV-1, appeared to compound the distinct phenotypes of each of the individual mutations. Thus these two highly conserved RT residues in the TRM, located in close proximity both sequentially and spatially, appear to affect HIV-1 replication by two independent mechanisms.

As Tachedjian and colleagues (2003) had not analysed the effect of the T409I mutation alone in recombinant RT, this was performed as the first part of this study. T409I had no affect on RT secondary structure as determined by CD analysis. A wild-type like profile in terms of bacterial expression of p66 and generation of the RT heterodimer also suggest that the T409I mutation did not adversely affect RT expression or structure. However, the RDDP activity of recombinant T409I RT was 55% of wild-type. Whether DDDP or RNase H activities were also decreased by T409I compared to wild-type was not investigated in this study. Nevertheless, the impact of T409I on RT activity is consistent with previous studies showing an interplay between the RT heterodimer interface and the polymerase active site (Tachedjian *et al.*, 2000; Tachedjian *et al.*, 2005b.

Similar to T409I, the W401F mutation does not adversely affect recombinant RT subunit dimerisation or RT secondary structure as assessed by CD analysis (Tachedjian *et al.*, 2003; Tachedjian *et al.*, 2005b). However, expression of W401F can adversely affect RDDP, DDDP and RNase H activity compared to wild-type, depending on the type and the amount of essential cation co-factor present (Tachedjian *et al.*, 2005b). Under the same conditions used in this study to measure RDDP activity, the W401F RT demonstrates RDDP activity that is 75% of wild-type (Tachedjian *et al.*, 2003). Tachedjian and colleagues (2000) propose that the architecture of the RT heterodimer interface is integral for construction of an optimal polymerase active site. Although located at the heterodimer interface, the $p66^{T409}$ side-chain preferentially orientates towards the core of the p66 subunit. This may explain why T409 is in not consistently identified as an important contributor to the RT heterodimer interface (Menendez-Arias *et al.*, 2001; Rodriguez-Barrios *et al.*, 2001) (Table 1.1). However, in recombinant protein studies the presence of both W401A and T409I in p66 enhances interaction with both $p51^{WT}$ and $p51^{W401A}$ above that of wild-type levels

(Tachedjian *et al.*, 2003), indicating subtle changes to subunit interaction conferred by T409I. Thus T409I may mediate changes at the heterodimer interface, which do not act to decrease RT subunit interaction or affect RT secondary structure observable by CD analysis, but result in suboptimal RT activity.

In recombinant RT, Tachedjian and colleagues (2003) report that the addition of T409I to W401A RT completely restores RT heterodimer formation, and partially restores RDDP activity to 50% of wild-type. In this regard, minor differences between the Tachedjian study and this study were observed. Quantification of the p51:p66 ratio indicated that the addition of T409I to W401A restored heterodimer formation and RDDP activity to 40% of wild-type. All attempts were made to replicate the parameters of the Tachedjian study, including construction of the expression vector and the protein affinity purification protocol. The RT coding region in the Tachedjian study was derived from pN5', which contains the *pol* coding region from the NL4.3 HIV-1 molecular clone (Adachi *et al.*, 1986). This study used RT derived from an independently sourced NL4.3 clone (Buxton *et al.*, 2005). A single polymorphism is observed at RT codon 549 resulting in a K to G change with respect to NL4.3. Moreover, there are 27 synonymous nucleotide polymorphisms, which could lead to differences in codon usage and protein expression. Therefore, it is possible that the observed differences in RT heterodimerisation and RDDP activity are due to the different genetic backgrounds of the RT used in these two studies. Despite these differences, T409I demonstrated the ability to increase both recombinant RT heterodimerisation and RDDP activity of the W401A mutant, and can still be viewed as a compensatory mutation. Thus the ability of T409I to suppress the defects conferred by W401A in HIV-1 was investigated, as well as the role of the T409I mutation itself. The high conservation of this residue, similar to that of the tryptophan residues in the TRM, suggests an important role for T409 in HIV-1 replication. Consistent with this notion, T409I was found to confer Gag-Pol processing defects, resulting in significantly decreased levels of Gag-Pol, RT and IN in the HIV-1 virion.

The affect of T409I on Gag-Pol processing was confirmed using the recombinant Gag-Pol processing assay developed by Pettit and colleagues (2003). Upon expression of a full-length Gag-Pol, Pettit and colleagues (2003) typically observe accumulation of Gag-Pol prior to cleavage mediated by the Gag-Pol embedded PR. The first cleavage occurs at the p2/NC site generating the 42 kDa MA-p2 and 120 kDa NC-IN intermediates. The latter is rapidly processed at the TFP/$p6^{Pol}$ site to generate a 113 kDa intermediate, $p6^{Pol}$-IN. No further cleavage events are observed for wild-type Gag-Pol in this system (Pettit *et al.*, 2003; Pettit *et al.*, 2004; Pettit *et al.*, 2005a). In contrast, it was found that expression of T409I resulted in the generation of an additional processing intermediate of 107 kDa. This is consistent with cleavage at the $p6^{Pol}$/PR site generating the PR-IN intermediate.

A decrease in total Gag-Pol and increase in processing intermediates in the 60-70 kDa range at later time points were also observed. Thus T409I alters the pattern and kinetics of Gag-Pol cleavage by the embedded HIV-1 PR *in vitro*.

Various mutations have been characterised that result in cleavage at the $p6^{Pol}$/PR site to generate the 107 kDa PR-IN intermediate in the recombinant Gag-Pol processing system. Blocking the TFP/$p6^{Pol}$ cleavage site (F440/L441) prevents generation of the 113-kDa $p6^{Pol}$-IN intermediate and enhances cleavage at the $p6^{Pol}$/PR site (Pettit *et al.*, 2004). Also, mutation of N- and C-terminal PR residues which interact to form the PR dimer interface (i.e. I3A, T96A, and F99A) result in a Gag-Pol processing profile including the 107 kDa PR-IN, but also with the persistence of the primary 120 kDa NC-IN intermediate (Pettit *et al.*, 2003).

A slightly different profile is observed upon mutation of the first PR residue (P1), to alanine (P1A) in the context of Gag-Pol. In contrast to the other PR interface mutants (I3A, T96A, and F99A), expression of P1A results in cleavage of the initial cleavage sites p2/NC and TFP/$p6^{Pol}$ to generate a 113 kDa intermediate, $p6^{Pol}$-IN, similarly to wild-type Gag-Pol. However the P1A mutation allows subsequent cleavage events at $p6^{Pol}$/PR, RT/IN and p51/RNase H, generating the processing intermediates PR-IN, the 67 kDa $p6^{Pol}$-p66 intermediate, 62 kDa PR-p51 intermediate, and the p66 subunit respectively (Pettit *et al.*, 2005a). These intermediates are not observed for wild-type Gag-Pol in this system. Pettit and colleagues (2005a) conclude that in the context of Gag-Pol, relieving the constraints of the rigid proline residue with the P1A mutation enhances flexibility of the Gag-Pol embedded PR facilitating cleavage of distal sites in addition to influencing the rate of cleavage at the $p6^{Pol}$/PR site. This effect is only observed in the context of the precursor associated PR. When the P1A mutation is expressed in the mature PR, the Gag-Pol processing profile is indistinguishable from that mediated by wild-type PR (Pettit *et al.*, 2005a).

Expression of the T409I mutation in the same recombinant Gag-Pol system resulted in a profile resembling that of P1A Gag-Pol. The 107 kDa intermediate corresponding to the PR-IN fragment was accurately identified by size migration analysis. However, the fragment sizes calculated from for intermediates in the range of 75-50 kDa did not correspond accurately with their molecular weight (± 3 kDa). It is suggested that these fragments observed in the T409I and W401A/T409I Gag-Pol processing profiles correspond to the 67 kDa $p6^{Pol}$-p66, p66 RT, and the 62 kDa PR-p51 products, based on the resemblance to the processing profile to that generated by the PR P1A mutant characterised previously (Pettit *et al.*, 2005a)

The Gag-Pol associated PR has different affinity for the cleavage sites compared to the mature free PR (Pettit *et al.*, 2005a). Cleavage of the $p6^{Pol}$/PR site in model systems is accompanied by an increase in wild-type like PR activity of the precursor associated PR (Louis *et al.*, 1994; Wondrak *et*

al., 1996; Pettit *et al.*, 2004). Thus accelerated cleavage at this site may result in expedited PR maturation. In the context of Gag-Pol, the T409I mutation may act similarly to facilitate cleavage at the $p6^{Pol}$/PR site, resulting in a PR intermediate with a wild-type like PR activity profile. Such an effect could explain the observation of decreased levels of Gag-Pol and enhanced Gag cleavage in viral and transfected cell lysates. To do so, T409I would confer increased flexibility to the Gag-Pol precursor, or facilitate exposure of cleavage sites. However, whether the activity of the precursor associated PR is responsible for aberrant cleavage of RT and IN containing processing intermediates, or whether this mutation results in conformational changes to RT and IN processing intermediates that are susceptible to proteolysis is unknown. In this regard, it would be of interest to examine the effect of the P1A mutation in HIV-1. First to determine whether this mutation has a similar effect compared to T409I on Gag-Pol processing in the context of the virion, including whether P1A enhances PR mediated decreases in virion RT and IN. If the phenotypes were similar for P1A and T409I it would suggest that the latter mediates conformational changes in Gag-Pol that relaxes constraints on the Gag-Pol embedded PR.

Another potential mechanism of action describing the effects of the T409I mutation could be related to the recently described interaction of Gag-Pol with the host cell factor clathrin. Clathrin interacts with multiple domains of Pol and acts either to regulate PR mediated processing of Gag-Pol or stabilise Pol processing intermediates in the presence of an active HIV-1 PR (Popov *et al.*, 2011; Zhang *et al.*, 2011). Reducing virion clathrin incorporation results in reduced HIV-1 infectivity, with no effect on viral particle production. Interestingly, expression of L234A in HIV-1 with an inactivated PR reduces clathrin incorporation in the virion (Zhang *et al.*, 2011). It is proposed that part of the effect of the L234A mutation on HIV-1 replication could be due to loss of interaction with clathrin. T409I results in a decrease in HIV-1 infectivity independent of a decrease in viral particle production, and a reduction in Gag-Pol RT and IN, which correspond with the proposed roles of clathrin in HIV-1 maturation. However, there is no described effect of clathrin on Gag processing. NL-T409I demonstrated a small but measurable increase in Gag processing in viral and cell lysates. Nevertheless, the possibility remains that T409I may affect Gag-Pol interaction with clathrin, which may be responsible for the instability in Pol products demonstrated by this mutant. Studies are currently in progress to determine whether NL-T409I packages clathrin into the virion at lower levels compared to wild-type.

Another possibility is that the T409I mutation, similarly to L234D (Yu *et al.*, 1998a), induces long-range conformational changes resulting in Gag-Pol instability and PR mediated degradation of Gag-Pol. This, however, is considered a less likely explanation. Premature PR activation or Gag-Pol instability is associated with a loss of Pol proteins from the budding virion into the cytoplasm of the producer cell (Yu *et al.*, 1998a; Olivares *et al.*, 2004).

While NL-T409I demonstrated consistent decreases in virion Gag-Pol, RT and IN, there was no evidence of a concomitant increase of Gag-Pol or RT in transfected cell lysates. Examination of IN would be a more appropriate indicator, as this protein carried no mutation. Unfortunately, due to technical difficulties with the preparation of monoclonal antibodies, detection of IN in transfected cell lysates was poor for all viruses, and no reliable data was obtained. However, wild-type levels of viral particle production indicate that premature PR activation was not a significant phenotype mediated by this mutation (Figueiredo *et al.*, 2006). While a substantial defect in particle production would be required for detection in the robust HEK293T transfection system used here, premature PR activation was not evident in the processing profile of recombinant Gag-Pol. The T409I Gag-Pol processing profile was characteristic of enhanced processing at additional sites, rather than premature activation.

To more completely address the effect of the T409I mutation further studies are proposed. These include expression of the T409I with an inactivated PR in recombinant Gag-Pol to confirm the lack of effect on Gag-Pol stability. Generation of NL-T409I in the presence of a protease inhibitor could confirm the role of PR activity in degradation of Gag-Pol processing intermediates, and to further examine the role of T409I in Gag-Pol stability in the context of HIV-1. Also, a more sensitive method for detection of viral particle production (Figueiredo *et al.*, 2006) would demonstrate whether T409I can result in a decrease in viral particle production not observed by the techniques used within this study. Finally, assessment of clathrin incorporation into NL-T409I virions to determine the role of this host cell factor in the defects observed for NL-T409I.

Given the association of T409I with increased Gag-Pol cleavage and reduced levels of virion-associated RT and IN, it was perhaps not surprising to find that co-expression of T409I did not act to suppress the defects conferred by W401A in HIV-1. NL-W401A/T409I demonstrated greater decreases in steady-state virion protein levels, viral infectivity and RT activity compared to the W401A mutant. Interestingly, the processing profile of recombinant Gag-Pol resembled that of T409I, with the presence of a 107 kDa intermediate indicating cleavage of the $p6^{Pol}$/PR site, and increase in processing intermediates in the 60-70 kDa range. While the presence of T409I in the context of W401A appeared to confer a similar in vitro Gag-Pol processing profile to T409I alone, levels of Gag-Pol, IN, and Gag processing profiles in viral and transfected cell lysates bore a greater resemblance to that of NL-W401A, compared to the NL-T409I mutant. The exception was levels of virion RT that demonstrated a greater decrease compared to that seen in the presence of either mutation alone.

This reduction in virion RT conferred by the T409I mutation may also form the basis for the apparent disparity in RDDP activity of recombinant RT compared to viral lysates. For recombinant RT heterodimers, equivalent amounts of p66-HIS assayed, whereas viral lysates were normalised

according to equivalent amounts virus as determined by p24/CA. Hence the RDDP activity for T409I and W401A/T409I double mutant in viral lysates is representative of the decreased levels of virion RT affected by these mutations, as well as the effect on RT function. In contrast, as the W401A mutation confers a dimerisation defect, and subunit dimerisation is a requisite for RT activity, the reduction in RDDP activity is more consistently observed, regardless of the input.

Both the effect of T409I on PR activity and the ability of the W401A mutation to mitigate its detrimental effect on virion Gag-Pol and IN levels are reminiscent of a study by Chiang and colleagues (2010). The expression of a non-conservative mutation at W402 in VSV-G pseudotyped HIV-1 results in significant reductions in viral particle release and enhances Gag cleavage in transfected cell lysates (Chiang *et al.*, 2010). Chiang and colleagues (2010) propose that mutation of W402 accelerates Gag-Pol multimerisation resulting in premature PR activation. Correspondingly, generation of W402A expressing HIV-1 in the presence of PR inhibitors mitigates this effect, as does co-expression with the W401A mutation, which has also been found to partially negate the Gag-Pol dimerisation enhancement effect of efavirenz on PR-mediated processing (Chiang *et al.*, 2009). Chiang and colleagues conclude that the HIV-1 RT tryptophan repeat motif, in the context of Gag-Pol, may play an important role in suppressing premature activation of HIV-1 PR during the late-stage of virus replication. Interestingly, this is similar to the role that has been ascribed to clathrin in the HIV-1 maturation (Zhang et al 2011; Popov et al 2011).

It is possible, given the proximity of W402 and T409, that mutation of these residues result in a similar phenotype. Given the high conservation of the TRM and the residues that fall within the TRM, the observation that mutation of many of the TRM residues has little or no effect on RT subunit interaction and activity, these suggest an essential role of this region in HIV-1 replication that is distinct to reverse transcriptase function. This could indeed be regulation of Gag-Pol processing by the embedded PR, and may involve the recently described role for the host cell factor clathrin. While differences are observed between this study and the study by Chiang and colleagues (2009), these may be attributed to differences in experimental systems.

With respect to expression of mature RT in HIV-1, it is clear that T409I does not act as a second-site suppressor of the W401A mutation. The low levels of RT in NL-W401A/T409I viral lysates suggests that the mutant RT is unstable or is selectively degraded by PR. In terms of the RT profile in transfected cell lysates, the W401A/T409I mutant demonstrated a W401A-like profile with a significantly decreased ratio of p51:p66. As proposed in Chapter 3, inability of the W401A RT mutant to form stable homodimers and heterodimers in HIV-1 resulted in aberrant proteolysis in the high PR concentration environment of the virion, and defects in RT maturation in the comparatively low PR concentration environment of the cell. If co-expression of T409I partially restores RT subunit interaction, why does the W401A/T409I phenotype in cell lysates resemble that of W401A?

A simple explanation may be that the effect is concentration dependent. As observed for wild-type HIV-1, the p51:p66 does not achieve a 1:1 ratio, indicating that cleavage of the p51/RNase H site is not efficiently mediated in cell lysates. Due to proteolysis of processing intermediates, less RT is present in NL-W401A/T409I transfected cell lysates, which may directly restrict the opportunity for RT maturation. It is also possible that bacterial expression of p66 subunit and HIV-1 PR mediated maturation is not representative of the situation in transfected cell lysates. Thus the observations in this recombinant protein assay are not transferable to the generation of mature RT *in situ*. Regardless, these data suggest that the earlier conclusion that a decrease in the p51:p66 ratio in cell lysates is indicative of an RT dimerisation defect (Chapter 3) may need to be reconsidered.

In summary, it is evident that while the T409I mutation does not mediate changes to RT secondary structure, it is detrimental to RT function as demonstrated by the reduction of RDDP activity compared to wild-type. It is likely that changes are mediated at the dimer interface and lead to conformational changes in the polymerase active site, as proposed for the W401F mutation (Tachedjian *et al.*, 2005b). In the context of Gag-Pol, T409I is also proposed to induce local conformational changes, which translate to increased flexibility or exposure of the $p6^{Pol}$/PR cleavage site leading to enhanced cleavage at this site. As described in previous studies, this PR intermediate is more representative of the mature PR than precursor associated PR intermediates (Pettit *et al.*, 2005a). This may result in the increased processing of the viral precursor proteins and intermediates observed for this mutant. This study demonstrates that residues important in the formation of a mature RT do not necessarily play the same role in Gag-Pol dimerisation and vice versa. In conclusion, the high conservation of TRM and residues contained within this motif, i.e. T409I, suggests that this region is not only important for RT dimerisation but also for Gag-Pol interactions and regulation of Gag-Pol maturation.

Chapter 5

Generation and analysis of W401A compensatory mutations in HIV-1

5.1 Introduction

Introduction of a non-conservative mutation at the highly conserved RT TRM residue, W401, results in a RT heterodimerisation defect mediated by the p66 subunit. In p66, W401 is located in the αL secondary structure, at the base of the αL-β20 loop, which forms multiple interactions with the p51 subunit at the heterodimer interface (Menendez-Arias *et al.*, 2001; Rodriguez-Barrios *et al.*, 2001; Srivastava *et al.*, 2006). The bulky aromatic side-chain of W401 is proposed to have an essential role in positioning the αL-β20 loop, and the W401A mutation is proposed to collapse the αL-β20 loop, resulting in the loss of multiple heterodimer interface interactions (Tachedjian *et al.*, 2003; Tachedjian *et al.*, 2005b, Chapter 3). In the context of HIV-1 replication, the W401A mutation results in a significant reduction in HIV-1 infectivity, RT activity and changes to the HIV-1 RT protein profile indicative of a RT maturation defect (Wapling *et al.*, 2005, Chapter 3). It is proposed that these effects are a direct consequence of the effect of the mutation on RT dimerisation, both in the context of the mature RT, and as part of RT containing processing intermediates during HIV-1 maturation. The conclusion that these defects are representative of the role of RT dimerisation in HIV-1 replication is supported by the observation that W401F, which does not affect RT subunit dimerisation (Tachedjian *et al.*, 2003; Tachedjian *et al.*, 2005b), confers no significant effects on HIV-1 replication (Wapling *et al.*, 2005, Chapter 3). The association between RT dimerisation and defects in HIV-1 replication would be supported by the identification of second-site mutations, that by acting to restore RT subunit dimerisation to the W401A mutant, also suppress the defects in HIV-1 replication.

The RT mutation, T409I, partially restores subunit dimerisation and RT activity to recombinant RT expressing the W401A mutation (Tachedjian *et al.*, 2003). However, due the role of T409 in Gag-Pol processing, the T409I mutation does not act to suppress defects conferred by W401A on HIV-1 replication (Chapter 4). The nature of spontaneous mutations are known to correlate with the selection pressure under which they were generated (Kimura, 1985). The T409I mutation was identified by selecting for mutations in $p66^{W401A}$ that restored interaction with the p51 subunit (Tachedjian *et al.*, 2003). Consistent with the selection pressure, T409I acts as a W401A suppressor mutation under the specific condition of forming a recombinant RT heterodimer, and may not necessarily suppress defects in the context of HIV-1 replication.

This Chapter describes the characterisation of mutations that act to suppress defects in HIV-1 replication conferred by W401A. Following 25 passages of the NL-W401A mutant HIV-1 in MT-2

cells, HIV-1 with increased infectivity was selected. In addition to the parent W401A mutation, three second-site mutations in the RT domain were identified, C162Y, K366R and A534T. Expression of these mutations suppressed defects conferred by W401A in HIV-1 replication, in addition to restoring recombinant RT subunit interaction. This study provides further evidence for the essential role of RT dimerisation in HIV-1 replication. These data also support the proposed mechanism of action of the W401A mutation, perturbing RT dimerisation by disturbing the positioning of the p66 αL-β20 loop at the RT heterodimer interface.

5.2 Results

5.2.1 Identification of second-site suppressor mutations generated upon serial passage of NL-W401A in MT-2 cells

The NL-W401A mutant demonstrates significantly reduced infectivity with low levels of CPE (Section 3.2.2). In order to establish a productive infection with NL-W401A, MT-2 cells were infected with a concentrated stock of NL-W401A. In contrast to standard infections where clarified supernatants from transfected HEK293T cultures are used, 30 mL of clarified supernatant was concentrated by ultracentrifugation, and the entire resuspended viral pellet used to infect 4×10^5 MT-2 cells (Section 2.4.1). An infection with wild-type HIV-1 (NL-WT) was established and passaged in parallel using 1 mL of clarified supernatant from pNL4.3 transfected HEK293T cells as described (Section 2.4). Infected cultures were passaged approximately every four days by a 1:4 dilution in fresh culture medium (Section 2.4.1).

HIV-1 specific CPE was observed in NL-W401A infected cultures at passage 14, and approached that of wild-type virus at passage 25. Aliquots of NL-WT and NL-W401A from passage 14 and 25 were biologically cloned by three sets of terminal dilutions in MT-2 cells (Section 2.4.2). The infectivity of NL-WT increased by approximately 60-fold at passage 25 (p.25) compared to the transfection derived stock (p.0) (Section 2.6, Fig. 5.1). NL-W401A increased from an undetectable titre at p.0, to a titre approaching that of wild-type virus at passage 14, which was comparable to the titre of wild-type virus at passage 25 (Fig. 5.1).

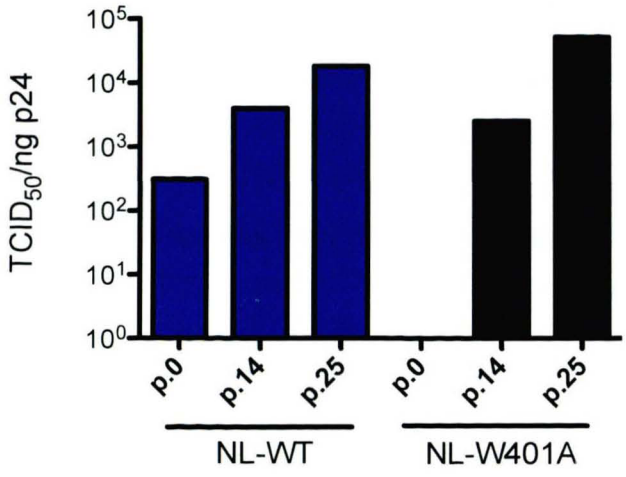

Figure 5.1. Infectivity of NL-WT and NL-W401A upon serial passage in MT-2 cells. Wild-type (NL-WT) and W401A mutant HIV-1 (NL-W401A) derived from HEK293T cell cultures transfected with HIV-1 constructs were used to infect MT-2 cells. Infected cultures were passaged in parallel until virus specific CPE of cells infected with NL-W401A approached that of wild-type. Aliquots of passage 14 and 25 virus were biologically cloned by terminal dilution in MT-2 cells. The original transfection derived stock (p.0) and stocks generated from passage 14 (p.14), and 25 (p.25) were subjected to p24 ELISA and equivalent amounts used to infect MT-2 cells. Infected MT-2 cells were scored for CPE at 6 days post infection. The $TCID_{50}$/ng was calculated using the Karber formula.

To a large degree the increase in infectivity observed after serial passage of NL-WT in MT-2 cells would be due to adaptation of the HIV-1 envelope to the MT-2 cell line. This adaptation would also be responsible in part for the increased infectivity observed for the MT-2 passaged NL-W401A. Other factors attributing to the increased infectivity of NL-W401A during MT-2 passage would be expected to be either due to a reversion of the W401A mutation to wild-type, or the generation of second-site mutations that compensate for the decreased infectivity mediated by W401A.

The RT coding region of biologically cloned, serially passaged HIV-1 was PCR amplified and the amplicons cloned into pBluescript (Section 2.4.3). Multiple clones were subjected to DNA sequencing. All RT sequences derived from NL-W401A at p.25 maintained the parent W401A mutation (Table 5.1). Additionally, three non-synonymous mutations were present in all six molecular clones. These mutations were C162Y in the palm subdomain, K366R in the connection subdomain, and A534T in the RNase H domain (Table 5.1). Each amino acid substitution was generated by a single nucleotide G to A or A to G transition. Comparison with the Los Alamos HIV/SIV protein sequence database (Los Alamos National Laboratory, 2008c) identified these three non-synonymous mutations as naturally occurring polymorphisms. Interestingly, a synonymous mutation at S163 was common to all NL-W401A p.25 sequences. This synonymous mutation (AGC to AGT) was the result of a C to T transition. These mutations were not present in either the original NL4.3 molecular clone or in NL-WT p.25 (Table 5.1). Other mutations identified in the NL-W401A p.25 RT coding region were not observed in more than one molecular clone and were not further investigated. Examination of sequences derived from an earlier passage (p.14) provided no information on the temporal selection of the second-site mutations (Table 5.2). Each individual mutation was present in a single clone as well as in combination. Interestingly the silent S163 mutation was not present at this earlier passage.

Both the PR and IN coding regions from NL-W401A at p.25 were also examined for the presence of second-site mutations (Table 5.3). There was no evidence of second-site mutations in the PR domain that were consistently associated with the NL-W401A and not NL-WT (Table 5.3). Analysis of the IN coding region revealed the presence of D279N in four of 10 sequences examined from NL-W401A p.25 (Table 5.4). Similar to mutations identified in the RT coding region, D279N is a naturally occurring polymorphism (Los Alamos National Laboratory, 2008c). This mutation was absent from the original NL-WT and NL-WT at p.25 suggesting that D279N was selected in response to either W401A, or the second-site mutations C162Y, K366R or A534T identified in the RT coding region. Since D279N was not detected in all W401A sequences examined, it was not investigated further.

Table 5.1. RT genotype of NL-WT and NL-W401A at passage 25

WT[a]	M16	I94	V111	K154	C162	S163	I167	N192	S251	G273	G316	K366	W401	P468	A502	A534
WT codon[a]	ATG	ATA	GTG	AAA	TGT	AGC	ATC	GAC	AGC	GGG	GGA	AAA	TGG	CCC	GCA	GCA
mutant codon	ACG	ATG	GCG	AAG	TAT	AGT	AAC	GGC	GGC	GAG	GAA	AGA	GCG	CAC	GCG	ACA
WT-1											E					
WT-2							N			E						
W401A-1		M			Y	S			G			R	A			T
W401A-2	T				Y	S						R	A			T
W401A-3			A		Y	S						R	A			T
W401A-4					Y	S		G				R	A			T
W401A-5				K	Y	S						R	A		A	T
W401A-6					Y	S						R	A	H		T
polymorphism, prevalence (%)[b]		L, 0.7			S, 68 C, 20 A, 6.6 Y, 3.6 H, 1.5 N, 0.7			N, 0.7	V, 5.1 Y, 0.7 E, 0.7 D, 0.7 Q, 0.7 I, 0.7	N, 0.7		R, 30		S, 61 P, 9.5 A, 2.2 K, 2.2 N, 0.7 D, 0.7 H, 0.7 I, 0.7 L, 0.7		S, 80 T, 3.6 P, 0.7 X, 0.7

[a] HIV-1 molecular clone NL4.3

[b] According to the 2008 Los Alamos compendium for HIV-1/SIVcpz sequences

Table 5.2. RT genotype of NL-WT and NL-W401A at passage 14

WT[a]	G51	K65	R78	G99	T139	W153	C162	I178	R206	F227	L246	K249	I329	K366	W401	I411	D443	R448	E514	K527	A534
WT codon[a]	GGG	AAA	AGA	GGG	ACA	TGG	TGT	ATA	AGA	TTC	CTG	AAG	ATA	AAA	TGG	ATT	GAT	AGG	GAA	AAA	GCA
mutant codon	AGG	AGA	AAA	AGG	GCA	CGG	TAT	GTA	AAA	CTC	CCG	AGG	GTA	AGA	GCG	ATG	AAT	AAG	AAA	GAA	ACA
WT-1	R			R				V			P									D	
WT-2									K												
W401A-1		R				R	Y					R		R	A						T
W401A-2							Y			L					A				K		
W401A-3			K			R	Y					R			A				K		T
W401A-4													V	R	A				K		
W401A-5					A										A	M	N	K			
W401A-6															A						T

[a] amino acid or codon of the HIV-1 molecular clone NL4.3

Table 5.3. PR genotype of NL-WT and NL-W401A at passage 25

WT[a]	I50	G57	T96
WT codon[a]	ATT	GGA	ACT
mutant codon	ATC	AGA	GCT
WT-1			
WT-2		R	A
WT-3		R	
W401A-1			
W401A-2	I		
W401A-3		R	
W401A-4		R	
polymorphism, prevalence (%)[b]	V, 0.6	R, 76 K, 23 Q, 0.6 S, 0.6	

[a] HIV-1 molecular clone NL4.3

[b] According to the 2008 Los Alamos compendium for HIV-1/SIVcpz sequences

Table 5.4. IN genotype of NL-WT and NL-W401A at passage 25

WT[a]	V31	I141	M154	K211	G256	D279	S283
WT codon[a]	GTA	ATT	ATG	AAA	GGG	GAT	AGT
mutant codon	ATA	ACT	ATA	GAA	GGT	AAT	GGT
WT-1					G		
WT-2							
WT-3							G
WT-4		T	I				
WT-5			I				
W401A-1				E		N	
W401A-2							
W401A-3							
W401A-4						N	
W401A-5							
W401A-6						N	
W401A-7							
W401A-8							
W401A-9	I						
W401A-10						N	
polymorphism, prevalance (%)[b]	I, 47	W 0.5 X, 0.5	I, 1.8 L, 0.5	R, 12 T, 11 D, 0.5 S, 0.5 X, 0.5		G, 6.5 A, 0.5 N, 0.5	G, 65 N, 1.2 D, 0.5

[a] HIV-1 molecular clone NL4.3

[b] According to the 2008 Los Alamos compendium for HIV-1/SIVcpz sequences

5.2.2 W401A second-site mutations increase viral infectivity and virion-associated RT activity

To confirm that the increase in infectivity of NL-W401A observed after passage in MT-2 cells was due to the presence of RT second-site mutations, each mutation was introduced into the pNL4.3-W401A molecular clone individually (+C162Y, +K366R, +A534T) and in combination (+3x), and these clones used to produce HIV-1 by transfection of HEK293T cells (Section 2.3). Wild-type and RT mutant HIV-1 demonstrated similar levels of viral particle production from transfected HEK293T cells (Fig. 5.2). Cell-free supernatants normalised to equivalent amounts of p24 were used to determine viral infectivity by end-point titration in MT-2 cells, and the titre determined in TZM-bl cells (Section 2.6). Virion-associated RDDP activity of mutant viruses was also determined (Section 2.7.1).

Expression of all three second-site RT mutations in concert with the W401A mutation resulted in a significant increase in HIV-1 infectivity in both MT-2 (Fig. 5.3A) and TZM-bl cells (Fig. 5.3B), and significant increases in RDDP activity compared to NL-W401A (Fig. 5.3C). Individually, addition of K366R conferred the greatest increase in infectivity and RDDP activity compared to NL-W401A, and significantly increased HIV-1 infectivity. In contrast, neither the C162Y nor A534T mutations conferred a significant increase in RDDP activity compared to NL-W401A. While these second-site mutations demonstrated increased infectivity in both MT-2 and TZM-bl cells, these increases were not significant compared to NL-W401A.

These studies demonstrate that the three second-site mutations, C162Y, K366R and A534T, contribute to overcome defects conferred by W401A on HIV-1 infectivity and virion-associated RDDP activity with K366R having the greatest effect on both HIV-1 infectivity and virion-associated RT activity.

5.2.3 Effect of W401A suppressor mutations on the viral protein profile in viral and transfected cell lysates

The defects conferred by W401A upon expression in HIV-1 include changes to the HIV-1 protein profile (Chapter 3). Since the C162Y, K366R and A534T second-site mutations suppressed defects in HIV-1 infectivity and RDDP activity conferred by W401A, their impact on the virion RT protein profile was examined in viral and transfected cell lysates by Western blot analysis.

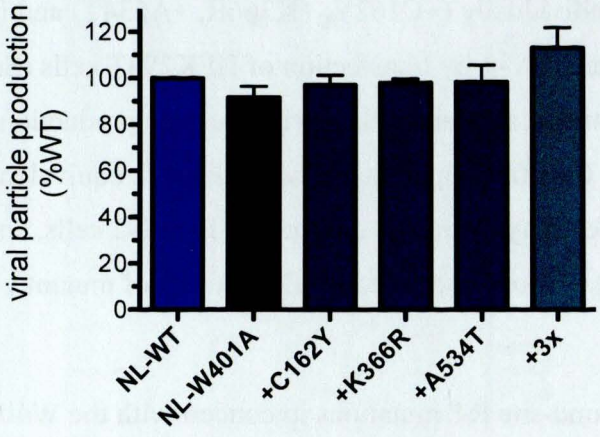

Figure 5.2. Effect of W401A second-site mutations on HIV-1 particle production.
HIV-1 particle production from transfected HEK293T cell cultures was determined by Western blot analysis. Transfection efficiency of wild-type and mutant RT HIV-1 constructs was monitored by co-transfection with an eGFP producing plasmid. Equivalents amounts of viral and transfected cell lysates, as determined by transfection efficiency, were subjected to Western blot analysis using p24 primary antibody 183-H12-5C and Alexa Fluor 680 anti-mouse secondary antibody. Western blots were visualised and quantified using the Odyssey IR imaging system. Viral particle production was calculated as the ratio of virion associated $Pr55^{Gag}$ and p24 to the total $Pr55^{Gag}$ and p24 in viral and transfected cell lysates as previously described (Shehu-Xhilaga *et al.*, 2004) and expressed as the percentage of wile-type viral particle production. Bars represent mean of nine independent assays and error bars denote the standard error of the mean. No significant difference in viral particle production was observed for all mutants compared to wild-type using the Kruskal-Wallis test ($p = 0.47$).

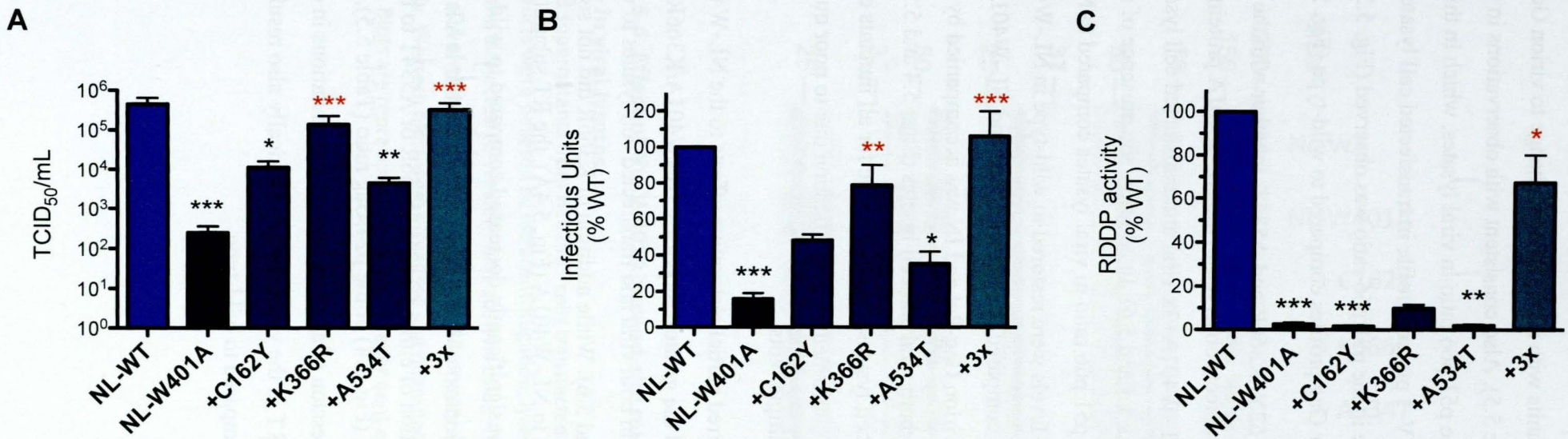

Figure 5.3. Effect of W401A second-site mutations on infectivity and RDDP activity of HIV-1 expressing the RT mutation W401A.

Clarified supernatants from transfected HEK293T cells were normalised to equivalent amounts of p24 by Western blot and used to infect MT-2 and TZM-bl cells, and tested for RDDP activity. (A) Infected MT-2 cells were scored for CPE six days post infection and the $TCID_{50}$/mL calculated using the Karber formula. (B) Infected TZM-bl cells were fixed 48 h post infection and stained to detect activity of the Tat activated reporter, β-galactosidase. Infected blue-stained foci were counted by light microscopy to determine the infectious units. (C) Virion-associated RDDP activity was assessed on a homopolymeric poly(rA)/oligo(dT) T/P. Incorporated ^{33}P-dTTP radiolabel was quantified using the Fujifilm FLA-3000 Phosphor Imager. Infectious units (B) and RDDP activity (C) was expressed as the percentage of wild-type for each individual experiment. Each bar represents the mean of at least five independent assays and error bars indicate standard error. Statistical analysis was performed using the Kruskal-Wallis with Dunn's post test. Significant differences compared to NL-WT are indicated by * when $p < 0.05$, ** when $p < 0.01$, and *** when $p < 0.001$. Comparisons to the NL-W401A mutant are in red text (*).

The HIV-1 protein profile of NL-W401A was consistent with results reported in previous chapters, demonstrating a decrease in virion RT subunits with no significant change to virion Gag-Pol, IN or Gag compared to wild-type (Fig. 5.4, Table 5.5). Also consistent with observations in Chapter 4, NL-W401A demonstrated an increase in the p51:p66 ratio in viral lysates, which in this case was significantly higher than wild-type. The HIV-1 protein profile in transfected cell lysates was as expected for NL-W401A, where a decrease in the p51:p66 ratio was observed (Fig. 5.5A, Table 5.6) with no change to the virion or cellular Gag profiles compared to wild-type (Fig. 5.5B).

The presence of all three RT mutations, C162Y, K366R and A534T, together with the parent W401A mutation appeared to suppress the defects observed in the NL-W401A protein profile. Levels of p66 and p51 were increased in NL-W401A+3x viral and transfected cell lysates compared to NL-W401A (Figs. 5.4A and 5.5A, Tables 5.5 and 5.6). In addition, the presence of all three suppressor mutations acted to decrease the p51:p66 ratio in viral lysates compared to NL-W401A (Fig. 5.4A, Table 5.5). However, while RT levels were restored to wild-type in NL-W401A+3x, virion Gag-Pol and IN levels were reduced compared to both wild-type and NL-W401A (Fig. 5.4, Table 5.5). Interestingly, this reduction in virion Gag-Pol and IN was accompanied by a trend towards an increase in the p24:Gag ratio in both viral and cell lysates (Figs. 5.4 and 5.5, Tables 5.5 and 5.6). Levels of Gag-Pol in transfected cell lysates appeared stable for all mutants compared to wild-type (Fig. 5.5). This was unable to be confirmed by quantification due to poor quality imaging of Gag-Pol in transfected cell lysates in multiple blots.

The individual suppressor mutations conferred partial restorative effects to the NL-W401A mutant, and of these the K366R mutation conferred the greatest increases. NL-W401A/K366R (+K366R) resulted in restoration of the p51:p66 ratio in both viral and transfected cell lysates to wild-type levels (Figs. 5.4A and 5.5A) (Tables 5.5 and 5.6). While addition of K366R did not significantly increase the levels of p66 or p51 compared to NL-W401A (Fig. 5.4A), the RT subunits in viral lysates of NL-W401A/K366R were also not significantly decreased compared to wild-type. The addition of either C162Y or A534T in the context of W401A resulted in similar levels of viral RT compared to the NL-W401A mutant. Addition of either C162Y, K366R or A534T to NL-W401A did not adversely affect virion Gag-Pol, IN (Fig. 5.4) or the p24:Gag ratio (Table 5.5), which were similar to NL-W401A and wild-type. Expression of all three second-site mutations in concert resulted in significant increases in mature RT in the virion but paradoxically also resulted in significant reductions in virion Gag-Pol compared to wild-type.

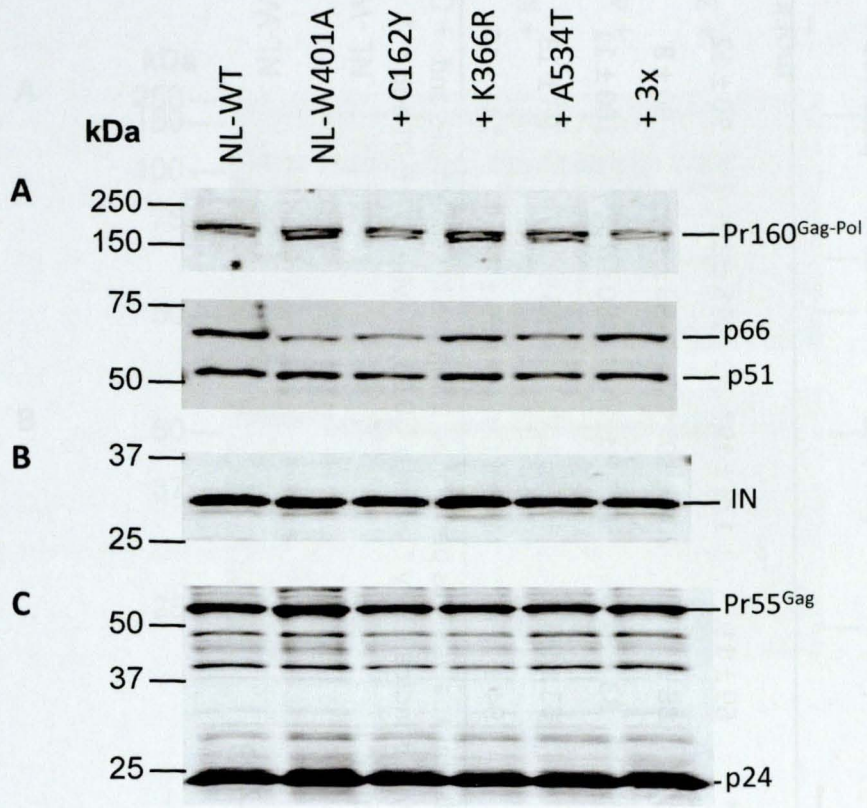

Figure 5.4. Effect of the W401A second-site mutations on the HIV-1 protein profile in viral lysates.

Clarified supernatants from HEK293T cells transfected with wild-type or W401A mutant HIV-1 constructs were pelleted by ultracentrifugation, lysed, normalised to equivalent amounts of p24 and subjected to Western blot analysis using RT antibody 11G10 (A), IN antibody 8E5 (C) and p24 antibody 183-H12-5C (D) with secondary antibody Alexa Fluor 680 anti-mouse antibody. Western blots were visualised and quantitated using the Odyssey IR imaging system. Blots are representative of five independent experiments.

Table 5.5. Quantification of HIV-1 proteins from viral lysates of NL-W401A with second-site mutations

Mutant	Protein or Ratio as indicated compared to WT(%)[a]							
	$Pr160^{Gag\text{-}Pol}$ 11G10[b]	$Pr160^{Gag\text{-}Pol}$ 8E5[c]	$Pr160^{Gag\text{-}Pol}$ 183-H12-5C[d]	p66	p51	p51:p66	IN	$p24:Pr55^{Gag}$
NL-W401A	131 ± 17	118 ± 15	109 ± 20	38 ± 7***	69 ± 11	178 ± 19*	115 ± 10	90 ± 12
+ C162Y	135 ± 20	98 ± 12	79 ± 12	46 ± 7**	88 ± 12	201 ± 30***	93 ± 9	90 ± 8
+ K366R	126 ± 11	100 ± 15	75 ± 9	74 ± 13	83 ± 8	137 ± 17	100 ± 15	100 ± 11
+ A534T	83 ± 6	98 ± 26	57 ± 9	39 ± 6**	63 ± 9*	166 ± 10*	98 ± 26	93 ± 13
+ 3x	53 ± 6**	55 ± 11*	34 ± 9*	80 ± 8*	94 ± 11	112 ± 12*	60 ± 8**	134 ± 12

[a] Mean ± the standard error of five independent experiments. Statistical analysis was performed using the Kruskal-Wallis and Dunn's post test. A significantly different value compared to wild-type is indicated by * when $p < 0.05$, ** when $p < 0.01$ and *** when $p < 0.001$. Comparisons to NL-W401A are indicated by red type (*).

[b] Quantification of $Pr160^{Gag\text{-}Pol}$ detected using RT antibody 11G10

[c] Quantification of $Pr160^{Gag\text{-}Pol}$ detected using IN antibody 8E5

[d] Quantification of $Pr160^{Gag\text{-}Pol}$ detected using p24 antibody 183-H12-5b

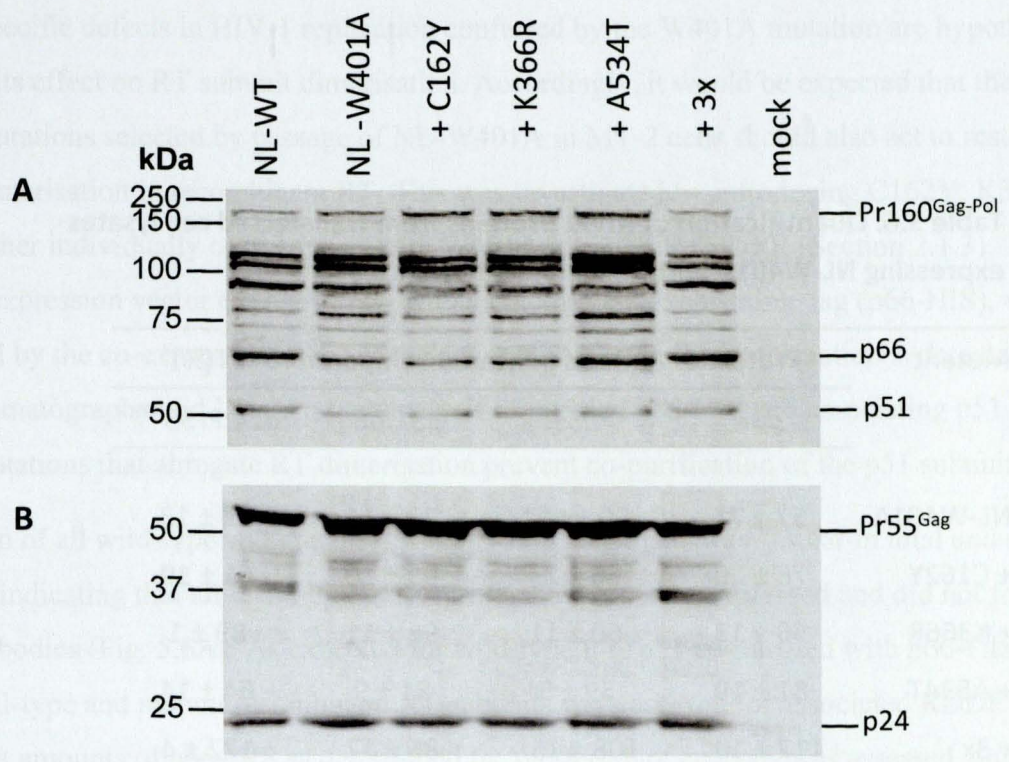

Figure 5.5. Effect of the W401A second-site mutations on the HIV-1 protein profile in transfected cell lysates

HEK293T cells transfected with wild-type (NL-WT) or mutant RT constructs were normalised to equivalent amounts of p24 and subjected to Western blot analysis using RT antibody 11G10 (A) and p24 antibody 183-H12-5C (B) with Alexa Fluor 680 anti-mouse secondary antibody. Western blots were visualised and quantitated using the Odyssey IR imaging system. Blots are representative of five independent experiments.

Table 5.6. Quantification of HIV-1 proteins from transfected cell lysates expressing NL-W401A with second-site mutations

Mutant	Protein or Ratio as indicated compared to WT(%)[a]			
	p66	p51	p51:p66	p24:Pr55^{Gag}
NL-W401A	57 ± 7*	50 ± 5**	77 ± 11	83 ± 13
+ C162Y	76 ± 20	66 ± 13	95 ± 10	61 ± 19
+ K366R	56 ± 13	60 ± 11	96 ± 11	89 ± 1
+ A534T	81 ± 19	59 ± 5	81 ± 9	64 ± 14
+ 3x	112 ± 10*	108 ± 15*	85 ± 12	127 ± 4

[a] Mean ± the standard error of five independent experiments. Statistical analysis was performed using the Kruskal-Wallis and Dunn's post test. A significantly different value compared to wild-type is indicated by * when $p < 0.05$, ** when $p < 0.01$. Text in red (*) denonte comparisons to NL-W401A.

5.2.4 Role of C162Y, K366R and A534T in suppressing RT dimerisation and RT activity defects conferred by W401A in recombinant RT

The RT specific defects in HIV-1 replication conferred by the W401A mutation are hypothesised to be due to its effect on RT subunit dimerisation. Accordingly, it would be expected that the second-site RT mutations selected by passage of NL-W401A in MT-2 cells should also act to restore RT subunit dimerisation in recombinant RT. This was investigated by introducing C162Y, K366R and A534T either individually or in concert with W401A into pNLRT6H/PR (Section 2.1.3). This bacterial expression vector expresses p66 with a C-terminal hexahistidine tag (p66-HIS), which can be cleaved by the co-expressed HIV-1 PR (Section 2.8). Heterodimer formation is detected by Ni-NTA chromatography and Western blot analysis of purified p66-HIS and associating p51 (Section 2.5.3). Mutations that abrogate RT dimerisation prevent co-purification of the p51 subunit.

Expression of all wild-type and mutant RT expression constructs was similar in total and soluble fractions, indicating that all recombinant RT proteins were stably expressed and did not form inclusion bodies (Fig. 5.6A). As expected for wild-type RT, p51 co-purified with p66-HIS in a 1:1 ratio. Wild-type and mutant recombinant RT subunits were assayed for associated RDDP activity. Equivalent amounts of p66-HIS as determined by Western blot analysis was assessed, and compared to wild-type. Both heterodimer formation and RDDP activity of W401A mutant RT was significantly decreased to approximately 10% of wild-type (Fig. 5.6). The presence of the three second-site mutations in combination with W401A generated a wild-type profile, restoring both RT subunit interaction and RT activity to 96% and 118% of wild-type, respectively (Fig. 5.6B and C, respectively). Of the three second-site mutations, K366R was the only one that conferred both a significant increase in RT subunit interaction and RDDP activity (68% and 148%, respectively) compared to the W401A mutant RT. Interestingly, while C162Y partially restored RT heterodimer interaction in the context of W401A (50% of wild-type), RDDP activity was significantly increased (120% of wild-type). The presence of A534T in the context of W401A marginally increased both heterodimer interaction and associated RDDP activity. Thus the ability of the three second-site mutations to restore recombinant RT dimerisation and activity was associated with their effects on NL-W401A, with the presence of all three second-site mutations conferring the most dramatic W401A suppressor effect and K366R being the most potent of the individual mutations.

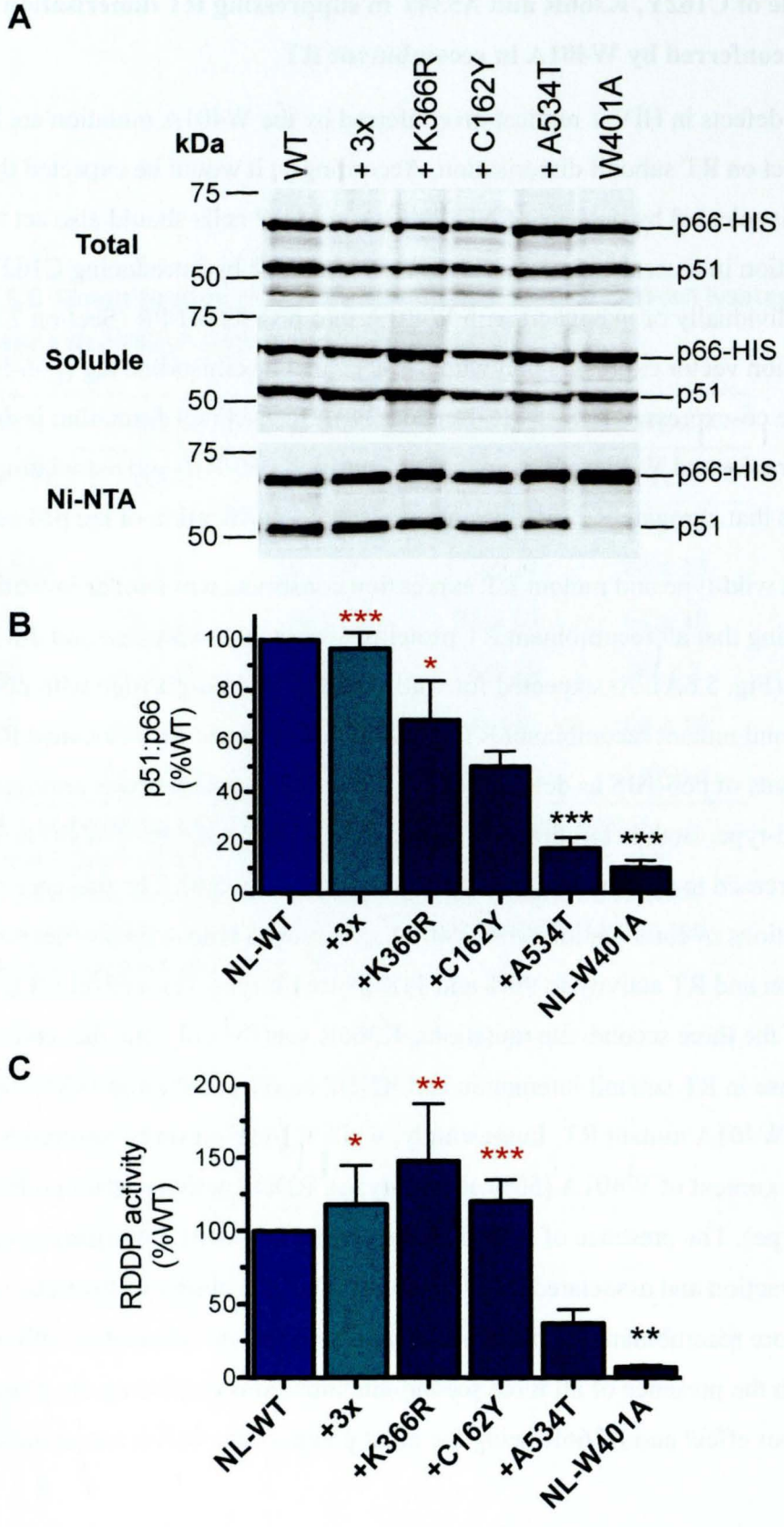
A
kDa
WT
+ 3x
+ K366R
+ C162Y
+ A534T
W401A
75
50
Total
Soluble
Ni-NTA
p66-HIS
p51
B
p51:p66 (%WT)
100
80
60
40
20
0
***
*
***
***
NL-WT
+3x
+K366R
+C162Y
+A534T
NL-W401A
C
RDDP activity (%WT)
200
150
100
50
0
*
**
***
**
NL-WT
+3x
+K366R
+C162Y
+A534T
NL-W401A

Figure 5.6. Effect of the W401A second-site mutations on RT heterodimer formation and RDDP activity.

HIV-1 RT heterodimer formation from a p66 precursor was assessed using the bacterial expression vector, pNLRT6H/PR, encoding wild-type or mutant RT. (A) Bacteria transformed with the RT expression vector were treated with IPTG to induce RT expression and then lysed (total). The soluble fraction (soluble) was affinity purified on Ni-NTA agarose and the eluate subjected to Western blot analysis using monoclonal anti-RT 11G10 and Alexa Fluor 680 anti-mouse secondary antibody. Western blots were visualised and quantitated using the Odyssey IR imaging system. The ratio of p51:p66-HIS was determined and expressed as the percentage of wild-type (B). Purified RT was normalised to equivalent amounts of p66 and assayed for RDDP activity on a poly(rA)/oligo(dT) T/P. Incorporation of ^{33}P dTTP was quantified using the Fujifilm FLA-3000 Phosphor Imager. RDDP activity was expressed as the percentage of wild-type activity (C). Each bar represents the mean of five independent assays and error bars denote the standard error. Statistical analysis employed the Kruskal-Wallis and Dunn's post test. A significant difference compared to wild-type is indicated with * when $p < 0.05$, and ** when $p < 0.01$). Text in red (*) denotes a comparison to the W401A mutant.

5.2.5 Location of the W401A RT second-site mutations

The C162Y, K366R and A534T second-site mutations were mapped onto the three dimensional structure of the HIV-1 RT to give insight into their possible mechanism of action in suppressing defects conferred by W401A. C162 is located in the palm subdomain, K366 is located in the connection subdomain, and A534 in the RNase H domain. The positioning of these residues in the p66 subunit was striking, with C162Y and A534T located at the dimer interface (Fig. 5.7). Of note, in the p66 subunit K366R is proximal to both W401A in p66 and the dimer interface (Fig. 5.8). In the p51 subunit, K366 and C162 do not contribute to the dimer interface and are located on solvent exposed faces of the subunit (Fig. 5.8A and Fig. 5.9A). As A534 is located in the RNase H domain, it is not present in the p51 subunit.

In the p66 subunit K366 is located adjacent to the secondary structure αL and the αL-β20 loop, and is within interacting distance of W401A (3-6 Å) (Fig. 5.8B). The replacement of lysine with an arginine introduces a longer side-chain with increased steric bulk while maintaining the positively charged nature of the amino acid. In the context of W401A, K366R may act to stabilise the π-stack formed between W401, Y405, W406 and $p51^{P420}$ and correct the position of the αL-β20 loop (personal communication, M. Kuiper). In the p51 subunit K366R is expected to have little effect, as this residue is located on a solvent exposed face of the subunit. Furthermore, the presence of arginine at this position is a naturally occurring polymorphism (Table 5.1), suggesting that this mutation is likely to be well tolerated.

In the p66 subunit, mutation of cysteine to the bulky hydrophobic tyrosine at codon 162 may provide increased opportunities for hydrogen bonding both within p66 and with the p51 subunit (Fig. 5.9B) and act to increase heterodimer stability. Of note is the potential interaction between $p66^{C162Y}$ and $p51^{P140}$, the latter bracketing the p51 β7-β8 loop. This structural motif is known to have an important role in RT heterodimer stability (Pandey *et al.*, 2001; Balzarini *et al.*, 2005; Mulky *et al.*, 2007). Mutation of the small hydrophobic alanine at codon 534 to the polar threonine residue provides both an additional hydroxyl and a methyl group that have the potential to increase intra- and inter- subunit interactions. This includes H-bonding with p51 residues N255 and Q258, and hydrophobic interactions with L289, and intra-subunit interactions with V496 and T532 (Fig. 5.10).

Hence the location of the second-site mutations in the RT structure appears to correlate with their relative suppressive effects on defects conferred by the W401A RT mutation as observed in the HIV-1 and recombinant RT protein studies.

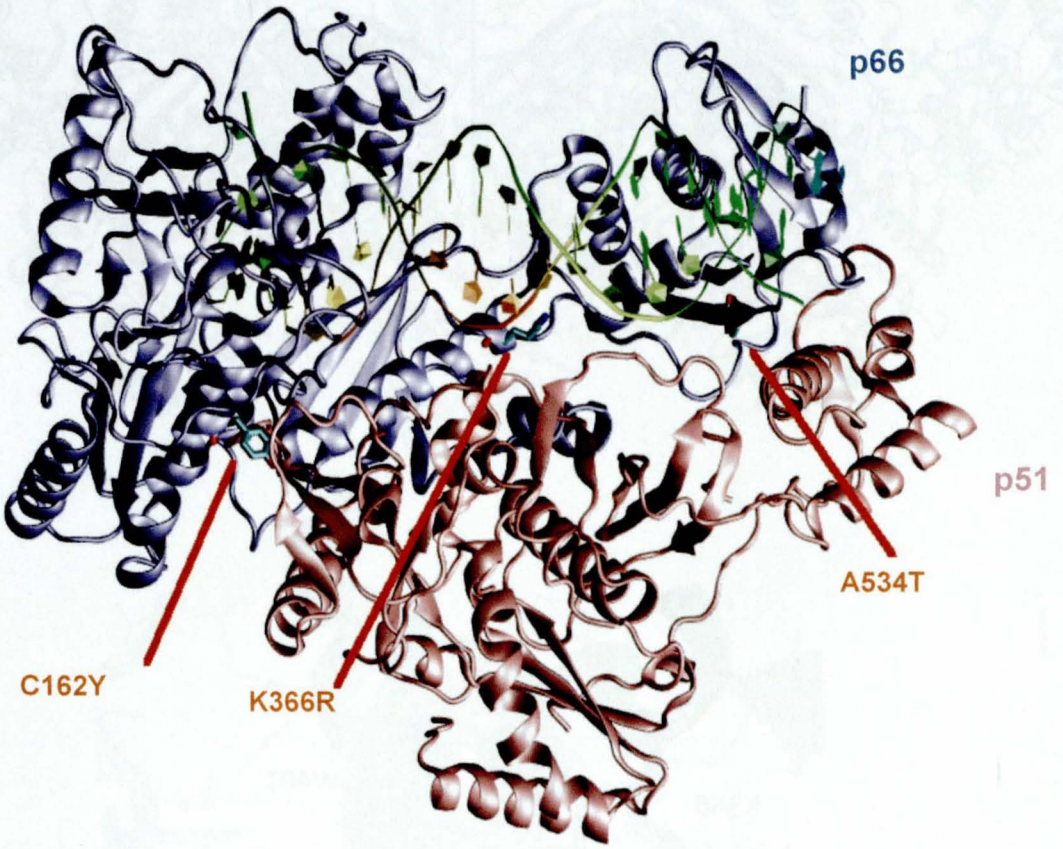

Figure 5.7. Location of second-site mutations in the p66 subunit of the RT heterodimer identified upon serial passage of W401A HIV-1.

Ribbon diagram of the RT heterodimer with the p66 subunit in blue, p51 subunit in pink and bound T/P in green. The mutations identified upon serial passage of NL-W401A, C162Y, K336R and A534T, were mapped onto the p66 subunit. This image was generated by M. Kuiper using the RT structure 1RTD (Huang *et al.*, 1998). The images were generated using the Visual Molecular Dynamics (VMD) program and rendered using POV-Ray (http://www.povray.org).

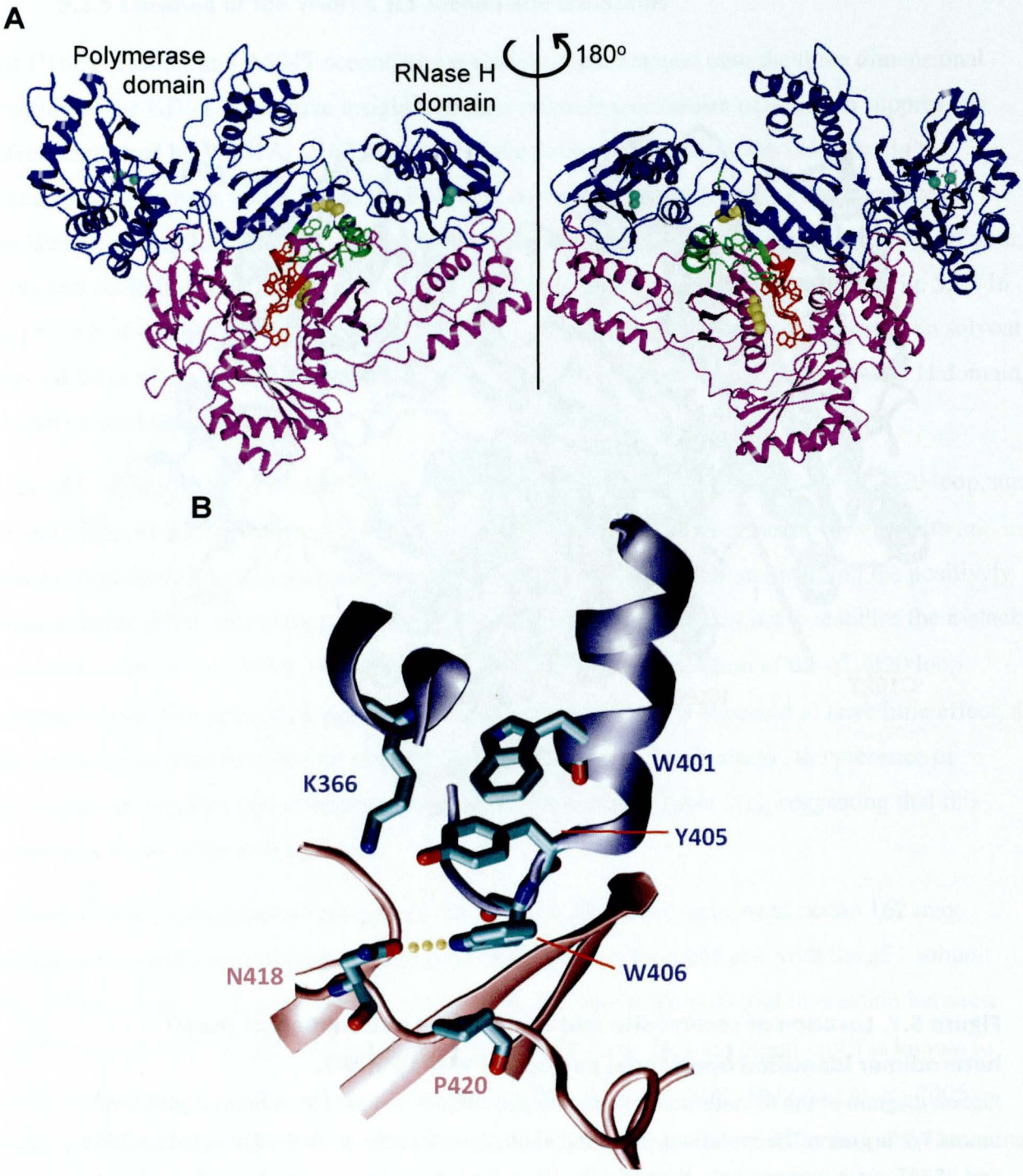

Figure 5.8. Location of K366 in the HIV-1 RT heterodimer.

(A) Ribbon diagram of the RT heterodimer with the p66 subunit in blue, p51 subunit in pink, and active site cations in teal. The RT heterodimer is displayed from the traditional perspective, and rotated 180°. Residues contributing to the TRM are coloured green or red in the p66 and p51 subunits, respectively. K366 is highlighted in yellow space fill representation in both subunits. (B) Magnified representation of the location of K366 in the p66 subunit and its proximity to the π-stack spanning the dimer interface formed by p66 residues W401, Y405, W406 and $p51^{P420}$. Images were created using the RT structure 1RTD (Huang *et al.*, 1998). Image (A) was generated with YASARA (Krieger *et al.*, 2002), and (B) was created by M. Kuiper using the Visual Molecular Dynamics (VMD) program and rendered using POV-Ray (http://www.povray.org).

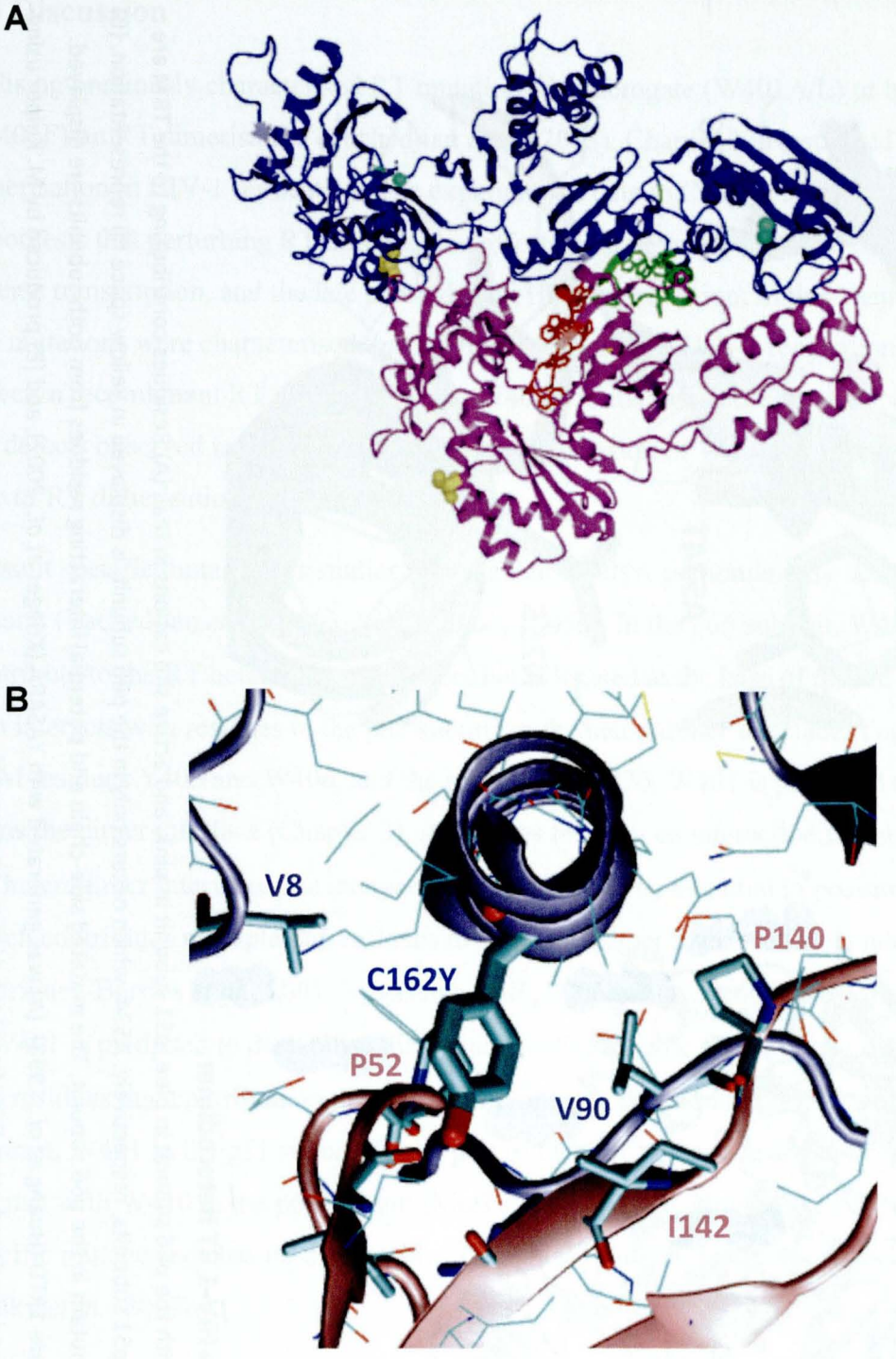

Figure 5.9. Location of C162 in the HIV-1 RT heterodimer.

Ribbon diagram of the RT heterodimer with the p66 subunit in blue, p51 subunit in pink, and active site cations in teal. (A) Residues contributing to the TRM are highlighted in green and red in the p66 and p51 subunits, respectively. C162 is displayed in yellow space fill representation in both subunits. (B) Magnified representation of the C162Y mutant in the p66 subunit. The mutated side-chain and potential interacting residues from both subunits are displayed. Images were created using the RT structure 1RTD (Huang *et al.*, 1998). (A) was generated with YASARA (Krieger *et al.*, 2002), and (B) was produced by M. Kuiper using the Visual Molecular Dynamics program and rendered using POV-Ray (http://www.povray.org).

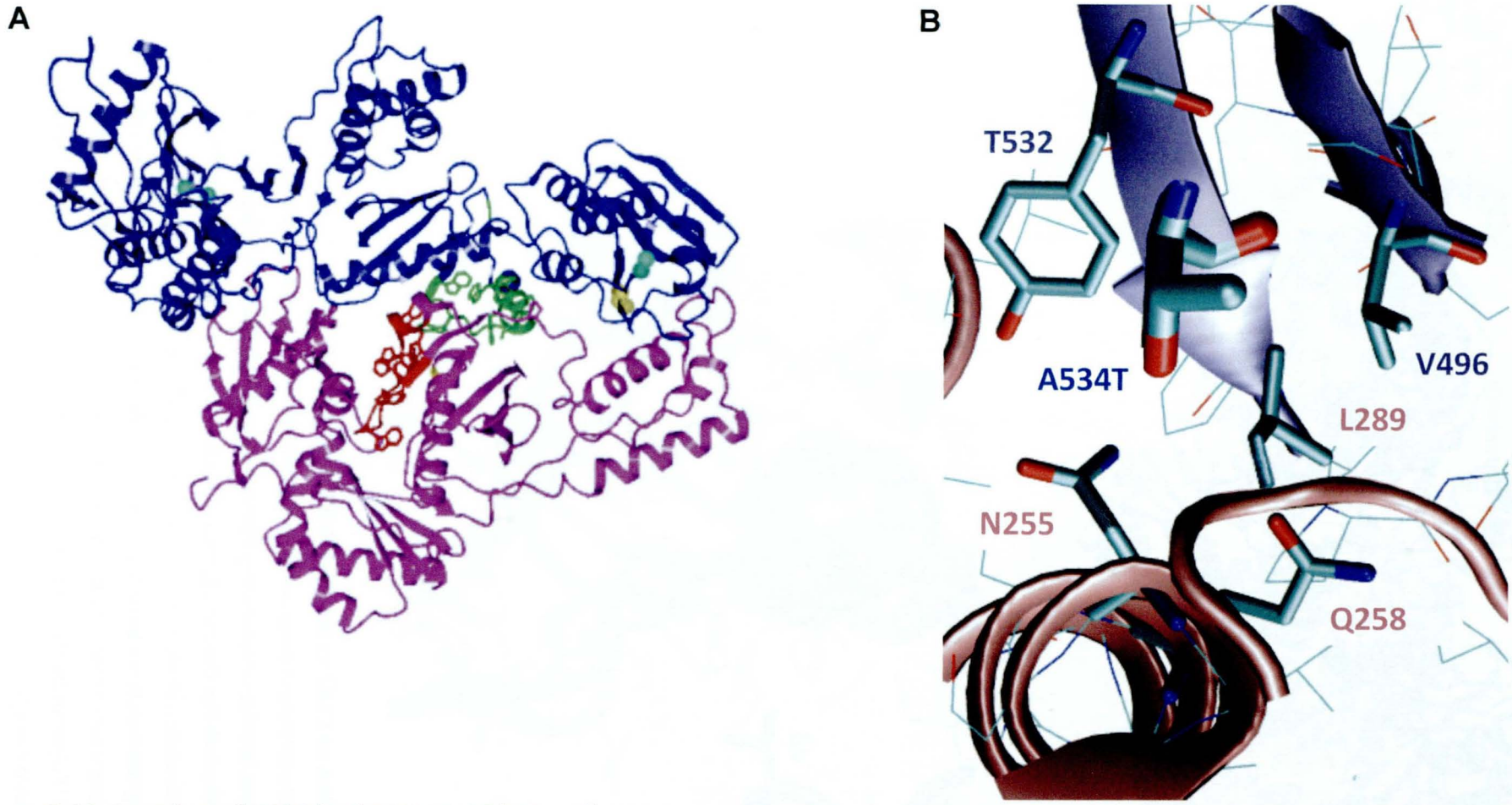

Figure 5.10. Location of A534 in the HIV-1 RT heterodimer.

Ribbon diagram of the RT heterodimer with the p66 subunit in blue, p51 subunit in pink, and active site cations in teal. (A) Residues contributing to the TRM are highlighted in green or red in the p66 or p51 subunits, respectively. A534, which occurs only in the p66 subunit, is displayed in yellow space fill representation. (B) Magnified representation of the A534T mutant in the p66 subunit. The mutated side-chain and potential interacting residues from both subunits are displayed. Images were created using the RT structure 1RTD (Huang *et al.*, 1998). (A) was generated with YASARA (Krieger *et al.*, 2002), and (B) produced by M. Kuiper using the Visual Molecular Dynamics program and rendered using POV-Ray (http://www.povray.org).

5.3 Discussion

Utilising previously characterised RT mutations that abrogate (W401A/L) or have no adverse effect (W401F) on RT dimerisation (Tachedjian *et al.*, 2003), Chapter 3 investigated the role of RT dimerisation in HIV-1 replication. The experimental data in Chapter 3 strongly supports the hypothesis that perturbing RT dimerisation affects both the early phase of HIV-1 replication at reverse transcription, and the late phase during HIV-1 maturation. In this chapter, W401A second-site mutations were characterised that suppress the defect in HIV-1 replication, and the dimerisation defect in recombinant RT conferred by the W401A mutation. These data support the conclusion that the defects observed in HIV-1 replication upon expression of W401A were representative of the role of RT dimerisation in HIV-1 replication.

Subunit specific mutagenesis studies indicate that W401A predominantly acts through the p66 RT subunit (Tachedjian *et al.*, 2003; Mulky *et al.*, 2005a). In the p66 subunit, W401 does not directly contribute to the RT heterodimer interface, but is located at the base of the αL-β20 loop, which in turn interacts with residues in the p51 subunit at the heterodimer interface. Together with the p66 TRM residues Y405 and W406, and the p51 residue P420, W401 is proposed to form a π-stack that spans the dimer interface (Chapter 3). As well as forming an interaction that directly contributes to the heterodimer interface, this interaction is proposed to be essential in positioning the αL-β20 loop which contributes multiple p66 residues to the heterodimer interface (Menendez-Arias *et al.*, 2001; Rodriguez-Barrios *et al.*, 2001; Srivastava *et al.*, 2006). Introduction of a non-conservative mutation at W401 is predicted to destabilise the π-stack, collapsing the αL-β20 loop and disturbing multiple p66 residues that contribute to the heterodimer interface (personal communication, M. Kuiper). In contrast, W401 in the p51 subunit forms part of the dimer interface and is predicted to directly interact with W410 in the p66 subunit (Mulky *et al.*, 2005b). However, loss of $p51^{W401}$ upon subunit specific mutagenesis has no discernable effect on RT subunit interaction (Tachedjian *et al.*, 2003; Mulky *et al.*, 2005b).

There are three main points of contact between the subunits at the RT heterodimer interface; the p66 palm with the p51 fingers subdomain, the connection subdomains of each subunit, and the RNase H domain with the p51 thumb subdomain (Wang *et al.*, 1994; Bahar *et al.*, 1999; Menendez-Arias *et al.*, 2001; Rodriguez-Barrios *et al.*, 2001; Srivastava *et al.*, 2006). In the context of the p66 subunit, the three W401A second-site mutations identified in this study, C162Y, K366R and A534T, are located within each of these three points of contact. In the p51 subunit these residues were on a solvent exposed face, or in the case of A534, not present in the subunit. This suggests that the mechanism of suppression of these mutations is also through the p66 subunit.

Expression of each suppressor mutation individually with the W401A mutant resulted in an increase in RT subunit interaction as observed in recombinant RT that was also associated with increases in HIV-1 infectivity. However, only K366R conferred significant increases in RT dimerisation and infectivity compared to the W401A mutant. The potency of the second-site mutations corresponded to their location and proposed mechanism of action based on structural analysis. K366R is predicted to act directly on the proposed structural defects mediated by W401A in the context of the p66 subunit. In this regard, W401A is proposed to affect the positioning of the p66 αL-β20 loop by disturbing the π-stack formed by W401, Y405, W406 and $p51^{P420}$. The increase in steric bulk upon mutation from a lysine to an arginine side-chain is proposed to stabilise the π-stack upon the loss of the bulky tryptophan residue at codon 401. This would assist in correct positioning of the p66 αL-β20 loop while maintaining the interactions contributed by the original, similarly charged lysine residue. In contrast, the C162Y and A534T mutations are unlikely to directly affect the position of the αL-β20 loop. Located at the dimer interface in the palm and RNase H of the p66 subunit, respectively these mutations are predicted to increase subunit interaction, and perhaps also contribute to subunit stability. The location of C162Y is of particular interest as structural analysis indicates that the tyrosine mutant side-chain of the mutant may interact with P140 in p51, which is located at the C-terminal end of the β7-β8 loop - an essential structure for RT heterodimer stability (Pandey *et al.*, 2001; Balzarini *et al.*, 2005; Mulky *et al.*, 2007). However, none of these mutations conferred a wild-type like phenotype in this study.

While each mutation individually acted to partially suppress the defects conferred by W401A, the combination of C162Y, K366R and A534T comprehensively suppressed the defects conferred by the W401A mutation in both recombinant protein and HIV-1 replication. However, NL-W401A+3x demonstrated decreased virion Gag-Pol and IN of approximately 50% and 40%, respectively compared to wild-type. This raises the question of why three second-site suppressor mutations were selected in cell culture, when the addition of a single suppressor mutation, K366R, conferred significant increases to NL-W401A infectivity, while not conferring any additional defects in the viral protein profile.

A possible explanation is that the presence of all three suppressor mutations in concert result in RT with increased stability and functionality compared to HX-W401A harbouring only K336R. Notably, virion-associated RDDP activity of NL-W401A+K366R was only 10% of wild-type, whereas that of to NL-W401A+3x was 67% of wild-type, despite these mutants displaying similar amounts of virion RT. Thus the amount of virion RT did wholly account for the low levels of virion associated RDDP activity, particularly with regards to high levels of RDDP observed for recombinant RT.

Addition of K366R or C162Y to recombinant RT expressing the W401A mutation conferred a significant increase in RDDP activity compared to W401A alone. However the observation of RDDP activity levels above that of wild-type may be indicative of an defect in the enzymatic activity of these mutants. A comprehensive analysis of RDDP, DDDP and RNase H activity, such as that conducted by Tachedjian and colleagues (2005b) could address this possibility.

Both the ratio of the RT subunits and RDDP activity of recombinant RT most closely resembled that of wild-type when all three suppressor mutations were present in concert with W401A. Accordingly, NL-W401A+3x was the only mutant to display a significant increase in virion associated RDDP activity compared to NL-W401A. NL-W401A+3x also demonstrated a two-fold increase in $TCID_{50}$ and 20% greater infectivity in the TZM-bl cell line compared to NL-W401A+K366R.

In terms of the RT protein profile, expression of W401A alone resulted in a significant increase of the p51:p66 ratio in the virion. As discussed in Chapter 4 this may be due to RT heterodimer instability or dissociation and proteolysis of mutant subunits. Inability to form a stable RT heterodimer can decrease the levels of p66 relative to the p51 subunit in viral lysates (Abram *et al.*, 2005; Dunn *et al.*, 2009). Expression of A534T had no discernable effect on the p51:p66 ratio, while C162Y increased the ratio compared to W401A alone. K336R was the only mutation that decreased the ratio, although not significantly. Expression of all three W401A suppressor mutations did significantly reduce this ratio compared to wild-type. These data suggest that these mutations work in concert to restore optimum RT subunit interaction and RT activity. Also, generation and the selection of the K336R mutation may not have been possible without the presence of the other second-site mutations. While this was briefly investigated by sequence analysis of an earlier passage HIV-1 (passage 14)(Table 5.4), no clear consensus was gained on the temporal selection of these mutations.

While decreases in virion Gag-Pol and IN were observed for NL-W401A+3x, it is unlikely that this was due to significant Gag-Pol instability or premature PR activation. Loss of viral proteins in the producer cell due to RT mutations that confer Gag-Pol instability (Yu *et al.*, 1998a; Olivares *et al.*, 2004; Chiang *et al.*, 2010) or premature PR activation mediated by enhanced RT dimerisation in the context of Gag-Pol (Figueiredo *et al.*, 2006) confer a universal decrease in Pol proteins and reduction in viral particle production. In addition, the Gag-Pol processing cascade can be affected without decreasing viral particle production, as described for the previously examined W401A suppressor mutation, T409I (Chapter 4). However, while a trend towards an increase in the p24:Gag ratio in viral and transfected cell lysates is reminiscent of the T409I defect, the global decrease in virion Pol products seen with T409I was not observed in NL-W401A+3x. Thus the combination of C162Y, K366R and A534T restored levels of virion RT while adversely affecting virion IN, and

possibly allowed for enhanced PR mediated processing of RT, without requiring premature PR activation.

While the Gag-Pol processing cascade remains somewhat of an enigma, data indicate that IN is cleaved prior to the cleavages required for RT maturation (Bukovsky *et al.*, 1996; Quillent *et al.*, 1996; Cherry *et al.*, 1998a; Liao *et al.*, 2004; Pettit *et al.*, 2005a; Pettit *et al.*, 2005b)(Fig. 1.9B). The addition of the second-site RT mutations C162Y, K366R and A534T to NL-W401A resulted in a partial, but significant increase in virion RT protein profile, however with a concomitant decrease in virion IN. This decrease in IN however did not result in a defect in HIV-1 replication as assayed in this study. Interestingly, the IN mutation, D279N, was detected in four of 10 molecular clones generated from serially passaged NL-W401A HIV-1 (NL-W401A p.25). This passaged virus also demonstrated no decrease in $TCID_{50}$ compared to serial passaged wild-type HIV-1. Thus it is possible that this second-site IN mutation may have been generated in response to the effect of the second-site RT mutations on virion IN observed for NL-W401A-3x. However, this was not investigated in this study, nor was the presence of other second-site mutations occurring outside of Pol.

A previous study of the F130W RT mutation that destabilises the RT heterodimer describes transitory PR mutations that reduce PR activity, allowing the generation and selection of an RT suppressor mutation (Olivares *et al.*, 2004). While no PR mutations were identified at either passage 14 or 25 of NL-W401A, the possibility of transitory PR mutations at other passages cannot be excluded.

In the sequential model of RT heterodimer formation, the p66 homodimer is an essential intermediate that regulates the formation of the mature heterodimer (Wang *et al.*, 1994). As W401A prevents both RT heterodimerisation (Tachedjian *et al.*, 2003) and p66 homodimerisation (unpublished data, G. Tachedjian), expression of W401A in HIV-1 could retard the generation of the p51 subunit. Experimental evidence for supporting this theory include RT formation observed in a bacterial expression construct (Sluis-Cremer *et al.*, 2004a), and the ability of W401A mutation to decrease the p51:p66 ratio in pNL-W401A transfected cell lysates compared to wild-type (Chapter 3 and Chapter 4). However, data presented in this Chapter is inconclusive as poor detection of HIV-1 proteins in transfected cell lysates made accurate detection of small differences in protein levels difficult. The decrease in the p51:p66 ratio mediated by W401A was small (77% ± 11). Consequently, the increase in the p51:p66 ratio conferred by the second-site mutations could also be marginal. Furthermore, the decrease in the p51:p66 ratio in cell lysates may not necessarily be an accurate measure of the presence of p66 homodimers or the effect of W401A on their formation (Chapter 4).

While the evidence for the role of the p66 homodimer as the immediate precursor to the RT heterodimer has not been directly proven, these data strongly support the essential role of RT domain interaction, both in the context of mature subunits and within precursor polyproteins in HIV-1 replication. The location of the second-site mutations strongly suggests a role in stabilising the RT heterodimer through the p66 subunit and mediating proper positioning of the αL-β20 loop in the context of W401A. In contrast to the previously identified W401A suppressor mutation, T409I (Chapter 4), the suppressor mutations identified in this Chapter were all polymorphic residues found in primate lentiviral RTs (Los Alamos National Laboratory, 2008c) and were not located within the αL-β20 loop. Together with the high conservation of αL-β20 loop residues, the pleiotropic effects of T409I on Gag-Pol processing, and the proximal location of K366R to the loop, these data strongly suggest an important role of the αL-β20 loop both in RT heterodimer stability and Gag-Pol processing.

Chapter 6

The role of highly conserved reverse transcriptase residues in HIV-1 replication

6.1 Introduction

Mutations within the HIV-1 RT can cause defects in HIV-1 replication by multiple mechanisms. Since HIV-1 RT is expressed as part of the $Pr160^{Gag\text{-}Pol}$ polyprotein, RT mutations have the potential to affect not only the mature protein, but also the function and/or structure of the Gag-Pol precursor protein (Huang *et al.*, 2003; Olivares *et al.*, 2004; Abram *et al.*, 2005; Buxton *et al.*, 2005; Dunn *et al.*, 2009; Chiang *et al.*, 2010) (Chapter 4). In terms of the effect of RT mutations on the mature RT, a further layer of complexity exists due to the structure and composition of the enzyme. Reverse transcriptase is an asymmetric heterodimer composed of a p66 and a p51 subunit, which are generated from the Gag-Pol precursor by a series of cleavage events. The p66 subunit consists of an N-terminal polymerase domain and C-terminal RNase H domain, while the p51 subunit consists solely of the polymerase domain. While these polymerase domains are identical in protein sequence, a contrasting conformation is assumed by each subunit in the heterodimer. Thus a mutation may affect either or both subunits depending on its location in the RT sequence and spatial location within the RT heterodimer. In addition, mutations that affect RT subunit dimerisation can also adversely affect both late and early stages of HIV-1 replication (Wapling *et al.*, 2005, Chapter 3). The multiple mechanisms by which a mutation in the RT domain can affect HIV-1 replication may be advantageous for the design of novel, multivalent antiretroviral drugs.

Previous studies indicate the RT TRM, located in the connection subdomain of the RT polymerase domain, is an important region both for RT function and HIV-1 replication. The TRM consists of six tryptophan residues at codons 401, 402, 406, 410 and 414, and a tyrosine residue at codon 405. In the asymmetric RT heterodimer, the TRM is unique as residues from each RT subunit contribute to, and interact at the heterodimer interface. The essential role of the TRM in RT dimerisation was first described by Divita and colleagues (1993). Subsequent studies have defined roles for specific TRM residues in RT dimerisation (Tachedjian *et al.*, 2003; Mulky *et al.*, 2005b) and further explored the structural and functional relationship between the TRM and RT heterodimerisation (Tachedjian *et al.*, 2003; Tachedjian *et al.*, 2005b).

The amino acids contributing to the TRM are located within the secondary structures αL, β20 and the αL-β20 loop linking these structures. In the p66 subunit the αL-β20 loop projects into the p51 subunit, forming a key point of subunit interaction (Tachedjian *et al.*, 2003; Mulky *et al.*, 2005b). In the p51 subunit, the majority of the αL-β20 loop is buried with only W401 and Y405 directly

contributing to the heterodimer interface (Tachedjian *et al.*, 2003; Mulky *et al.*, 2005b; Srivastava *et al.*, 2006). Introduction of a non-conservative mutation at TRM residue W401 prevents RT subunit interaction. This effect is mediated through the p66 subunit instead of p51, where it is proposed to disturb the position of the p66 αL-β20 loop (Tachedjian *et al.*, 2005b). Data supporting this hypothesis include observation of an RT dimerisation defect upon mutation of K331 in the p51 subunit and W414 in p66 (Tachedjian *et al.*, 2003). W414 is the last residue of the TRM, located in β20 at the terminus of the αL-β20 loop (Chapter 3). Mutation of W414 is proposed to abrogate RT subunit dimerisation by the same mechanism as a non-conservative mutation at W401, by the loss of interactions between the p66 αL-β20 loop and the p51 subunit (Tachedjian et al 2003). In contrast, mutation of K331 is hypothesised to act through the p51 subunit where the K331 side-chain potentially interacts with the backbone carbonyl groups of the p66 αL-β20 loop residues W402, Y405 and Q407 (Tachedjian *et al.*, 2003; Grohmann *et al.*, 2008).

With the aim to further define the role of the TRM and the αL-β20 loop in HIV-1 replication, the RT mutations W414A and K331A were examined in this study. In addition, the effect of mutating the highly conserved TRM residue W398, and the αL-β20 loop residue Q407 was investigated. The rationale for evaluating Q407 includes its high conservation in primate lentiviral RT, its location within in the p66 αL-β20 loop, and its potential interaction with K331 in the p51 RT subunit.

With regards to W398, previous studies indicate a potential role for W398 in p51 and heterodimer stability. Non-conservative mutation of W398 does not prevent RT subunit dimerisation (Tachedjian *et al.*, 2003; Mulky *et al.*, 2005b). Expression of the W398A mutation in a Vpr-p51 fusion protein does not affect interaction with or co-packaging of wild-type p66 into *trans*-complemented viral particles (Mulky *et al.*, 2005b). However, within these particles the p66 subunit is aberrantly cleaved or degraded (Mulky *et al.*, 2005b). Expression of the W398L mutation in p66 bait and p51 prey fusion proteins in the Y2H system prevented expression of the p51 fusion protein, GAL4AD-p51 (Tachedjian *et al.*, 2003). The role of W398 in HIV-1 replication is unknown, however its high conservation in lentiviral RTs indicates an important role.

This study confirms that the integrity of the TRM and the αL-β20 loop is essential for HIV-1 replication, and that it has a role in both Gag-Pol maturation and RT dimerisation. The defects conferred upon expression of K331A in HIV-1 resemble that of the W401A mutation and is consistent with the proposed role of the p66 αL-β20 loop in RT dimerisation and HIV-1 replication. In contrast, the W414A mutation resulted in defects in Gag-Pol processing, as did W398A. As for T409 (Chapter 4), the role of these residues in Gag-Pol or RT heterodimerisation and function appear to be independent. Interestingly, the Q407A mutation had little effect on heterodimer formation and polymerase activity in recombinant RT, or HIV-1. Taken together with previous

studies, these data indicate that the p66 αL-β20 loop has a key role in RT subunit interaction that is required for both RT activity and HIV-1 infectivity. An essential role for the αL-β20 loop residues in Gag-Pol maturation is indicated, which appears to be mediated independently of the role of the loop in RT subunit interaction. However, the flexibility and dynamic nature of this region also allows for particular mutations, such as Q407A, to be surprisingly well tolerated.

6.2 Results

6.2.1 Conservation and location of HIV-1 RT residues K331, W398, Q407 and W414

Residues that contribute to protein:protein interactions correlate with structurally conserved residues (Keskin *et al.*, 2005). Consistent with this observation, analysis of multiple RT structures reveals that the overall composition of the RT heterodimer interface is generally conserved (Mulky *et al.*, 2005b) (Chapter 3). An alignment of RT amino acid sequences from representative strains of primate and non-primate lentiviruses (Fig. 6.1A) shows that residues contributing to the TRM (i.e. W398, W401, W402, Y405, W406, W410, W414) are strictly conserved across HIV-1 and HIV-2, and are generally conserved across SIV RT. Of the residues contributing to the tryptophan repeat motif, W414 is the least highly conserved in SIV RT. Polymorphisms at this location maintain a hydrophobic, but not necessarily an aromatic residue. W398 is the most widely conserved across all lentiviral RTs. Neither TRM residue W398 nor W414 contribute directly to the heterodimer interface in either RT subunit (Fig. 6.1B and C).

Q407 is strictly conserved across all primate lentiviral RTs. K331, which is reported to interact with TRM residues in the p66 subunit (Tachedjian *et al.*, 2003; Grohmann *et al.*, 2008), is highly conserved in HIV with low levels of polymorphism observed in SIV RT sequences. Both Q407 and K331 contribute to the heterodimer interface in the context of the p66 and p51 subunits, respectively (Fig. 6.1C) (Menendez-Arias *et al.*, 2001; Rodriguez-Barrios *et al.*, 2001; Srivastava *et al.*, 2006). The Q407 side-chain in p66 is within interacting distance of p51 residues V417 and N418. As previously reported (Tachedjian *et al.*, 2003), the K331 side-chain can potentially establish hydrogen bonds with the backbone carbonyl groups of Q407, W402 and Y405 in p66. The asymmetric nature of the RT heterodimer results in distinct spatial locations of these residues in the two RT subunits. In the context of p66, K331 is located on a solvent exposed face of the heterodimer and Q407 is buried within the p51 subunit.

A

	331	//	398	399	400	401	402	403	404	405	406	407	408	409	410	411	412	413	414	415	416
HIV-1 M group consensus	K		W	E	T	W	W	T	E	Y	W	Q	A	T	W	I	P	E	W	E	F
HIV-1 N YBF106	K		W	E	T	W	W	T	E	H	W	Q	A	T	W	I	P	E	W	E	F
HIV-1 N YBF30	K		W	E	A	W	W	T	D	H	W	Q	A	T	W	I	P	E	W	E	F
HIV-1 O ANT	K		W	E	T	W	W	A	D	Y	W	Q	A	T	W	I	P	E	W	E	F
HIV-1 O MVP5180	K		W	E	T	W	W	A	E	Y	W	Q	A	T	W	I	P	E	W	E	F
HIV-2 BEN	K		W	E	Q	W	W	D	N	Y	W	Q	V	T	W	I	P	E	W	D	F
HIV-2 ROD	K		W	E	Q	W	W	D	N	Y	W	Q	V	T	W	I	P	D	W	D	F
HIV-2 EHO	K		W	D	Q	W	W	T	D	Y	W	Q	V	T	W	I	P	E	W	D	F
HIV-2 UC1	K		W	D	Q	W	W	T	D	Y	W	Q	V	T	W	I	P	E	W	D	F
SIVagm155	K		W	E	Q	W	W	A	D	Y	W	Q	V	S	W	I	P	E	W	D	F
SIVagm3	K		W	E	Q	W	W	A	D	Y	W	Q	V	S	W	I	P	D	W	E	F
SIVagm TYO1	K		W	E	Q	W	W	A	D	Y	W	Q	V	S	W	I	P	E	W	D	F
SIVcpz EK505	K		W	E	T	W	W	T	E	Y	E	Q	A	T	W	I	P	D	W	E	F
SIVcpz MB66	K		W	E	A	W	W	T	D	Y	W	Q	A	T	W	I	P	E	W	E	Y
SIVcpz TAN1	K		W	S	Q	W	W	T	D	Y	W	Q	V	T	W	V	P	E	W	E	F
SIVmac 17E-Cl	K		W	E	Q	W	W	T	D	Y	W	Q	V	T	W	I	P	E	W	D	F
SIVmac 17E-Fr	K		W	E	Q	W	W	T	D	Y	W	Q	V	T	W	I	P	E	W	D	F
SIVmac K6W	K		W	E	Q	W	W	T	D	Y	W	Q	V	T	W	I	P	-	W	D	F
SIVmac Mm142-83	K		W	E	Q	W	W	T	D	Y	W	Q	V	T	W	I	P	E	W	D	F
SIVmnd GB1	K		W	E	D	W	W	H	E	Y	W	Q	C	T	W	I	P	E	V	E	F
SIVmnd-2	K		W	D	Q	W	W	P	E	Y	W	Q	A	T	W	I	P	E	W	E	F
SIVmon	S		W	D	T	W	W	A	D	N	W	Q	V	T	W	I	P	E	I	E	P
SIVolc	C		W	E	A	W	A	F	D	D	W	Q	V	H	W	I	P	D	I	E	F
SIVsm F236/smH4	K		W	E	Q	W	W	T	D	Y	W	Q	V	T	W	I	P	D	W	D	F
SIVsm PBj14/BCL-3	K		W	E	Q	W	W	T	D	Y	W	Q	V	T	W	I	P	E	W	D	F
SIVwrc	K		W	D	M	W	W	S	E	Y	W	Q	A	T	W	I	P	E	V	E	H
SIVqu	S		W	N	T	W	W	A	E	H	W	Q	A	N	W	I	P	E	V	K	A

Figure 6.1 Conservation and location of RT residues K331, W398, Q407 and W414.

(A) Lentiviral Pol or RT protein sequences obtained from the NCBI Entrez Protein Database (accession numbers detailed in Fig. 1.7) were aligned using ClustalW2 (Chenna *et al.*, 2003). K331, W398, Q407, W414 and the previously described W401 are highlighted in grey. (B) displays the location of these residues in the HIV-1 RT heterodimer. The heterodimer is shown in ribbon representation with the p66 subunit coloured blue and p51 coloured pink. The side-chains of the residues of interests are shown in ball and stick representation coloured green or magenta in the p66 and p51 subunits, respectively. An enlarged view of the p66 αL-β20 region (boxed) is shown in (C). These images were generated with YASARA (Krieger *et al.*, 2002) using coordinates for the RT structure 1RTD (Huang *et al.*, 1998).

B

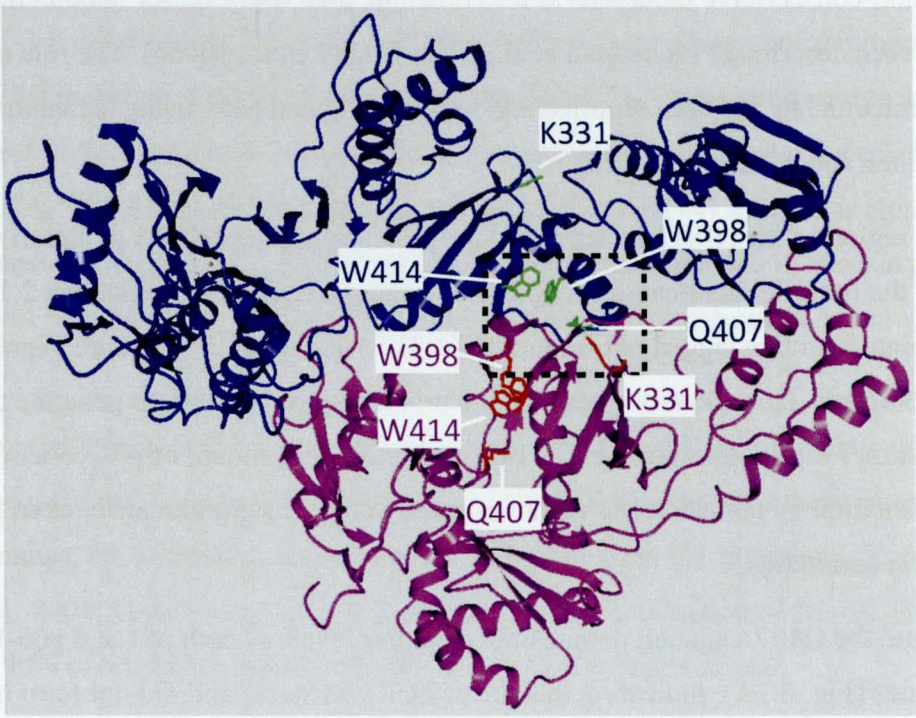

C

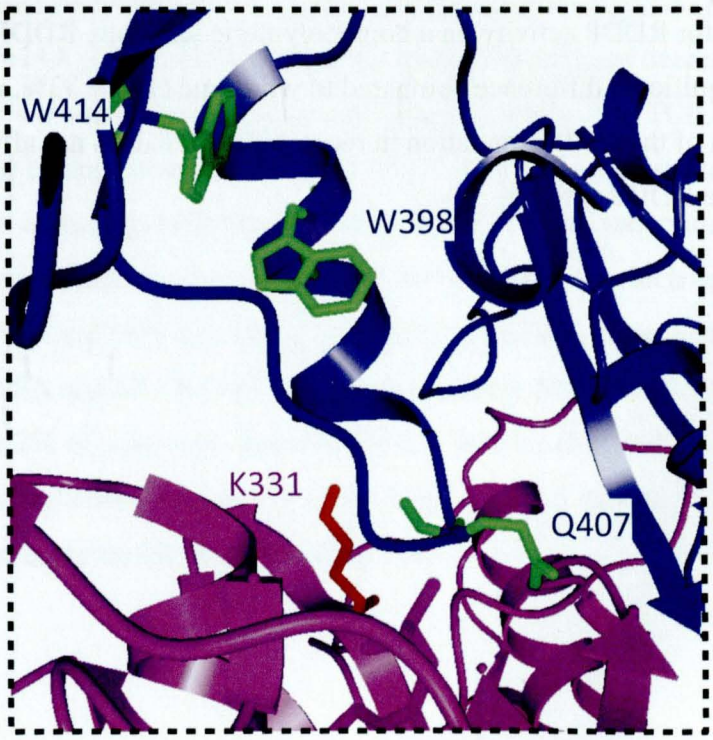

6.2.2 Expression of Q407A does not affect subunit interaction or RDDP activity of recombinant RT

The impact of non-conservative mutations at K331, W398, and W414 on RT subunit dimerisation has previously been described (Tachedjian et al., 2003; Mulky et al., 2005b). The role of Q407 in RT subunit interaction has not been reported and was investigated here, using techniques previously used by Tachedjian and colleagues (2003).

The RT coding region of the HIV-1 molecular clone NL carrying the Q407A mutation was introduced into the bacterial dual-cassette expression vector pNLRT6H/PR (Section 2.1.3-1). In this vector a C-terminal histidine tagged p66 subunit (p66-HIS) and the HIV-1 PR are expressed from independent promoters. This allows expression and processing of p66-HIS to generate the p51 subunit. Heterodimer formation was assessed by quantitating the amount of p51 co-associated with p66-HIS upon isolation by metal chelate chromatography and Western blot analysis of the eluates using RT specific antibodies.

Wild-type RT and the Q407A mutant demonstrated similar levels of both p51 and p66-HIS in total and soluble lysates (Fig. 6.2A), indicating that the protein was stable and did not form inclusion bodies. Purified Q407A RT was similar to wild-type where an approximate 1:1 ratio of the p51 subunit and p66-HIS was observed (Fig. 6.2A and B). These data indicate that Q407A does not affect HIV-1 PR-mediated cleavage of recombinant p66, or RT subunit heterodimerisation.

Purified RT was tested for RDDP activity on a homopolymeric template. RDDP activity of Q407A RT demonstrated no significant difference compared to wild-type (142 ± 33%, n = 9, p =0.39, Fig. 6.2C). Thus, expression of the Q407A mutation in recombinant RT does not affect recombinant RT dimerisation or decrease RDDP activity.

6.2.3 Impact of RT mutations W398A, Q407A, W414A and K331A on HIV-1 particle production, infectivity and virion-associated RT activity

A role in HIV-1 replication has been demonstrated for specific residues contributing to or located within the TRM, including W401 and T409 (Chapters 3 and 4). To further examine the role of conserved residues located within or identified to interact with the TRM and the αL-β20 loop, W398A, Q407A, W414A and K331A were introduced into the HIV-1 molecular clone, NL, by site directed mutagenesis (Section 2.1.2-2). The W401A mutant was included in these experiments to provide a direct comparison to this previously characterised RT dimerisation defective mutant (Chapter 3).

Viral particle production of all RT mutant HIV-1 from transfected HEK293T cells (Section 2.5.4-1) did not vary significantly compared to wild-type (Fig. 6.3), indicating that these mutations do not result in premature PR activation, as has been described for other RT mutations (Yu *et al.*, 1998a; Olivares *et al.*, 2004; Chiang *et al.*, 2010). However, particle production of NL-W398A was decreased at 90% of wild-type, which may be indicative of a minor defect.

The effect of the mutations on HIV-1 infectivity was examined by end-point titration to determine the $TCID_{50}$/mL in MT-2 cells (Section 2.6.2), and the effects on the early stages of infection examined using the TZM-bl reporter cell line (Section 2.6.3). Virion-associated RDDP activity was also determined as described (Section 2.7.1). HIV-1 expressing the K331A (NL-K331A), W398A (NL-W398A) and W414A (NL-W414A) mutations showed significant decreases in infectivity in both cell lines (Fig. 6.4A and B) compared to wild-type (NL-WT). The $TCID_{50}$/mL of these mutant viruses was decreased by approximately 10^2-fold (Fig. 6.4A) and demonstrated an approximate 80% decrease in infectious units (Fig. 6.4B) compared to NL-WT. These reductions were of a similar magnitude, but not as substantial as those observed for NL-W401A, which demonstrated a 10^3-fold reduction in $TCID_{50}$/mL and 86% decrease in infectious units. Virion-associated RDDP activities of NL-K331A, NL-W398A and NL-W414A were approximately 5% of wild-type, which again was in a similar range to the 2% of wild-type observed for NL-W401A (Fig. 6.4C). In contrast, the infectivity and virion-associated RT activity of the Q407A HIV-1 mutant (NL-Q407A) was not significantly different compared to wild-type (Fig. 6.4).

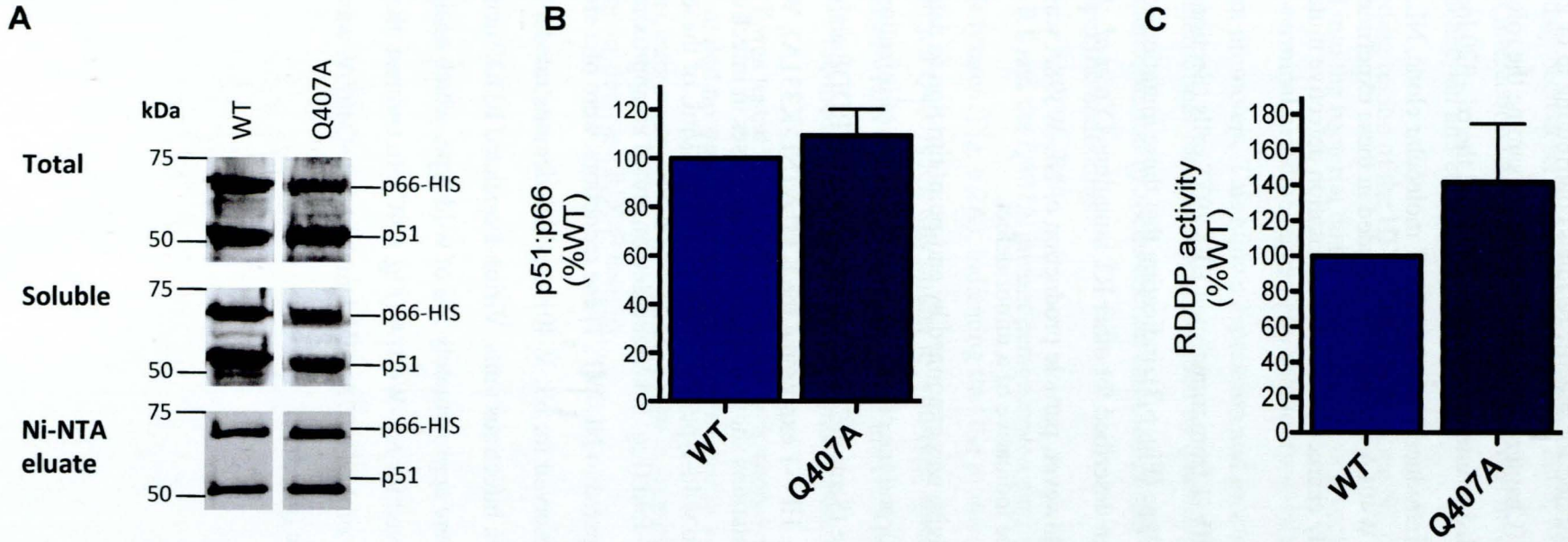

Figure 6.2. Heterodimer formation and associated RDDP activity of recombinant RT expressing the Q407A mutation.

RT heterodimer formation from a p66 precursor was assessed using the dual bacterial expression vector pNLRT6H/PR, encoding wild-type or the Q407A RT mutation. (A) Transformed bacteria were incubated with IPTG during propagation to induce expression of the HIV-1 RT and PR proteins. Bacteria were lysed (total) and the soluble fraction (soluble) affinity purified on Ni-NTA agarose. The eluate (Ni-NTA) was subjected to Western blot analysis using monoclonal RT antibody 11G10 and Alexa Fluor 680 anti-mouse secondary antibody. Western blots were visualised and quantitated using the Odyssey IR imaging system. The ratio of p51:p66-HIS was determined and expressed as the percentage of wild-type (B). Purified RT was normalised to equivalent amounts of p66 and assayed for RDDP activity on a poly(rA)/oligo(dT) T/P. Incorporation of ^{33}P dTTP was quantified using the Fujifilm FLA-3000 Phosphor Imager. RDDP activity was expressed as the percentage of wild-type activity (C). Each bar represents the mean of nine independent assays and error bars denote the standard error. Statistical analysis using the Wilcoxon matched-pairs signed rank test indicated no significant difference between wild-type and Q407A RT for either (B) $p = 0.48$, or (C) $p = 0.39$.

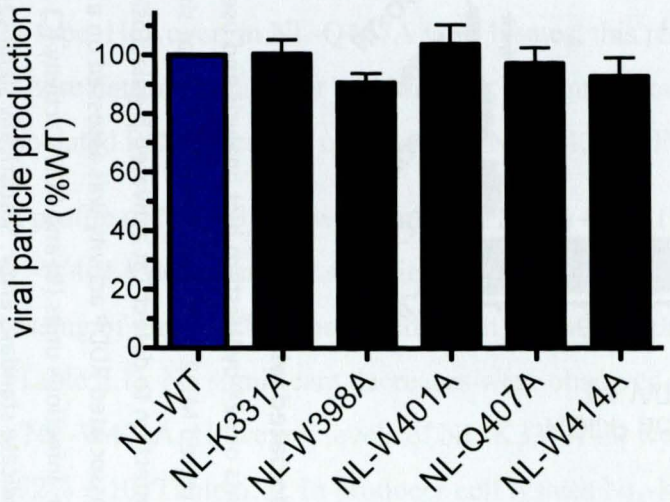

Figure 6.3. HIV-1 particle production of mutants with mutations in or associated with the RT TRM.

HIV-1 particle production from transfected HEK293T cell cultures was determined by Western blot analysis. Transfection efficiency of wild-type and mutant RT HIV-1 constructs was monitored by co-transfection with an eGFP producing plasmid. Equivalents amounts of viral and transfected cell lysates, as determined by transfection efficiency, were subjected to Western blot analysis using p24 primary antibody 183-H12-5C and Alexa Fluor 680 anti-mouse secondary antibody. Western blots were visualised and quantified using the Odyssey IR imaging system. Viral particle production was calculated as the ratio of virion-associated $Pr55^{Gag}$ and p24 to the total $Pr55^{Gag}$ and p24 in viral and cell lysates as previously described (Shehu-Xhilaga *et al.*, 2004) and expressed as the percentage of wile-type viral particle production. Bars represent the mean of seven independent assays and error bars denote the standard error of the mean. No significant differences in viral particle production was observed compared to wild-type ($p=0.46$) as determined using the Kruskal-Wallis test.

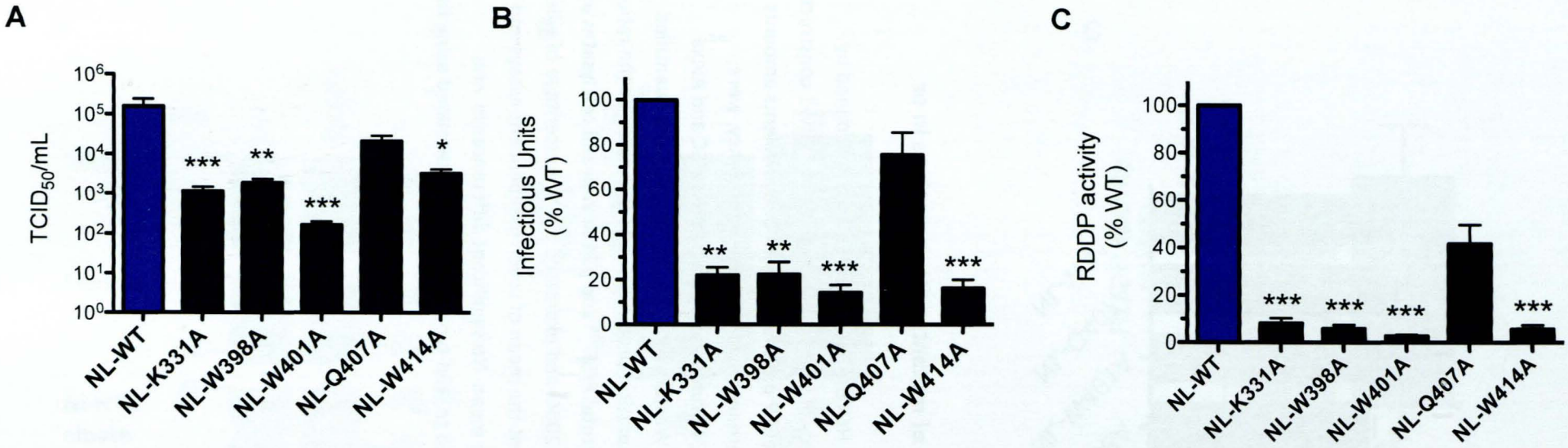

Figure 6.4. Infectivity and virion-associated RDDP activity of HIV-1 with mutations in or associated with the RT TRM

Clarified supernatants from HIV-1 transfected HEK293T cell cultures were normalised to equivalent amounts of p24 by Western blot analysis and used to determine the $TCID_{50}$/mL in MT-2 cells (A), infectious units in TZM-bl cells (B), and virion-associated RT activity (C). Infected MT-2 cells were scored for CPE at six days post infection and the $TCID_{50}$/mL calculated using the Karber formula. (B) TZM-bl cells were stained 48 h post infection to detect Tat activated β-galactosidase activity. Infected blue-stained foci were counted by light microscopy to determine infectious units/mL. (C) Virion-associated RDDP activity was assessed on a homopolymeric poly(rA)/oligo(dT) T/P. Incorporated ^{33}P-dTTP was quantified using the Fujifilm FLA-3000 Phosphor Imager. Infectious units (B) and RDDP activity (C) are presented as the percentage of wild-type. Each bar represents the mean of seven independent assays and error bars indicate standard error. Statistically significant differences between wild-type and mutant HIV-1 were calculated using the Kruskal-Wallis and Dunn's post test. A significant difference is indicated by * when $p < 0.05$, ** when $p < 0.01$, and *** when $p < 0.001$.

6.2.4 Effect of RT mutations W398A, Q407A, W414A and K331A on the HIV-1 protein profile

The HIV-1 protein profile in viral lysates (Fig. 6.5) and transfected cell lysates (Fig. 6.6) were examined. All mutant HIV-1 demonstrated a decrease in the steady-state levels of RT in viral lysates compared to wild-type. However, in NL-Q407A viral lysates, this reduction was not significant (Table 6.1). These data are consistent with the lack of significant inhibition of viral infectivity and virion-associated RDDP activity observed for NL-Q407A (Fig. 6.4).

Overall, the viral protein profile of NL-K331A was similar to NL-W401A (Fig 6.5 and Table 6.1). Both NL-K331A and NL-W401A demonstrated significant reductions in virion RT levels with a trend towards over processing of virion RT as measured by an increase in the p51:p66 ratio compared to wild-type (Table 6.1). No significant decreases were observed in virion Gag-Pol or IN for either NL-K331A or NL-W401A. However, levels of NL-K331A IN were slightly decreased compared to wild-type (72% ± 10, Table 6.1). In producer cell lysates NL-K331A and NL-W401A were the only mutants to demonstrate significant decreases in the levels of both RT subunits compared to wild-type (Table 6.2).

NL-W398A and NL-W414A also demonstrated significant reductions in virion RT. However, in contrast to NL-W401A and NL-K331A, the levels of virion Gag-Pol and IN were reduced (Table 6.1). A significant reduction in virion Gag-Pol was observed using antibodies directed against p24 (183-H12-5C) or RT (11G10), with the exception of NL-W398A Gag-Pol detected using p24 antibodies in which the 31% ± 11 decrease compared to wild-type did not achieve statistical significance (Table 6.1). Since the epitope recognised by 11G10 (Szilvay *et al.*, 1993) is distal to this RT mutation it is unlikely that the RT mutations significantly affect antibody recognition. Thus the reduced Gag-Pol levels observed with both RT and p24 antibodies strongly suggests that W398A and W414A cause a reduction in virion Gag-Pol, which is consistent with significant reductions observed in virion IN (Fig. 6.5 and Table 6.1).

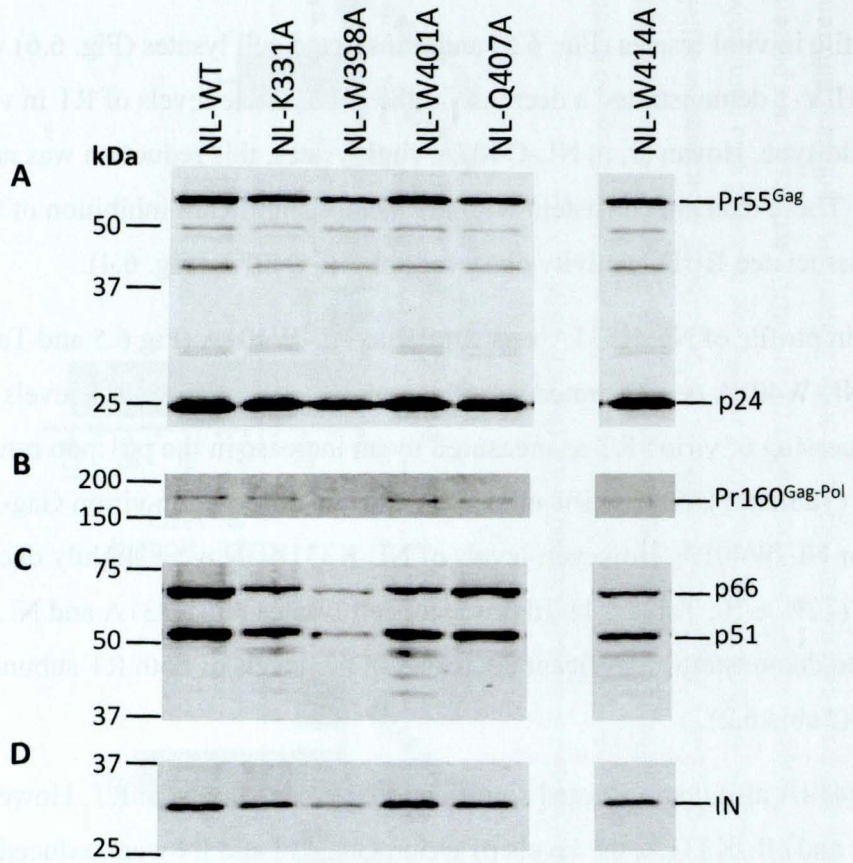

Figure 6.5. Western blot analysis of viral lysates of HIV-1 expressing RT mutations in or associated with the RT TRM.

Clarified supernatants from HEK293T cell cultures transfected with wild-type (NL-WT) or constructs containing the RT mutations as noted were normalised to equivalent amounts of p24 and subjected to Western blot analysis using p24 antibody 183-H12-5C (A) and (B), RT antibody 11G10 (C) or IN antibody 8E5 (D) and secondary antibody Alexa Fluor 680 anti-mouse antibody. Western blots were visualised and quantitated using the Odyssey IR imaging system.

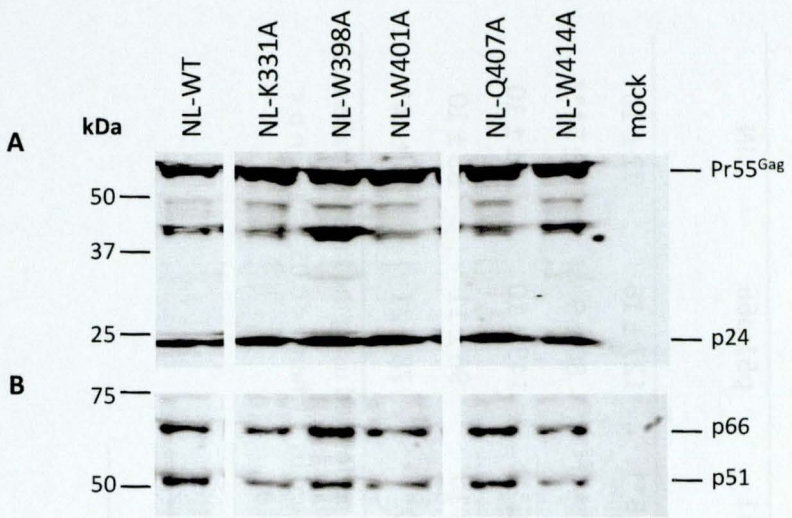

Figure 6.6. Western blot analysis of transfected cell lysates producing HIV-1 with RT mutations in or associated with the RT TRM.

HEK293T cell cultures transfected with wild-type (NL-WT) or constructs containing the RT mutations as noted were normalised to equivalent amounts of p24 and subjected to Western blot analysis using p24 antibody 183-H12-5C (A) and RT antibody 11G10 (B) and secondary Alexa Fluor 680 anti-mouse antibody. Western blots were visualised and quantitated using the Odyssey IR imaging system.

Table 6.1. Quantification of HIV-1 protein profile in viral lysates of RT mutants of or associated with the TRM.

Mutant	Protein or protein ratio relative to wild-type (%)[a]						
	p24:Pr55^{Gag}	Pr160$^{Gag\text{-}Pol}$ 183-H12-5C[b]	Pr160$^{Gag\text{-}Pol}$ 11G10[c]	p66	p51	p51:p66	IN
NL-K331A	101 ± 8	109 ± 16	99 ± 20	28 ± 7**	36 ± 6**	127 ± 16	72 ± 10
NL-W398A	114 ± 6	69 ± 13	34 ± 6***	14 ± 4***	21 ± 7***	86 ± 9	38 ± 5***
NL-W401A	102 ± 9	93 ± 10	80 ± 13	19 ± 3***	32 ± 6***	149 ± 10	101 ± 10
NL-Q407A	110 ± 8	116 ± 9	88 ± 8	80 ± 9	83 ± 10	96 ± 11	88 ± 10
NL-W414A	135 ± 18	56 ± 9*	44 ± 10**	15 ± 4***	21 ± 7***	78 ± 21	50 ± 14*

[a] Mean ± the standard error from five independent experiments. Statistical analysis was performed using the Kruskal-Wallis and Dunn's post test. Values that are significantly different compared to wild-type are indicated by * when $p < 0.05$, ** when $p < 0.01$, and *** when $p < 0.001$.

[b] Quantification of Pr160$^{Gag\text{-}Pol}$ detected using RT antibody 11G10

[c] Quantification of Pr160$^{Gag\text{-}Pol}$ detected using IN antibody 183-H12-5c

Table 6.2. Quantification of HIV-1 proteins in transfected cell lysates producing HIV-1 with mutations in or associated with the TRM.

Mutant	Protein or Ratio as relative to WT (%)[a]			
	p24:Pr55^{Gag}	p66	p51	p51:p66
NL-K331A	88 ± 13	47 ± 9***	60 ± 10**	100 ± 9
NL-W398A	114 ± 12	86 ± 7	69 ± 10	72 ± 9*
NL-W401A	93 ± 7	52 ± 7***	51 ± 4***	87 ± 6
NL-Q407A	92 ± 9	93 ± 16	96 ± 13	104 ± 8
NL-W414A	87 ± 10	85 ± 2	64 ± 9	71 ± 6*

[a]Mean ± the standard error from five independent experiments. Statistical analysis was performed using the Kruskal-Wallis and Dunn's post test. Values that are significantly different compared to wild-type are indicated by * when $p < 0.05$, ** when $p < 0.01$, and *** when $p < 0.001$.

6.2.5 RT mutations W398A and W414A affect processing of recombinant Gag-Pol

The decreased steady-state levels of virion Gag-Pol, RT and IN compared to wild-type suggest a Gag-Pol processing defect conferred by W398A and W414A. To examine this further, the effect to these mutations on the initial Gag-Pol cleavage events mediated by the embedded PR were examined using the recombinant Gag-Pol processing assay developed by Pettit and colleagues (2003) and described in Section 3.2.6.

Consistent with previous reports (Pettit *et al.*, 2003; Pettit *et al.*, 2004; Pettit *et al.*, 2005a), expression of wild-type Gag-Pol resulted in production of 120 kDa and 113 kDa processing intermediates detectable after 1 h incubation (Fig. 6.7). These polypeptides correspond to Gag-Pol processing intermediates NC-IN and $p6^{Pol}$-IN generated by cleavage at the p2/NC and TFP/$p6^{Pol}$ sites, respectively. In contrast to wild-type, expression of the W398A or W414A mutations in Gag-Pol resulted in the appearance of an additional 107 kDa fragment (Fig. 6.7). This corresponds to the PR-IN processing intermediate generated by cleavage at the $p6^{Pol}$/PR site (see Fig. 1.9)

The appearance of the 107 kDa processing intermediate PR-IN in W398A and W414A mutant Gag-Pol was accompanied by a decrease in full-length Gag-Pol compared to wild-type at the at the 2, 4 and 6 h time points, which was more pronounced for the W398A mutant. This effect was consistently observed across three independent assays. Thus in this system both W398A and W414A alter the Gag-Pol cleavages mediated by the embedded PR. These data are consistent with the decreased levels of virion Gag-Pol, RT and IN observed in NL-W398A and NL-W414A (Fig. 6.5 and Table 6.1).

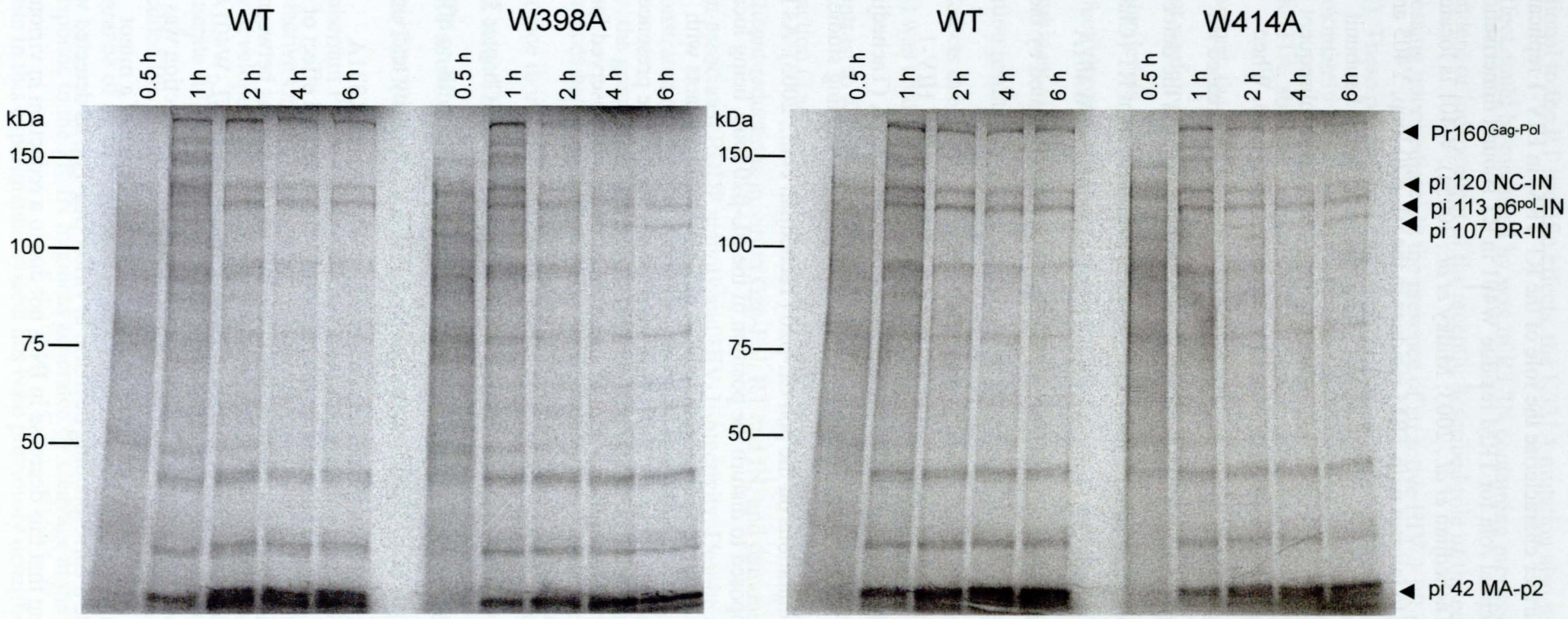

Figure 6.7. Effect of RT mutations W398A and W414A on the Gag-Pol cleavage events mediated by the Gag-Pol embedded PR.

The full-length Gag-Pol coding region derived from NL with a constitutive frameshift mutation was expressed in the Promega RRL Transcription/Translation system encoding wild-type Gag-Pol or Gag-Pol with the RT mutations W398A and W414A. The full-length Gag-Pol and its processing intermediates were detected by incorporation of ^{35}S radiolabelled methionine and cysteine. Aliquots were removed at the indicated time points, added to an excess of 2× SDS sample buffer. Samples were resolved by SDS-PAGE and proteins visualised using the Fujifilm FLA-3000 Phosphor Imager. Gag-Pol processing intermediates (pi) were identified by the molecular mass and are denoted by solid arrowheads and abbreviated nomenclature as previously defined by Pettit and colleagues (2003). Solid red arrows denote processing intermediates in the 60 to 70 kDa range that are predicted to correspond to $p6^{pol}$-p51, p66 and PR-p51. Molecular weight markers are indicated on the left of each blot. Representative data from three independent assays.

6.3 Discussion

This investigation endeavoured to further characterise the role of the RT TRM in HIV-1 replication. Previous studies demonstrate an essential role for TRM residue W401 in RT subunit dimerisation mediated through the p66 subunit (Tachedjian *et al.*, 2003; Mulky *et al.*, 2005a). W401 is located at the C-terminus of αL, and proposed to interact with TRM residues in the αL-β20 loop, Y405 and W406, to stabilise the position of the αL-β20 loop for optimal interaction with the p51 subunit (Chapter 3). Mutation of W401 results in the loss of this stabilising interaction, and subsequent loss of the multiple heterodimer interface interactions contributed by the p66 αL-β20 loop. When expressed in HIV-1, W401A confers reduced HIV-1 infectivity, RT activity, and decreased RT protein levels compared to wild-type (Chapter 3). Second-site mutations that suppress the defects conferred by W401A in HIV-1, also restore subunit heterodimerisation in recombinant RT (Chapter 5). The location and nature of these second-site mutations supports the assertion that W401A mediates its effect in HIV-1 as it does in recombinant RT; a dimerisation defect mediated by the p66 αL-β20 loop (Chapter 5).

To provide further information on the p66 αL-β20 loop in RT subunit interaction and HIV-1 replication, this Chapter examined the effect of the RT mutations W414A and K331A (Tachedjian *et al.*, 2003). Both mutations confer a RT dimerisation defect in recombinant RT binding studies, putatively due to the effect of these mutations on the p66 αL-β20 (Tachedjian *et al.*, 2003). As for the W401A mutation, W414A is proposed to disturb the position of the αL-β20 loop, being located at the N-terminus of β20. In the p51 subunit, K331 is predicted to make multiple contacts with residues in the p66 αL-β20 loop (Tachedjian *et al.*, 2003; Grohmann *et al.*, 2008). The presence of these mutations in HIV-1 was expected to result in a similar spectrum of defects as observed for the dimerisation defective W401A mutation, which was examined concurrently.

NL-K331A revealed similar defects compared to NL-W401A (Wapling *et al.*, 2005) (Chapter 3). This included a specific and significant reduction in steady-state levels of virion RT with no effects on virion Gag-Pol. This was accompanied by significant reductions in HIV-1 infectivity and virion-associated RT activity. The similarity between the defects conferred by W401A and K331A suggested a common mechanism of action. This could be the previously characterised effect of K331A in recombinant RT, a subunit dimerisation defect due to the loss of interactions between the $p51^{K331}$ side-chain and the p66 αL-β20 loop (Tachedjian *et al.*, 2003). In contrast to NL-W401A, levels of virion IN for NL-K331A were decreased (72% ± 10 of wild-type). This reduction was not significantly different to NL-WT or NL-W401A, and may or may not be indicative of a minor defect. NL-K331 did not demonstrate a corresponding decrease in virion Gag-Pol, as detected with both p24 and RT antibodies, implying that this decrease in IN is not due to a reduction in virion

Gag-Pol incorporation. The decrease in virion IN observed for NL-K331 may indicate that additional to the RT specific effects, the K331A mutation also partially affects IN maturation. Such an effect could be mediated by way of RT/IN containing processing intermediates, and could be dependent or independent of the recently described role of the cell factor clathrin in stabilising Pol processing intermediates in the presence of an active HIV-1 PR (Popov *et al.*, 2011; Zhang *et al.*, 2011). These possibilities remain unconfirmed, however the specific decrease in virion RT to approximately 30% of wild-type, which was not observed for any other viral protein examined in NL-K331A, strongly suggests that the defect conferred by the K331A is primarily RT specific.

In contrast, the W414A mutant resulted in a virion protein profile indicative of a distinct phenotype to that conferred by W401A and K331A. NL-W414A demonstrated decreases not only in virion RT but also levels of virion Gag-Pol and IN. These defects were accompanied by significant decreases in infectivity and virion-associated RDDP activity. Examination of the W414A mutation in a recombinant Gag-Pol processing assay developed by Petit and colleagues (2003) confirmed that this mutation resulted in an aberrant Gag-Pol processing profile compared to wild-type. Thus attributing the defects in HIV-1 replication to the role of W414 in RT subunit dimerisation (Tachedjian *et al.*, 2003) was confounded by its effect on Gag-Pol processing.

In contrast to K331 and W414, there was no evidence that mutation of W398 affects RT subunit interaction (Tachedjian *et al.*, 2003; Mulky *et al.*, 2005b). In this study NL-W398A demonstrated significant reductions in virion Gag-Pol, RT and IN, and demonstrated significant decreases in virion-associated RDDP activity and HIV-1 infectivity. Despite the fact that NL-W398A demonstrated the greatest reduction in steady-state virion RT levels of all mutants examined in this study, the greatest reduction in infectivity and RDDP activity was observed for NL-W401A. The differences between these mutants were small, with a 3% difference in RDDP activity, an 8% difference in infectious units in TZM-bl cells, and a 10-fold difference in $TCID_{50}$/mL observed in MT-2 cells. These differences may be attributed to the role of W401A on RT subunit dimerisation and RT activity, whereas previous data demonstrates that the W398L recombinant RT mutant has similar RDDP activity compared to wild-type (Tachedjian *et al.*, 2003).

The aberrant Pol protein profile in virions observed for NL-W398A and NL-W414A is due in part to defective Gag-Pol processing, which was confirmed in the recombinant Gag-Pol processing assay developed by Pettit and colleagues (2003). This assay uses a transcription/translation system to generate full-length Gag-Pol and observe the initial cleavage events mediated by the Gag-Pol embedded PR. Expression of the W398A and W414A mutations in this system resulted in the appearance of an additional 107 kDa processing intermediate compared to wild-type Gag-Pol. This corresponds to the PR-IN fragment generated by cleavage at the $p6^{Pol}$/PR site (Fig. 1.9). Cleavage at this site in this experimental system has been previously described upon mutation of downstream

cleavage sites, or mutation of N- or C terminal PR residues in the context of Gag-Pol (Pettit *et al.*, 2003; Pettit *et al.*, 2004; Pettit *et al.*, 2005a). The most potent of these mutations, the PR P1A mutation is hypothesised to enhance the flexibility of the Gag-Pol embedded PR, facilitating additional cleavage events. Cleavage at the $p6^{Pol}$/PR site also results in a mature-like PR activity in recombinant protein studies (Wondrak *et al.*, 1996). Thus cleavage at this site would appear to expedite Gag-Pol processing and generation of a precursor associated PR with characteristics of the mature PR (Pettit *et al.*, 2005a). Upon expression of the PR P1A mutation in Gag-Pol, cleavage at the $p6^{Pol}$/PR site is followed by cleavage at the RT/IN and p51/RNase H sites (Pettit *et al.*, 2005a).

Whether the W398A and W414A RT mutations similarly enhance Gag-Pol flexibility, or affect the Gag-Pol conformation allowing access to downstream processing sites is unknown. Furthermore, it is also unknown whether the RT mutations affect a purely PR mediated defect, as would be expected for the PR P1A mutation, or whether these RT mutations also affect further processing of RT containing processing intermediates. In this respect it would be of interest to examine the effect of the P1A mutation characterised by Pettit and colleagues (2005a) in HIV-1 to determine whether the P1A mutation results simply in enhanced processing, or aberrant processing of Pol products. In addition, generation of NL-W398A and NL-W414A in the presence of a PI, as described for the W401L mutant in Chapter 3, could confirm the role of PR in the defect conferred by these mutations.

The effect of the W398A or W414A mutations in RT subunit interaction has also been examined in *trans*-complemented virions where incorporation of RT is dependent on packaging of a Vpr-p51 fusion protein, and any co-associating p66 subunit (Mulky *et al.*, 2005b). Interestingly, p66 that is co-packaged by Vpr-p51 fusion proteins harbouring the W398A or the W414A mutation is aberrantly cleaved in the viral particle. This cleavage is not mediated by the HIV-1 PR (Mulky *et al.*, 2005b). A similar defect is also observed with mutation of TRM residues at codons W402, W406 and W414. These residues are located within the p51 subunit beneath residues Y405, W401, and N363, which contribute to the p51 heterodimer interface (Mulky *et al.*, 2005b). Thus Mulky and colleagues (2005b) propose that these mutations indirectly affect heterodimer stability.

In bacterially expressed recombinant RT, no such RT subunit degradation was reported (Tachedjian *et al.*, 2003). However, mutation of each of these residues, in this case to leucine (W398L, W402L, W406L and W414L), resulted in instability of p51-prey fusion protein for use in the Y2H system (Tachedjian *et al.*, 2003). These observations may be indicative of the role of these TRM residues in structural stability of the subunit, which may be indicative of their role in Gag-Pol observed here. Also of note is that the phenotype conferred by the W398A mutation was more dramatic than that of W414A, as observed in this study and by Mulky and colleagues (2005b). This is consistent with the strict conservation of W398 in lentiviral RTs compared to that of W414.

The viral protein processing profiled observed for NL-W398 and NL-W414, where decreases in steady-state levels of all Gag-Pol, RT and IN were observed with little defect in viral particle production and Gag processing, may also suggest that the mutants prevent interaction with the host cell factor clathrin (Popov *et al.*, 2011; Zhang *et al.*, 2011). Clathrin is specifically incorporated in HIV-1 virions by interaction with multiple regions of HIV-1 Pol. RT mutations proposed to affect the conformation of Gag-Pol (i.e. L234A), or deletion of IN or RT in the context of Gag-Pol abrogates clathrin incorporation into the virion (Popov *et al.*, 2011; Zhang *et al.*, 2011). A decrease in clathrin incorporation is associated with defects in virion Pol protein stability in the presence of an active PR. It is possible that in the context of Gag-Pol, the W398A and W414A mutations alter the conformation of Gag-Pol, decreasing clathrin incorporation and resulting in aberrant Pol processing.

With respect to this study, a recent publication by Chiang and colleagues (2010), report the effect of the W402A mutation in VSV-G pseudotyped viral particles. Expression of W402A completely abolished production of VSV-G pseudotyped particles from transiently transfected HEK293T cells (Chiang *et al.*, 2010). This phenotype is dependent on HIV-1 PR activity, as no decrease in viral particle production is observed in the presence of protease inhibitors (Chiang *et al.*, 2010). While this phenotype is distinct to the effect of the W398A and W414A mutations described here, some similarities can be seen.

Previous studies in recombinant RT demonstrate that the W402L mutation does not prevent RT subunit heterodimerisation or reduce associated RDDP activity (Tachedjian *et al.*, 2003). As previously mentioned, expression of W402A specifically in the p51 subunit does not inhibit subunit interaction, but results in breakdown of co-packaged wild-type p66 in *trans*-complemented viral particles (Mulky *et al.*, 2005b). A similar phenotype is also observed for $p51^{W398A}$, and to a lesser degree, $p51^{W414A}$ in this system (Mulky *et al.*, 2005b).

Both Chiang and colleagues (2010) and this study demonstrate a role for the HIV-1 PR in mediating the effects of these TRM mutations. Given the location and conservation of W402 and lack of effect on RT subunit interaction, it is suggested that W402 has a similar role with respect to Gag-Pol processing in HIV-1 replication as described here for W398 and W414. The differences observed between these studies may be explained by difference in the experimental conditions.

Chiang and colleagues (2010) suggest that the PR mediated defect in viral particle production is due to enhanced Gag-Pol multimerisation and premature PR activation. Here it is suggested that W398 and W414 do no promote Gag-Pol dimerisation or PR activation, rather they result in changes to Gag-Pol flexibility or conformation, facilitating Gag-Pol processing events that in expedite PR maturation. Thus changes in Gag-Pol flexibility, rather than the enhancement of Gag-Pol

dimerisation represents an alternative explanation for the W402A phenotype reported by Chiang and colleagues (2010). Interestingly, viral particle production of NL-W398A was only 10% less compared to wild-type. This may be indicative of an effect on viral particle production that was not accurately assessed in the robust transfection system used in this study. Ultimately, these mutations need to be examined within the same system to comment on the potential of a common mechanism of action. Accurate detection of viral particle production, as described by Figueiredo and colleagues (2006) should be employed to determine any effect of W398, W414 and the previously characterised T409 (Chapter 4) on viral particle production. Furthermore, the role of the HIV-1 PR in mediating the defects conferred by W398A and W414A in HIV-1 replication should be confirmed by generation of virus expressing these mutations in the presence of a PI. Thus although the precise mechanism remains undefined, these data suggest a fundamental role for TRM in Gag-Pol processing, and as indicated by Mulky et al (2005a) and Tachedjian et al (2003), in RT subunit stability.

This study also aimed to confirm that the defects in HIV-1 replication conferred by the W401A mutation were due to the dimerisation defect mediated by the αL-β20 loop. The observation of a similar range of RT specific defects in HIV-1 replication upon expression of K331A supports this conclusion, as the K331A mutation also results in an RT dimerisation defect, mediated by the αL-β20 loop, in recombinant RT studies (Tachedjian *et al.*, 2003; Grohmann *et al.*, 2008). Together with the identification and characterisation of W401A second-site mutations that suppress the defects in HIV-1 replication, and restore RT heterodimerisation and activity in recombinant protein studies (Chapter 5), these data support the role of a dimerisation defect mediated by the αL-β20 loop in HIV-1 replication. The possibility of another mechanism of action that results in similar defects, such as p51 instability (Dunn *et al.*, 2009) or conformational changes (Zhang *et al.*, 2009), is considered unlikely.

As discussed in Chapter 3, the reduction in p51 compared to p66 in transfected cell lysates upon expression of mutations at W401 that abrogate RT dimerisation was proposed to be indicative of the role for p66 homodimer formation in RT maturation (Chapter 3). A similar effect would be expected for the K331A mutation, as the p66 homodimer is assumed to adopt the asymmetric structure of the heterodimer (Wang *et al.*, 1994). Thus a mutation that abrogates RT heterodimerisation through either subunit should also affect p66 homodimer formation. However, as discussed in Chapters four and five, the decrease in the p51:p66 ratio in HIV transfected cell lysates was observed to be variable, or not strongly associated with a characterised dimerisation defect. In this series of experiments a significant decrease in the ratio of p51:p66 in producer cell lysates was not observed for NL-K331A or NL-W401A, although the latter demonstrated a small but insignificant decrease (87% ± 6) compared to wild-type. To a certain degree, the low levels of

RT subunits detected in cell lysates may have masked this observation. However, a significant decrease in the p51:p66 ratio was observed for NL-W398A, a mutation hypothesised not to act through RT subunit dimerisation. In this case the decrease in ratio may be due to loss of Pol processing intermediates to the producer cells during viral budding and inefficient RT maturation in cell lysates. These observations indicate that the change in ratio of RT subunits in transfected cell lysates is an unreliable indicator of an RT dimerisation defect, and cannot be used to make conclusions regarding the presence or absence of the p66 homodimer in RT heterodimer formation.

The role of Q407 was also investigated due to its location in the p66 αL-β20 loop and its proposed interaction with the p51 subunit. However, this mutation conferred no defects in recombinant RT subunit interaction or function, HIV-1 infectivity, virion-associated RT activity or Pol steady-state protein levels in viral particles. The lack of an effect of the Q407A mutation on RT subunit dimerisation could be explained by a previous structural analysis indicating that the carbonyl backbone of Q407 contributes to RT heterodimer interface interactions rather than the side-chain (Tachedjian *et al.*, 2003). The lack of effect of the p66 αL-β20 loop residues W402L, Y405L, W406L and W410L on RT subunit dimerisation has been described (Tachedjian *et al.*, 2003; Mulky *et al.*, 2005a). Additionally, Q407A also appeared to have no significant detrimental effect on Gag-Pol, in contrast to mutations at codon W398 and T409 in this region, that have no detectable role in RT subunit dimerisation (Chapter 4). What was surprising was the strict conservation of Q407 across primate lentiviral RT sequences, yet very little impact was observed on viral infectivity and the viral protein profile upon mutation in HIV-1. Compared to wild-type, RDDP activity and infectivity was decreased, but the decrease was not significant. Thus, it is possible that Q407 affects HIV-1 replication by a mechanism that was not directly tested in this study, and that mutation to alanine was particularly well tolerated.

It was the potential role of the TRM in RT subunit dimerisation that initially attracted attention as a novel therapeutic drug target (Restle *et al.*, 1990). While the role of the p66 αL-β20 loop in RT subunit interaction and HIV-1 replication was supported by the findings of this study, another potential means of inhibition by targeting this conserved motif was demonstrated – that is affecting early Gag-Pol processing events mediated by the embedded PR. Findings in this and previous studies suggest that specific residues of the TRM have a role in regulating PR activity in the context of Gag-Pol. This has been observed for TRM residues W398 and W414 in this study and W402 as described by Chiang and colleagues (2010). Due to the observation of similar defects upon mutation of this residue in other systems (Tachedjian *et al.*, 2003; Mulky *et al.*, 2005a), such an effect may also be observed upon mutation of W406 in HIV-1 replication (Tachedjian *et al.*, 2003; Mulky *et al.*, 2005a). A similar effect on Gag-Pol processing is also observed upon mutation of αL-β20 loop residue T409I (Chapter 4), and may be indicative of an essential structural role of this region in the

context of Gag-Pol. This effect may be mediated by the ability of Gag-Pol to bind and incorporate clathrin (Popov *et al.*, 2011; Zhang *et al.*, 2011). To confirm both the role of these highly conserved residues and the mechanism of action, examination in HIV-1 clinical isolates and primary cells, rather than adapted experimental systems such as VSV-G pseudotyping, would be more appropriate, particularly for validation as a novel target for chemotherapeutic intervention. As a basic research investigation, this study demonstrates the ability of the RT domain in Gag-Pol to affect the activity of the embedded PR, and provides evidence for the dynamic nature of the RT heterodimer interface during HIV-1 maturation. These data point towards a much greater story for the role of Gag-Pol conformation in the budding virion and in regulation of PR activity, consistent with the recent discovery that clathrin is involved in regulation of PR processing of HIV-1 Pol.

Chapter 7

General discussion and conclusions

The HIV-1 RT TRM is a series of aromatic residues, highly conserved in primate lentiviral RTs but absent in other lentiviral RTs known to form heterodimers. Amino acids that constitute the TRM are located in the connection subdomain in secondary structures αL, β20 and the loop that links these elements. In the p66 subunit the amino acids that form the αL-β20 loop, including the TRM, make significant contributions to the RT heterodimer interface, whereas the majority of the p51 TRM is buried within the subunit (Kohlstaedt *et al.*, 1992; Srivastava *et al.*, 2006). An important role for this motif in RT subunit dimerisation was originally suggested by structural analysis (Baillon *et al.*, 1991) and biochemical studies (Divita *et al.*, 1993). However, it was not until a decade later that the roles of particular TRM residues in RT subunit interaction were defined by mutagenic analysis of recombinant HIV-1 RT (Tachedjian *et al.*, 2003; Mulky *et al.*, 2005b). While these later studies demonstrated that non-conservative mutations at W401 abrogate RT subunit dimerisation, mutagenesis of several other TRM residues failed to result in adverse effects on RT subunit interaction or polymerase activity. Nonetheless, the high conservation of the TRM suggests an important role for these residues, and if not in RT subunit interaction, then in other aspects of HIV-1 replication.

Six highly conserved tryptophan residues and a tyrosine comprise the TRM, those being W398, W401, W402, Y405, W406, W410 and W414. In the context of the asymmetric RT heterodimer, both the connection subdomain and TRM are unique as residues from each subunit interact at the heterodimer interface. Residues located in the p66 αL-β20 loop from W402 to W410 make significant contributions to the RT heterodimer interface (Menendez-Arias *et al.*, 2001; Rodriguez-Barrios *et al.*, 2001; Srivastava *et al.*, 2006). For the same region in the p51 subunit, only T400, W401 and Y405 have been identified to contribute to the heterodimer interface (Mulky *et al.*, 2005b; Srivastava *et al.*, 2006). Introduction of non-conservative mutations at W401 or W414 result in a dimerisation defect mediated principally by the p66 subunit (Tachedjian *et al.*, 2003; Mulky *et al.*, 2005b). While not directly contributing to the heterodimer interface, these residues are proposed to be essential in positioning the p66 αL-β20 loop for optimal interaction with the p51 subunit (Tachedjian *et al.*, 2003). This hypothesis is supported by the observation of a dimerisation defect upon mutation K331 and consequent loss of multiple interactions formed between the $p51^{K331}$ side-chain and the p66 αL-β20 loop (Tachedjian, 2003; Grohmann *et al.*, 2008). Further, the W401A second-site compensatory mutation, T409I, is located within the p66 αL-β20 loop, and proposed to act by restoring the position of the loop (Tachedjian *et al.*, 2003).

This study investigated the role of the TRM in HIV-1 replication by mutational analysis in HIV-1, complemented by examination in recombinant Gag-Pol and RT. The dimerisation competent (W401F) and incompetent (W401A/L) TRM mutants characterised by Tachedjian and colleagues (2003, 2005b) were utilised to specifically investigate the role of RT dimerisation in HIV-1 replication. This study provides multiple lines of evidence supporting the hypothesis that perturbing RT dimerisation can inhibit both early and late phases of HIV-1 replication. This included the observation of a specific decrease in virion RT in the absence of corresponding decreases in Gag-Pol or IN, and significant decreases in reverse transcription and HIV-1 infectivity. These defects were observed upon expression of mutations that abrogate RT subunit interaction including W401A/L (Chapter 3) and K331A (Chapter 6), and absent upon expression of the dimerisation competent mutation W401F (Chapter 3). Further, W401A second-site suppressor mutations were identified that that restored HIV-1 replication to wild-type levels, and correspondingly acted to restore dimerisation of recombinant RT subunits (Chapter 5).

This study also described a novel role for particular TRM and αL-β20 loop residues in Gag-Pol processing. An aberrant processing was observed in the presence of TRM mutations that were either independent of (T409I, Chapter 4 and W398A, Chapter 6), or associated with an RT dimerisation defect in recombinant RT (W414A in Chapter 6). These observations suggested a critical role not only for the TRM. but the αL-β20 structural motif. Thus this study reveals independent roles for highly conserved residues contributing to the TRM and the αL-β20 loop in HIV-1 replication, namely modulation of interaction of the RT domain, and PR-mediated processing of Gag-Pol.

A comprehensive range of HIV-1 RT crystal structures were reviewed in the course of this study, including unliganded RT, NNRTI or T/P bound RT, and the quaternary enzymatic complex (Section 3.2.7). The location of the TRM residues within the secondary structure elements was relatively consistent, with W401 and W402 located at the C-terminus of αL, and W414 at the N-terminus of β20. The location of Y405 in either αL or the loop varied depending on the RT structure analysed. The remaining TRM residues, W406 and W410, were located in the αL-β20 loop.

From this review a mechanism was proposed for how $p66^{W401}$ may act to stabilise the position of the αL-β20 loop in the RT heterodimer. The aromatic side-chains of W401, Y405 and W406 pack against each other in an interaction referred to as a π-stack. This interaction extends across the heterodimer interface to involve the side-chain $p51^{P420}$. In addition to directly contributing to RT interface interactions, the π-stack acts to tether the αL-β20 loop (Chapter 3). Non-conservative mutation of W401 is hypothesised to prevent formation of the π-stack, whereas substitution with a bulky aromatic, i.e. W401F, maintains this hydrophobic interaction. W401, located at the base of

the π-stack, appears to be essential for establishing this interaction, whereas mutation of either Y405 or W406, located within the π-stack, is tolerated (Tachedjian *et al.*, 2003). Loss of the π-stack is predicted to relax the structure of the αL-β20 loop, and consequently, multiple interactions contributed by the αL-β20 loop to the RT heterodimer interface. Thus a non-conservative mutation at W401 in p66 accounts for the loss of multiple subunit interactions. This is in contrast to the role of W401 in the p51 subunit where it directly contributes to the heterodimer interface, and loss of this single point of interaction is not sufficient to prevent subunit association (Tachedjian *et al.*, 2003; Mulky *et al.*, 2005a).

These observations fit with the theory of hot spots and hot regions in protein:protein interaction, where multiple densely packed hot spots contribute in a cumulative manner to form a hot region, and multiple hot regions at the dimer interface contribute to the stability of the complex in an additive manner (Section 1.9). The loss of a single point of interaction, as for W401 at the p51 heterodimer interface, or T409 and Q407 at the p66 heterodimer interface, are not sufficient to prevent subunit association (Chapter 4 and 6, respectively). In contrast, both W401 and K331 potentially affect multiple interactions through the αL-β20 loop, hence conferring a RT dimerisation defect (Tachedjian *et al.*, 2003).

One of the major aims of this study was to examine the role of RT dimerisation in HIV-1 replication. Extensive characterisation of the TRM mutations W401A, W401L and W401F in recombinant RT by Tachedjian and colleagues (2003, 2005) allowed for these mutations to be utilised to examine the effect of perturbing RT dimerisation in HIV-1 replication. It was hypothesised that expression of W401A or W401L, which abrogate RT dimerisation, would result in HIV-1 with significantly reduced infectivity due to defects in the early and late phases of replication at reverse transcription and proteolytic maturation of the RT heterodimer, respectively. Structural analysis suggests that the defect mediated by the W401A or W401L mutations is localised to interactions between the p66 αL-β20 loop and p51 subunit. This is supported by the absence of changes to standard secondary structure elements as observed by CD analysis of mutant RT subunits (Tachedjian *et al.*, 2005b). As such expression of these mutations in HIV-1 were hypothesised to result in defects specific to RT and independent of pleiotropic effects on Gag-Pol stability and virion incorporation. As the W401A/L mutations prevent both RT heterodimerisation and p66 homodimerisation (unpublished data, G. Tachedjian), if the p66 homodimer is an essential processing intermediate as proposed in the sequential model of RT maturation (Sluis-Cremer *et al.*, 2004a), these mutations were expected to retard heterodimer maturation. Finally, any defects in HIV-1 replication would be specific to the dimerisation defective mutants W401A and W401L, and would not be observed upon expression of the dimerisation competent W401F mutation.

Consistent with these hypotheses, expression of the W401A and W401L resulted in HIV-1 with significantly reduced infectivity due to RT specific defects that were not observed for the W401F mutant. The decrease in virion RT was observed exclusive of defects in virion incorporation of Gag-Pol incorporation or Gag-Pol processing as indicated by wild-type levels of virion Gag-Pol, IN and a wild-type Gag processing profile. The absence of defects in the early PR mediated processing events in recombinant Gag-Pol indicated that these dimerisation defective mutants did not affect PR activation. However, the HIV-1 PR did have a role in the aberrant proteolysis of mutant RT. In addition to reductions in virion RT, W401A and W401L mutants displayed defects in reverse transcription that were most prominent for late transcripts. The relatively subtle changes in RT activity and HIV-1 infectivity observed for the W401F mutant compared to wild-type corresponded to fine changes in RT activity previously reported for the W401F RT mutant (Tachedjian *et al.*, 2005b).

Interestingly, the defect conferred by the W401A mutation in the NL4.3 HIV-1 molecular clone compared to HXB2 appeared more severe in terms of defects in reverse transcription and HIV-1 infectivity. This may be due to sequence polymorphisms, but is more likely explained by the presence of accessory proteins Vif, Nef, and Vpu, which are absent in the HXB2. In this regard, both Vif (Dettenhofer *et al.*, 2000) and Nef (Aiken *et al.*, 1995; Schwartz *et al.*, 1995; Fournier, 2002) have been shown to enhance the efficiency of reverse transcription. All further investigations in this study were conducted in NL4.3 due to the potential impact of these accessory proteins on the observed phenotypes.

Further evidence that these defects were associated with the effect of the mutation on the ability of the RT domain to dimerise, was the identification of second-site mutations that suppressed defects conferred by the W401A mutation in HIV-1 replication. That these second-site mutations acted to restore subunit interaction and polymerase activity in recombinant RT supports the conclusion that the defects observed in HIV-1 replication upon expression of W401A, were due to its effects on RT subunit interaction. Furthermore, the location and proposed mechanism of action of the most effective second-site mutation, K366R, supports the role of the αL-β20 loop in mediating this defect.

Evidence to supporting the proposed role of the αL-β20 loop in RT dimerisation and HIV-1 replication is provided by the phenotype conferred by the K331A mutation. Introduction of the K331A mutation results in a dimerisation defect in recombinant RT (Tachedjian *et al.*, 2003). The presence of K331A in HIV-1 resulted in a similar range of defects compared to the W401A mutant. Originally characterised by Tachedjian and colleagues (2003), the K331 side-chain is predicted to form multiple interactions with the backbone residues of the p66 αL-β20 loop. Accordingly,

expression of the K331A mutation in both subunits, or specifically in the p51 subunit inhibits heterodimer formation (Tachedjian *et al.*, 2003; Grohmann *et al.*, 2008). The role of K331 specifically in the p66 subunit has not been characterised. As it is located on the solvent exposed face and does not contribute to the heterodimer interface, it is presumed that mutation of $p66^{K331}$ does not contribute to the dimerisation defect. However, a precedent does exist in the L289K mutation. This mutation confers a dimerisation defect mediated through the p66 subunit where it is located on the solvent exposed face of the heterodimer, rather than the p51 subunit where L289 is located at the heterodimer interface (Goel *et al.*, 1993; Zheng *et al.*, 2010). Hence the presumption that $p66^{K331A}$ has a negligible effect on RT heterodimerisation would be strengthened by RT subunit specific analysis. Nevertheless, the similar phenotype in HIV-1 caused by the W401A and K331A mutations is supportive of a common defect mediated by a common mechanism.

RT mutations have been described that result in a similar HIV-1 viral protein profile as observed here for the W401A and K331A mutants. Most significantly, similar phenotypes have been observed upon mutation of β7-β8 loop residue N136 (Mulky *et al.*, 2007). Both the p51 β7-β8 loop (Pandey *et al.*, 2001) and N136 (Balzarini *et al.*, 2005) have an important role in formation of a stable RT heterodimer. Mutation of the p51/RNase H cleavage site (Abram *et al.*, 2005), or mutation of residues in the thumb subdomain (Dunn *et al.*, 2009, Zhang *et al.*, 2009) result in a range of defects for distinct mutations, however include HIV-1 phenotypes with specific decreases in levels of virion RT independent of decreases in Gag-Pol or other Pol proteins. Consequently it appears that the inability to form a stable RT heterodimer within the viral particle, whether due to RT subunit instability, prevention of p51 formation, or a dimerisation defect, results in PR mediated proteolysis of mutant RT.

Dunn and colleagues (2009) observe that the RT fragments generated upon proteolysis of mutant RT subunits are generally consistently, regardless of the mutation. They propose that this is indicative of exposure of pre-existing PR cleavages sites in RT, rather than these RT mutations creating novel PR cleavage sites (Dunn *et al.*, 2009). In this study small molecular weight RT reactive fragments were observed in viral lysates of HIV-1 mutants expressing mutations that abrogate RT subunit dimerisation (Chapter 4, Chapter 6). This is also observed upon expression of p51/RNase cleavage site mutations in HIV-1 (Abram *et al.*, 2005). Within each study a relatively consistent pattern of RT breakdown products was observed. Both Dunn and colleagues (2009) and this study defined a role for the HIV-1 PR in the proteolysis of mutant RT subunits. Abram and colleagues (2005) identified a second-site RT mutation that facilitated generation of the p51 subunit in HIV-1 by cleavage at an alternative site in p51/RNase H cleavage site mutants, implying a role for the HIV-1 RT. The possible role for cellular proteases was not been investigated in any of the aforementioned studies. However these data are suggestive of a dominant role for the HIV-1 PR in

proteolysis of mutant RT subunits for which formation of a stable heterodimer is retarded - regardless of the mechanism – at common sites susceptible to proteolysis.

Mutations at W401 that prevent RT heterodimer formation also prevent p66 homodimer formation in recombinant protein studies (unpublished data, G. Tachedjian). Thus, if the p66 homodimer was an essential processing intermediate in the generation of the mature heterodimer, as proposed in the sequential model of RT maturation (Sluis-Cremer *et al.*, 2004a), expression of W401A and W401L in HIV-1 would be expected to retard heterodimer formation. Unfortunately, the data presented in this study does not provide unequivocal evidence for the necessity of p66 homodimer formation in heterodimer maturation.

The effect of W401L (Tachedjian *et al.*, 2003) and W401A (Tachedjian, 2003; Mulky *et al.*, 2005b) on RT subunit interaction has been investigated under physiologically relevant conditions, those being within yeast cells and *trans*-complemented viral particles, respectively. However, in the virion or infected cell, with the presence of multiple interacting partners, it is likely that these mutations would not completely prevent RT subunit interaction. This is supported by the observation of mature RT subunits the viral lysates of these mutants, although at significantly reduced levels compared to wild-type. It is proposed that these mutations that abrogate RT dimerisation in recombinant protein binding studies, when expressed in the context of HIV-1, result in a shift in the monomer-dimer equilibrium towards monomeric subunits, or the construction of unstable dimers. It is also proposed that this would be the case for the mature RT, but also RT containing processing intermediates. Further studies involving native PAGE analysis of RT subunits in virion and transfected cell lysates could provide data to further elucidate this proposition.

The observation of a decrease in the p51:p66 ratio in cell lysates in the W401A/L HIV-1 mutants, which was not observed for the dimerisation competent W401F mutant, was originally suggested to be representative of the inability to form a stable p66 homodimer, and a subsequent reduction in RT maturation and p51 production (Chapter 3). However, the data presented in following Chapters challenge this conclusion. Unfortunately the background reactivity of antibody stocks did vary during the study. Consequently, quantitation of HIV-1 proteins in transfected cell lysates was at the limit of detection, and correspondingly any variation detected was also minimal. More pertinently however, the decrease in p51:p66 ratio was not exclusively observed for mutations that abrogate RT dimerisation.

A decrease in the p51:p66 ratio in HIV-1 transfected cell lysates was also observed in HIV-1 expressing RT mutations proposed to have no effect on RT subunit dimerisation (i.e. W398A, Chapter 6) and mutants characterised to restore subunit interaction (i.e. W401A/T409I, Chapter 4).

For the latter, the effect of the T409I in the recombinant RT expression system may not be analogous to PR mediated processing in the transfected cell, and the ability of T409I to restore p66 homodimerisation to the W401A mutant has not been directly observed. Thus the T409I may not act to restore RT heterodimer maturation in transfected cell lysates. Additionally, the role of T409I in Gag-Pol processing may have influenced the RT profile in transfected cell lysates. With respect to the W398A mutant, loss of Gag-Pol or Pol proteins to the transfected cell lysate upon enhanced precursor associated PR activity conferred by this mutation may have resulted in an increase in Pol proteins in transfected cell lysates. Indeed, even in cell lysates transfected with wild-type constructs, the p51:p66 ratio was not 1:1 as usually observed in viral lysates, indicating that RT maturation in transfected cells is inefficient. Thus the p51:p66 ratio in transfected cell lysates was subsequently found to be a poor indicator of the effect of these mutations on RT maturation.

The data presented in this study data does not provide evidence for or against a role of RT dimerisation in RT maturation, nor the necessity for p66 homodimer formation. What can be concluded is that expression of mutations that abrogate RT dimerisation in HIV-1 results in virus with significantly reduced infectivity compared to wild-type, which appears to be due both to a reduction in virion RT and a defect in RT function. In addition, the phenotype is dependent on an active HIV-1 PR resulting in proteolysis of mutant RT or RT containing processing intermediates. A goal of this study was to define the Gag-Pol cleavage events necessary for RT maturation, and the role of dimerisation in this process. Unfortunately, attempts to perform pulse-chase analysis of Gag-Pol processing in infected cell culture were unsuccessful. Ultimately even if successful, the dynamic environment of the maturing virion would not be recapitulated in these studies. Thus whether heterodimer formation proceeds via a single Gag-Pol processing pathway that necessitates formation of a p66 homodimer for RT maturation or can be generated by multiple processing pathways that incorporate dimeric intermediates, as implied by Pettit and colleagues (2005a), remains to be determined.

Independent of the role of particular TRM residues in RT dimerisation, another essential role for this motif in HIV-1 replication was identified in this study. TRM residues W398 and W414, and the αL-β20 loop residue T409, are essential for Gag-Pol processing. Mutation of these residues resulted in a Gag-Pol processing defect, observed in mutant HIV-1 as decreased levels of virion Gag-Pol, RT and IN, and in the case of T409I, significantly enhanced Gag processing. Expression of these mutations in the recombinant Gag-Pol processing assay developed by Pettit and colleagues (2003) were found to closely resemble the profile of the PR mutant P1A mutant. In the context of the Gag-Pol embedded PR, the P1A mutation enhances processing of the $p6^{Pol}$/PR cleavage site, and subsequent cleavage of the RT/IN and p51/RH sites.

The striking similarity between the Gag-Pol processing profile of the PR mutant, P1A, and the RT mutations examined here may be indicative of a similar mechanism of action. The PR P1A mutation is proposed to enhance the flexibility of the embedded precursor facilitating enhanced cleavage. Interestingly, cleavage of $p6^{Pol}$/PR has been characterised to result in a precursor associated PR with an activity profile that resembles that of the mature PR (Wondrak *et al.*, 1996; Pettit *et al.*, 2005a). This could inturn explain the enhanced cleavage of downstream PR cleavage sites demonstrated by the P1A mutant.

The RT mutants examined here demonstrate presence of small molecular weight products likely to correspond to processing intermediates generated by cleavage at RT/IN, and p51/RNase H ($p6^{Pol}$-p51, p66, and PR-p51). These products were less pronounced for the RT mutations W398A and W414A compared to T409I. This may be due to further proteolysis of these processing intermediates due to the proposed roles for W398 in p51 subunit stability (Tachedjian *et al.*, 2003; Mulky *et al.*, 2005b), and W414 in RT subunit dimerisation (Tachedjian *et al.*, 2003).

Whether the RT mutations also act to enhance flexibility in the context of Gag-Pol is unknown. The effect of P1A in HIV-1 replication has not been examined to draw a comparison on the effects in HIV-1. While it is proposed that premature PR activation is not a significant effect of these mutations, it may comprise part of the defect as indicated by a non-significant reduction in viral particle production observed for the W398A mutant (90 % of wild-type). To address this possibility, a more sensitive method of assaying viral particle production, such as that used by Figueiredo and colleagues (2006), should be employed.

A recent study revealing the role of the host cell factor clathrin in virion morphogenesis leads to the proposition of whether the effect of these RT mutations on Gag-Pol processing is direct or indirect. Clathrin is selectively incorporated into the budding virion by interaction with multiple, as yet uncharacterised domains of Pol (Popov *et al.*, 2011; Zhang *et al.*, 2011). Clathrin is proposed to have a role in regulating protease activity, retaining Pol products or stabilising Pol containing processing intermediates in the presence of an active PR during HIV-1 morphogenesis. Inability to package clathrin has no effect on viral particle production (Popov *et al.*, 2011; Zhang *et al.*, 2011). Thus the virion profile observed upon expression of RT mutations W398A, T409I and W414 is remarkably similar to the proposed role for clathrin in HIV-1 maturation. Interestingly, the Pol domain of HIV is responsible for interaction with clathrin, and in SIV both Gag and Pol appear to have a role. In other retroviruses this interaction occurs entirely with Gag. This broadly corresponds with the conservation of the TRM in primate lentiviral RTs, and its absence in non-primate lentiviruses. This may indicate an interplay between lentiviral TRM and clathrin that is yet to be fully characterised.

Interestingly, the non-conservative mutation of TRM residues, W402A, has been described to abolish the production of VSV-G pseudotyped HIV-1 particles from transiently transfected HEK293T cells (Chiang *et al.*, 2010). Co-expression of the W401A mutation with W402A in this system partially restored viral particle production. Chiang and colleagues (2010) suggest that the W402A mutation enhances Gag-Pol multimerisation resulting in premature PR activation. This effect is partially mitigated by the expression of the dimerisation defective W401A mutation.

This phenotype is distinct to the effect of mutating TRM residues on HIV-1 viral particle production and replication described in this study. The data presented here for the W398A, T409I and W414A mutants does not imply a role in mediating premature PR activation; rather they support the conclusion that these mutations induce conformational changes in Gag-Pol that facilitate Gag-Pol processing events that in turn result in expedited PR maturation. It is suggested that the W402A mutation described by Chiang and colleagues (2010), and W398A, W414A and T409I, mediate a similar effect on PR mediated Gag-Pol processing, and that the differences between these studies is largely due to differences in experimental systems. In addition, changes in Gag-Pol conformation, rather than the enhancement of Gag-Pol dimerisation represents an alternative explanation for the W402A phenotype reported by Chiang and colleagues (2010).

Interestingly, the virion Gag-Pol and Gag processing profile of the W401A/T409I double mutant was more similar to wild-type compared to that of the T409I mutant alone (Chapter 4), which is reminiscent of the action of W401A in restoring the W402A profile in terms of particle production (Chiang *et al.*, 2010).

While VSV-G pseudotyped HIV-1 is a convenient experimental system, differences in the effect of the same variable in pseudotyped versus HIV-1 systems have been described. For example, the magnitude of the effect of clathrin on viral infectivity varies depending on the experimental system used (Zhang *et al.*, 2011), as does the effect of EFV on viral particle production (Figueiredo *et al.*, 2006; Chiang *et al.*, 2009). To determine whether the effect of mutating W402 is analogous to the effect of TRM mutations W398A, W414A and T409I, W402A should be examined in both the recombinant Gag-Pol processing assay and in HIV-1 with its native envelope.

This study used statistical analysis to identify significant variations from wild-type for HIV-1 infectivity and RT activity assays, and quantifications of the HIV-1 proteins. This was limited by the inherent variability in biological systems. This datasets lacked the power to identify variables that were small, but consistent in their effect. For example, the variation between W401F mutant HIV-1 and wild-type was not statistically significant, however the infectivity of HX-W401F was consistently lower than its respective wild-type. Statistical analysis on a larger dataset would presumably identify a significant difference between wild-type or HIV-1 expressing the W401F

mutation. Thus while statistical analysis aids in identifying biologically relevant variables, it should be considered with the entirety of the biological data. In this study the statistical analysis was observed to support the conclusions drawn from the biological data.

The data presented in this study describes two essential roles for TRM residues in HIV-1 replication. TRM residues are essential in regulating the position of the p66 αL-β20 loop, which is a critical interaction for RT heterodimerisation. This study provides multiple lines of evidence supporting the conclusion that RT dimerisation is essential for optimal HIV-1 replication. These data indicate that complete RT subunit dissociation is not necessary, and that disturbing the dimer interface is sufficient to significantly reduce HIV-1 infectivity and associated RT activity. Specific residues contributing to, or located within the TRM, have an essential role in regulating the early Gag-Pol cleavage events mediated by the Gag-Pol embedded PR. Given the importance of TRM residues and the αL-β20 loop, this region should be considered as an important structural motif, similar to the β7-β8 loop. While the role of this region in RT dimerisation and Gag-Pol processing can be considered completely independent, there is evidence that both can occur in concert as demonstrated by W414, and co-expression of the W401A and T409I mutations. RT subunit dimerisation has been considered a potential target for the design of novel antiretroviral agents. This study indicates that targeting of this region could effectively inhibit HIV-1 replication by multiple mechanisms.

Abbink, T. E. and B. Berkhout (2008). "HIV-1 reverse transcription initiation: a potential target for novel antivirals?" Virus Res **134**(1-2): 4-18.

Abbondanzieri, E. A., G. Bokinsky, J. W. Rausch, J. X. Zhang, S. F. Le Grice and X. Zhuang (2008). "Dynamic binding orientations direct activity of HIV reverse transcriptase." Nature **453**(7192): 184-9.

Abram, M. E. and M. A. Parniak (2005). "Virion instability of human immunodeficiency virus type 1 reverse transcriptase (RT) mutated in the protease cleavage site between RT p51 and the RT RNase H domain." J Virol **79**(18): 11952-61.

Abram, M. E., S. G. Sarafianos and M. A. Parniak (2010). "The mutation T477A in HIV-1 reverse transcriptase (RT) restores normal proteolytic processing of RT in virus with Gag-Pol mutated in the p51-RNH cleavage site." Retrovirology **7**: 6.

Adachi, A., H. E. Gendelman, S. Koenig, T. Folks, R. Willey, A. Rabson and M. A. Martin (1986). "Production of acquired immunodeficiency syndrome-associated retrovirus in human and nonhuman cells transfected with an infectious molecular clone." J Virol **59**(2): 284-91.

Ahn, J., I. J. Byeon, S. Dharmasena, K. Huber, J. Concel, A. M. Gronenborn and N. Sluis-Cremer (2010). "The RNA binding protein HuR does not interact directly with HIV-1 reverse transcriptase and does not affect reverse transcription in vitro." Retrovirology **7**: 40.

Aiken, C. and D. Trono (1995). "Nef stimulates human immunodeficiency virus type 1 proviral DNA synthesis." J Virol **69**(8): 5048-56.

Almog, N., R. Roller, G. Arad, L. Passi-Even, M. A. Wainberg and M. Kotler (1996). "A p6Pol-protease fusion protein is present in mature particles of human immunodeficiency virus type 1." J Virol **70**(10): 7228-32.

Amacker, M., M. Hottiger, R. Mossi and U. Hubscher (1997). "HIV-1 nucleocapsid protein and replication protein A influence the strand displacement DNA synthesis of lentiviral reverse transcriptase." Aids **11**(4): 534-6.

Amacker, M. and U. Hubscher (1998). "Chimeric HIV-1 and feline immunodeficiency virus reverse transcriptases: critical role of the p51 subunit in the structural integrity of heterodimeric lentiviral DNA polymerases." J Mol Biol **278**(4): 757-65.

Anderson, S. F. and J. E. Coleman (1992). "Conformational changes of HIV reverse transcriptase subunits on formation of the heterodimer: correlation with kcat and Km." Biochemistry **31**(35): 8221-8.

Anderson, W. K. (2002). Fever hospital : a history of Fairfield Infectious Diseases Hospital. Carlton South, Vic., Melbourne University Press.

Anthony, R. M. and J. J. Destefano (2007). "In vitro synthesis of long DNA products in reactions with HIV-RT and nucleocapsid protein." J Mol Biol **365**(2): 310-24.

Antiretroviral Therapy Cohort Collaboration (2008). "Life expectancy of individuals on combination antiretroviral therapy in high-income countries: a collaborative analysis of 14 cohort studies." Lancet **372**(9635): 293-9.

Argyris, E. G., J. M. Vanderkooi, P. S. Venkateswaran, B. K. Kay and Y. Paterson (1999). "The connection domain is implicated in metalloporphyrin binding and inhibition of HIV reverse transcriptase." J Biol Chem **274**(3): 1549-56.

Argyris, E. G., J. M. Vanderkooi and Y. Paterson (2001). "Mutagenesis of key residues identifies the connection subdomain of HIV-1 reverse transcriptase as the site of inhibition by heme." Eur J Biochem **268**(4): 925-31.

Arion, D., N. Sluis-Cremer, K. L. Min, M. E. Abram, R. S. Fletcher and M. A. Parniak (2002). "Mutational analysis of Tyr-501 of HIV-1 reverse transcriptase. Effects on ribonuclease H activity and inhibition of this activity by N-acylhydrazones." J Biol Chem **277**(2): 1370-4.

Arnold, E., A. Jacobo-Molina, R. G. Nanni, R. L. Williams, X. Lu, J. Ding, A. D. Clark, Jr., A. Zhang, A. L. Ferris, P. Clark and et al. (1992). "Structure of HIV-1 reverse transcriptase/DNA complex at 7 A resolution showing active site locations." Nature **357**(6373): 85-9.

Arts, E. J., J. Mak, L. Kleiman and M. A. Wainberg (1994). "Mature reverse transcriptase (p66/p51) is responsible for low levels of viral DNA found in human immunodeficiency virus type 1 (HIV-1)." Leukemia **8 Suppl 1**: S175-8.

Arts, E. J., M. Ghosh, P. S. Jacques, B. Ehresmann and S. F. Le Grice (1996). "Restoration of tRNA3Lys-primed(-)-strand DNA synthesis to an HIV-1 reverse transcriptase mutant with extended tRNAs. Implications for retroviral replication." J Biol Chem **271**(15): 9054-61.

Arts, E. J., J. T. Miller, B. Ehresmann and S. F. Le Grice (1998). "Mutating a region of HIV-1 reverse transcriptase implicated in tRNA(Lys-3) binding and the consequences for (-)-strand DNA synthesis." J Biol Chem **273**(23): 14523-32.

Artzi, H. B., J. Shemesh, E. Zeelon, B. Amit, L. Kleiman, M. Gorecki and A. Panet (1996). "Ribonuclease H activity during initiation of reverse transcription using tRNA(lys)/RNA primer/template of human immunodeficiency virus." Arch Biochem Biophys **325**(2): 209-16.

Auwerx, J., J. Van Nieuwenhove, F. Rodriguez-Barrios, S. de Castro, S. Velazquez, F. Ceccherini-Silberstein, E. De Clercq, M. J. Camarasa, C. F. Perno, F. Gago and J. Balzarini (2005). "The N137 and P140 amino acids in the p51 and the P95 amino acid in the p66 subunit of human immunodeficiency virus type 1 (HIV-1) reverse

transcriptase are instrumental to maintain catalytic activity and to design new classes of anti-HIV-1 drugs." FEBS Lett **579**(11): 2294-300.
Bahar, I., B. Erman, R. L. Jernigan, A. R. Atilgan and D. G. Covell (1999). "Collective motions in HIV-1 reverse transcriptase: examination of flexibility and enzyme function." J Mol Biol **285**(3): 1023-37.
Baillon, J. G., N. T. Nashed, A. Kumar, S. H. Wilson and D. M. Jerina (1991). "A leucine zipper-like motif may mediate HIV reverse transcriptase subunit binding." New Biol **3**(10): 1015-9.
Baltimore, D. (1970). "RNA-dependent DNA polymerase in virions of RNA tumour viruses." Nature **226**(252): 1209-11.
Balzarini, J. (2004). "Current status of the non-nucleoside reverse transcriptase inhibitors of human immunodeficiency virus type 1." Curr Top Med Chem **4**(9): 921-44.
Balzarini, J., J. Auwerx, F. Rodriguez-Barrios, A. Chedad, V. Farkas, F. Ceccherini-Silberstein, C. Garcia-Aparicio, S. Velazquez, E. De Clercq, C. F. Perno, M. J. Camarasa and F. Gago (2005). "The amino acid Asn136 in HIV-1 reverse transcriptase (RT) maintains efficient association of both RT subunits and enables the rational design of novel RT inhibitors." Mol Pharmacol **68**(1): 49-60.
Barre-Sinoussi, F., J. C. Chermann, F. Rey, M. T. Nugeyre, S. Chamaret, J. Gruest, C. Dauguet, C. Axler-Blin, F. Vezinet-Brun, C. Rouzioux, W. Rozenbaum and L. Montagnier (1983). "Isolation of a T-lymphotropic retrovirus from a patient at risk for acquired immune deficiency syndrome (AIDS)." Science **220**(4599): 868-71.
Basu, A., S. Basu and M. J. Modak (1992). "Structure-activity analyses of HIV-1 reverse transcriptase." Biochem Biophys Res Commun **183**(3): 1131-8.
Bauman, J. D., K. Das, W. C. Ho, M. Baweja, D. M. Himmel, A. D. Clark, Jr., D. A. Oren, P. L. Boyer, S. H. Hughes, A. J. Shatkin and E. Arnold (2008). "Crystal engineering of HIV-1 reverse transcriptase for structure-based drug design." Nucleic Acids Res **36**(15): 5083-92.
Bavand, M. R., R. Wagner and T. J. Richmond (1993). "HIV-1 reverse transcriptase: polymerization properties of the p51 homodimer compared to the p66/p51 heterodimer." Biochemistry **32**(40): 10543-52.
Beard, W. A. and S. H. Wilson (1993). "Kinetic analysis of template.primer interactions with recombinant forms of HIV-1 reverse transcriptase." Biochemistry **32**(37): 9745-53.
Bebenek, K., J. Abbotts, J. D. Roberts, S. H. Wilson and T. A. Kunkel (1989). "Specificity and mechanism of error-prone replication by human immunodeficiency virus-1 reverse transcriptase." J Biol Chem **264**(28): 16948-56.
Becerra, S. P., A. Kumar, M. S. Lewis, S. G. Widen, J. Abbotts, E. M. Karawya, S. H. Hughes, J. Shiloach and S. H. Wilson (1991). "Protein-protein interactions of HIV-1 reverse transcriptase: implication of central and C-terminal regions in subunit binding." Biochemistry **30**(50): 11707-19.
Bogan, A. A. and K. S. Thorn (1998). "Anatomy of hot spots in protein interfaces." J Mol Biol **280**(1): 1-9.
Borkow, G., R. S. Fletcher, J. Barnard, D. Arion, D. Motakis, G. I. Dmitrienko and M. A. Parniak (1997). "Inhibition of the ribonuclease H and DNA polymerase activities of HIV-1 reverse transcriptase by N-(4-tert-butylbenzoyl)-2-hydroxy-1-naphthaldehyde hydrazone." Biochemistry **36**(11): 3179-85.
Brass, A. L., D. M. Dykxhoorn, Y. Benita, N. Yan, A. Engelman, R. J. Xavier, J. Lieberman and S. J. Elledge (2008). "Identification of host proteins required for HIV infection through a functional genomic screen." Science **319**(5865): 921-6.
Brierley, I. and F. J. Dos Ramos (2006). "Programmed ribosomal frameshifting in HIV-1 and the SARS-CoV." Virus Res **119**(1): 29-42.
Briggs, J. A., J. D. Riches, B. Glass, V. Bartonova, G. Zanetti and H. G. Krausslich (2009). "Structure and assembly of immature HIV." Proc Natl Acad Sci U S A **106**(27): 11090-5.
Brown, F. (1986). "Human immunodeficiency virus." Science **232**(4757): 1486.
Brown, P. O. (1997). Integration. Retroviruses. M. Coffin J, H. Hughes S and E. Varmus H, Cold Spring Habor Laboratory Press.
Bryant, M. and L. Ratner (1990). "Myristoylation-dependent replication and assembly of human immunodeficiency virus 1." Proc Natl Acad Sci U S A **87**(2): 523-7.
Buchschacher, G. L., Jr., L. Yu, F. Murai, T. Friedmann and A. Miyanohara (1999). "Association of murine leukemia virus pol with virions, independent of Gag-Pol expression." J Virol **73**(11): 9632-7.
Bukovsky, A. and H. Gottlinger (1996). "Lack of integrase can markedly affect human immunodeficiency virus type 1 particle production in the presence of an active viral protease." J Virol **70**(10): 6820-5.
Buxton, P., G. Tachedjian and J. Mak (2005). "Analysis of the contribution of reverse transcriptase and integrase proteins to retroviral RNA dimer conformation." J Virol **79**(10): 6338-48.
Cabodevilla, J. F., L. Odriozola, E. Santiago and J. J. Martinez-Irujo (2001). "Factors affecting the dimerization of the p66 form of HIV-1 reverse transcriptase." Eur J Biochem **268**(5): 1163-72.
Camarasa, M. J., S. Velazquez, A. San Felix, M. J. Perez-Perez and F. Gago (2006). "Dimerization inhibitos of HIV-1 reverse transcriptase, protease and integrase: A single mode of inhibition for three HIV enzymes?" Antiviral Res **71**: 260-7.
Campbell, W., L. Kleiman, L. Barany, Z. Li, A. Khorchid, E. Fujita, N. Okada and H. Okada (2002). "A novel genetic algorithm for designing mimetic peptides that interfere with the function of a target molecule." Microbiol Immunol **46**(3): 211-5.

Campiani, G., A. Ramunno, G. Maga, V. Nacci, C. Fattorusso, B. Catalanotti, E. Morelli and E. Novellino (2002). "Non-nucleoside HIV-1 reverse transcriptase (RT) inhibitors: past, present, and future perspectives." Curr Pharm Des **8**(8): 615-57.

Candotti, D., C. Chappey, M. Rosenheim, P. M'Pele, J. M. Huraux and H. Agut (1994). "High variability of the gag/pol transframe region among HIV-1 isolates." C R Acad Sci III **317**(2): 183-9.

Carlson, L. A., J. A. Briggs, B. Glass, J. D. Riches, M. N. Simon, M. C. Johnson, B. Muller, K. Grunewald and H. G. Krausslich (2008). "Three-dimensional analysis of budding sites and released virus suggests a revised model for HIV-1 morphogenesis." Cell Host Microbe **4**(6): 592-9.

Cen, S., M. Niu and L. Kleiman (2004a). "The connection domain in reverse transcriptase facilitates the in vivo annealing of tRNALys3 to HIV-1 genomic RNA." Retrovirology **1**: 33.

Cen, S., M. Niu, J. Saadatmand, F. Guo, Y. Huang, G. J. Nabel and L. Kleiman (2004b). "Incorporation of pol into human immunodeficiency virus type 1 Gag virus-like particles occurs independently of the upstream Gag domain in Gag-pol." J Virol **78**(2): 1042-9.

Centers for Disease Control (1981). "Kaposi's sarcoma and Pneumocystis pneumonia among homosexual men--New York City and California." Morbidity and Mortality Weekly Report **30**(25): 305-8.

Centers for Disease Control (1985). Acquired Immunodeficiency Syndrome: Meeting of the WHO Collaborating Centres on AIDS Morbidity and Mortality Weekly Report. Atlanta, Centers for Disease Control and Prevention. **34:** 678-9.

Centers for Disease Control (2001). "HIV and AIDS--United States, 1981-2000." MMWR Morb Mortal Wkly Rep **50**(21): 430-4.

Charneau, P., M. Alizon and F. Clavel (1992). "A second origin of DNA plus-strand synthesis is required for optimal human immunodeficiency virus replication." J Virol **66**(5): 2814-20.

Chatterjee, A., P. Mridula, R. K. Mishra, R. Mittal and R. V. Hosur (2005). "Folding regulates autoprocessing of HIV-1 protease precursor." J Biol Chem **280**(12): 11369-78.

Chattopadhyay, D., D. B. Evans, M. R. Deibel, Jr., A. F. Vosters, F. M. Eckenrode, H. M. Einspahr, J. O. Hui, A. G. Tomasselli, H. A. Zurcher-Neely, R. L. Heinrikson and et al. (1992). "Purification and characterization of heterodimeric human immunodeficiency virus type 1 (HIV-1) reverse transcriptase produced by in vitro processing of p66 with recombinant HIV-1 protease." J Biol Chem **267**(20): 14227-32.

Cheng, Y. S., F. H. Yin, S. Foundling, D. Blomstrom and C. A. Kettner (1990). "Stability and activity of human immunodeficiency virus protease: comparison of the natural dimer with a homologous, single-chain tethered dimer." Proc Natl Acad Sci U S A **87**(24): 9660-4.

Chenna, R., H. Sugawara, T. Koike, R. Lopez, T. J. Gibson, D. G. Higgins and J. D. Thompson (2003). "Multiple sequence alignment with the Clustal series of programs." Nucleic Acids Res **31**(13): 3497-500.

Cherry, E., C. Liang, L. Rong, Y. Quan, P. Inouye, X. Li, N. Morin, M. Kotler and M. A. Wainberg (1998a). "Characterization of human immunodeficiency virus type-1 (HIV-1) particles that express protease-reverse transcriptase fusion proteins." J Mol Biol **284**(1): 43-56.

Cherry, E., N. Morin and M. A. Wainberg (1998b). "Effect of HIV constructs containing protease-reverse transcriptase fusion proteins on viral replication." Aids **12**(9): 967-75.

Chesebro, B., K. Wehrly, J. Nishio and S. Perryman (1992). "Macrophage-tropic human immunodeficiency virus isolates from different patients exhibit unusual V3 envelope sequence homogeneity in comparison with T-cell-tropic isolates: definition of critical amino acids involved in cell tropism." J Virol **66**(11): 6547-54.

Chiang, C. C., S. M. Wang, Y. T. Tseng, K. J. Huang and C. T. Wang (2009). "Mutations at human immunodeficiency virus type 1 reverse transcriptase tryptophan repeat motif attenuate the inhibitory effect of efavirenz on virus production." Virology **383**(2): 261-70.

Chiang, C. C., S. M. Wang, Y. Y. Pan, K. J. Huang and C. T. Wang (2010). "A single amino acid substitution in HIV-1 reverse transcriptase significantly reduces virion release." J Virol **84**(2): 976-82.

Chiu, H. C., S. Y. Yao and C. T. Wang (2002). "Coding sequences upstream of the human immunodeficiency virus type 1 reverse transcriptase domain in Gag-Pol are not essential for incorporation of the Pr160(gag-pol) into virus particles." J Virol **76**(7): 3221-31.

Chiu, H. C., W. H. Liao, S. W. Chen and C. T. Wang (2004a). "The human immunodeficiency virus type 1 carboxyl-terminal third of capsid sequence in Gag-Pol is essential but not sufficient for efficient incorporation of Pr160(gag-pol) into virus particles." J Biomed Sci **11**(3): 398-407.

Chiu, T. K. and D. R. Davies (2004b). "Structure and function of HIV-1 integrase." Curr Top Med Chem **4**(9): 965-77.

Clavel, F., D. Guetard, F. Brun-Vezinet, S. Chamaret, M. A. Rey, M. O. Santos-Ferreira, A. G. Laurent, C. Dauguet, C. Katlama, C. Rouzioux and et al. (1986). "Isolation of a new human retrovirus from West African patients with AIDS." Science **233**(4761): 343-6.

Clavel, F. and A. J. Hance (2004). "HIV drug resistance." N Engl J Med **350**(10): 1023-35.

Clore, G. M., J. Ernst, R. Clubb, J. G. Omichinski, W. M. Kennedy, K. Sakaguchi, E. Appella and A. M. Gronenborn (1995). "Refined solution structure of the oligomerization domain of the tumour suppressor p53." Nat Struct Biol **2**(4): 321-33.

Co, E., G. Koelsch, Y. Lin, E. Ido, J. A. Hartsuck and J. Tang (1994). "Proteolytic processing mechanisms of a miniprecursor of the aspartic protease of human immunodeficiency virus type 1." Biochemistry **33**(5): 1248-54.

Coffin, J., A. Haase, J. A. Levy, L. Montagnier, S. Oroszlan, N. Teich, H. Temin, K. Toyoshima, H. Varmus, P. Vogt and et al. (1986). "What to call the AIDS virus?" Nature **321**(6065): 10.

Concorde Coordinating Committee (1994). "Concorde: MRC/ANRS randomised double-blind controlled trial of immediate and deferred zidovudine in symptom-free HIV infection. Concorde Coordinating Committee." Lancet **343**(8902): 871-81.

Cote, H. C., Z. L. Brumme and P. R. Harrigan (2001). "Human immunodeficiency virus type 1 protease cleavage site mutations associated with protease inhibitor cross-resistance selected by indinavir, ritonavir, and/or saquinavir." J Virol **75**(2): 589-94.

Cote, M. L. and M. J. Roth (2008). "Murine leukemia virus reverse transcriptase: structural comparison with HIV-1 reverse transcriptase." Virus Res **134**(1-2): 186-202.

Daniel, M. D., N. L. Letvin, N. W. King, M. Kannagi, P. K. Sehgal, R. D. Hunt, P. J. Kanki, M. Essex and R. C. Desrosiers (1985). "Isolation of T-cell tropic HTLV-III-like retrovirus from macaques." Science **228**(4704): 1201-4.

Das, K., S. G. Sarafianos, E. Arnold and S. H. Hughes (2004). HIV-1 Reverse Transcriptase Structure. Encylopedia of Biological Chemistry. W. Lennarz, P. Modrich, J. Dixon, E. Carafoli, J. Exton and D. Cleveland, Academic Press. **2**.

Das, K., S. G. Sarafianos, A. D. Clark, Jr., P. L. Boyer, S. H. Hughes and E. Arnold (2007). "Crystal structures of clinically relevant Lys103Asn/Tyr181Cys double mutant HIV-1 reverse transcriptase in complexes with ATP and non-nucleoside inhibitor HBY 097." J Mol Biol **365**(1): 77-89.

Das, K., J. D. Bauman, A. D. Clark, Jr., Y. V. Frenkel, P. J. Lewi, A. J. Shatkin, S. H. Hughes and E. Arnold (2008). "High-resolution structures of HIV-1 reverse transcriptase/TMC278 complexes: strategic flexibility explains potency against resistance mutations." Proc Natl Acad Sci U S A **105**(5): 1466-71.

Das, K., J. D. Bauman, A. S. Rim, C. Dharia, A. D. Clark, Jr., M. J. Camarasa, J. Balzarini and E. Arnold (2011). "Crystal structure of tert-butyldimethylsilyl-spiroaminooxathioledioxide-thymine (TSAO-T) in complex with HIV-1 reverse transcriptase (RT) rededfines the elastic limits of the non-nucleoside inhibitor-binding pocket." J Med Chem **54**(8): 2727-37.

Davey, R. T., Jr., R. L. Dewar, G. F. Reed, M. B. Vasudevachari, M. A. Polis, J. A. Kovacs, J. Falloon, R. E. Walker, H. Masur, S. E. Haneiwich and et al. (1993). "Plasma viremia as a sensitive indicator of the antiretroviral activity of L-697,661." Proc Natl Acad Sci U S A **90**(12): 5608-12.

Davies, J. F., 2nd, Z. Hostomska, Z. Hostomsky, S. R. Jordan and D. A. Matthews (1991). "Crystal structure of the ribonuclease H domain of HIV-1 reverse transcriptase." Science **252**(5002): 88-95.

Dayton, A. I., J. G. Sodroski, C. A. Rosen, W. C. Goh and W. A. Haseltine (1986). "The trans-activator gene of the human T cell lymphotropic virus type III is required for replication." Cell **44**(6): 941-7.

De Vivo, M., M. Dal Peraro and M. L. Klein (2008). "Phosphodiester cleavage in ribonuclease H occurs via an associative two-metal-aided catalytic mechanism." J Am Chem Soc **130**(33): 10955-62.

Debyser, Z. and E. De Clercq (1996). "Chemical crosslinking of the subunits of HIV-1 reverse transcriptase." Protein Sci **5**(2): 278-86.

Delaney, M. (2005). AIDS Activisim and the Pharmaceutical Industry. Ethics and the Pharmaceutical Industry. M. A. Santoro and T. M. Gorrie. New York, CAMBRIDGE UNIVERSITY PRESS 300-25.

Depollier, J., M. L. Hourdou, G. Aldrian-Herrada, P. Rothwell, T. Restle and G. Divita (2005). "Insight into the mechanism of a peptide inhibitor of HIV reverse transcriptase dimerization." Biochemistry **44**(6): 1909-18.

Derdeyn, C. A., J. M. Decker, J. N. Sfakianos, X. Wu, W. A. O'Brien, L. Ratner, J. C. Kappes, G. M. Shaw and E. Hunter (2000). "Sensitivity of human immunodeficiency virus type 1 to the fusion inhibitor T-20 is modulated by coreceptor specificity defined by the V3 loop of gp120." J Virol **74**(18): 8358-67.

DeStefano, J. J., R. G. Buiser, L. M. Mallaber, T. W. Myers, R. A. Bambara and P. J. Fay (1991). "Polymerization and RNase H activities of the reverse transcriptases from avian myeloblastosis, human immunodeficiency, and Moloney murine leukemia viruses are functionally uncoupled." J Biol Chem **266**(12): 7423-31.

Dettenhofer, M. and X. F. Yu (1999). "Proline residues in human immunodeficiency virus type 1 p6(Gag) exert a cell type-dependent effect on viral replication and virion incorporation of Pol proteins." J Virol **73**(6): 4696-704.

Dettenhofer, M., S. Cen, B. A. Carlson, L. Kleiman and X. F. Yu (2000). "Association of human immunodeficiency virus type 1 Vif with RNA and its role in reverse transcription." J Virol **74**(19): 8938-45.

di Marzo Veronese, F., T. D. Copeland, A. L. DeVico, R. Rahman, S. Oroszlan, R. C. Gallo and M. G. Sarngadharan (1986). "Characterization of highly immunogenic p66/p51 as the reverse transcriptase of HTLV-III/LAV." Science **231**(4743): 1289-91.

Ding, J., K. Das, C. Tantillo, W. Zhang, A. D. Clark, Jr., S. Jessen, X. Lu, Y. Hsiou, A. Jacobo-Molina, K. Andries and et al. (1995). "Structure of HIV-1 reverse transcriptase in a complex with the non-nucleoside inhibitor alpha-APA R 95845 at 2.8 A resolution." Structure **3**(4): 365-79.

Ding, J., K. Das, Y. Hsiou, S. G. Sarafianos, A. D. Clark, Jr., A. Jacobo-Molina, C. Tantillo, S. H. Hughes and E. Arnold (1998). "Structure and functional implications of the polymerase active site region in a complex of HIV-1 RT with a double-stranded DNA template-primer and an antibody Fab fragment at 2.8 A resolution." J Mol Biol **284**(4): 1095-111.

Ding, L., A. Derdowski, J. J. Wang and P. Spearman (2003). "Independent segregation of human immunodeficiency virus type 1 Gag protein complexes and lipid rafts." J Virol **77**(3): 1916-26.

Divita, G., T. Restle and R. S. Goody (1993). "Characterization of the dimerization process of HIV-1 reverse transcriptase heterodimer using intrinsic protein fluorescence." FEBS Lett **324**(2): 153-8.

Divita, G., T. Restle, R. S. Goody, J. C. Chermann and J. G. Baillon (1994). "Inhibition of human immunodeficiency virus type 1 reverse transcriptase dimerization using synthetic peptides derived from the connection domain." J Biol Chem **269**(18): 13080-3.

Divita, G., K. Rittinger, C. Geourjon, G. Deleage and R. S. Goody (1995a). "Dimerization kinetics of HIV-1 and HIV-2 reverse transcriptase: a two step process." J Mol Biol **245**(5): 508-21.

Divita, G., K. Rittinger, T. Restle, U. Immendorfer and R. S. Goody (1995b). "Conformational stability of dimeric HIV-1 and HIV-2 reverse transcriptases." Biochemistry **34**(50): 16337-46.

Dunn, L. L., M. J. McWilliams, K. Das, E. Arnold and S. H. Hughes (2009). "Mutations in the thumb allow human immunodeficiency virus type 1 reverse transcriptase to be cleaved by protease in virions." J Virol **83**(23): 12336-44.

Eggink, D., B. Berkhout and R. W. Sanders (2010). "Inhibition of HIV-1 by fusion inhibitors." Current pharmaceutical design **16**(33): 3716-28.

Esnouf, R., J. Ren, C. Ross, Y. Jones, D. Stammers and D. Stuart (1995). "Mechanism of inhibition of HIV-1 reverse transcriptase by non-nucleoside inhibitors." Nat Struct Biol **2**(4): 303-8.

Espeseth, A. S., P. Felock, A. Wolfe, M. Witmer, J. Grobler, N. Anthony, M. Egbertson, J. Y. Melamed, S. Young, T. Hamill, J. L. Cole and D. J. Hazuda (2000). "HIV-1 integrase inhibitors that compete with the target DNA substrate define a unique strand transfer conformation for integrase." Proceedings of the National Academy of Sciences of the United States of America **97**(21): 11244-9.

Facke, M., A. Janetzko, R. L. Shoeman and H. G. Krausslich (1993). "A large deletion in the matrix domain of the human immunodeficiency virus gag gene redirects virus particle assembly from the plasma membrane to the endoplasmic reticulum." J Virol **67**(8): 4972-80.

Fassati, A. and S. P. Goff (2001). "Characterization of intracellular reverse transcription complexes of human immunodeficiency virus type 1." J Virol **75**(8): 3626-35.

Figueiredo, A., K. L. Moore, J. Mak, N. Sluis-Cremer, M. P. de Bethune and G. Tachedjian (2006). "Potent Nonnucleoside Reverse Transcriptase Inhibitors Target HIV-1 Gag-Pol." PLoS Pathog **2**(11).

Filler, A. G. and A. M. Lever (1997). "Effects of cation substitutions on reverse transcriptase and on human immunodeficiency virus production." AIDS Res Hum Retroviruses **13**(4): 291-9.

Fischl, M. A., D. D. Richman, M. H. Grieco, M. S. Gottlieb, P. A. Volberding, O. L. Laskin, J. M. Leedom, J. E. Groopman, D. Mildvan, R. T. Schooley and et al. (1987). "The efficacy of azidothymidine (AZT) in the treatment of patients with AIDS and AIDS-related complex. A double-blind, placebo-controlled trial." N Engl J Med **317**(4): 185-91.

Fisher, A. G., M. B. Feinberg, S. F. Josephs, M. E. Harper, L. M. Marselle, G. Reyes, M. A. Gonda, A. Aldovini, C. Debouk, R. C. Gallo and et al. (1986). "The trans-activator gene of HTLV-III is essential for virus replication." Nature **320**(6060): 367-71.

Folks, T. M., K. A. Clouse, J. Justement, A. Rabson, E. Duh, J. H. Kehrl and A. S. Fauci (1989). "Tumor necrosis factor alpha induces expression of human immunodeficiency virus in a chronically infected T-cell clone." Proc Natl Acad Sci U S A **86**(7): 2365-8.

Forshey, B., U. v. Schwedler, U. S. WI and A. C (2002). "Formation of a human immunodeficiency virus type 1 core of optimal stability is crucial for viral replication." Journal of Virology **76**: 5667-77.

Fournier, C. (2002). "The HIV-1 Nef protein enhances the affinity of reverse transcriptase for RNA in vitro." Virus Genes **25**: 255-69.

Francis, D. P. and J. C. Petricciani (1985). "The prospects for and pathways toward a vaccine for AIDS." N Engl J Med **313**(25): 1586-90.

Freed, E. O. (1998). "HIV-1 gag proteins: diverse functions in the virus life cycle." Virology **251**(1): 1-15.

Furfine, E. S. and J. E. Reardon (1991). "Reverse transcriptase.RNase H from the human immunodeficiency virus. Relationship of the DNA polymerase and RNA hydrolysis activities." J Biol Chem **266**(1): 406-12.

Gallo, R. C., S. Z. Salahuddin, M. Popovic, G. M. Shearer, M. Kaplan, B. F. Haynes, T. J. Palker, R. Redfield, J. Oleske, B. Safai and et al. (1984). "Frequent detection and isolation of cytopathic retroviruses (HTLV-III) from patients with AIDS and at risk for AIDS." Science **224**(4648): 500-3.

Ganser-Pornillos, B. K., M. Yeager and W. I. Sundquist (2008). "The structural biology of HIV assembly." Curr Opin Struct Biol **18**(2): 203-17.

Garforth, S. J., T. W. Kim, M. A. Parniak, E. T. Kool and V. R. Prasad (2007). "Site-directed mutagenesis in the fingers subdomain of HIV-1 reverse transcriptase reveals a specific role for the beta3-beta4 hairpin loop in dNTP selection." J Mol Biol **365**(1): 38-49.

Garrus, J. E., U. K. von Schwedler, O. W. Pornillos, S. G. Morham, K. H. Zavitz, H. E. Wang, D. A. Wettstein, K. M. Stray, M. Cote, R. L. Rich, D. G. Myszka and W. I. Sundquist (2001). "Tsg101 and the vacuolar protein sorting pathway are essential for HIV-1 budding." Cell **107**(1): 55-65.

Gheysen, D., E. Jacobs, F. de Foresta, C. Thiriart, M. Francotte, D. Thines and M. De Wilde (1989). "Assembly and release of HIV-1 precursor Pr55gag virus-like particles from recombinant baculovirus-infected insect cells." Cell **59**(1): 103-12.

Ghosh, M., P. S. Jacques, D. W. Rodgers, M. Ottman, J. L. Darlix and S. F. Le Grice (1996). "Alterations to the primer grip of p66 HIV-1 reverse transcriptase and their consequences for template-primer utilization." Biochemistry **35**(26): 8553-62.

Goel, R., W. A. Beard, A. Kumar, J. R. Casas-Finet, M. P. Strub, S. J. Stahl, M. S. Lewis, K. Bebenek, S. P. Becerra, T. A. Kunkel and et al. (1993). "Structure/function studies of HIV-1(1) reverse transcriptase: dimerization-defective mutant L289K." Biochemistry **32**(48): 13012-8.

Goff, S. P. (1990). "Retroviral reverse transcriptase: synthesis, structure, and function." Journal of acquired immune deficiency syndromes **3**(8): 817-31.

Goody, R. S., B. Muller and T. Restle (1991). "Factors contributing to the inhibition of HIV reverse transcriptase by chain-terminating nucleotides in vitro and in vivo." FEBS Lett **291**(1): 1-5.

Gopalakrishnan, V., J. A. Peliska and S. J. Benkovic (1992). "Human immunodeficiency virus type 1 reverse transcriptase: spatial and temporal relationship between the polymerase and RNase H activities." Proc Natl Acad Sci U S A **89**(22): 10763-7.

Gorry, P. R., J. Sterjovski, M. Churchill, K. Witlox, L. Gray, A. Cunningham and S. Wesselingh (2004). "The role of viral coreceptors and enhanced macrophage tropism in human immunodeficiency virus type 1 disease progression." Sex Health **1**(1): 23-34.

Gotte, M. (2006). "Effects of nucleotides and nucleotide analogue inhibitors of HIV-1 reverse transcriptase in a ratchet model of polymerase translocation." Curr Pharm Des **12**(15): 1867-77.

Gottlieb, M. S., H. M. Schanker, P. T. Fan, A. Saxon and J. D. Weisman (1981). "Pneumocystis pneumonia--Los Angeles." Morbidity and Mortality Weekly Report **30**(21): 250-2.

Gottlinger, H. G., J. G. Sodroski and W. A. Haseltine (1989). "Role of capsid precursor processing and myristoylation in morphogenesis and infectivity of human immunodeficiency virus type 1." Proc Natl Acad Sci U S A **86**(15): 5781-5.

Gottlinger, H. G., T. Dorfman, J. G. Sodroski and W. A. Haseltine (1991). "Effect of mutations affecting the p6 gag protein on human immunodeficiency virus particle release." Proc Natl Acad Sci U S A **88**(8): 3195-9.

Graves, M. C., M. C. Meidel, Y. C. Pan, M. Manneberg, H. W. Lahm and F. Gruninger-Leitch (1990). "Identification of a human immunodeficiency virus-1 protease cleavage site within the 66,000 Dalton subunit of reverse transcriptase." Biochem Biophys Res Commun **168**(1): 30-6.

Grinsztejn, B., B. Y. Nguyen, C. Katlama, J. M. Gatell, A. Lazzarin, D. Vittecoq, C. J. Gonzalez, J. Chen, C. M. Harvey and R. D. Isaacs (2007). "Safety and efficacy of the HIV-1 integrase inhibitor raltegravir (MK-0518) in treatment-experienced patients with multidrug-resistant virus: a phase II randomised controlled trial." Lancet **369**(9569): 1261-9.

Grohmann, D., V. Corradi, M. Elbasyouny, A. Baude, F. Horenkamp, S. D. Laufer, F. Manetti, M. Botta and T. Restle (2008). "Small molecule inhibitors targeting HIV-1 reverse transcriptase dimerization." Chembiochem **9**(6): 916-22.

Hahn, B. H., G. M. Shaw, K. M. De Cock and P. M. Sharp (2000). "AIDS as a zoonosis: scientific and public health implications." Science **287**(5453): 607-14.

Halperin, I., H. Wolfson and R. Nussinov (2004). "Protein-protein interactions; coupling of structurally conserved residues and of hot spots across interfaces. Implications for docking." Structure **12**(6): 1027-38.

Halwani, R., A. Khorchid, S. Cen and L. Kleiman (2003). "Rapid localization of Gag/GagPol complexes to detergent-resistant membrane during the assembly of human immunodeficiency virus type 1." J Virol **77**(7): 3973-84.

Hang, J. Q., S. Rajendran, Y. Yang, Y. Li, P. W. In, H. Overton, K. E. Parkes, N. Cammack, J. A. Martin and K. Klumpp (2004). "Activity of the isolated HIV RNase H domain and specific inhibition by N-hydroxyimides." Biochem Biophys Res Commun **317**(2): 321-9.

Hang, J. Q., Y. Li, Y. Yang, N. Cammack, T. Mirzadegan and K. Klumpp (2007). "Substrate-dependent inhibition or stimulation of HIV RNase H activity by non-nucleoside reverse transcriptase inhibitors (NNRTIs)." Biochem Biophys Res Commun **352**(2): 341-50.

Harada, S., Y. Koyanagi and N. Yamamoto (1985). "Infection of HTLV-III/LAV in HTLV-I-carrying cells MT-2 and MT-4 and application in a plaque assay." Science **229**(4713): 563-6.

Harris, D., R. Lee, H. S. Misra, P. K. Pandey and V. N. Pandey (1998). "The p51 subunit of human immunodeficiency virus type 1 reverse transcriptase is essential in loading the p66 subunit on the template primer." Biochemistry **37**(17): 5903-8.

Hawkes, R. (1979). General principles underlying laboratory diagnosis in viral infections. Diagnostic procedures for viral, rickettsial and chlamydial infections. E. H. Lennette and N. J. Schmidt. Washington, D.C., American Public Health Association: 34-5.

Hazuda, D. J., P. Felock, M. Witmer, A. Wolfe, K. Stillmock, J. A. Grobler, A. Espeseth, L. Gabryelski, W. Schleif, C. Blau and M. D. Miller (2000). "Inhibitors of strand transfer that prevent integration and inhibit HIV-1 replication in cells." Science **287**(5453): 646-50.

Hill, M., G. Tachedjian and J. Mak (2005). "The packaging and maturation of the HIV-1 Pol proteins." Curr HIV Res **3**(1): 73-85.

Hill, M. K., M. Shehu-Xhilaga, S. M. Crowe and J. Mak (2002). "Proline residues within spacer peptide p1 are important for human immunodeficiency virus type 1 infectivity, protein processing, and genomic RNA dimer stability." J Virol **76**(22): 11245-53.

Hizi, A., C. McGill and S. H. Hughes (1988). "Expression of soluble, enzymatically active, human immunodeficiency virus reverse transcriptase in Escherichia coli and analysis of mutants." Proc Natl Acad Sci U S A **85**(4): 1218-22.

Hizi, A. and A. Herschhorn (2008). "Retroviral reverse transcriptases (other than those of HIV-1 and murine leukemia virus): a comparison of their molecular and biochemical properties." Virus Res **134**(1-2): 203-20.

Ho, D. D., A. U. Neumann, A. S. Perelson, W. Chen, J. M. Leonard and M. Markowitz (1995). "Rapid turnover of plasma virions and CD4 lymphocytes in HIV-1 infection." Nature **373**(6510): 123-6.

Holm, K., K. Weclewicz, R. Hewson and M. Suomalainen (2003). "Human immunodeficiency virus type 1 assembly and lipid rafts: Pr55(gag) associates with membrane domains that are largely resistant to Brij98 but sensitive to Triton X-100." J Virol **77**(8): 4805-17.

Hopkins, A. L., J. Ren, J. Milton, R. J. Hazen, J. H. Chan, D. I. Stuart and D. K. Stammers (2004). "Design of non-nucleoside inhibitors of HIV-1 reverse transcriptase with improved drug resistance properties. 1." J Med Chem **47**(24): 5912-22.

Hosokawa, M., M. Imai, H. Okada and N. Okada (2004). "Inhibition of HIV-1 infection in cells expressing an artificial complementary peptide." Biochem Biophys Res Commun **324**(1): 236-40.

Hostomska, Z., D. A. Matthews, J. F. Davies, 2nd, B. R. Nodes and Z. Hostomsky (1991). "Proteolytic release and crystallization of the RNase H domain of human immunodeficiency virus type 1 reverse transcriptase." J Biol Chem **266**(22): 14697-702.

Hostomsky, Z., Z. Hostomska, T. B. Fu and J. Taylor (1992). "Reverse transcriptase of human immunodeficiency virus type 1: functionality of subunits of the heterodimer in DNA synthesis." J Virol **66**(5): 3179-82.

Hsiou, Y., J. Ding, K. Das, A. D. Clark, Jr., S. H. Hughes and E. Arnold (1996). "Structure of unliganded HIV-1 reverse transcriptase at 2.7 A resolution: implications of conformational changes for polymerization and inhibition mechanisms." Structure **4**(7): 853-60.

Hu, W. S. and H. M. Temin (1990). "Retroviral recombination and reverse transcription." Science **250**(4985): 1227-33.

Huang, H., R. Chopra, G. L. Verdine and S. C. Harrison (1998). "Structure of a covalently trapped catalytic complex of HIV-1 reverse transcriptase: implications for drug resistance." Science **282**(5394): 1669-75.

Huang, M., J. M. Orenstein, M. A. Martin and E. O. Freed (1995). "p6Gag is required for particle production from full-length human immunodeficiency virus type 1 molecular clones expressing protease." J Virol **69**(11): 6810-8.

Huang, W., A. Gamarnik, K. Limoli, C. J. Petropoulos and J. M. Whitcomb (2003). "Amino acid substitutions at position 190 of human immunodeficiency virus type 1 reverse transcriptase increase susceptibility to delavirdine and impair virus replication." J Virol **77**(2): 1512-23.

Huang, Y., J. Wang, A. Shalom, Z. Li, A. Khorchid, M. A. Wainberg and L. Kleiman (1997). "Primer tRNA3Lys on the viral genome exists in unextended and two-base extended forms within mature human immunodeficiency virus type 1." J Virol **71**(1): 726-8.

Huet, T., R. Cheynier, A. Meyerhans, G. Roelants and S. Wain-Hobson (1990). "Genetic organization of a chimpanzee lentivirus related to HIV-1." Nature **345**(6273): 356-9.

Hungnes, O., E. Tjotta and B. Grinde (1992). "Mutations in the central polypurine tract of HIV-1 result in delayed replication." Virology **190**(1): 440-2.

Hymes, K. B., T. Cheung, J. B. Greene, N. S. Prose, A. Marcus, H. Ballard, D. C. William and L. J. Laubenstein (1981). "Kaposi's sarcoma in homosexual men-a report of eight cases." Lancet **2**(8247): 598-600.

Iordanskiy, S., R. Berro, M. Altieri, F. Kashanchi and M. Bukrinsky (2006). "Intracytoplasmic maturation of the human immunodeficiency virus type 1 reverse transcription complexes determines their capacity to integrate into chromatin." Retrovirology **3**: 4.

Jacks, T. and H. E. Varmus (1985). "Expression of the Rous sarcoma virus pol gene by ribosomal frameshifting." Science **230**(4731): 1237-42.

Jacks, T., K. Townsley, H. E. Varmus and J. Majors (1987). "Two efficient ribosomal frameshifting events are required for synthesis of mouse mammary tumor virus gag-related polyproteins." Proc Natl Acad Sci U S A **84**(12): 4298-302.

Jacks, T., H. D. Madhani, F. R. Masiarz and H. E. Varmus (1988a). "Signals for ribosomal frameshifting in the Rous sarcoma virus gag-pol region." Cell **55**(3): 447-58.

Jacks, T., M. D. Power, F. R. Masiarz, P. A. Luciw, P. J. Barr and H. E. Varmus (1988b). "Characterization of ribosomal frameshifting in HIV-1 gag-pol expression." Nature **331**(6153): 280-3.

Jacobo-Molina, A., J. Ding, R. G. Nanni, A. D. Clark, Jr., X. Lu, C. Tantillo, R. L. Williams, G. Kamer, A. L. Ferris, P. Clark and et al. (1993). "Crystal structure of human immunodeficiency virus type 1 reverse transcriptase complexed with double-stranded DNA at 3.0 A resolution shows bent DNA." Proc Natl Acad Sci U S A **90**(13): 6320-4.

Jacques, P. S., B. M. Wohrl, K. J. Howard and S. F. Le Grice (1994a). "Modulation of HIV-1 reverse transcriptase function in "selectively deleted" p66/p51 heterodimers." J Biol Chem **269**(2): 1388-93.

Jacques, P. S., B. M. Wohrl, M. Ottmann, J. L. Darlix and S. F. Le Grice (1994b). "Mutating the "primer grip" of p66 HIV-1 reverse transcriptase implicates tryptophan-229 in template-primer utilization." J Biol Chem **269**(42): 26472-8.

James, J. S. (1997). "T-20: entirely new antiretroviral." AIDS Treat News(No 279): 5-6.

Janssen, P. A., P. J. Lewi, E. Arnold, F. Daeyaert, M. de Jonge, J. Heeres, L. Koymans, M. Vinkers, J. Guillemont, E. Pasquier, M. Kukla, D. Ludovici, K. Andries, M. P. de Bethune, R. Pauwels, et al. (2005). "In search of a

novel anti-HIV drug: multidisciplinary coordination in the discovery of 4-[[4-[[4-[(1E)-2-cyanoethenyl]-2,6-dimethylphenyl]amino]-2- pyrimidinyl]amino]benzonitrile (R278474, rilpivirine)." Journal of medicinal chemistry **48**(6): 1901-9.

Johnson, M. S., M. A. McClure, D. F. Feng, J. Gray and R. F. Doolittle (1986). "Computer analysis of retroviral pol genes: assignment of enzymatic functions to specific sequences and homologies with nonviral enzymes." Proc Natl Acad Sci U S A **83**(20): 7648-52.

Jonckheere, H., J. M. Taymans, J. Balzarini, S. Velazquez, M. J. Camarasa, J. Desmyter, E. De Clercq and J. Anne (1994). "Resistance of HIV-1 reverse transcriptase against [2',5'-bis-O-(tert-butyldimethylsilyl)-3'-spiro-5"-(4"-amino-1",2"- oxathiole-2",2"-dioxide)] (TSAO) derivatives is determined by the mutation Glu138-->Lys on the p51 subunit." J Biol Chem **269**(41): 25255-8.

Joshi, A. and K. T. Jeang (1993). "Reduction in growth temperature minimizes instability of large plasmids containing HIV-1 proviral genomes." Biotechniques **14**(6): 880, 4-6.

Joshi, A., S. D. Ablan, F. Soheilian, K. Nagashima and E. O. Freed (2009). "Evidence That Productive Human Immunodeficiency Virus Type 1 Assembly Can Occur in an Intracellular Compartment." J Virol.

Jouvenet, N., S. J. Neil, C. Bess, M. C. Johnson, C. A. Virgen, S. M. Simon and P. D. Bieniasz (2006). "Plasma membrane is the site of productive HIV-1 particle assembly." PLoS Biol **4**(12): e435.

Julias, J. G., M. J. McWilliams, S. G. Sarafianos, E. Arnold and S. H. Hughes (2002). "Mutations in the RNase H domain of HIV-1 reverse transcriptase affect the initiation of DNA synthesis and the specificity of RNase H cleavage in vivo." Proc Natl Acad Sci U S A **99**(14): 9515-20.

Jupp, R. A., L. H. Phylip, J. S. Mills, S. F. Le Grice and J. Kay (1991). "Mutating P2 and P1 residues at cleavage junctions in the HIV-1 pol polyprotein. Effects on hydrolysis by HIV-1 proteinase." FEBS Lett **283**(2): 180-4.

Kameoka, M., L. Rong, M. Gotte, C. Liang, R. S. Russell and M. A. Wainberg (2001). "Role for human immunodeficiency virus type 1 Tat protein in suppression of viral reverse transcriptase activity during late stages of viral replication." J Virol **75**(6): 2675-83.

Kaplan, A. H. and R. Swanstrom (1991). "Human immunodeficiency virus type 1 Gag proteins are processed in two cellular compartments." Proc Natl Acad Sci U S A **88**(10): 4528-32.

Kaplan, A. H., M. Manchester and R. Swanstrom (1994). "The activity of the protease of human immunodeficiency virus type 1 is initiated at the membrane of infected cells before the release of viral proteins and is required for release to occur with maximum efficiency." J Virol **68**(10): 6782-6.

Karim, Q. A., S. A. Karim, J. Frolich, A. Grobler, C. Baxter, L. Mansoor, A. Kharsany, S. Sibeko, K. Milsana, Z. Omar, T. Gengiah, S. Maarshalk, N. Arulappan, M. Mlotshwa, L. Morris, et al. (2010). "Effectivemess and safety of tenofovir gel, an antiretroviral microbicide, for the prevention of HIV infection in women." Science **329**(5996): 1168-74.

Kati, W. M., K. A. Johnson, L. F. Jerva and K. S. Anderson (1992). "Mechanism and fidelity of HIV reverse transcriptase." J Biol Chem **267**(36): 25988-97.

Keele, B. F., F. Van Heuverswyn, Y. Li, E. Bailes, J. Takehisa, M. L. Santiago, F. Bibollet-Ruche, Y. Chen, L. V. Wain, F. Liegeois, S. Loul, E. M. Ngole, Y. Bienvenue, E. Delaporte, J. F. Brookfield, et al. (2006). "Chimpanzee reservoirs of pandemic and nonpandemic HIV-1." Science **313**(5786): 523-6.

Keskin, O., B. Ma and R. Nussinov (2005). "Hot regions in protein-protein interactions: the organization and contribution of structurally conserved hot spot residues." J Mol Biol **345**(5): 1281-94.

Kew, Y., L. R. Olsen, A. J. Japour and V. R. Prasad (1998). "Insertions into the beta3-beta4 hairpin loop of HIV-1 reverse transcriptase reveal a role for fingers subdomain in processive polymerization." J Biol Chem **273**(13): 7529-37.

Kiernan, R. E., A. Ono, G. Englund and E. O. Freed (1998). "Role of matrix in an early postentry step in the human immunodeficiency virus type 1 life cycle." J Virol **72**(5): 4116-26.

Kimura, M. (1985). "The role of compensatory neutral mutations in molecular evolution." Journal of Genetics **64**: 7-19.

Kitchen, D. B., H. Decornez, J. R. Furr and J. Bajorath (2004). "Docking and scoring in virtual screening for drug discovery: methods and applications." Nat Rev Drug Discov **3**(11): 935-49.

Klatzmann, D., E. Champagne, S. Chamaret, J. Gruest, D. Guetard, T. Hercend, J. C. Gluckman and L. Montagnier (1984). "T-lymphocyte T4 molecule behaves as the receptor for human retrovirus LAV." Nature **312**(5996): 767-8.

Klein, J. R. and B. D. Jones (2001). "Salmonella pathogenicity island 2-encoded proteins SseC and SseD are essential for virulence and are substrates of the type III secretion system." Infect Immun **69**(2): 737-43.

Klumpp, K., J. Q. Hang, S. Rajendran, Y. Yang, A. Derosier, P. Wong Kai In, H. Overton, K. E. Parkes, N. Cammack and J. A. Martin (2003). "Two-metal ion mechanism of RNA cleavage by HIV RNase H and mechanism-based design of selective HIV RNase H inhibitors." Nucleic Acids Res **31**(23): 6852-9.

Klumpp, K. and T. Mirzadegan (2006). "Recent progress in the design of small molecule inhibitors of HIV RNase H." Curr Pharm Des **12**(15): 1909-22.

Kohl, N. E., E. A. Emini, W. A. Schleif, L. J. Davis, J. C. Heimbach, R. A. Dixon, E. M. Scolnick and I. S. Sigal (1988). "Active human immunodeficiency virus protease is required for viral infectivity." Proc Natl Acad Sci U S A **85**(13): 4686-90.

Kohlstaedt, L. A., J. Wang, J. M. Friedman, P. A. Rice and T. A. Steitz (1992). "Crystal structure at 3.5 A resolution of HIV-1 reverse transcriptase complexed with an inhibitor." Science **256**(5065): 1783-90.

Kollmus, H., A. Honigman, A. Panet and H. Hauser (1994). "The sequences of and distance between two cis-acting signals determine the efficiency of ribosomal frameshifting in human immunodeficiency virus type 1 and human T-cell leukemia virus type II in vivo." J Virol **68**(9): 6087-91.

Krausslich, H. G., R. H. Ingraham, M. T. Skoog, E. Wimmer, P. V. Pallai and C. A. Carter (1989). "Activity of purified biosynthetic proteinase of human immunodeficiency virus on natural substrates and synthetic peptides." Proc Natl Acad Sci U S A **86**(3): 807-11.

Krausslich, H. G. (1991). "Human immunodeficiency virus proteinase dimer as component of the viral polyprotein prevents particle assembly and viral infectivity." Proc Natl Acad Sci U S A **88**(8): 3213-7.

Krieger, E., G. Koraimann and G. Vriend (2002). "Increasing the precision of comparative models with YASARA NOVA--a self-parameterizing force field." Proteins **47**(3): 393-402.

Larder, B. A., D. J. Purifoy, K. L. Powell and G. Darby (1987). "Site-specific mutagenesis of AIDS virus reverse transcriptase." Nature **327**(6124): 716-7.

Larder, B. A., G. Darby and D. D. Richman (1989). "HIV with reduced sensitivity to zidovudine (AZT) isolated during prolonged therapy." Science **243**(4899): 1731-4.

Le Grice, S. F., T. Naas, B. Wohlgensinger and O. Schatz (1991). "Subunit-selective mutagenesis indicates minimal polymerase activity in heterodimer-associated p51 HIV-1 reverse transcriptase." Embo J **10**(12): 3905-11.

Lebowitz, J., S. Kar, E. Braswell, S. McPherson and D. L. Richard (1994). "Human immunodeficiency virus-1 reverse transcriptase heterodimer stability." Protein Sci **3**(9): 1374-82.

Lee, T. H., F. J. Sunzeri, L. H. Tobler, B. G. Williams and M. P. Busch (1991). "Quantitative assessment of HIV-1 DNA load by coamplification of HIV-1 gag and HLA-DQ-alpha genes." Aids **5**(6): 683-91.

Lemay, J., P. Maidou-Peindara, T. Bader, E. Ennifar, J. C. Rain, R. Benarous and L. X. Liu (2008a). "HuR interacts with human immunodeficiency virus type 1 reverse transcriptase, and modulates reverse transcription in infected cells." Retrovirology **5**: 47.

Lemay, J., P. Maidou-Peindara, R. Cancio, E. Ennifar, G. Coadou, G. Maga, J. C. Rain, R. Benarous and L. X. Liu (2008b). "AKAP149 binds to HIV-1 reverse transcriptase and is involved in the reverse transcription." J Mol Biol **383**(4): 783-96.

Lener, D., V. Tanchou, B. P. Roques, S. F. Le Grice and J. L. Darlix (1998). "Involvement of HIV-I nucleocapsid protein in the recruitment of reverse transcriptase into nucleoprotein complexes formed in vitro." J Biol Chem **273**(50): 33781-6.

Leszczynski, J. F. and G. D. Rose (1986). "Loops in globular proteins: a novel category of secondary structure." Science **234**(4778): 849-55.

Letvin, N. L., M. D. Daniel, P. K. Sehgal, R. C. Desrosiers, R. D. Hunt, L. M. Waldron, J. J. MacKey, D. K. Schmidt, L. V. Chalifoux and N. W. King (1985). "Induction of AIDS-like disease in macaque monkeys with T-cell tropic retrovirus STLV-III." Science **230**(4721): 71-3.

Levy, J. A., A. D. Hoffman, S. M. Kramer, J. A. Landis, J. M. Shimabukuro and L. S. Oshiro (1984). "Isolation of lymphocytopathic retroviruses from San Francisco patients with AIDS." Science **225**(4664): 840-2.

Liao, W. H. and C. T. Wang (2004). "Characterization of human immunodeficiency virus type 1 Pr160 gag-pol mutants with truncations downstream of the protease domain." Virology **329**(1): 180-8.

Liao, W. H., K. J. Huang, Y. F. Chang, S. M. Wang, Y. T. Tseng, C. C. Chiang, J. J. Wang and C. T. Wang (2007). "Incorporation of human immunodeficiency virus type 1 reverse transcriptase into virus-like particles." J Virol **81**(10): 5155-65.

Lightfoote, M. M., J. E. Coligan, T. M. Folks, A. S. Fauci, M. A. Martin and S. Venkatesan (1986). "Structural characterization of reverse transcriptase and endonuclease polypeptides of the acquired immunodeficiency syndrome retrovirus." J Virol **60**(2): 771-5.

Lindhofer, H., K. von der Helm and H. Nitschko (1995). "In vivo processing of Pr160gag-pol from human immunodeficiency virus type 1 (HIV) in acutely infected, cultured human T-lymphocytes." Virology **214**(2): 624-7.

Lindwasser, O. W. and M. D. Resh (2001). "Multimerization of human immunodeficiency virus type 1 Gag promotes its localization to barges, raft-like membrane microdomains." J Virol **75**(17): 7913-24.

Liu, R., W. A. Paxton, S. Choe, D. Ceradini, S. R. Martin, R. Horuk, M. E. MacDonald, H. Stuhlmann, R. A. Koup and N. R. Landau (1996). "Homozygous defect in HIV-1 coreceptor accounts for resistance of some multiply-exposed individuals to HIV-1 infection." Cell **86**(3): 367-77.

Lochelt, M. and R. M. Flugel (1996). "The human foamy virus pol gene is expressed as a Pro-Pol polyprotein and not as a Gag-Pol fusion protein." J Virol **70**(2): 1033-40.

Loregian, A., H. S. Marsden and G. Palu (2002). "Protein-protein interactions as targets for antiviral chemotherapy." Rev Med Virol **12**(4): 239-62.

Lori, F., F. di Marzo Veronese, A. L. de Vico, P. Lusso, M. S. Reitz, Jr. and R. C. Gallo (1992). "Viral DNA carried by human immunodeficiency virus type 1 virions." J Virol **66**(8): 5067-74.

Los Alamos National Laboratory. (2008a, Tue Apr 22 12:37 2008). "HIV and SIV Nomenclature." Retrieved 30-11-2008, 2008, from http://www.hiv.lanl.gov/content/sequence/HelpDocs/subtypes-more.htm.

Los Alamos National Laboratory. (2008b, Wed Nov 26 14:00 2008). "The Circulating Recombinant Forms (CRFs)." from http://www.hiv.lanl.gov/content/sequence/HIV/CRFs/CRFs.html.

Los Alamos National Laboratory. (2008c, Thu Jun 18 14:21 2009). "HIV Sequence Database." Retrieved 30/06/08, 2008, from http://www.hiv.lanl.gov.

Louis, J. M., R. A. McDonald, N. T. Nashed, E. M. Wondrak, D. M. Jerina, S. Oroszlan and P. T. Mora (1991a). "Autoprocessing of the HIV-1 protease using purified wild-type and mutated fusion proteins expressed at high levels in Escherichia coli." Eur J Biochem **199**(2): 361-9.

Louis, J. M., S. Oroszlan and P. T. Mora (1991b). "Studies of the autoprocessing of the HIV-1 protease using cleavage site mutants." Adv Exp Med Biol **306**: 499-502.

Louis, J. M., N. T. Nashed, K. D. Parris, A. R. Kimmel and D. M. Jerina (1994). "Kinetics and mechanism of autoprocessing of human immunodeficiency virus type 1 protease from an analog of the Gag-Pol polyprotein." Proc Natl Acad Sci U S A **91**(17): 7970-4.

Louis, J. M., F. Dyda, N. T. Nashed, A. R. Kimmel and D. R. Davies (1998). "Hydrophilic peptides derived from the transframe region of Gag-Pol inhibit the HIV-1 protease." Biochemistry **37**(8): 2105-10.

Louis, J. M., G. M. Clore and A. M. Gronenborn (1999a). "Autoprocessing of HIV-1 protease is tightly coupled to protein folding." Nat Struct Biol **6**(9): 868-75.

Louis, J. M., E. M. Wondrak, A. R. Kimmel, P. T. Wingfield and N. T. Nashed (1999b). "Proteolytic processing of HIV-1 protease precursor, kinetics and mechanism." J Biol Chem **274**(33): 23437-42.

Lowe, D. M., A. Aitken, C. Bradley, G. K. Darby, B. A. Larder, K. L. Powell, D. J. Purifoy, M. Tisdale and D. K. Stammers (1988). "HIV-1 reverse transcriptase: crystallization and analysis of domain structure by limited proteolysis." Biochemistry **27**(25): 8884-9.

Ludwig, C., A. Leiherer and R. Wagner (2008). "Importance of protease cleavage sites within and flanking human immunodeficiency virus type 1 transframe protein p6* for spatiotemporal regulation of protease activation." J Virol **82**(9): 4573-84.

Ma, B. and R. Nussinov (2007). "Trp/Met/Phe hot spots in protein-protein interactions: potential targets in drug design." Curr Top Med Chem **7**(10): 999-1005.

Maddon, P. J., A. G. Dalgleish, J. S. McDougal, P. R. Clapham, R. A. Weiss and R. Axel (1986). "The T4 gene encodes the AIDS virus receptor and is expressed in the immune system and the brain." Cell **47**(3): 333-48.

Mak, J., M. Jiang, M. A. Wainberg, M. L. Hammarskjold, D. Rekosh and L. Kleiman (1994). "Role of Pr160gag-pol in mediating the selective incorporation of tRNA(Lys) into human immunodeficiency virus type 1 particles." J Virol **68**(4): 2065-72.

Mak, J., A. Khorchid, Q. Cao, Y. Huang, I. Lowy, M. A. Parniak, V. R. Prasad, M. A. Wainberg and L. Kleiman (1997). "Effects of mutations in Pr160gag-pol upon tRNA(Lys3) and Pr160gag-plo incorporation into HIV-1." J Mol Biol **265**(4): 419-31.

Markowitz, M., J. O. Morales-Ramirez, B. Y. Nguyen, C. M. Kovacs, R. T. Steigbigel, D. A. Cooper, R. Liporace, R. Schwartz, R. Isaacs, L. R. Gilde, L. Wenning, J. Zhao and H. Teppler (2006). "Antiretroviral activity, pharmacokinetics, and tolerability of MK-0518, a novel inhibitor of HIV-1 integrase, dosed as monotherapy for 10 days in treatment-naive HIV-1-infected individuals." Journal of acquired immune deficiency syndromes **43**(5): 509-15.

Marsden, M. D. and J. A. Zack (2007). "Human immunodeficiency virus bearing a disrupted central DNA flap is pathogenic in vivo." J Virol **81**(11): 6146-50.

Marsh, M., K. Theusner and A. Pelchen-Matthews (2009). "HIV assembly and budding in macrophages." Biochem Soc Trans **37**(Pt 1): 185-9.

Martin-Serrano, J., T. Zang and P. D. Bieniasz (2001). "HIV-1 and Ebola virus encode small peptide motifs that recruit Tsg101 to sites of particle assembly to facilitate egress." Nat Med **7**(12): 1313-9.

McDonald, D., M. A. Vodicka, G. Lucero, T. M. Svitkina, G. G. Borisy, M. Emerman and T. J. Hope (2002). "Visualization of the intracellular behavior of HIV in living cells." J Cell Biol **159**(3): 441-52.

McWilliams, M. J., J. G. Julias, S. G. Sarafianos, W. G. Alvord, E. Arnold and S. H. Hughes (2006). "Combining mutations in HIV-1 reverse transcriptase with mutations in the HIV-1 polypurine tract affects RNase H cleavages involved in PPT utilization." Virology **348**(2): 378-88.

Melikyan, G. B., R. M. Markosyan, H. Hemmati, M. K. Delmedico, D. M. Lambert and F. S. Cohen (2000). "Evidence that the transition of HIV-1 gp41 into a six-helix bundle, not the bundle configuration, induces membrane fusion." J Cell Biol **151**(2): 413-23.

Menendez-Arias, L., A. Abraha, M. E. Quinones-Mateu, A. Mas, M. J. Camarasa and E. J. Arts (2001). "Functional characterization of chimeric reverse transcriptases with polypeptide subunits of highly divergent HIV-1 group M and O strains." J Biol Chem **276**(29): 27470-9.

Mitsuya, H., K. J. Weinhold, P. A. Furman, M. H. St Clair, S. N. Lehrman, R. C. Gallo, D. Bolognesi, D. W. Barry and S. Broder (1985). "3'-Azido-3'-deoxythymidine (BW A509U): an antiviral agent that inhibits the infectivity and cytopathic effect of human T-lymphotropic virus type III/lymphadenopathy-associated virus in vitro." Proc Natl Acad Sci U S A **82**(20): 7096-100.

Mizrahi, V., G. M. Lazarus, L. M. Miles, C. A. Meyers and C. Debouck (1989). "Recombinant HIV-1 reverse transcriptase: purification, primary structure, and polymerase/ribonuclease H activities." Arch Biochem Biophys **273**(2): 347-58.

Mizrahi, V., R. L. Brooksbank and N. C. Nkabinde (1994). "Mutagenesis of the conserved aspartic acid 443, glutamic acid 478, asparagine 494, and aspartic acid 498 residues in the ribonuclease H domain of p66/p51 human immunodeficiency virus type I reverse transcriptase. Expression and biochemical analysis." J Biol Chem **269**(30): 19245-9.

Moore, J. P. and D. R. Kuritzkes (2009). "A piece de resistance: how HIV-1 escapes small molecule CCR5 inhibitors." Curr Opin HIV AIDS **4**(2): 118-24.
Moreira, I. S., P. A. Fernandes and M. J. Ramos (2007a). "Hot spots--a review of the protein-protein interface determinant amino-acid residues." Proteins **68**(4): 803-12.
Moreira, I. S., P. A. Fernandes and M. J. Ramos (2007b). "Hot spot occlusion from bulk water: a comprehensive study of the complex between the lysozyme HEL and the antibody FVD1.3." J Phys Chem B **111**(10): 2697-706.
Morikawa, Y., S. Hinata, H. Tomoda, T. Goto, M. Nakai, C. Aizawa, H. Tanaka and S. Omura (1996). "Complete inhibition of human immunodeficiency virus Gag myristoylation is necessary for inhibition of particle budding." J Biol Chem **271**(5): 2868-73.
Morris, M. C., C. Berducou, J. Mery, F. Heitz and G. Divita (1999a). "The thumb domain of the P51-subunit is essential for activation of HIV reverse transcriptase." Biochemistry **38**(46): 15097-103.
Morris, M. C., V. Robert-Hebmann, L. Chaloin, J. Mery, F. Heitz, C. Devaux, R. S. Goody and G. Divita (1999b). "A new potent HIV-1 reverse transcriptase inhibitor. A synthetic peptide derived from the interface subunit domains." J Biol Chem **274**(35): 24941-6.
Mulky, A., S. G. Sarafianos, E. Arnold, X. Wu and J. C. Kappes (2004). "Subunit-specific analysis of the human immunodeficiency virus type 1 reverse transcriptase in vivo." J Virol **78**(13): 7089-96.
Mulky, A. and J. C. Kappes (2005a). "Analysis of human immunodeficiency virus type 1 reverse transcriptase subunit structure/function in the context of infectious virions and human target cells." Antimicrob Agents Chemother **49**(9): 3762-9.
Mulky, A., S. G. Sarafianos, Y. Jia, E. Arnold and J. C. Kappes (2005b). "Identification of amino acid residues in the human immunodeficiency virus type-1 reverse transcriptase tryptophan-repeat motif that are required for subunit interaction using infectious virions." J Mol Biol **349**(4): 673-84.
Mulky, A., B. C. Vu, J. A. Conway, S. H. Hughes and J. C. Kappes (2007). "Analysis of amino acids in the beta7-beta8 loop of human immunodeficiency virus type 1 reverse transcriptase for their role in virus replication." J Mol Biol **365**(5): 1368-78.
Muller, B., T. Restle, S. Weiss, M. Gautel, G. Sczakiel and R. S. Goody (1989). "Co-expression of the subunits of the heterodimer of HIV-1 reverse transcriptase in Escherichia coli." J Biol Chem **264**(24): 13975-8.
Navia, M. A. and B. M. McKeever (1990). "A role for the aspartyl protease from the human immunodeficiency virus type 1 (HIV-1) in the orchestration of virus assembly." Ann N Y Acad Sci **616**: 73-85.
Nilsen, B. M., I. R. Haugan, K. Berg, L. Olsen, P. O. Brown and D. E. Helland (1996). "Monoclonal antibodies against human immunodeficiency virus type 1 integrase: epitope mapping and differential effects on integrase activities in vitro." J Virol **70**(3): 1580-7.
Ofran, Y. and B. Rost (2007). "Protein–Protein Interaction Hotspots Carved into Sequences." PLoS Computational Biology **3**(7): e119.
Olivares, I., M. Gutierrez-Rivas, C. Lopez-Galindez and L. Menendez-Arias (2004). "Tryptophan scanning mutagenesis of aromatic residues within the polymerase domain of HIV-1 reverse transcriptase: critical role of Phe-130 for p51 function and second-site revertant restoring viral replication capacity." Virology **324**(2): 400-11.
Olivares, I., A. Mulky, P. I. Boross, J. Tozser, J. C. Kappes, C. Lopez-Galindez and L. Menendez-Arias (2007). "HIV-1 protease dimer interface mutations that compensate for viral reverse transcriptase instability in infectious virions." J Mol Biol **372**(2): 369-81.
Ollis, D. L., P. Brick, R. Hamlin, N. G. Xuong and T. A. Steitz (1985). "Structure of large fragment of Escherichia coli DNA polymerase I complexed with dTMP." Nature **313**(6005): 762-6.
Ono, A. and E. O. Freed (1999). "Binding of human immunodeficiency virus type 1 Gag to membrane: role of the matrix amino terminus." J Virol **73**(5): 4136-44.
Ono, A., J. M. Orenstein and E. O. Freed (2000). "Role of the Gag matrix domain in targeting human immunodeficiency virus type 1 assembly." J Virol **74**(6): 2855-66.
Oude Essink, B. B., A. T. Das and B. Berkhout (1996). "HIV-1 reverse transcriptase discriminates against non-self tRNA primers." J Mol Biol **264**(2): 243-54.
Pal, R., M. S. Reitz, Jr., E. Tschachler, R. C. Gallo, M. G. Sarngadharan and F. D. Veronese (1990). "Myristoylation of gag proteins of HIV-1 plays an important role in virus assembly." AIDS Res Hum Retroviruses **6**(6): 721-30.
Palaniappan, C., M. Wisniewski, P. S. Jacques, S. F. Le Grice, P. J. Fay and R. A. Bambara (1997). "Mutations within the primer grip region of HIV-1 reverse transcriptase result in loss of RNase H function." J Biol Chem **272**(17): 11157-64.
Pandey, P. K., N. Kaushik, T. T. Talele, P. N. Yadav and V. N. Pandey (2001). "The beta7-beta8 loop of the p51 subunit in the heterodimeric (p66/p51) human immunodeficiency virus type 1 reverse transcriptase is essential for the catalytic function of the p66 subunit." Biochemistry **40**(32): 9505-12.
Pandey, P. K., N. Kaushik, K. Singh, B. Sharma, A. K. Upadhyay, S. Kumar, D. Harris and V. N. Pandey (2002). "Insertion of a small peptide of six amino acids into the beta7-beta8 loop of the p51 subunit of HIV-1 reverse transcriptase perturbs the heterodimer and affects its activities." BMC Biochem **3**: 18.
Park, J. and C. D. Morrow (1991). "Overexpression of the gag-pol precursor from human immunodeficiency virus type 1 proviral genomes results in efficient proteolytic processing in the absence of virion production." J Virol **65**(9): 5111-7.
Park, J. and C. D. Morrow (1992). "The nonmyristylated Pr160gag-pol polyprotein of human immunodeficiency virus type 1 interacts with Pr55gag and is incorporated into viruslike particles." J Virol **66**(11): 6304-13.

Partin, K., H. G. Krausslich, L. Ehrlich, E. Wimmer and C. Carter (1990). "Mutational analysis of a native substrate of the human immunodeficiency virus type 1 proteinase." J Virol **64**(8): 3938-47.

Partin, K., G. Zybarth, L. Ehrlich, M. DeCrombrugghe, E. Wimmer and C. Carter (1991). "Deletion of sequences upstream of the proteinase improves the proteolytic processing of human immunodeficiency virus type 1." Proc Natl Acad Sci U S A **88**(11): 4776-80.

Paulus, C., S. Hellebrand, U. Tessmer, H. Wolf, H. G. Krausslich and R. Wagner (1999). "Competitive inhibition of human immunodeficiency virus type-1 protease by the Gag-Pol transframe protein." J Biol Chem **274**(31): 21539-43.

Pear, W. S., G. P. Nolan, M. L. Scott and D. Baltimore (1993). "Production of high-titer helper-free retroviruses by transient transfection." Proc Natl Acad Sci U S A **90**(18): 8392-6.

Pearl, L. H. and W. R. Taylor (1987). "Sequence specificity of retroviral proteases." Nature **328**(6130): 482.

Peeters, M., C. Honore, T. Huet, L. Bedjabaga, S. Ossari, P. Bussi, R. W. Cooper and E. Delaporte (1989). "Isolation and partial characterization of an HIV-related virus occurring naturally in chimpanzees in Gabon." Aids **3**(10): 625-30.

Pelchen-Matthews, A., B. Kramer and M. Marsh (2003). "Infectious HIV-1 assembles in late endosomes in primary macrophages." J Cell Biol **162**(3): 443-55.

Peliska, J. A. and S. J. Benkovic (1992). "Mechanism of DNA strand transfer reactions catalyzed by HIV-1 reverse transcriptase." Science **258**(5085): 1112-8.

Penny, R., R. Marks, J. Berger, D. Marriott and D. Bryant (1983). "Acquired immune deficiency syndrome." Med J Aust **1**(12): 554-7.

Perelson, A. S., A. U. Neumann, M. Markowitz, J. M. Leonard and D. D. Ho (1996). "HIV-1 dynamics in vivo: virion clearance rate, infected cell life-span, and viral generation time." Science **271**(5255): 1582-6.

Pettit, S. C., J. Simsic, D. D. Loeb, L. Everitt, C. A. Hutchison, 3rd and R. Swanstrom (1991). "Analysis of retroviral protease cleavage sites reveals two types of cleavage sites and the structural requirements of the P1 amino acid." J Biol Chem **266**(22): 14539-47.

Pettit, S. C., M. D. Moody, R. S. Wehbie, A. H. Kaplan, P. V. Nantermet, C. A. Klein and R. Swanstrom (1994). "The p2 domain of human immunodeficiency virus type 1 Gag regulates sequential proteolytic processing and is required to produce fully infectious virions." J Virol **68**(12): 8017-27.

Pettit, S. C., N. Sheng, R. Tritch, S. Erickson-Viitanen and R. Swanstrom (1998). "The regulation of sequential processing of HIV-1 Gag by the viral protease." Adv Exp Med Biol **436**: 15-25.

Pettit, S. C., G. J. Henderson, C. A. Schiffer and R. Swanstrom (2002). "Replacement of the P1 amino acid of human immunodeficiency virus type 1 Gag processing sites can inhibit or enhance the rate of cleavage by the viral protease." J Virol **76**(20): 10226-33.

Pettit, S. C., S. Gulnik, L. Everitt and A. H. Kaplan (2003). "The dimer interfaces of protease and extra-protease domains influence the activation of protease and the specificity of GagPol cleavage." J Virol **77**(1): 366-74.

Pettit, S. C., L. E. Everitt, S. Choudhury, B. M. Dunn and A. H. Kaplan (2004). "Initial cleavage of the human immunodeficiency virus type 1 GagPol precursor by its activated protease occurs by an intramolecular mechanism." J Virol **78**(16): 8477-85.

Pettit, S. C., J. C. Clemente, J. A. Jeung, B. M. Dunn and A. H. Kaplan (2005a). "Ordered processing of the human immunodeficiency virus type 1 GagPol precursor is influenced by the context of the embedded viral protease." J Virol **79**(16): 10601-7.

Pettit, S. C., J. N. Lindquist, A. H. Kaplan and R. Swanstrom (2005b). "Processing sites in the human immunodeficiency virus type 1 (HIV-1) Gag-Pro-Pol precursor are cleaved by the viral protease at different rates." Retrovirology **2**: 66.

Piot, P., T. C. Quinn, H. Taelman, F. M. Feinsod, K. B. Minlangu, O. Wobin, N. Mbendi, P. Mazebo, K. Ndangi, W. Stevens and et al. (1984). "Acquired immunodeficiency syndrome in a heterosexual population in Zaire." Lancet **2**(8394): 65-9.

Pitt, V. M., P. Chapman and ABC-TV (Australia) (2007). Rampant how a city stopped a plague. Hindmarsh, S. Aust., Tape Services,.

Platt, E. J., K. Wehrly, S. E. Kuhmann, B. Chesebro and D. Kabat (1998). "Effects of CCR5 and CD4 cell surface concentrations on infections by macrophagetropic isolates of human immunodeficiency virus type 1." J Virol **72**(4): 2855-64.

Popov, S., B. Strack, V. Sanchez-Merino, E. Popova, H. Rosin and H. G. Gottlinger (2011). "Human immunodeficiency virus type 1 and related primate lentiviruses engage clathrin through Gag-Pol or Gag." Journal of Virology **85**(8): 3792-801.

Popper, S. J., A. D. Sarr, K. U. Travers, A. Gueye-Ndiaye, S. Mboup, M. E. Essex and P. J. Kanki (1999). "Lower human immunodeficiency virus (HIV) type 2 viral load reflects the difference in pathogenicity of HIV-1 and HIV-2." J Infect Dis **180**(4): 1116-21.

Powell, M. D., M. Ghosh, P. S. Jacques, K. J. Howard, S. F. Le Grice and J. G. Levin (1997). "Alanine-scanning mutations in the "primer grip" of p66 HIV-1 reverse transcriptase result in selective loss of RNA priming activity." J Biol Chem **272**(20): 13262-9.

Prabu-Jeyabalan, M., E. Nalivaika and C. A. Schiffer (2002). "Substrate shape determines specificity of recognition for HIV-1 protease: analysis of crystal structures of six substrate complexes." Structure **10**(3): 369-81.

Purcell, D. F. and M. A. Martin (1993). "Alternative splicing of human immunodeficiency virus type 1 mRNA modulates viral protein expression, replication, and infectivity." J Virol **67**(11): 6365-78.

Quillent, C., A. M. Borman, S. Paulous, C. Dauguet and F. Clavel (1996). "Extensive regions of pol are required for efficient human immunodeficiency virus polyprotein processing and particle maturation." Virology **219**(1): 29-36.

Ratner, L., R. C. Gallo and F. Wong-Staal (1985). "HTLV-III, LAV, ARV are variants of same AIDS virus." Nature **313**(6004): 636-7.

Ratner, L., A. Fisher, L. L. Jagodzinski, H. Mitsuya, R. S. Liou, R. C. Gallo and F. Wong-Staal (1987). "Complete nucleotide sequences of functional clones of the AIDS virus." AIDS Res Hum Retroviruses **3**(1): 57-69.

Rausch, J. W., D. Lener, J. T. Miller, J. G. Julias, S. H. Hughes and S. F. Le Grice (2002). "Altering the RNase H primer grip of human immunodeficiency virus reverse transcriptase modifies cleavage specificity." Biochemistry **41**(15): 4856-65.

Ren, J., R. Esnouf, E. Garman, D. Somers, C. Ross, I. Kirby, J. Keeling, G. Darby, Y. Jones, D. Stuart and et al. (1995). "High resolution structures of HIV-1 RT from four RT-inhibitor complexes." Nat Struct Biol **2**(4): 293-302.

Ren, J., C. Nichols, L. Bird, P. Chamberlain, K. Weaver, S. Short, D. I. Stuart and D. K. Stammers (2001). "Structural mechanisms of drug resistance for mutations at codons 181 and 188 in HIV-1 reverse transcriptase and the improved resilience of second generation non-nucleoside inhibitors." J Mol Biol **312**(4): 795-805.

Resnik, S. (1999). Blood saga : hemophilia, AIDS, and the survival of a community. Berkeley, Calif. ; London, University of California Press.

Restle, T., B. Muller and R. S. Goody (1990). "Dimerization of human immunodeficiency virus type 1 reverse transcriptase. A target for chemotherapeutic intervention." J Biol Chem **265**(16): 8986-8.

Restle, T., B. Muller and R. S. Goody (1992a). "RNase H activity of HIV reverse transcriptases is confined exclusively to the dimeric forms." FEBS Lett **300**(1): 97-100.

Restle, T., M. Pawlita, G. Sczakiel, B. Muller and R. S. Goody (1992b). "Structure-function relationships of HIV-1 reverse transcriptase determined using monoclonal antibodies." J Biol Chem **267**(21): 14654-61.

Richman, D. D., D. Havlir, J. Corbeil, D. Looney, C. Ignacio, S. A. Spector, J. Sullivan, S. Cheeseman, K. Barringer, D. Pauletti and et al. (1994). "Nevirapine resistance mutations of human immunodeficiency virus type 1 selected during therapy." J Virol **68**(3): 1660-6.

Rodgers, D. W., S. J. Gamblin, B. A. Harris, S. Ray, J. S. Culp, B. Hellmig, D. J. Woolf, C. Debouck and S. C. Harrison (1995). "The structure of unliganded reverse transcriptase from the human immunodeficiency virus type 1." Proc Natl Acad Sci U S A **92**(4): 1222-6.

Rodriguez-Barrios, F., C. Perez, E. Lobaton, S. Velazquez, C. Chamorro, A. San-Felix, M. J. Perez-Perez, M. J. Camarasa, H. Pelemans, J. Balzarini and F. Gago (2001). "Identification of a putative binding site for [2',5'-bis-O-(tert-butyldimethylsilyl)-beta-D-ribofuranosyl]-3'-spiro-5"- (4"-amino-1",2"-oxathiole-2",2"-dioxide)thymine (TSAO) derivatives at the p51-p66 interface of HIV-1 reverse transcriptase." J Med Chem **44**(12): 1853-65.

Roth, M. J., N. Tanese and S. P. Goff (1985). "Purification and characterization of murine retroviral reverse transcriptase expressed in Escherichia coli." J Biol Chem **260**(16): 9326-35.

Rumbaugh, J. A., G. M. Fuentes and R. A. Bambara (1998). "Processing of an HIV replication intermediate by the human DNA replication enzyme FEN1." J Biol Chem **273**(44): 28740-5.

Saag, M. S., E. A. Emini, O. L. Laskin, J. Douglas, W. I. Lapidus, W. A. Schleif, R. J. Whitley, C. Hildebrand, V. W. Byrnes, J. C. Kappes and et al. (1993). "A short-term clinical evaluation of L-697,661, a non-nucleoside inhibitor of HIV-1 reverse transcriptase. L-697,661 Working Group." N Engl J Med **329**(15): 1065-72.

Sambrook, J., Fritsch, E.F. & Maniatis, T. (1989). Molecular Cloning: a laboratory manual. New York, Cold Spring Harbor Laboratory Press.

Samson, M., F. Libert, B. J. Doranz, J. Rucker, C. Liesnard, C. M. Farber, S. Saragosti, C. Lapoumeroulie, J. Cognaux, C. Forceille, G. Muyldermans, C. Verhofstede, G. Burtonboy, M. Georges, T. Imai, et al. (1996). "Resistance to HIV-1 infection in caucasian individuals bearing mutant alleles of the CCR-5 chemokine receptor gene." Nature **382**(6593): 722-5.

Sarafianos, S. G., K. Das, C. Tantillo, A. D. Clark, Jr., J. Ding, J. M. Whitcomb, P. L. Boyer, S. H. Hughes and E. Arnold (2001). "Crystal structure of HIV-1 reverse transcriptase in complex with a polypurine tract RNA:DNA." Embo J **20**(6): 1449-61.

Sarafianos, S. G., A. D. Clark, Jr., K. Das, S. Tuske, J. J. Birktoft, P. Ilankumaran, A. R. Ramesha, J. M. Sayer, D. M. Jerina, P. L. Boyer, S. H. Hughes and E. Arnold (2002). "Structures of HIV-1 reverse transcriptase with pre- and post-translocation AZTMP-terminated DNA." Embo J **21**(23): 6614-24.

Sarafianos, S. G., B. Marchand, K. Das, D. M. Himmel, M. A. Parniak, S. H. Hughes and E. Arnold (2009). "Structure and function of HIV-1 reverse transcriptase: molecular mechanisms of polymerization and inhibition." J Mol Biol **385**(3): 693-713.

Schatz, O., J. Mous and S. F. Le Grice (1990). "HIV-1 RT-associated ribonuclease H displays both endonuclease and 3'----5' exonuclease activity." Embo J **9**(4): 1171-6.

Schroder, A. R., P. Shinn, H. Chen, C. Berry, J. R. Ecker and F. Bushman (2002). "HIV-1 integration in the human genome favors active genes and local hotspots." Cell **110**(4): 521-9.

Schultz, S. J. and J. J. Champoux (2008). "RNase H activity: structure, specificity, and function in reverse transcription." Virus Res **134**(1-2): 86-103.

Schwartz, O., V. Marechal, O. Danos and J. M. Heard (1995). "Human immunodeficiency virus type 1 Nef increases the efficiency of reverse transcription in the infected cell." J Virol **69**(7): 4053-9.
Sendziuk, P. (2003). Learning to trust : Australian responses to AIDS. Sydney, UNSW Press.
Serwadda, D., R. D. Mugerwa, N. K. Sewankambo, A. Lwegaba, J. W. Carswell, G. B. Kirya, A. C. Bayley, R. G. Downing, R. S. Tedder, S. A. Clayden and et al. (1985). "Slim disease: a new disease in Uganda and its association with HTLV-III infection." Lancet **2**(8460): 849-52.
Shafer, R. W. and J. M. Schapiro (2008). "HIV-1 Drug Resistance Mutations: an Updated Framework for the Second Decade of HAART." AIDS Reviews **10**: 67-84.
Sharp, P. M. and B. H. Hahn (2011). "Origins of HIV and the AIDS Pandemic." Cold Spring Harb Perspect Med **1**(1): a006841.
Shehu-Xhilaga, M., S. M. Crowe and J. Mak (2001). "Maintenance of the Gag/Gag-Pol ratio is important for human immunodeficiency virus type 1 RNA dimerization and viral infectivity." J Virol **75**(4): 1834-41.
Shehu-Xhilaga, M., S. D. Ablan, D. G. Demirov, C. Chen, R. C. Montelaro and E. O Freed (2004). "Late domain-dependent inhibition of equine infectious anemia virus budding." J Virol **78**: 724-32.
Sluis-Cremer, N., G. I. Dmitrienko, J. Balzarini, M. J. Camarasa and M. A. Parniak (2000). "Human immunodeficiency virus type 1 reverse transcriptase dimer destabilization by 1-[Spiro[4"-amino-2",2" -dioxo-1",2" -oxathiole-5",3'-[2', 5'-bis-O-(tert-butyldimethylsilyl)-beta-D-ribofuranosyl]]]-3-ethylthy mine." Biochemistry **39**(6): 1427-33.
Sluis-Cremer, N., D. Arion and M. A. Parniak (2002). "Destabilization of the HIV-1 reverse transcriptase dimer upon interaction with N-acyl hydrazone inhibitors." Mol Pharmacol **62**(2): 398-405.
Sluis-Cremer, N., D. Arion, M. E. Abram and M. A. Parniak (2004a). "Proteolytic processing of an HIV-1 pol polyprotein precursor: insights into the mechanism of reverse transcriptase p66/p51 heterodimer formation." Int J Biochem Cell Biol **36**(9): 1836-47.
Sluis-Cremer, N., N. A. Temiz and I. Bahar (2004b). "Conformational changes in HIV-1 reverse transcriptase induced by nonnucleoside reverse transcriptase inhibitor binding." Curr HIV Res **2**(4): 323-32.
Sluis-Cremer, N. and G. Tachedjian (2008). "Mechanisms of inhibition of HIV replication by non-nucleoside reverse transcriptase inhibitors." Virus Res **134**(1-2): 147-56.
Smerdon, S. J., J. Jager, J. Wang, L. A. Kohlstaedt, A. J. Chirino, J. M. Friedman, P. A. Rice and T. A. Steitz (1994). "Structure of the binding site for nonnucleoside inhibitors of the reverse transcriptase of human immunodeficiency virus type 1." Proc Natl Acad Sci U S A **91**(9): 3911-5.
Smith, J. S. and M. J. Roth (1993). "Purification and characterization of an active human immunodeficiency virus type 1 RNase H domain." J Virol **67**(7): 4037-49.
Sonza, S., A. Maerz, N. Deacon, J. Meanger, J. Mills and S. Crowe (1996). "Human immunodeficiency virus type 1 replication is blocked prior to reverse transcription and integration in freshly isolated peripheral blood monocytes." J Virol **70**(6): 3863-9.
Srivastava, S., N. Sluis-Cremer and G. Tachedjian (2006). "Dimerization of human immunodeficiency virus type 1 reverse transcriptase as an antiviral target." Curr Pharm Des **12**(15): 1879-94.
Sterjovski, J., M. J. Churchill, S. L. Wesselingh and P. R. Gorry (2006). "HIV-1 entry inhibitors: classes, applications and factors affecting potency." Curr HIV Res **4**(4): 387-400.
Strack, B., A. Calistri, S. Craig, E. Popova and H. G. Gottlinger (2003). "AIP1/ALIX is a binding partner for HIV-1 p6 and EIAV p9 functioning in virus budding." Cell **114**(6): 689-99.
Swanstrom, R. and J. W. Will (1997). Synthesis, assembly, and processing of viral proteins. Retroviruses. M. H. S. Coffin J, H. Varmus H, E. NY, Cold Spring Harbor Laboratory Press: 263-334.
Szilvay, A. M., S. Nornes, I. R. Haugan, L. Olsen, V. R. Prasad, C. Endresen, S. P. Goff and D. E. Helland (1992). "Epitope mapping of HIV-1 reverse transcriptase with monoclonal antibodies that inhibit polymerase and RNase H activities." J Acquir Immune Defic Syndr **5**(7): 647-57.
Szilvay, A. M., S. Nornes, A. Kannapiran, B. I. Haukanes, C. Endresen and D. E. Helland (1993). "Characterization of HIV-1 reverse transcriptase with antibodies indicates conformational differences between the RNAse H domains of p 66 and p 15." Arch Virol **131**(3-4): 393-403.
Tachedjian, G., H. E. Aronson and S. P. Goff (2000). "Analysis of mutations and suppressors affecting interactions between the subunits of the HIV type 1 reverse transcriptase." Proc Natl Acad Sci U S A **97**(12): 6334-9.
Tachedjian, G., M. Orlova, S. G. Sarafianos, E. Arnold and S. P. Goff (2001). "Nonnucleoside reverse transcriptase inhibitors are chemical enhancers of dimerization of the HIV type 1 reverse transcriptase." Proc Natl Acad Sci U S A **98**(13): 7188-93.
Tachedjian, G., H. E. Aronson, M. de los Santos, J. Seehra, J. M. McCoy and S. P. Goff (2003). "Role of residues in the tryptophan repeat motif for HIV-1 reverse transcriptase dimerization." J Mol Biol **326**(2): 381-96.
Tachedjian, G., K. L. Moore, S. P. Goff and N. Sluis-Cremer (2005a). "Efavirenz enhances the proteolytic processing of an HIV-1 pol polyprotein precursor and reverse transcriptase homodimer formation." FEBS Lett **579**(2): 379-84.
Tachedjian, G., J. Radzio and N. Sluis-Cremer (2005b). "Relationship between enzyme activity and dimeric structure of recombinant HIV-1 reverse transcriptase." Proteins: Structure, Function, and Bioinformatics **60**: 5-13.
Tachedjian, G., Goff, S. P (2003). "The effect of NNRTIs on HIV reverse transcriptase dimerisation." Current Opinion in Investigational Drugs **4**(8): 966-73.

Telesnitsky, A. and S. P. Goff (1993). "RNase H domain mutations affect the interaction between Moloney murine leukemia virus reverse transcriptase and its primer-template." Proc Natl Acad Sci U S A **90**(4): 1276-80.
Telesnitsky, A. and S. P. Goff (1997). Reverse Transcriptase and the Generation of Retroviral DNA. Retroviruses. M. Coffin J, H. Hughes S and E. Varmus H, Cold Spring Habor Laboratory Press.
Temin, H. M. and S. Mizutani (1970). "RNA-dependent DNA polymerase in virions of Rous sarcoma virus." Nature **226**(252): 1211-3.
Temiz, N. A. and I. Bahar (2002). "Inhibitor binding alters the directions of domain motions in HIV-1 reverse transcriptase." Proteins **49**(1): 61-70.
Tessmer, U. and H. G. Krausslich (1998). "Cleavage of human immunodeficiency virus type 1 proteinase from the N-terminally adjacent p6* protein is essential for efficient Gag polyprotein processing and viral infectivity." J Virol **72**(4): 3459-63.
Tomasselli, A. G., J. L. Sarcich, L. J. Barrett, I. M. Reardon, W. J. Howe, D. B. Evans, S. K. Sharma and R. L. Heinrikson (1993). "Human immunodeficiency virus type-1 reverse transcriptase and ribonuclease H as substrates of the viral protease." Protein Sci **2**(12): 2167-76.
Tozser, J., P. Bagossi, I. T. Weber, J. M. Louis, T. D. Copeland and S. Oroszlan (1997). "Studies on the symmetry and sequence context dependence of the HIV-1 proteinase specificity." J Biol Chem **272**(27): 16807-14.
Trono, D. (1992). "Partial reverse transcripts in virions from human immunodeficiency and murine leukemia viruses." J Virol **66**(8): 4893-900.
Turner, B. G. and M. F. Summers (1999). "Structural biology of HIV." J Mol Biol **285**(1): 1-32.
U.S. Department of Health and Human Services. (2009). "Antiretroviral drugs used in the treatment of HIV infection." Retrieved 20 June 2009, 2009, from http://www.fda.gov/ForConsumers/byAudience/ForPatientAdvocates/HIVandAIDSActivities/ucm118915.htm.
Ulich, C., A. Dunne, E. Parry, C. W. Hooker, R. B. Gaynor and D. Harrich (1999). "Functional domains of Tat required for efficient human immunodeficiency virus type 1 reverse transcription." J Virol **73**(3): 2499-508.
UNAIDS (2002). AIDS epidemic update December 2001. Geneva, Joint United Nations Programme on HIV/AIDS (UNAIDS) & World Health Organization (WHO).
UNAIDS (2008). 2008 Report on the global AIDS epidemic. Geneva, Joint United Nations Programme on HIV/AIDS (UNAIDS),.
UNAIDS (2010). 2010 Report on the global AIDS epidemic. Geneva, Joint United Nations Programme on HIV/AIDS (UNAIDS),.
Van de Perre, P., D. Rouvroy, P. Lepage, J. Bogaerts, P. Kestelyn, J. Kayihigi, A. C. Hekker, J. P. Butzler and N. Clumeck (1984). "Acquired immunodeficiency syndrome in Rwanda." Lancet **2**(8394): 62-5.
Van Heuverswyn, F., Y. Li, E. Bailes, C. Neel, B. Lafay, B. F. Keele, K. S. Shaw, J. Takehisa, M. H. Kraus, S. Loul, C. Butel, F. Liegeois, B. Yangda, P. M. Sharp, E. Mpoudi-Ngole, et al. (2007). "Genetic diversity and phylogeographic clustering of SIVcpzPtt in wild chimpanzees in Cameroon." Virology **368**(1): 155-71.
Venezia, C. F., K. J. Howard, M. E. Ignatov, L. A. Holladay and M. D. Barkley (2006). "Effects of efavirenz binding on the subunit equilibria of HIV-1 reverse transcriptase." Biochemistry **45**(9): 2779-89.
Venezia, C. F., B. J. Meany, V. A. Braz and M. D. Barkley (2009). "Kinetics of association and dissociation of HIV-1 reverse transcriptase subunits." Biochemistry **48**(38): 9084-93.
VerPlank, L., F. Bouamr, T. J. LaGrassa, B. Agresta, A. Kikonyogo, J. Leis and C. A. Carter (2001). "Tsg101, a homologue of ubiquitin-conjugating (E2) enzymes, binds the L domain in HIV type 1 Pr55(Gag)." Proc Natl Acad Sci U S A **98**(14): 7724-9.
Vogt, V. M. (1997). Retroviral Virions and Genomes. Retroviruses. J. M. Coffin, S. H. Hughes and H. E. Varmus, Cold Spring Harbor Laboratory Press.
Wang, C. T., Y. C. Chou and C. C. Chiang (2000). "Assembly and processing of human immunodeficiency virus Gag mutants containing a partial replacement of the matrix domain by the viral protease domain." J Virol **74**(7): 3418-22.
Wang, J., S. J. Smerdon, J. Jager, L. A. Kohlstaedt, P. A. Rice, J. M. Friedman and T. A. Steitz (1994). "Structural basis of asymmetry in the human immunodeficiency virus type 1 reverse transcriptase heterodimer." Proc Natl Acad Sci U S A **91**(15): 7242-6.
Wang, Y. X., H. J. Zhang, J. Xu, B. J. Zheng and Y. M. Wen (2008). "Mutational analysis of the "turn" of helix clamp motif of HIV-1 reverse transcriptase." Biochem Biophys Res Commun **377**(3): 915-20.
Wapling, J., K. L. Moore, S. Sonza, J. Mak and G. Tachedjian (2005). "Mutations that abrogate human immunodeficiency virus type 1 reverse transcriptase dimerization affect maturation of the reverse transcriptase heterodimer." J Virol **79**(16): 10247-57.
Wapling, J., S. Srivastava, M. Shehu-Xhilaga and G. Tachedjian (2007). "Targeting Human Immunodefi ciency Virus Type 1 Assembly, Maturation and Budding." Drug Target Insights **2**: 159-82.
Warren, K., D. Warrilow, L. Meredith and D. Harrich (2009). "Reverse Transcriptase and Cellular Factors: Regulators of HIV-1 Reverse Transcription." Viruses **1**(3): 873-94.
Warrilow, D., D. Stenzel and D. Harrich (2007). "Isolated HIV-1 core is active for reverse transcription." Retrovirology **4**: 77.
Warrilow, D., L. Meredith, A. Davis, C. Burrell, P. Li and D. Harrich (2008). "Cell factors stimulate human immunodeficiency virus type 1 reverse transcription in vitro." J Virol **82**(3): 1425-37.

Wei, P., M. E. Garber, S. M. Fang, W. H. Fischer and K. A. Jones (1998). "A novel CDK9-associated C-type cyclin interacts directly with HIV-1 Tat and mediates its high-affinity, loop-specific binding to TAR RNA." Cell **92**(4): 451-62.

Wei, X., J. M. Decker, H. Liu, Z. Zhang, R. B. Arani, J. M. Kilby, M. S. Saag, X. Wu, G. M. Shaw and J. C. Kappes (2002). "Emergence of resistant human immunodeficiency virus type 1 in patients receiving fusion inhibitor (T-20) monotherapy." Antimicrob Agents Chemother **46**(6): 1896-905.

Weiss, E. R. and H. Gottlinger (2011). "The role of cellular factors in promoting HIV budding." Journal of molecular biology **410**(4): 525-33.

Wellcome Photo Library, W. I. (2008). HIV virus budding from T lymphocyte. Wellcome Images. N0013888. London, Wellcome Images: TEM digitized, coloured. CMSP ref: Z500-LL-10866

E4 immunology.

Welsch, S., O. T. Keppler, A. Habermann, I. Allespach, J. Krijnse-Locker and H. G. Krausslich (2007). "HIV-1 buds predominantly at the plasma membrane of primary human macrophages." PLoS Pathog **3**(3): e36.

Weng, Y. and C. D. Weiss (1998). "Mutational analysis of residues in the coiled-coil domain of human immunodeficiency virus type 1 transmembrane protein gp41." Journal of Virology **72**(12): 9676-82.

Wiegers, K., G. Rutter, H. Kottler, U. Tessmer, H. Hohenberg and H. G. Krausslich (1998). "Sequential steps in human immunodeficiency virus particle maturation revealed by alterations of individual Gag polyprotein cleavage sites." J Virol **72**(4): 2846-54.

Wild, C. T., D. C. Shugars, T. K. Greenwell, C. B. McDanal and T. J. Matthews (1994). "Peptides corresponding to a predictive alpha-helical domain of human immunodeficiency virus type 1 gp41 are potent inhibitors of virus infection." Proceedings of the National Academy of Sciences of the United States of America **91**(21): 9770-4.

Wisniewski, M., C. Palaniappan, Z. Fu, S. F. Le Grice, P. Fay and R. A. Bambara (1999). "Mutations in the primer grip region of HIV reverse transcriptase can increase replication fidelity." J Biol Chem **274**(40): 28175-84.

Wisniewski, M., M. Balakrishnan, C. Palaniappan, P. J. Fay and R. A. Bambara (2000a). "The sequential mechanism of HIV reverse transcriptase RNase H." J Biol Chem **275**(48): 37664-71.

Wisniewski, M., M. Balakrishnan, C. Palaniappan, P. J. Fay and R. A. Bambara (2000b). "Unique progressive cleavage mechanism of HIV reverse transcriptase RNase H." Proc Natl Acad Sci U S A **97**(22): 11978-83.

Wlodawer, A. and J. Vondrasek (1998). "Inhibitors of HIV-1 protease: A major success of structure-assisted drug design." Annual review of biophysics and biomolecular structure **27**: 249-84.

Wohrl, B. M., R. Krebs, S. H. Thrall, S. F. Le Grice, A. J. Scheidig and R. S. Goody (1997). "Kinetic analysis of four HIV-1 reverse transcriptase enzymes mutated in the primer grip region of p66. Implications for DNA synthesis and dimerization." J Biol Chem **272**(28): 17581-7.

Wondrak, E. M., N. T. Nashed, M. T. Haber, D. M. Jerina and J. M. Louis (1996). "A transient precursor of the HIV-1 protease. Isolation, characterization, and kinetics of maturation." J Biol Chem **271**(8): 4477-81.

Wood, A. and D. Armour (2005). "The discovery of the CCR5 receptor antagonist, UK-427,857, a new agent for the treatment of HIV infection and AIDS." Prog Med Chem **43**: 239-71.

Woody, R. W. (1996). Theory of Circular Dichroism of Proteins. Circular Dichroism and the Conformational Analysis of Biomolecules. G. D. Fasman. New York, Plenum Press.

Worobey, M., M. Gemmel, D. E. Teuwen, T. Haselkorn, K. Kunstman, M. Bunce, J. J. Muyembe, J. M. Kabongo, R. M. Kalengayi, E. Van Marck, M. T. Gilbert and S. M. Wolinsky (2008). "Direct evidence of extensive diversity of HIV-1 in Kinshasa by 1960." Nature **455**(7213): 661-4.

Wu, X., H. Liu, H. Xiao, J. A. Conway, E. Hunter and J. C. Kappes (1997). "Functional RT and IN incorporated into HIV-1 particles independently of the Gag/Pol precursor protein." Embo J **16**(16): 5113-22.

Wu, X., H. Liu, H. Xiao, J. A. Conway, E. Hehl, G. V. Kalpana, V. Prasad and J. C. Kappes (1999). "Human immunodeficiency virus type 1 integrase protein promotes reverse transcription through specific interactions with the nucleoprotein reverse transcription complex." J Virol **73**(3): 2126-35.

Xiong, Y. and T. H. Eickbush (1990). "Origin and evolution of retroelements based upon their reverse transcriptase sequences." Embo J **9**(10): 3353-62.

Yarchoan, R., R. W. Klecker, K. J. Weinhold, P. D. Markham, H. K. Lyerly, D. T. Durack, E. Gelmann, S. N. Lehrman, R. M. Blum, D. W. Barry and et al. (1986). "Administration of 3'-azido-3'-deoxythymidine, an inhibitor of HTLV-III/LAV replication, to patients with AIDS or AIDS-related complex." Lancet **1**(8481): 575-80.

Yu, Q., M. Ottmann, C. Pechoux, S. Le Grice and J. L. Darlix (1998a). "Mutations in the primer grip of human immunodeficiency virus type 1 reverse transcriptase impair proviral DNA synthesis and virion maturation." J Virol **72**(9): 7676-80.

Yu, S. F., D. N. Baldwin, S. R. Gwynn, S. Yendapalli and M. L. Linial (1996). "Human foamy virus replication: a pathway distinct from that of retroviruses and hepadnaviruses." Science **271**(5255): 1579-82.

Yu, X. F., L. Dawson, C. J. Tian, C. Flexner and M. Dettenhofer (1998b). "Mutations of the human immunodeficiency virus type 1 p6Gag domain result in reduced retention of Pol proteins during virus assembly." J Virol **72**(4): 3412-7.

Yusim, K., M. Peeters, O. G. Pybus, T. Bhattacharya, E. Delaporte, C. Mulanga, M. Muldoon, J. Theiler and B. Korber (2001). "Using human immunodeficiency virus type 1 sequences to infer historical features of the acquired immune deficiency syndrome epidemic and human immunodeficiency virus evolution." Philos Trans R Soc Lond B Biol Sci **356**(1410): 855-66.

Zack, J. A., S. J. Arrigo, S. R. Weitsman, A. S. Go, A. Haislip and I. S. Chen (1990). "HIV-1 entry into quiescent primary lymphocytes: molecular analysis reveals a labile, latent viral structure." Cell **61**(2): 213-22.

Zhang, F., T. Zang, S. J. Wilson, M. C. Johnson and P. D. Bieniasz (2011). "Clathrin facilitates the morphogenesis of retrovirus particles." PLoS pathogens **7**(6): e1002119.

Zhang, H. J., Y. X. Wang, H. Wu, D. Y. Jin, Y. M. Wen and B. J. Zheng (2009). "The y271 and i274 amino acids in reverse transcriptase of human immunodeficiency virus-1 are critical to protein stability." PLoS One **4**(7): e6108.

Zheng, X., G. A. Mueller, M. J. Cuneo, E. F. Derose and R. E. London (2010). "Homodimerization of the p51 subunit of HIV-1 reverse transcriptase." Biochemistry **49**(13): 2821-33.

Zhu, T., B. T. Korber, A. J. Nahmias, E. Hooper, P. M. Sharp and D. D. Ho (1998). "An African HIV-1 sequence from 1959 and implications for the origin of the epidemic." Nature **391**(6667): 594-7.

Zybarth, G., H. G. Krausslich, K. Partin and C. Carter (1994). "Proteolytic activity of novel human immunodeficiency virus type 1 proteinase proteins from a precursor with a blocking mutation at the N terminus of the PR domain." J Virol **68**(1): 240-50.

Zybarth, G. and C. Carter (1995). "Domains upstream of the protease (PR) in human immunodeficiency virus type 1 Gag-Pol influence PR autoprocessing." J Virol **69**(6): 3878-84.

A1. Buffers and their constitution

2x HBS	280mM NaCl
	50mM HEPES
	1.5mM Na2HPO4
	adjust pH to 7.05 with 5M NaOH
2x SDS sample buffer	62.5 mM Tris pH 6.8
	10% v/v glycerol
	2% w/v SDS
	0.01 mg/mL Bromophenol Blue
	5% 2-Mercaptoethanol
2× SSC	300 mM NaCl
	30 mM Sodium Citrate
A/78	50 mM sodium phosphate buffer pH 7.8
	2 µg/ml Leupeptin
	2 µg/ml Aprotinin
	2 µg/ml Pepstatin
A/78+	50 mM sodium phosphate buffer pH 7.8
	2 µg/ml Leupeptin
	2 µg/ml Aprotinin
	2 µg/ml Pepstatin
	300 mM NaCl
	10% v/v glycerol
Dialysis buffer	50 mM Tris pH 7.0
	25 mM NaCl
	1 mM EDTA
	10% glycerol
Dilution Buffer	50 mM Tris pH 7.0
	25 mM NaCl
	10% glycerol
	0.1 mM dithiothreitol
PCR lysis buffer	1x HotStarTaq PCR buffer (QIAGEN)
	0.5% v/v IGEPAL CA-630 (Sigma Aldrich)
	0.5% v/v Tween 20 (Sigma Aldrich)
	0.5% v/v Triton X (Sigma Aldrich)
RT buffer	50 mM Tris pH 7.8
	7.5 mM KCl
	5 mM MgCl2
	2 mM DTT
	10 µCi 33P dTTP
	5 µg/mL Poly(rA)/Oligo(dT)
TBS	137 mM NaCl
	20 mM Tris pH7.6

TBST-(0.2%)	137 mM NaCl 20 mM Tris pH7.6 0.2% v/v Tween 20
TBST-(0.5%)	137 mM NaCl 20 mM Tris pH7.6 0.5% v/v Tween 20
TEN Buffer	10 mM Tris pH 8.0 1 mM EDTA pH 8.0 50 mM NaCl
TNEN Lysis buffer	100 mM Tris pH 8.0 100 mM NaCl 20 mM EDTA 1.0% v/v IGEPAL CA-630 (Sigma Aldrich) 2µg/ml Leupeptin 2µg/ml Aprotinin 2µg/ml Pepstatin

A2. Publications arising from this study

Wapling, J., K. L. Moore, S. Sonza, J. Mak and G. Tachedjian (2005). "Mutations that abrogate human immunodeficiency virus type 1 reverse transcriptase dimerization affect maturation of the reverse transcriptase heterodimer." J Virol **79**(16): 10247-57.

JOURNAL OF VIROLOGY, Aug. 2005, p. 10247–10257 Vol. 79, No. 16
0022-538X/05/$08.00+0 doi:10.1128/JVI.79.16.10247–10257.2005

Mutations That Abrogate Human Immunodeficiency Virus Type 1 Reverse Transcriptase Dimerization Affect Maturation of the Reverse Transcriptase Heterodimer

Johanna Wapling,[1,2] Katie L. Moore,[1] Secondo Sonza,[2,3] Johnson Mak,[4,5] and Gilda Tachedjian[1,2,6]*

Molecular Interactions Group, Macfarlane Burnet Institute for Medical Research and Public Health, Melbourne, Victoria 3001, Australia[1];Department of Microbiology, Monash University, Clayton, Victoria 3168, Australia[2]; HIV Regulation Laboratory, Macfarlane Burnet Institute for Medical Research and Public Heath, Melbourne, Victoria 3001, Australia[3]; HIV Assembly Group, Macfarlane Burnet Institute for Medical Research and Public Health, Melbourne, Victoria 3001, Australia[4]; Department of Biochemistry and Molecular Biology, Monash University, Clayton, Victoria 3168, Australia[5]; and Department of Medicine, Monash University, Prahran, Victoria 3181, Australia[6]

Received 8 February 2005/Accepted 16 May 2005

The specific impact of mutations that abrogate human immunodeficiency virus type 1 (HIV-1) reverse transcriptase (RT) dimerization on virus replication is not known, as mutations shown previously to inhibit RT dimerization also impact Gag-Pol stability, resulting in pleiotropic effects on HIV-1 replication. We have previously characterized mutations at codon 401 in the HIV-1 RT tryptophan repeat motif that abrogate RT dimerization in vitro, leading to a loss in polymerase activity. The introduction of the RT dimerization-inhibiting mutations W401L and W401A into HIV-1 resulted in the formation of noninfectious viruses with reduced levels of both virion-associated and intracellular RT activity compared to the wild-type virus and the W401F mutant, which does not inhibit RT dimerization in vitro. Steady-state levels of the p66 and p51 RT subunits in viral lysates of the W401L and W401A mutants were reduced, but no significant decrease in Gag-Pol was observed compared to the wild type. In contrast, there was a decrease in processing of p66 to p51 in cell lysates for the dimerization-defective mutants compared to the wild type. The treatment of transfected cells with indinavir suggested that the HIV-1 protease contributed to the degradation of virion-associated RT subunits. These data demonstrate that mutations near the RT dimer interface that abrogate RT dimerization in vitro result in the production of replication-impaired viruses without detectable effects on Gag-Pol stability or virion incorporation. The inhibition of RT activity is most likely due to a defect in RT maturation, suggesting that RT dimerization represents a valid drug target for chemotherapeutic intervention.

The human immunodeficiency virus type 1 (HIV-1) reverse transcriptase (RT) is critical for HIV-1 replication and is required for the conversion of the genomic viral RNA into a double-stranded proviral DNA precursor, catalyzed by the RNA- and DNA-dependent polymerase and RNase H activities of the enzyme. The biologically relevant form of HIV-1 RT is a heterodimer composed of 66 (p66)- and 51-kDa (p51) polypeptides. The p51 subunit is derived from and is identical to the N-terminal polymerase domain of p66 (9). The p66 subunit can be divided structurally into the polymerase and RNase H domains, with the polymerase domain further divided into the fingers, palm, thumb, and connection subdomains (24, 29). One functional polymerase and RNase H active site is located on the p66 subunit, which adopts an "open" structure to accommodate the nucleic acid template/primer (24, 29). The p51 subunit has the same polymerase subdomains as p66. However, the spatial orientations of the individual subdomains differ from those in p66, with the p51 subunit assuming a "closed" structure and playing a largely structural role in the heterodimer (2, 23, 32). Structural analyses reveal three major contacts between the p66 and p51 subunits, which include interactions between the connection subdomains of both subunits, with most of the interaction surface being largely hydrophobic (4, 59).

The appropriate association of the p66 and p51 RT subunits is required for activation of the enzyme, as monomeric subunits are devoid of polymerase activity (41, 51, 53). In vitro dimerization of the p66 and p51 subunits can be achieved under nonphysiological conditions and appears to occur by a two-step process involving the initial formation of an intermediate that can bind the template/primer but lacks polymerase activity followed by conformational changes resulting in an active enzyme (11). While this in vitro study may not exactly represent how RT maturation occurs in infected cells, it does demonstrate the absolute requirement for RT dimerization to activate polymerase function, making RT dimerization an attractive drug target (21, 48, 51, 53). Despite several in vitro studies demonstrating the critical role of RT dimerization in enzyme activation (51, 53), the specific impact of abrogating RT dimerization on HIV-1 replication has not been determined.

The HIV-1 RT is expressed as part of a Gag-Pol polyprotein ($Pr160^{gag\text{-}pol}$), which consists of the structural proteins matrix

* Corresponding author. Mailing address: Molecular Interactions Group, Macfarlane Burnet Institute for Medical Research and Public Health, 85 Commercial Road, GPO Box 2284, Melbourne, Victoria 3001, Australia. Phone: (61) 3 9282 2256. Fax: (61) 3 9282 2100. E-mail: gildat@burnet.edu.au.

(MA), capsid (CA), p2, and nucleocapsid (NC) and the Pol-encoded functional enzymes protease (PR), RT, and integrase (IN) (20). A transframe region links the Gag and the Pol domains and consists of an N-terminal octapeptide and $p6^{pol}$ that are separated by an HIV-1 protease cleavage site (15). $Pr160^{gag\text{-}pol}$ is translated from a full-length viral RNA once every 20 Gag ($Pr55^{gag}$) translation events by a ribosomal frameshift mechanism (66). Proteolytic processing by the *pol*-encoded PR results in the sequential cleavage of Gag and Gag-Pol during or shortly after viral particle release (27), resulting in the formation of mature structural proteins and viral enzymes (58). The precise pathway for the formation of RT heterodimers in HIV-1-infected cells is not established, although it is proposed to occur through a p66/p66 homodimer intermediate (59). Recent data based on a model 90-kDa Pol polyprotein (which consists of the transframe region, PR, RT, and the N terminus of IN) support this model (45). The study of mutations that abrogate RT dimerization is likely to shed light on the intermediates involved in the formation of stable RT heterodimers in HIV-1-infected cells.

The RT tryptophan repeat motif represents a remarkable cluster of six tryptophan residues, at codons 398, 401, 402, 406, 410, and 414, five of which are separated by three amino acid residues (3). The tryptophan repeat motif is found in the connection subdomain of both HIV-1 RT subunits. This hydrophobic cluster is highly conserved among primate lentiviral reverse transcriptases (3), although it is not found in other lentiviral RTs known to form heterodimers, including feline immunodeficiency virus RT. The tryptophan repeat motif is also absent from RTs from other retrovirus families, including those of the heterodimeric avian sarcoma leukosis virus and Moloney murine leukemia virus, which may dimerize when presented with a template (56). Previous studies suggested that the tryptophan repeat motif is important for RT heterodimerization, as the elucidation of the kinetics of the association of p66 and p51 RT subunits in vitro implicates the RT tryptophan residues as being involved in the initial interaction of the two monomers (10). These data are supported by our studies, which demonstrate that mutations of the highly conserved tryptophans at codons 401 and 414 in the context of the p66 subunit abrogate RT heterodimerization, as observed in both a yeast two-hybrid system for RT dimerization and in vitro binding assays (51).

The study and interpretation of the impact of mutations in RT and IN on HIV-1 replication are usually complicated by their effects on the stability and function of the Gag-Pol polyprotein from which RT and IN are expressed (34, 44, 65). A *trans*-complementation system has been developed to study the impact of mutations in specific subunits of the HIV-1 RT, where RT and IN are delivered into viral particles in *trans* fused to HIV-1 Vpr (35, 64). While this system is useful for examining the effect of RT mutations on intracellular reverse transcription, it is unlikely to recapitulate the maturation of the HIV-1 RT heterodimer from the Gag-Pol polyprotein as it occurs in HIV-1-infected cells. Hence, to examine the impact of RT dimerization-blocking mutations on RT maturation and function, it is necessary to perform these experiments in the context of the full-length virus, using mutations that are not expected to impact Gag-Pol stability or its packaging into the virion.

Examples of RT mutations at primer grip residues L234 and W229 that abrogate RT dimerization have been described (6, 14, 26, 52, 62). The primer grip region of HIV-1 RT is important for maintaining the primer terminus in an orientation appropriate for nucleophilic attack by the incoming deoxynucleoside triphosphate (37) and is not near the RT dimer interface (24, 29). Previous studies which examined the impact of mutations in or near the RT primer grip region on HIV-1 replication demonstrated decreased viral infectivity due to defects in Gag-Pol stability (65). The L234D primer grip mutant produced HIV-1 with a reduced infectivity as a result of defects in virion maturation that were ascribed to the premature cleavage of $Pr160^{gag\text{-}pol}$ in the cell, leading to a reduction in the virion incorporation of *pol* gene products (65). Since the primer grip region is far from the dimer interface, mutations at L234 that negate RT dimerization are likely to do so through long-range conformational changes that may also impact the conformation and stability of $Pr160^{gag\text{-}pol}$. In contrast, W401 is close to the RT dimer interface, and mutation of this residue to either an alanine or leucine in the context of p66 abrogates the interaction with p51 in vitro (51). Our studies demonstrate that the effect of mutating W401 is mainly localized to the repositioning of a loop region between amino acids W401 and W414 in the p66 subunit (51). Furthermore, a circular dichroism analysis of recombinant RT heterodimers expressing either the W401A or W401L mutation demonstrated no significant change in secondary structure or misfolding of the protein compared to wild-type RT (53). Since RT W401 is near the dimer interface, we hypothesized that the impact of mutations at this residue on the stability and structure of $Pr160^{gag\text{-}pol}$ would be minimal, enabling us to probe the specific effect of mutations that abrogate RT dimerization on RT maturation in the context of a full-length infectious virus.

In this study, we show that RT dimer interface mutations at amino acid W401 result in the production of viral particles with dramatically reduced infectivities and specific defects in RT maturation and function. Notably, this phenotype was observed in the absence of detectable Gag-Pol instability and virion packaging defects. Furthermore, our data provide evidence in support of the ideas that the immediate precursor of the RT heterodimer is the p66 homodimer and that the abrogation of RT dimerization represents a valid drug target for chemotherapeutic intervention.

MATERIALS AND METHODS

Cell culture. The 293T and TZM-bl (60) cell lines were maintained in Dulbecco's modified Eagle's medium (DMEM) containing 10% fetal calf serum (Progen, Darra, Queensland), glutamine (292 μg/ml), penicillin (100 U/ml), and streptomycin (100 μg/ml) (DMEM-10). TZM-bl cells were obtained through the NIH AIDS Research and Reference Reagent Program, Division of AIDS, National Institute for Allergy and Infectious Diseases (NIAID), National Institutes of Health (NIH), and were contributed by John C. Kappes, Xiaoyun Wu, and Tanzyme Inc. MT-2 cells (16) were maintained in RPMI 1640 supplemented with 10% fetal calf serum, glutamine (29.2 μg/ml), penicillin (100 U/ml), and streptomycin (100 μg/ml).

Antibodies. The monoclonal antibodies 11G10 and 5B2 recognize HIV-1 RT epitope 1 (codons 193 to 284) and HIV-1 RT epitope 2 (codons 294 to 319), respectively, and were generously provided by Dag Helland (University of Bergen, Norway) (50). The monoclonal antibody 8E5 recognizes the C-terminal epitope (codons 262 to 271) of HIV-1 IN (36) and was provided by Dag Helland. A p24 monoclonal antibody to the HIV-1 capsid (p24), purified by Andy Poumbourios (St. Vincent's Institute of Medical Research, Melbourne, Australia)

from an HIV-1 p24 hybridoma (183-H12-5C), was obtained through the NIH AIDS Research and Reference Reagent Program, Division of AIDS, NIAID, NIH, and was contributed by Bruce Chesebro (7). Pooled sera from HIV-infected patients were also used to detect HIV-1 *gag* and *pol* gene products (22).

Drug. Indinavir sulfate was prepared as a 10 mM stock in sterile water and was obtained through the NIH AIDS Research and Reference Reagent Program.

HIV-1 proviral clones and site-directed mutagenesis. The plasmid pSVC21 contains the infectious HXB2 molecular clone of HIV-1 (12). Mutations at RT amino acid W401 were introduced by site-directed mutagenesis using a Gene-Editor mutagenesis kit (Promega, Madison, Wis.) into the clone pBPol containing the ApaI-SalI fragment of HXB2 (nucleotides 2006 to 5786) cloned into the ApaI-SalI sites of pBluescript II SK(+) (Stratagene, La Jolla, CA). The mutagenic oligonucleotides 5′-GGAAACATGGGAAACCGCGTGGACAGAGTA TTGG-3′, 5′-GGAAACATGGGAAACGTTGTGGACAGAGTATTGG-3′, and 5′-GGAAACATGGGAAACATTCTGGACAGAGTATTGG-3′ were used to introduce the W401A, W401L, and W401F mutations, respectively, into the RT gene in pBPol. Following site-directed mutagenesis, the ApaI-SalI fragment in pBPol was subcloned into the ApaI-SalI sites of pSVC21 to generate the proviral mutants HX-W401A, HX-W401L, and HX-W401F. The construct pDRNL, containing the infectious NL4-3 molecular clone of HIV-1 (1), was used to generate a clone containing the W401A mutation in the RT gene (NL-W401A) by stitch PCR mutagenesis (6).

Transfections. 293T cells were seeded at 2×10^6 cells in 10-cm-diameter tissue culture plates in DMEM-10 1 day prior to transfection. Proviral DNA constructs (10 μg/plate) were introduced into cells by using the calcium phosphate procedure as previously described (38). An enhanced green fluorescent protein (EGFP; Clontech)-expressing reporter plasmid (2 μg) was cotransfected with the HIV-1 plasmids to determine the transfection efficiency. At 8 h posttransfection, cells were washed with phosphate-buffered saline without magnesium and calcium [PBS(−)] and replenished with fresh DMEM-10. At 36 h posttransfection, viruses and cells were harvested, and cell lysates were normalized according to their transfection efficiency for Western blot analysis. For the examination of viral protein profiles in viral lysates, infectivity assays, and cell-free RT assays, the amounts of virus were normalized according to equivalent amounts of virion-associated p24, as determined by Western blot analysis using p24 antibodies. For transfections performed in the presence of indinavir, cells were pretreated with 0, 0.1, 1, or 10 μM of drug, which was added to cells 1 h prior to transfection and was maintained in the culture up to the time of harvesting of cells and virus.

Infectivity assays. The titer of HIV-1 produced from 293T cell transfections was determined by end-point dilution in MT-2 cells. MT-2 cells (30,000 cells/ml) were seeded into a 96-well tissue culture plate and inoculated with 10-fold serial dilutions of virus in quintuplicate wells. Following day 6 postinfection, the virus-specific cytopathic effect was scored in each well as either positive or negative in order to calculate the 50% tissue culture infective dose using the Karber formula (18). The amount of infectious virus was determined by using the TZM-bl reporter cell line. TZM-bl cells were seeded in a 24-well tissue culture plate at 5×10^4 cells per well 1 day prior to infection. Duplicate wells were infected with a viral inoculum diluted in DMEM-10 containing DEAE-dextran (Amersham Biosciences) at a final concentration of 40 μg/ml. Cultures were incubated at 37°C in 5% CO_2 for 48 h postinfection, fixed in 0.25% glutaraldehyde-0.8% formaldehyde in PBS for 5 min at room temperature, and then stained with 400 μg/ml of X-Gal (5-bromo-4-chloro-3-indolyl-β-D-galactopyranoside), 4 mM $MgCl_2$, 4 mM potassium ferrocyanide, and 4 mM potassium ferricyanide in PBS for 1 h at 37°C. Mock-infected cells were included and used to determine the background. Following two washes with PBS, blue foci were counted by microscopy as previously described (8). The presence of equivalent amounts of virion-associated p24 in culture supernatants for mutant and wild-type strains was confirmed by a Western blot analysis of viral lysates purified through a 25% (wt/vol) sucrose cushion prior to the infectivity assays. Since the numbers of viral particles produced were similar for wild-type and mutant viruses, virus infectivity in MT-2 and TZM-bl cells was expressed per ml of culture supernatant.

Viral protein analysis. For an analysis of viral proteins by Western blotting, culture supernatants from transfected 293T cells were harvested at 36 h post-transfection and clarified by low-speed centrifugation (2,000 rpm for 30 min; Beckman GS-6R rotor), followed by concentration and partial purification of the virus through a 25% (wt/vol) sucrose cushion (26,500 rpm, 1 h, 4°C) using an SW41 rotor (Beckman). Viral pellets were solubilized in 80 μl of 2× sodium dodecyl sulfate (SDS) loading buffer and heated to 95°C for 3 min prior to the separation of proteins in a 7.5% polyacrylamide gel containing sodium dodecyl sulfate (SDS-polyacrylamide gel electrophoresis [SDS-PAGE]). For the analysis of intracellular viral protein expression, transfected 293T cells were washed twice with PBS(−), collected in 5 ml of PBS(−), and pelleted at 1,500 rpm for 10 min. The cell pellet was lysed in 500 μl of TNEN (10 mM Tris, pH 8.0, 50 mM NaCl, 1 mM EDTA, 1.0% Igepal CA-630 [Sigma-Aldrich, Castle Hill, NSW, Australia]) containing 1 μg/ml each of aprotinin, leupeptin, and pepstatin. For experiments performed with indinavir, the lysis buffer was also supplemented with 10 μM drug. Lysates were centrifuged at 13,000 × *g* at 4°C for 20 min, and the supernatants were removed, added to an equal volume of 2× SDS loading buffer, heated to 95°C for 3 min, and then subjected to SDS-PAGE. Following electrophoresis, proteins were transferred to polyvinylidene difluoride membranes (Millipore, North Ryde, NSW, Australia) by electroblotting and blocked for 1 h at room temperature with 5% skim milk power in TBST (0.5% Tween 20, 137 mM NaCl, 20 mM Tris), followed by incubation with primary and secondary antibodies conjugated to horseradish peroxidase (Amersham Biosciences). Viral proteins were detected by chemiluminescence per the manufacturer's instructions (Amersham Biosciences). The quantitation of viral protein bands from Western blots was performed by densitometry using ScienceLab 99 Image Gauge, version 3.3, software (Fuji Photo Film Co. Ltd.) as previously described (28). The statistical significance of differences between mutant and wild-type proteins was determined using the Wilcoxon rank sum test (5, 42) for a minimum of three independent assays, with data expressed as average relative intensities ± standard deviations. The relative viral release efficiency (viral production) was calculated as the amount of viral particle-associated Gag divided by the total (cell- and viral particle-associated) amount of Gag as described previously (43).

Cell-free reverse transcriptase assay. Clarified viral lysates from transfections were applied to an equal volume of 0.3% Igepal CA-630. The RT activity of viral lysates (20 μl) was assayed in the presence of 5 μg/ml poly(rA)/oligo(dT) (Amersham Biosciences), 10 μCi [α-^{33}P]dTTP (Perkin-Elmer, Boston, MA), 50 mM Tris, pH 7.8, 7.5 mM KCl, 2 mM dithiothreitol, and 5 mM $MgCl_2$ for 2 h at 37°C. Samples were applied to DE 81 membranes and washed, and incorporated counts were quantified by phosphorimager analysis as previously described (52).

Intracellular reverse transcriptase assay. Semiquantitative PCR was used to detect reverse transcripts in lysates of MT-2 cells (4×10^5 cells/10 ml) infected with wild-type and mutant viruses (500 ng of p24 quantified using the Vironostika HIV-1 Antigen MicroElisa system [Biomerieux, Baulkham Hills, NSW, Australia]) which were harvested at 6 h postinfection. Cells were washed with PBS(−) and prepared for PCR as previously described (49), except that cells were lysed with 100 μl of lysis buffer (1× HotStarTaq PCR buffer [QIAGEN, Clifton Hill, Victoria, Australia], 0.5% Igepal CA-630, 0.5% Tween 20). Prior to infection, viral stocks were filtered through 0.45-μm filters and pretreated with 10 U of RNase-free DNase I (Roche, Castle Hill, NSW, Australia) for 30 min at 37°C in the presence of 10 mM $MgCl_2$ to remove contaminating plasmid DNA. Ten-microliter aliquots of undiluted cell lysates and either a 1/3, 1/10, or 1/30 dilution of the cell lysates were assayed by PCR using HotStarTaq DNA polymerase (QIAGEN) in a 50-μl reaction mixture to detect early viral DNA synthesis (R/U5) using the primer pair M667 (5′-GGCTAACTAGGGAACCCACTG-3′) and AA55 (5′-CTGCTAGAGATTTTCCACACTGAC-3′) (66). The presence of full-length or nearly full-length (long terminal repeat [LTR]/*gag*) viral DNA transcripts was detected by PCR using the primer pair M667 and M661 (5′-CC TGCGTCGAGAGAGCTCCTCTGG-3′) (66).

The amount of DNA in the lysates was standardized by PCR using the HLA-DQα-specific primers GH26 (5′-GTGCTGCAGGTGTAAACTTGTACCAG-3′) and GH27 (5′-CACGGATCCGGTAGCAGCGGTAGAGTTG-3′ (30). Lysates from ACH2 cells, which contain a single copy of proviral DNA per cell (13), were used for PCR quantitation as previously described (49).

Protein purification and size exclusion chromatography. Recombinant p66-His and p66W401A-His were purified by Ni-nitrilotriacetic acid and DEAE-Sepharose chromatography as previously described (31). The separation of RT monomers and homodimers was performed by size exclusion chromatography (SEC) using a Superdex 200 column (Amersham Biosciences) and a Pharmacia fast-performance liquid chromatography system. The elution of RT subunits was compared to the elution profiles of a mixture of eight molecular size standards for gel filtration (range, 669 to 13.7 kDa) per the manufacturer's instructions (Amersham Biosciences). Samples (200 μl) were resolved using a mobile-phase (50 mM sodium phosphate, pH 7.8, 150 mM NaCl) flow rate of 0.25 ml/min. To examine the proportions of monomers versus homodimers, purified wild-type p66 or mutant p66W401A-His was diluted in the mobile phase to a final concentration of 3.8 μM and resolved by SEC after 2 h of incubation on ice.

RESULTS

Mutations at RT codon 401 do not affect viral particle production and Gag processing in virions. We have previously demonstrated that the RT mutations W401A and W401L negate RT dimerization both in vitro and in the yeast two-hybrid

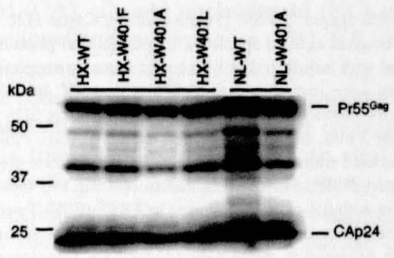

FIG. 1. Viral lysates probed with p24 antibodies. 293T cells were cotransfected with an EGFP reporter plasmid and infectious molecular clones of wild-type HIV-1 (HX-WT and NL-WT) or the W401 RT mutants HX-W401F, HX-W401A, HX-W401L, and NL-W401A. At 36 h posttransfection, viruses and cells were harvested and normalized to the transfection efficiency (according to EGFP expression) and virion-associated p24 by Western blot analysis for the elucidation of viral protein profiles in viral and cell lysates. Viruses were purified from cell culture supernatants at 36 h posttransfection by centrifugation through a 25% (wt/vol) sucrose cushion. Viral pellets were solubilized in 2× SDS loading buffer, and proteins were separated by SDS-PAGE on a 7.5% polyacrylamide gel and subjected to Western blot analysis using p24 antibodies. Viral bands were visualized by chemiluminescence.

system, while W401F has no effect on RT dimerization (51). To determine if mutations that abrogate RT dimerization affect viral production, we transfected 293T cells with infectious molecular clones of HIV-1 expressing the W401A (HX-W401A and NL-W401A), W401L (HX-W401L), and W401F (HX-W401F) RT mutations and compared the viral protein profiles of the mutants to those of the corresponding isogenic wild-type strains (HX-WT or NL-WT) (51) in both viral and cell lysates. We examined the effect of the W401A mutation in the HXB-2 and NL4-3 genetic backgrounds to ensure that any observed phenotypic effects were not strain dependent.

A Western blot analysis of both viral (Fig. 1) and cell lysates (data not shown) from HIV-transfected cells probed with p24 antibodies demonstrated similar expression levels of viral Gag for the mutant and isogenic wild-type strains. The relative viral release efficiencies ± standard errors for the mutant viruses normalized to that of the wild type were 101 ± 12 for HX-W401F, 100 ± 14 for HX-W401A, 98 ± 13 for HX-W401L, and 109 ± 17 for NL-W401A. Statistical analysis demonstrated that viral production was not significantly different for the mutant W401 viruses compared to the isogenic wild-type strains. These data demonstrate that mutations at W401 do not affect viral particle production.

To determine whether the processing of $Pr55^{gag}$ to p24 was altered in the mutant viruses, we performed a Western blot analysis of viral lysates probed with p24 antibodies and determined the ratio of p24 to $Pr55^{gag}$ for HX-W401A, HX-W401L, and HX-W401F compared to that for the wild-type virus (Fig. 1). Our analysis revealed no significant difference in the p24/$Pr55^{gag}$ ratio for the mutants compared to that for the wild-type virus (HX-WT, 1.10 ± 0.05; HX-W401F, 1.05 ± 0.11; HX-W401A, 1.07 ± 0.04; HX-W401L, 1.04 ± 0.06). A similar investigation of HIV-1 containing the W401A mutation in the NL4-3 genetic backbone (NL-W401A) also revealed no significant difference in the processing pattern of $Pr55^{gag}$ to p24 compared to that for NL-WT (NL-WT, 1.05 ± 0.04; NL-W401A, 1.04 ± 0.05) (Fig. 1). Taken together, these data demonstrate that mutations near the RT dimer interface that abrogate RT dimerization result in viruses that produce normal levels of viral particles with no detectable defects in Gag processing.

The W401A/L RT mutations result in viral particles with reduced infectivities. Since RT dimerization is critical for activation of the RT enzyme (51, 53), we hypothesized that mutations that cause defects in RT subunit interactions would have detrimental effects on viral infectivity. In order to determine whether the viral particles with mutations at RT W401 were infectious, we subjected viruses obtained from the transfection of 293T cells with the HIV-1 wild type and with mutant clones to infectivity assays performed in MT-2 and TZM-bl cells. For the detection of virus replication in MT-2 cells, the virus must undergo multiple rounds of replication and spread through the culture to produce detectable virus-specific cytopathic effects by 6 days postinfection. Consequently, any differences in viral infectivity will be amplified in this system compared to assays in which the virus undergoes limited rounds of infection, such as assays with the TZM-bl cell line. The HIV-1 mutants HX-W401A, HX-W401L, and NL-W401A demonstrated undetectable levels of infectious virus in MT-2 cells, while the titer of HX-W401F was fourfold less than that of the wild type (Fig. 2A). We also assessed the infectivity of the mutant viruses in the TZM-bl indicator cell line, which contains a host cell chromosome-integrated LacZ gene under the control of the HIV-1 LTR promoter (8). These cells can measure a single round of infection, which is detected by transactivation of the LacZ reporter by newly synthesized Tat protein following integration of the viral DNA. Therefore, HIV-1 with defects in the early stage of replication up to and including integration and the production of Tat would be expected to display a reduced infectivity in this cell line. Under our assay conditions (48 h), the cells would have been subjected to limited rounds of HIV infection. In this assay, HX-W401L was noninfectious while HX-W401F was 2.5-fold less infectious than HX-WT (Fig. 2B), similar to the data we observed with the MT-2 infectivity assay. In contrast to the results of the infectivity assay performed with MT-2 cells, the HX-W401A and NL-W401A mutants demonstrated the presence of infectious virus. Nevertheless, their infectivities were significantly lower than that of the corresponding wild-type strains, with 100- and 50-fold decreases for HX-W401A and NL-W401A, respectively (Fig. 2B). These data demonstrate a correlation between the abrogation of RT dimerization in vitro and defects in viral infectivity.

The W401A/L RT mutations result in viral particles with defects in both virion particle-associated and intracellular RT activity. We have shown that the HIV-1 mutants displayed significant defects in infectivity (Fig. 2). We also know from previous studies that viruses with mutations at W401 that abrogate RT dimerization in vitro lack RT activity (51, 53). Therefore, we examined the RT activity present in viral particles and the capacity of the RT in these particles to initiate and complete intracellular reverse transcription. To measure RT activity in virions, viral particles from 293T transfections (normalized for p24) were subjected to a cell-free RT assay using poly(rA)/oligo(dT) as a template primer. HX-W401A, HX-W401L, and NL-W401A displayed <1% of the RT activity of the wild type in our assay, while the RT activity of the HX-

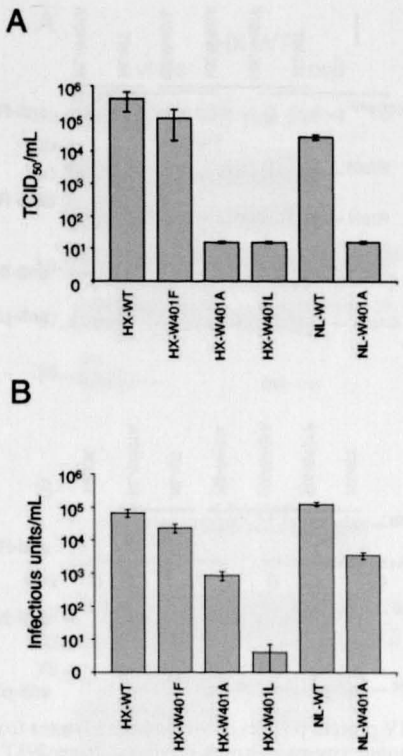

FIG. 2. Infectivities of wild-type and W401 mutant viruses produced by transfection of 293T cells. Prior to infection, clarified 293T cell supernatants containing wild-type or mutant virus were normalized to equivalent amounts of virion-associated p24, as determined by Western blot analysis. (A) Infectivities determined in a 6-day spreading assay performed with MT-2 cells. Cells were infected in quintuplicate wells with 10-fold serial dilutions of virus. At 6 days postinfection, the virus-specific cytopathic effect was scored and the 50% tissue culture infective dose ($TCID_{50}$) was calculated for each virus. Results were obtained from three independent assays. (B) Infectivities determined with TZM-bl cells. Serially diluted viruses were used to infect duplicate wells, and the numbers of blue-staining foci (infectious units) were determined at 48 h postinfection as described in Materials and Methods. Data were obtained from two independent assays. Error bars indicate standard deviations.

W401F virus was 80% that of the wild type (Fig. 3A). These data clearly show that viruses containing mutations known to abrogate RT dimerization in vitro are defective in RT function.

To determine whether viral particles could initiate and complete intracellular reverse transcription, we performed a semiquantitative PCR using primers that detect early transcripts (minus-strand strong-stop DNA) and primers designed to detect nearly complete viral DNA transcripts (66). MT-2 cells were infected with viruses (normalized for p24) and at 6 h postinfection were lysed for PCR analysis. A housekeeping gene, HLA-DQα, was amplified from cell lysates and used to normalize the cell lysates subjected to PCR for the detection of HIV-1 reverse transcripts (data not shown).

HX401L demonstrated dramatic decreases in both early and late transcripts (Fig. 3C). We also tested HIV-1 expressing the L234A RT mutation (NL-L234A). Mutations at this residue have been reported to confer a defect in Gag-Pol packaging, and as a result, decreased packaging of RT in the virion (6, 65). Hence, the NL-L234A mutant was expected to demonstrate a

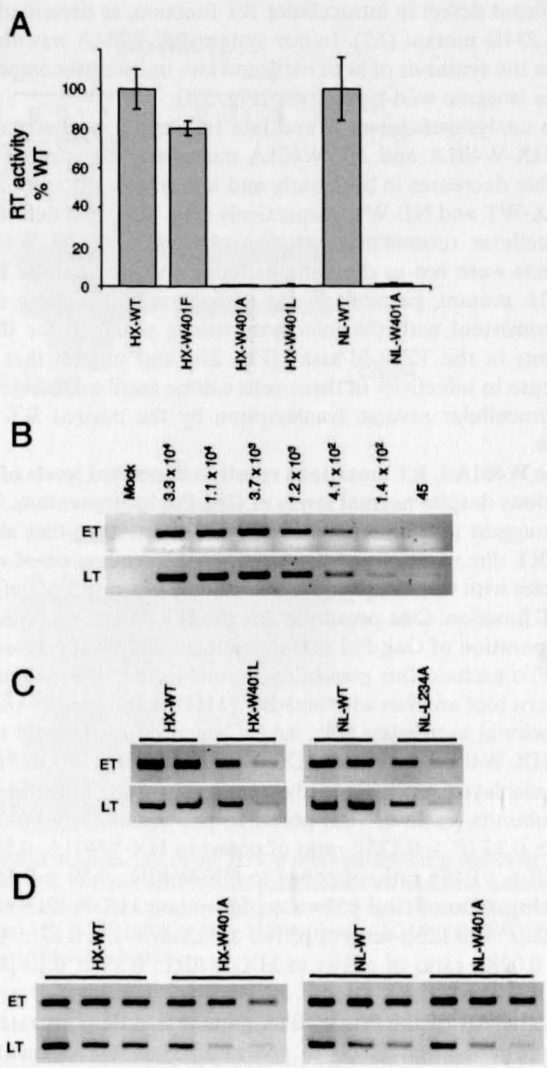

FIG. 3. RT activities of wild-type and W401 mutant viruses. (A) Viruses from cell culture supernatants obtained from transfected 293T cells expressing wild-type and W401 mutant viruses were normalized to equivalent amounts of virion-associated p24, as determined by Western blotting, lysed, and subjected to a cell-free RT assay using a poly(rA)/oligo(dT) template/primer and an [α-^{33}P]dTTP substrate. Incorporated counts were determined by phosphorimager analysis. Results were obtained from three independent assays. Error bars indicate standard deviations. (B, C, and D) Semiquantitative PCRs for viral DNA transcripts. The primer pair AA55 and MM67 was used to detect early transcripts (ET), and MM61 and MM67 were used to detect late transcripts (LT). (B) Dilution series of ACH2 cell lysate, which contains one integrated copy of the HIV-1 provirus per cell, in addition to PCR of uninfected MT-2 cells (mock). For panels C and D, supernatants from transfected 293T cells were clarified, treated with DNase I, and used to infect MT2 cells using 500 ng of p24/4 × 10^5 cells. At 6 hours postinfection, the cells were collected, lysed, and then subjected to PCR analysis. (C) PCRs were performed on undiluted (left) and diluted (1/10) (right) MT-2 cell lysates infected with HX-W401L, NL-L234A, and corresponding wild-type viruses. (D) MT-2 cell lysates from infections with HX-W401A, NL-W401A, and corresponding wild-type viruses were diluted 1/3, 1/10, and 1/30 (left to right). PCR products were resolved in a 2% agarose gel and visualized by ethidium bromide staining. The absence of contaminating plasmid DNA was confirmed by performing PCR on the DNase I-treated cell culture supernatant used for MT2 infection using both primer pairs (data not shown).

significant defect in intracellular RT function, as described for the L234D mutant (65). In our system, NL-L234A was defective in the synthesis of both early and late transcripts compared to the isogenic wild-type strain (Fig. 3B).

An analysis of the early and late transcripts synthesized by the HX-W401A and NL-W401A mutants demonstrated detectable decreases in both early and late transcripts compared to HX-WT and NL-WT, respectively (Fig. 3D). The defects in intracellular reverse transcription observed for the W401A mutants were not as dramatic as those observed for the HX-W401L mutant, particularly for early transcripts. These data are consistent with the infectivity results obtained for these mutants in the TZM-bl assay (Fig. 2B) and suggest that the decrease in infectivity in these cells can be ascribed to a defect in intracellular reverse transcription by the mutant RT enzymes.

The W401A/L RT mutations result in decreased levels of RT in virions despite normal levels of Gag-Pol incorporation. Our data suggest that mutations at the dimer interface that abrogate RT dimerization in vitro result in the production of viral particles with markedly reduced infectivity as a result of defects in RT function. One possibility for the RT defect is a reduced incorporation of Gag-Pol in the virion, as described previously (65). To exclude this possibility, we subjected viral lysates to Western blot analysis with anti-RT (11G10) and anti-IN (8E5) monoclonal antibodies (Fig. 4A). Compared to the wild type and HX-W401F, both the HX-W401A and HX-W401L mutants displayed reduced steady-state levels of the p66 and p51 RT subunits (ratio of viral p66wt to p66 mutant HX-W401F, 1.09 ± 0.37 [$P > 0.125$]; ratio of p66wt to HX-W401A, 0.59 ± 0.14 [$P = 0.048$]; ratio of p66wt to HX-W401L, 0.39 ± 0.16 [$P = 0.048$]; ratio of viral p51wt to p51 mutant HX-W401F, 1.06 ± 0.23 [$P > 0.125$]; ratio of p51wt to HX-W401A, 0.57 ± 0.16 [$P = 0.028$]; ratio of p51wt to HX-W401L, 0.35 ± 0.10 [$P = 0.008$]).

An analysis of the NL-W401A mutant also demonstrated a trend toward lower levels of p66 and p51 in the virion than those for NL-WT, which did not reach statistical significance for p51 (ratio of viral p66wt to p66 mutant NL-W401A, 0.62 ± 0.10 [$P = 0.048$]; ratio of viral p51wt to p51 mutant NL-W401A, 0.78 ± 0.11 [$P = 0.11$]). Decreased levels of the two RT subunits were also observed in viral lysates probed with another RT monoclonal antibody (5B2) and with pooled sera from HIV-infected individuals, indicating that the observed results were not RT antibody specific (data not shown).

In contrast, no significant decrease in steady-state protein levels of either Gag-Pol (the ratio of viral Gag-Pol to p24 for HX-W401F normalized to the wild type was 1.04 ± 0.18, that for HX-W401A was 0.96 ± 0.08, that for HX-W401L was 0.89 ± 0.19, and that for NL-W401A was 1.17 ± 0.24) or IN (the ratio of viral IN to p24 for HX-W401F normalized to the wild type was 1.1 ± 0.05, that for HX-W401A was 0.92 ± 0.14, that for HX-W401L was 1.01 ± 0.19, and that for NL-W401A was 1.01 ± 0.01) was detected in mutant virions compared to the corresponding wild-type virus, suggesting that the decreased levels of RT were unlikely to be a result of a defect in Gag-Pol incorporation (Fig. 4A). These data are also consistent with the lack of Gag processing defects observed in virions (Fig. 1) and indicate that normal levels of PR and therefore of Gag-Pol were incorporated into the mutant virus.

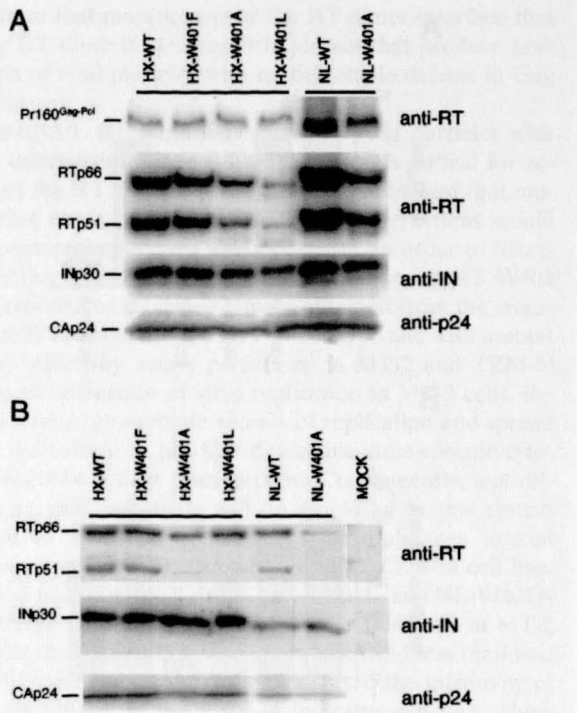

FIG. 4. HIV protein profiles of viral and cell lysates from wild-type and W401 mutant viruses. Viruses produced from 293T cells transfected with infectious molecular clones of HIV-1 expressing wild-type virus and the W401 RT mutants were purified through a 25% (wt/vol) sucrose cushion, and viral pellets were solubilized in 2× SDS loading buffer. 293T cells were washed, lysed, and clarified by centrifugation, and equal volumes were added to 2× SDS loading buffer. Viral (A) and cell (B) lysates were normalized according to virion-associated p24 (by Western blotting) and transfection efficiency, separated by SDS-PAGE on a 7.5% polyacrylamide gel, subjected to Western blot analysis using RT (11G10) and IN (8E5) antibodies, and visualized by chemiluminescence.

Intracellular processing of RT suggests a defect in p66 homodimer formation. It has been postulated that the immediate precursor to the HIV-1 RT heterodimer is the p66 homodimer (59). Since both p66 subunits contain an RNase H domain, it has been proposed that the RNase H domain of one of the subunits must unravel in the p66 homodimer, exposing the PR cleavage site between the Pol and RNase H domains and leading to a 1:1 ratio of p66 to p51 in the virion (59). In vitro studies using a minimal *pol* construct expressed in bacteria support this hypothesis (45), but there are no data to shed light on the mechanism of RT heterodimer formation in HIV-1-infected cells. We have demonstrated that the W401A RT mutation can abrogate RT heterodimerization (51) and p66 homodimerization (data not shown) in vitro. Hence, if the p66 homodimer is the immediate precursor to the RT heterodimer, then the abrogation of p66 homodimerization should lead to a decrease in processing to p51.

In order to gain insight into the nature of the immediate RT heterodimer precursor, we examined RT expression in cell lysates (Fig. 4B) of cells transfected with mutant and wild-type viruses. Cell lysates from cells transfected with the virus expressing the W401A or W401L mutant displayed altered RT processing profiles, where p51 was almost undetectable despite

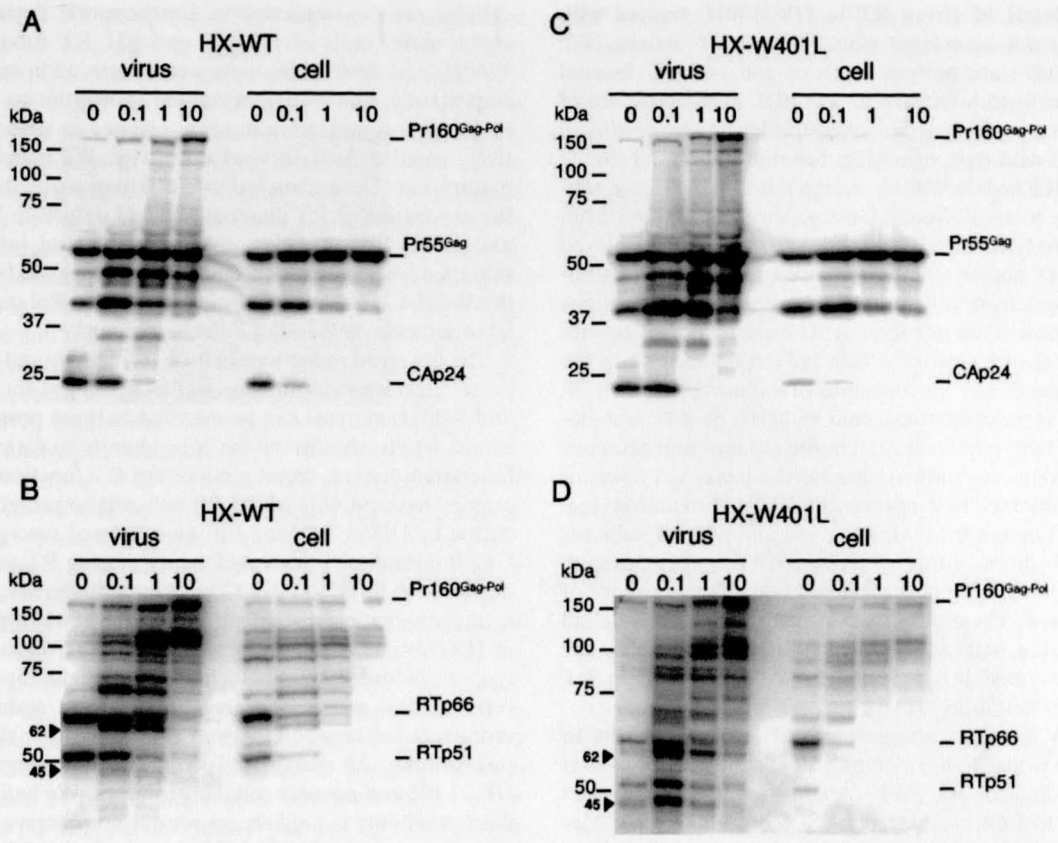

FIG. 5. Western blot analysis of wild-type and W401L mutant viruses generated in the presence of the HIV-1 protease inhibitor indinavir. 293T cells cultured in the presence of 0, 0.1, 1, or 10 μM indinavir were transfected with HX-WT and HX-W401L constructs. Cell and viral lysates were collected as described in Materials and Methods, normalized according to transfection efficiency, and subjected to SDS-PAGE and Western blot analysis. Viral and cell lysates were probed with a p24 antibody (HX-WT [A] and HX-W401L [C]) or the RT antibody 11G10 (HX-WT [B] and HX-W401L [D]). RT-related bands migrating at 62 and 45 kDa are denoted by solid arrowheads.

the presence of p66, compared with those from wild type-transfected cells and cells transfected with the dimerization-competent HX-W401F mutant (ratios of intracellular p66 to p51 for wild-type and mutant viruses were as follows: HX-WT, 1.97 ± 0.31; HX-W401F, 1.66 ± 0.42 [$P = 0.190$]; HX-W401A, 3.44 ± 0.94 [$P = 0.008$]; HX-W401L, 5.40 ± 2.17 [$P = 0.008$]; NL-WT, 1.98 ± 0.39; NL-W401A, 3.20 ± 0.48 [$P = 0.05$]). In contrast, there was no detectable change in the intracellular level of IN, suggesting that the defect was specific to RT processing (Fig. 4B). The defect in processing to p51 can be explained by the inability of p66 to form homodimers, which may be a prerequisite for heterodimer formation. Taken together, these data suggest that mutations near the dimer interface which negate RT dimerization in vitro lead to a defect in the processing of p66 to the p51 subunit inside the infected cell.

Mutant RT subunits are sensitive to proteolysis by HIV-1 protease. The decreased levels of RT in viral particles observed with the HX-W401A/L and NL-W401A mutants is likely a result of an increased susceptibility of the RT to proteolytic degradation by proteases and not of decreased expression or incorporation of Gag-Pol into the virion. To determine whether the RT subunits were degraded by HIV-1 protease, we transfected 293T cells with HX-WT and HX-W401L in the absence and presence of indinavir, a specific inhibitor of HIV-1 protease (57), and probed viral and cell lysates with either anti-p24 or the RT antibody 11G10. As expected, indinavir treatment resulted in a dose-dependent inhibition of $Pr55^{gag}$ processing to p24 for both wild-type (Fig. 5A) and mutant viruses (Fig. 5C). As shown in Fig. 4A, viral lysates from HX-WT obtained from transfections performed in the absence of indinavir demonstrated almost a 1:1 ratio of p66:p51 in the virion, and both subunits were also detectable in the cell lysates (Fig. 5B). In contrast, markedly reduced steady-state protein levels of p66 and p51 were observed in the HX-W401L viral lysates in the absence of indinavir, while in cell lysates there were decreased levels of p51 compared to HX-WT cell lysates (Fig. 5B and D). The treatment of cells transfected with HX-WT with increasing concentrations of indinavir led to a dose-dependent decrease in the processing of Gag-Pol to p66 and p51 in both viral and cell lysates (Fig. 5B). Notably, viral lysates from cells transfected with HX-W401L and treated with 0.1 μM indinavir demonstrated levels of p66 and p51 approaching those observed with the wild-type virus cultured in the absence of the drug. These data indicate that mutant RT is more susceptible to proteolytic degradation than wild-type RT and that HIV-1 PR is largely responsible for the reduced levels of RT observed in HX-W401L virions.

Restored levels of virion RT in HX-W401L treated with indinavir are not associated with restored RT activity. We observed steady-state protein levels of p66 and p51 in viral lysates from cells transfected with HX401L in the presence of 0.1 μM indinavir which approached the levels observed with the untreated wild-type virus (Fig. 5B and D). To determine whether the RT in HX-W401L virions was functional, we subjected virions to a cell-free RT assay. Virions obtained from cells transfected with HX-WT in the absence of drug displayed the highest RT activity, while decreased RT activity was observed in virions from cells treated with increasing concentrations of indinavir (data not shown). These data correlate with a decrease in the processing of Gag-Pol to p66 and p51 in the virion with increasing concentrations of indinavir (Fig. 5B). In contrast, RT from cells transfected with HX-W401L was devoid of RT activity when cultured in the absence and presence of indinavir (data not shown), despite the increased levels of p66 and p51 observed in the presence of 0.1 μM indinavir (Fig. 5D). Our data demonstrate that the p66 and p51 RT subunits in HX-W401L do not form a functional RT enzyme, despite increased expression levels of these subunits in the presence of 0.1 μM indinavir. These data suggest that the RT subunits fail to form a stable heterodimer, which is consistent with our previously described in vitro findings with recombinant RT expressing this mutation (51).

The W401A mutation abrogates p66 homodimerization in vitro. Our previous studies demonstrated that mutations that abrogate RT dimerization (W401A/L) result in a recombinant RT that fails to form a stable p66/p51 heterodimer. Furthermore, this dimerization-defective RT is devoid of RT activity, as measured in an assay using an exogenous template/primer (51). If the p66 homodimer is the immediate precursor of the RT heterodimer, it is important to establish that mutations that abrogate RT heterodimerization will also abrogate p66 homodimerization. Accordingly, we introduced the W401A mutation into a construct expressing p66 with a C-terminal histidine tag, expressed the mutant (p66W401A-His) in bacteria, and purified the protein using nickel-nitrilotriacetic acid and ion-exchange chromatography. Wild-type p66-His was also expressed and purified in the same way. The proportion of homodimer to monomer was resolved by SEC analysis on a Superdex 200 column. Wild-type His-p66 at a concentration of 3.8 μM was resolved as two peaks, representing p66 homodimers (132 kDa) and p66 monomers (data not shown), consistent with the known dissociation constant (K_D) for p66 homodimerization (59). In contrast, p66W401A at the same concentration was predominately monomeric (data not shown). These data demonstrate that mutations that abrogate RT heterodimerization also lead to defects in p66 homodimerization.

DISCUSSION

We used mutations near the RT dimer interface which were previously shown to inhibit RT heterodimerization in vitro to probe the specific effects of abrogating RT dimerization on HIV-1 replication. Our data show that the RT mutations W401A and W401L result in the production of viruses with markedly reduced infectivities due to decreased RT activity, as observed both in cell-free RT assays and at the level of intracellular reverse transcription. Furthermore, decreases in the steady-state levels of the p66 and p51 RT subunits for the W401L and W401A mutants were observed in virion lysates. Importantly, the W401F mutation, shown not to significantly inhibit RT dimerization in vitro, resulted in virions with relatively small defects in viral infectivity, RT activity, and RT maturation. These data indicate a strong correlation between the abrogation of RT dimerization and defects in RT function and maturation. Notably, the defect in viral infectivity was remarkably specific to RT and did not appear to be a result of the W401A/L mutations altering either Gag-Pol stability or the incorporation of Gag-Pol into the virions.

The observed reductions in both RT activity and steady-state protein levels of virion-associated p66 and p51 for the W401A and W401L mutants can be ascribed to three possible mechanisms: (i) an inability of the RT subunits to form stable and functional dimers, thereby inhibiting RT function; (ii) an increased susceptibility of the RT subunits to proteolytic degradation by HIV-1 PR; and (iii) an increased susceptibility of a Gag-Pol processing intermediate expressing RT to proteolytic degradation by HIV-1 PR. Consistent with the first mechanism is our observation that despite the restoration of p66 and p51 in HX-W401L virions to levels approaching those of the wild type by indinavir treatment, the RT was nonfunctional in a cell-free RT assay. The inability to form stable RT heterodimers and homodimers may also account for the increased susceptibility of mutant RT to proteolytic degradation by HIV-1 PR and possibly cellular proteases. We believe that the third possibility is unlikely, as we did not observe a concomitant degradation of HIV-1 IN along with the RT subunits in either viral or cell lysates.

HIV PR-mediated processing of Gag and Gag-Pol is critical for virus maturation (58). Gag processing occurs in a highly ordered and sequential manner which is crucial for the production of infectious virus (61). The processing of Gag-Pol is also likely to occur in a highly regulated and sequential manner for virion incorporation and proper maturation of the HIV-1 enzymes. The nature of the Gag-Pol cleavage intermediates in HIV-1-infected cells has been determined by immunoblotting using distinct antisera against HIV-1 proteins (33). The intermediates include the initial autocatalytic cleavage reaction products p120 and p113 (33). These products have also been observed with a cell-free rabbit reticulocyte lysate system for the study of PR activation in the context of full-length Gag-Pol and are generated by autocatalytic cleavage between p2/NC and transframe protein/$p6^{pol}$ (39, 40). Other processing intermediates identified in HIV-1-infected cells include PR-RT-IN (p107) and RT-IN (p97) (33). While the Gag-Pol processing intermediates have been identified, we still do not know the sequence of appearance of the processing products, which would shed light on the Gag-Pol processing precursors that are critical for RT maturation.

Two models have been proposed for the formation of the p66/p51 RT during HIV-1 PR-mediated processing of $Pr160^{gag\text{-}pol}$ (45). In the so-called sequential model, the RT heterodimer is formed from a p66/p66 homodimer intermediate, while in the concerted model, the p66 subunits are formed by processing from separate Gag-Pol molecules followed by cleavage of some of the p66 to p51, which then associates with the remaining p66. Structural studies (59) and experiments

using a model Pol polyprotein (45) support the sequential model, but no data exist to support this model in HIV-1-infected cells. Our data demonstrate that the intracellular processing of p66 to p51 in dimerization-defective mutants is not efficient and that recombinant p66W401A does not form stable p66/p66 homodimers in vitro. These data suggest that the reduced processing of p66 to p51 in cell lysates may be explained by a failure of the mutant p66 to form homodimers. An alternative explanation for the reduced intracellular processing of p66 to p51 is that the W401A/L mutations alter the conformation of p66 in such a way that the PR cleavage site between the polymerase and the RNase H domain is not accessible. However, this possibility is not consistent with our observation of a processing profile for the virion where the ratio of p66 to p51 was similar to that of the wild type. Furthermore, a circular dichroism analysis of recombinant RT mutants expressing either the W401A or W401L mutation demonstrated identical profiles to that of wild-type RT, indicating that these mutations do not lead to major changes in the RT secondary structure (53). Therefore, our data support the sequential model for p66/p51 heterodimer formation, as observed in cell lysates.

Paradoxically, while the processing of p66 to p51 was not efficient in cells transfected with HX-W401A, HX-W401L, and NL-W401A, the processing of p66 to p51 was not dramatically inhibited in the viral particles, although the steady-state levels of both subunits were less than those in the wild-type virus for the HX-W401L and HX-W401A mutants. Since the effective concentration of p66 subunits would be much higher in the confines of the viral particle than in the cell, a possible explanation for the difference in the RT processing pattern in cells compared to virions is that mutant p66 is able to form loose or transient homodimers in the virus, allowing cleavage of the RNase H domain from one of the p66 monomers to p51. Furthermore, the relative inability to form stable dimers may explain the decreased stability of the RT subunits in response to the high concentrations of HIV-1 PR in the virion, as monomeric or loose dimers of RT may be more susceptible to proteolysis than stable RT dimers. Our hypothesis of weak/transient dimer formation is consistent with the defects in RT activity observed for the dimerization-defective mutants, since it has been established that not only abrogation of RT dimerization but also destabilization of the RT dimer leads to defects in polymerase function (48). This has been demonstrated by studies with the nonnucleoside reverse transcriptase inhibitors 1-{spiro[4-amino-2,2-dioxo-1,2-oxathiole-5,3′-[2′,5′-bis-*O*-(*tert*-butyldimethylsilyl)-β-D-ribofuranosyl]]}-3-ethylthymine (TSAOe^{3}T) and (4-*tert*-butylbenzoyl)-2-hydroxy-1-naphthaldehyde hydrazone (BBSH), which both inhibit the HIV-1 RT DNA polymerase activity of the heterodimers and p66 homodimers by destabilization and not by abrogation of the RT subunit interaction (46, 47). The treatment of recombinant wild-type p66 and the W401A mutant RT with HIV-1 protease will help to determine the relative susceptibilities of monomeric and dimeric forms to proteolytic degradation in addition to whether the cleavage site between Pol and RNase H is accessible in the W401A mutant monomer.

Treatment with 0.1 μM indinavir resulted in a partial restoration of the steady-state levels of p66 and p51 in the HX-W401L mutant viral particles, but RT activity remained undetectable. We believe that the lack of RT activity in the cell-free RT assay was due to the inability of the p66 and p51 RT subunits to form stable heterodimers, as demonstrated in our previous in vitro studies (51, 53). The lack of activity is unlikely to be due to an inhibition of RT activity by the 62-kDa polypeptide (migrating immediately underneath RT p66 in Fig. 5D) recognized by the RT antibody. A peptide of this size was also observed for the wild-type virus treated with 0.1 μM indinavir (Fig. 5B), which, in contrast to the W401L mutant, displayed significant levels of RT activity (50%) compared to untreated wild-type virus (data not shown). An RT-specific band at 45 kDa was also observed in HX-W401L viral lysates harvested from 0.1 μM indinavir-treated cells. In other experiments, this band had similar intensities for both HX-WT and HX-W401L treated with 0.1 μM indinavir, indicating that it is unlikely to be specific to the HX-W401L mutant. Furthermore, the 45-kDa band is unlikely to interfere with heterodimer formation, as a deletion of as little as 26 amino acids from p51 negates the interaction with p66 (25, 52).

The W401A and W401L mutant RTs displayed a >99% reduction in RNA-dependent DNA polymerase activity compared to wild-type RT in the cell-free RT assay. A significant reduction was also observed for minus-strand strong-stop and late DNA synthesis for the W401L mutant and the L234A control compared to wild-type HIV-1. In contrast, while the virion-associated reverse transcriptase activity was dramatically reduced compared to that of the wild type, we could still detect significant levels of early DNA synthesis for NL-W401A and HX-W401A compared to the wild type, with reverse transcription defects becoming more apparent when we examined late DNA transcripts. The greater RT defect by the W401L mutation than by the W401A mutation correlates with the larger decrease in viral infectivity of HX-W401L than of HX-W401A in the infectivity assay performed with the TZM-bl cell line. One possible explanation for detectable intracellular reverse transcription, particularly for the W401A mutants, is that the RT may behave differently on an artificial template/primer from how it behaves when presented with the natural tRNA^{Lys} primer and genomic RNA template in the reverse transcription complex. In vitro studies of recombinant RT with either the W401L or W401A mutation also demonstrated a complete inhibition of RNA-dependent DNA polymerase activity using the same synthetic template/primer used for our RT assays (51) and also using a template/primer based on the HIV-1 sequence (53). Therefore, one explanation for the difference in RT activity in infected cells compared to that in vitro may be due to the stabilizing presence of other viral or host cell factors that modulate RT activity in the reverse transcription complex (17, 19, 54, 55, 63). Another possibility for the difference in RT activity of W401 mutants in cell-free assays compared to intracellular reverse transcription can be ascribed to the dimerization constant of the RT. The effective concentration of RT in the confines of the reverse transcription complex is likely higher than that in cell-free assays. Hence, the proportions of dimers and monomers in the reverse transcription complex would be higher, leading to a less dramatic defect than what we observed in the cell-free assays.

Our study demonstrates a clear correlation between RT dimerization-inhibiting mutations located near the RT dimer interface and defects in RT maturation and function. The defect in RT function was observed in the absence of detect-

able effects on Gag-Pol stability or Gag-Pol incorporation into the virion. Our studies suggest that the most likely precursor of the mature RT heterodimer in HIV-1-infected cells is the p66 homodimer, although further studies are needed to prove this assertion. Since the stability of the p66 homodimer is orders of magnitude lower than that of the RT heterodimer, the former represents a more attractive target for destabilization by small-molecule inhibitors of HIV-1 RT.

ACKNOWLEDGMENTS

G.T. was supported by NHMRC career development award 235102 and NHMRC project grant 235030. J.W. was supported by the Australian Postgraduate Award, Monash University.

We thank Dag Helland for the supply of RT and IN antibodies, Andy Poumbourios for the purification of p24 antibodies, and the NIH AIDS Research and Reference Reagent Program, Division of AIDS, NIAID, NIH, for the supply of indinavir, the TZM-bl cell line, and the p24 hybridoma (183-H12-5C). We thank Margaret Hellard for assistance with the statistical analyses performed for this study.

REFERENCES

1. **Adachi, A., H. E. Gendelman, S. Koenig, T. Folks, R. Willey, A. Rabson, and M. A. Martin.** 1986. Production of acquired immunodeficiency syndrome-associated retrovirus in human and nonhuman cells transfected with an infectious molecular clone. J. Virol. **59:**284–291.
2. **Amacker, M., and U. Hubscher.** 1998. Chimeric HIV-1 and feline immunodeficiency virus reverse transcriptases: critical role of the p51 subunit in the structural integrity of heterodimeric lentiviral DNA polymerases. J. Mol. Biol. **278:**757–765.
3. **Baillon, J. G., N. T. Nashed, A. Kumar, S. H. Wilson, and D. M. Jerina.** 1991. A leucine zipper-like motif may mediate HIV reverse transcriptase subunit binding. New Biol. **3:**1015–1019.
4. **Becerra, S. P., A. Kumar, M. S. Lewis, S. G. Widen, J. Abbotts, E. M. Karawya, S. H. Hughes, J. Shiloach, and S. H. Wilson.** 1991. Protein-protein interactions of HIV-1 reverse transcriptase: implication of central and C-terminal regions in subunit binding. Biochemistry **30:**11707–11719.
5. **Bhattacharyya, G. K., and R. A. Johnson.** 1997. Statistical concepts and methods. John Wiley and Sons, New York, N.Y.
6. **Buxton, P., G. Tachedjian, and J. Mak.** 2005. Analysis of the contribution of reverse transcriptase and integrase proteins to retroviral RNA dimer conformation. J. Virol. **79:**6338–6348.
7. **Chesebro, B., K. Wehrly, J. Nishio, and S. Perryman.** 1992. Macrophage-tropic human immunodeficiency virus isolates from different patients exhibit unusual V3 envelope sequence homogeneity in comparison with T-cell-tropic isolates: definition of critical amino acids involved in cell tropism. J. Virol. **66:**6547–6554.
8. **Derdeyn, C. A., J. M. Decker, J. N. Sfakianos, X. Wu, W. A. O'Brien, L. Ratner, J. C. Kappes, G. M. Shaw, and E. Hunter.** 2000. Sensitivity of human immunodeficiency virus type 1 to the fusion inhibitor T-20 is modulated by coreceptor specificity defined by the V3 loop of gp120. J. Virol. **74:**8358–8367.
9. **di Marzo Veronese, F., T. D. Copeland, A. L. DeVico, R. Rahman, S. Oroszlan, R. C. Gallo, and M. G. Sarngadharan.** 1986. Characterization of highly immunogenic p66/p51 as the reverse transcriptase of HTLV-III/LAV. Science **231:**1289–1291.
10. **Divita, G., T. Restle, and R. S. Goody.** 1993. Characterization of the dimerization process of HIV-1 reverse transcriptase heterodimer using intrinsic protein fluorescence. FEBS Lett. **324:**153–158.
11. **Divita, G., K. Rittinger, T. Restle, U. Immendorfer, and R. S. Goody.** 1995. Conformational stability of dimeric HIV-1 and HIV-2 reverse transcriptases. Biochemistry **34:**16337–16346.
12. **Fisher, A. G., E. Collalti, L. Ratner, R. C. Gallo, and F. Wong-Staal.** 1985. A molecular clone of HTLV-III with biological activity. Nature **316:**262–265.
13. **Folks, T. M., K. A. Clouse, J. Justement, A. Rabson, E. Duh, J. H. Kehrl, and A. S. Fauci.** 1989. Tumor necrosis factor alpha induces expression of human immunodeficiency virus in a chronically infected T-cell clone. Proc. Natl. Acad. Sci. USA **86:**2365–2368.
14. **Ghosh, M., P. S. Jacques, D. W. Rodgers, M. Ottman, J. L. Darlix, and S. F. Le Grice.** 1996. Alterations to the primer grip of p66 HIV-1 reverse transcriptase and their consequences for template-primer utilization. Biochemistry **35:**8553–8562.
15. **Gorelick, R. J., and L. E. Henderson.** 1994. Human retroviruses and AIDS: analyses (part III). The Los Alamos National Laboratory, Los Alamos, N.Mex.
16. **Harada, S., Y. Koyanagi, and N. Yamamoto.** 1985. Infection of HTLV-III/LAV in HTLV-I-carrying cells MT-2 and MT-4 and application in a plaque assay. Science **229:**563–566.
17. **Harrich, D., and B. Hooker.** 2002. Mechanistic aspects of HIV-1 reverse transcription initiation. Rev. Med. Virol. **12:**31–45.
18. **Hawkes, R.** 1979. General principles underlying laboratory diagnosis in viral infections, p. 34–35. *In* Diagnostic procedures for viral, rickettsial and chlamydial infection, 5th ed. American Public Health Association, Washington, D.C.
19. **Hehl, E. A., P. Joshi, G. V. Kalpana, and V. R. Prasad.** 2004. Interaction between human immunodeficiency virus type 1 reverse transcriptase and integrase proteins. J. Virol. **78:**5056–5067.
20. **Henderson, L. E., M. A. Bowers, R. C. Sowder II, S. A. Serabyn, D. G. Johnson, J. W. Bess, Jr., L. O. Arthur, D. K. Bryant, and C. Fenselau.** 1992. Gag proteins of the highly replicative MN strain of human immunodeficiency virus type 1: posttranslational modifications, proteolytic processing, and complete amino acid sequences. J. Virol. **66:**1856–1865.
21. **Hill, M., G. Tachedjian, and J. Mak.** 2005. The packaging and maturation of the HIV-1 Pol proteins. Curr. HIV Res. **3:**73–85.
22. **Hill, M. K., M. Shehu-Xhilaga, S. M. Crowe, and J. Mak.** 2002. Proline residues within spacer peptide p1 are important for human immunodeficiency virus type 1 infectivity, protein processing, and genomic RNA dimer stability. J. Virol. **76:**11245–11253.
23. **Hostomsky, Z., Z. Hostomska, T. B. Fu, and J. Taylor.** 1992. Reverse transcriptase of human immunodeficiency virus type 1: functionality of subunits of the heterodimer in DNA synthesis. J. Virol. **66:**3179–3182.
24. **Jacobo-Molina, A., J. Ding, R. G. Nanni, A. D. Clark, Jr., X. Lu, C. Tantillo, R. L. Williams, G. Kamer, A. L. Ferris, P. Clark, et al.** 1993. Crystal structure of human immunodeficiency virus type 1 reverse transcriptase complexed with double-stranded DNA at 3.0 A resolution shows bent DNA. Proc. Natl. Acad. Sci. USA **90:**6320–6324.
25. **Jacques, P. S., B. M. Wohrl, K. J. Howard, and S. F. Le Grice.** 1994. Modulation of HIV-1 reverse transcriptase function in "selectively deleted" p66/p51 heterodimers. J. Biol. Chem. **269:**1388–1393.
26. **Jacques, P. S., B. M. Wohrl, M. Ottmann, J. L. Darlix, and S. F. Le Grice.** 1994. Mutating the "primer grip" of p66 HIV-1 reverse transcriptase implicates tryptophan-229 in template-primer utilization. J. Biol. Chem. **269:**26472–26478.
27. **Kaplan, A. H., M. Manchester, and R. Swanstrom.** 1994. The activity of the protease of human immunodeficiency virus type 1 is initiated at the membrane of infected cells before the release of viral proteins and is required for release to occur with maximum efficiency. J. Virol. **68:**6782–6786.
28. **Klein, J. R., and B. D. Jones.** 2001. *Salmonella* pathogenicity island 2-encoded proteins SseC and SseD are essential for virulence and are substrates of the type III secretion system. Infect. Immun. **69:**737–743.
29. **Kohlstaedt, L. A., J. Wang, J. M. Friedman, P. A. Rice, and T. A. Steitz.** 1992. Crystal structure at 3.5 A resolution of HIV-1 reverse transcriptase complexed with an inhibitor. Science **256:**1783–1790.
30. **Lee, T. H., F. J. Sunzeri, L. H. Tobler, B. G. Williams, and M. P. Busch.** 1991. Quantitative assessment of HIV-1 DNA load by coamplification of HIV-1 gag and HLA-DQ-alpha genes. AIDS **5:**683–691.
31. **Le Grice, S. F., C. E. Cameron, and S. J. Benkovic.** 1995. Purification and characterization of human immunodeficiency virus type 1 reverse transcriptase. Methods Enzymol. **262:**130–144.
32. **Le Grice, S. F., T. Naas, B. Wohlgensinger, and O. Schatz.** 1991. Subunit-selective mutagenesis indicates minimal polymerase activity in heterodimer-associated p51 HIV-1 reverse transcriptase. EMBO J. **10:**3905–3911.
33. **Lindhofer, H., K. von der Helm, and H. Nitschko.** 1995. In vivo processing of Pr160gag-pol from human immunodeficiency virus type 1 (HIV) in acutely infected, cultured human T-lymphocytes. Virology **214:**624–627.
34. **Mak, J., A. Khorchid, Q. Cao, Y. Huang, I. Lowy, M. A. Parniak, V. R. Prasad, M. A. Wainberg, and L. Kleiman.** 1997. Effects of mutations in Pr160gag-pol upon tRNA(Lys3) and Pr160gag-pol incorporation into HIV-1. J. Mol. Biol. **265:**419–431.
35. **Mulky, A., S. G. Sarafianos, E. Arnold, X. Wu, and J. C. Kappes.** 2004. Subunit-specific analysis of the human immunodeficiency virus type 1 reverse transcriptase in vivo. J. Virol. **78:**7089–7096.
36. **Nilsen, B. M., I. R. Haugan, K. Berg, L. Olsen, P. O. Brown, and D. E. Helland.** 1996. Monoclonal antibodies against human immunodeficiency virus type 1 integrase: epitope mapping and differential effects on integrase activities in vitro. J. Virol. **70:**1580–1587.
37. **Patel, P. H., A. Jacobo-Molina, J. Ding, C. Tantillo, A. D. Clark, Jr., R. Raag, R. G. Nanni, S. H. Hughes, and E. Arnold.** 1995. Insights into DNA polymerization mechanisms from structure and function analysis of HIV-1 reverse transcriptase. Biochemistry **34:**5351–5363.
38. **Pear, W. S., G. P. Nolan, M. L. Scott, and D. Baltimore.** 1993. Production of high-titer helper-free retroviruses by transient transfection. Proc. Natl. Acad. Sci. USA **90:**8392–8396.
39. **Pettit, S. C., L. E. Everitt, S. Choudhury, B. M. Dunn, and A. H. Kaplan.** 2004. Initial cleavage of the human immunodeficiency virus type 1 GagPol precursor by its activated protease occurs by an intramolecular mechanism. J. Virol. **78:**8477–8485.
40. **Pettit, S. C., S. Gulnik, L. Everitt, and A. H. Kaplan.** 2003. The dimer interfaces of protease and extra-protease domains influence the activation of protease and the specificity of GagPol cleavage. J. Virol. **77:**366–374.

41. **Restle, T., B. Muller, and R. S. Goody.** 1990. Dimerization of human immunodeficiency virus type 1 reverse transcriptase. A target for chemotherapeutic intervention. J. Biol. Chem. **265:**8986–8988.
42. **Richardson, B. A., and J. Overbaugh.** 2005. Basic statistical considerations in virological experiments. J. Virol. **79:**669–676.
43. **Shehu-Xhilaga, M., S. Ablan, D. G. Demirov, C. Chen, R. C. Montelaro, and E. O. Freed.** 2004. Late domain-dependent inhibition of equine infectious anemia virus budding. J. Virol. **78:**724–732.
44. **Shin, C. G., B. Taddeo, W. A. Haseltine, and C. M. Farnet.** 1994. Genetic analysis of the human immunodeficiency virus type 1 integrase protein. J. Virol. **68:**1633–1642.
45. **Sluis-Cremer, N., D. Arion, M. E. Abram, and M. A. Parniak.** 2004. Proteolytic processing of an HIV-1 Pol polyprotein precursor: insights into the mechanism of reverse transcriptase p66/p51 heterodimer formation. Int. J. Biochem. Cell Biol. **36:**1836–1847.
46. **Sluis-Cremer, N., D. Arion, and M. A. Parniak.** 2002. Destabilization of the HIV-1 reverse transcriptase dimer upon interaction with *N*-acyl hydrazone inhibitors. Mol. Pharmacol. **62:**398–405.
47. **Sluis-Cremer, N., G. I. Dmitrienko, J. Balzarini, M. J. Camarasa, and M. A. Parniak.** 2000. Human immunodeficiency virus type 1 reverse transcriptase dimer destabilization by 1-[spiro[4"-amino-2",2"-dioxo-1",-2"-oxathiole-5",3'-[2',5'-*bis*-*O*-(*tert*-butyldimethylsilyl)-beta-D-ribofuranosyl]]]-3-ethylthymine. Biochemistry **39:**1427–1433.
48. **Sluis-Cremer, N., and G. Tachedjian.** 2002. Modulation of the oligomeric structures of HIV-1 retroviral enzymes by synthetic peptides and small molecules. Eur. J. Biochem. **269:**5103–5111.
49. **Sonza, S., A. Maerz, N. Deacon, J. Meanger, J. Mills, and S. Crowe.** 1996. Human immunodeficiency virus type 1 replication is blocked prior to reverse transcription and integration in freshly isolated peripheral blood monocytes. J. Virol. **70:**3863–3869.
50. **Szilvay, A. M., S. Nornes, I. R. Haugan, L. Olsen, V. R. Prasad, C. Endresen, S. P. Goff, and D. E. Helland.** 1992. Epitope mapping of HIV-1 reverse transcriptase with monoclonal antibodies that inhibit polymerase and RNase H activities. J. Acquir. Immune Defic. Syndr. **5:**647–657.
51. **Tachedjian, G., H. E. Aronson, M. de los Santos, J. Seehra, J. M. McCoy, and S. P. Goff.** 2003. Role of residues in the tryptophan repeat motif for HIV-1 reverse transcriptase dimerization. J. Mol. Biol. **326:**381–396.
52. **Tachedjian, G., H. E. Aronson, and S. P. Goff.** 2000. Analysis of mutations and suppressors affecting interactions between the subunits of the HIV type 1 reverse transcriptase. Proc. Natl. Acad. Sci. USA **97:**6334–6339.
53. **Tachedjian, G., J. Radzio, and N. Sluis-Cremer.** 2005. Relationship between enzyme activity and dimeric structure of recombinant HIV-1 reverse transcriptase. Proteins **60:**5–13.
54. **Tasara, T., M. O. Hottiger, and U. Hubscher.** 2001. Functional genomics in HIV-1 virus replication: protein-protein interactions as a basis for recruiting the host cell machinery for viral propagation. Biol. Chem. **382:**993–999.
55. **Tasara, T., G. Maga, M. O. Hottiger, and U. Hubscher.** 2001. HIV-1 reverse transcriptase and integrase enzymes physically interact and inhibit each other. FEBS Lett. **507:**39–44.
56. **Telesnitsky, A., and S. P. Goff.** 1993. Two defective forms of reverse transcriptase can complement to restore retroviral infectivity. EMBO J. **12:**4433–4438.
57. **Vacca, J. P., B. D. Dorsey, W. A. Schleif, R. B. Levin, S. L. McDaniel, P. L. Darke, J. Zugay, J. C. Quintero, O. M. Blahy, E. Roth, et al.** 1994. L-735,524: an orally bioavailable human immunodeficiency virus type 1 protease inhibitor. Proc. Natl. Acad. Sci. USA **91:**4096–4100.
58. **Vogt, V. M.** 1996. Morphogenesis and maturation of retroviruses, vol. 214. Springer-Verlag, Berlin, Germany.
59. **Wang, J., S. J. Smerdon, J. Jager, L. A. Kohlstaedt, P. A. Rice, J. M. Friedman, and T. A. Steitz.** 1994. Structural basis of asymmetry in the human immunodeficiency virus type 1 reverse transcriptase heterodimer. Proc. Natl. Acad. Sci. USA **91:**7242–7246.
60. **Wei, X., J. M. Decker, H. Liu, Z. Zhang, R. B. Arani, J. M. Kilby, M. S. Saag, X. Wu, G. M. Shaw, and J. C. Kappes.** 2002. Emergence of resistant human immunodeficiency virus type 1 in patients receiving fusion inhibitor (T-20) monotherapy. Antimicrob. Agents Chemother. **46:**1896–1905.
61. **Wiegers, K., G. Rutter, H. Kottler, U. Tessmer, H. Hohenberg, and H. G. Krausslich.** 1998. Sequential steps in human immunodeficiency virus particle maturation revealed by alterations of individual Gag polyprotein cleavage sites. J. Virol. **72:**2846–2854.
62. **Wohrl, B. M., R. Krebs, S. H. Thrall, S. F. Le Grice, A. J. Scheidig, and R. S. Goody.** 1997. Kinetic analysis of four HIV-1 reverse transcriptase enzymes mutated in the primer grip region of p66. Implications for DNA synthesis and dimerization. J. Biol. Chem. **272:**17581–17587.
63. **Wu, X., H. Liu, H. Xiao, J. A. Conway, E. Hehl, G. V. Kalpana, V. Prasad, and J. C. Kappes.** 1999. Human immunodeficiency virus type 1 integrase protein promotes reverse transcription through specific interactions with the nucleoprotein reverse transcription complex. J. Virol. **73:**2126–2135.
64. **Wu, X., H. Liu, H. Xiao, J. A. Conway, E. Hunter, and J. C. Kappes.** 1997. Functional RT and IN incorporated into HIV-1 particles independently of the Gag/Pol precursor protein. EMBO J. **16:**5113–5122.
65. **Yu, Q., M. Ottmann, C. Pechoux, S. Le Grice, and J. L. Darlix.** 1998. Mutations in the primer grip of human immunodeficiency virus type 1 reverse transcriptase impair proviral DNA synthesis and virion maturation. J. Virol. **72:**7676–7680.
66. **Zack, J. A., S. J. Arrigo, S. R. Weitsman, A. S. Go, A. Haislip, and I. S. Chen.** 1990. HIV-1 entry into quiescent primary lymphocytes: molecular analysis reveals a labile, latent viral structure. Cell **61:**213–222.